Early immune events in *Mycobacterium tuberculosis* infection and vaccination:

Protective role for GM-CSF in the primary immune response to Mycobacterium tuberculosis infection and recall responses following vaccination

Philippa Jay Stimpson

June 2015

Francis Crick Institute, Mill Hill Laboratories

The Ridgeway, Mill Hill

LONDON NW7 1AA

A thesis submitted to University College London for the degree of Doctor of Philosophy

I, Philippa Jay Stimpson confirm that the work presented in this thesis is my own. Where information has been derived from other sources, I confirm that this has been indicated in the thesis.

Abstract

Tuberculosis, caused by the intracellular bacterium *Mycobacterium tuberculosis* (*Mtb*), is the second leading cause of death from infectious disease. BCG, the only licensed vaccine to date, only provides variable protection against pulmonary disease. Although there is a broad understanding of protective factors in the immune response to *Mtb* infection, including TNFα, IFNγ and the Th1 axis, these are incompletely understood, hindering development of novel vaccine regimes. Factors that are detrimental to control of *Mtb* infection, such as the immunosuppressive cytokine IL-10, are also induced upon *Mtb* infection and BCG vaccination. Blockade of the IL-10 receptor during BCG vaccination enhances protection in both resistant and susceptible mouse models of *Mtb*.

Work in this thesis further investigated IL-10 mediated suppression of BCG-induced protection in *Mtb* susceptible mice and assessed how BCG vaccination in the context of IL-10 receptor blockade affected the onset of adaptive immunity. Vaccination in this context impacted the early immune response to *Mtb* challenge with accelerated and enhanced IL-17 and GM-CSF production. Furthermore, GM-CSF was required for optimal control of bacterial load upon *Mtb* challenge following BCG vaccination. GM-CSF was also required throughout primary *Mtb* infection as GM-CSF neutralisation was detrimental to control of bacterial load in both *Mtb* resistant and *Mtb* susceptible mouse models.

Previous work showed IFNγ and IL-17 production by an "innate-like lymphoid" population upon *Mtb* challenge, following vaccination. This thesis further studied the response and role of ILCs in the early innate response to both the lab-adapted *Mtb* strain H37Rv and the clinical isolate HN878. ILCs were identified as a source of GM-CSF upon HN878 infection and were protective in the innate response to HN878 infection.

Overall this thesis demonstrates the importance of GM-CSF in the primary and recall responses to *Mtb* infection and identifies ILCs as an early, innate source of GM-CSF.

Acknowledgments

Firstly I would like to thank my primary supervisor Professor Anne O'Garra for her guidance, encouragement and continuous support throughout my PhD. Her words of encouragement and guidance at crucial moments enabled me to improve and perform at the best of my ability. I would also like to thank my Thesis Committee Professor Douglas Young and Dr Greg Bancroft for their additional advice and support. I am also indebted to many people from the O'Garra lab, both past and present. My thanks go to Dr Paul Redford for his time and patience throughout my training in BSL-3; to Dr Finlay McNab for his advice, discussions and criticisms that taught me so much; to Vangelis Stavropoulos without whom many of my (sometimes very larger) *in vivo* experiments would not be possible, I am sure he will not miss my demands for early mornings; and finally to Dr Lucia Moreira-Teixeira whose insightful comments have challenged me and who has also been invaluable in performing the some of the large *in vivo* experiments. I would also like to thank Dr Xuemei Wu and Dr Damian Carragher for breeding all the mice I required throughout me project, making sure they were in the right place, and for their advice. My thanks also go to the rest of the AOG lab (and other members of the institute) who have made my PhD so enjoyable.

I would like to thank Ewelina Kozlowska and Kathleen Mathers of Biological Services and all the animal technicians in Laidlaw Yellow who have cared for my animals in BSL-3, notably Jackie Holland, Amanda Hewitt, Matthew Legate and more recently Daiva Poniskaitiene. I would like to thank Graham Preece and his team in the Flow Cytometery Facility for their technical assistance and patience. I would like to thank Simon Caidan and the rest of the Safety team, without whom my PhD would not have been possible. My thanks also go to the UCL MB PhD programme for awarding me my place and giving me such a wonderful opportunity.

On a personal note I would like to thank my parents and my siblings Cate, Hugh and Jo for their love, support and continued belief in me. Special thanks also go to Charlotte Whicher and

Victoria Pelly for their tremendous support and friendship. Finally I would like to thank my boyfriend Ali for dropping me off and picking me up at ungodly hours, for planning weekends around weighing my mice, and for his seemingly never-ending supply of encouragement, love and belief. Thank you.

Table of Contents

Table of Figures

Chapter 1: Introduction

Chapter 3: Determining whether IL-10 during BCG vaccination influences the early cytokine response to *Mtb* challenge in susceptible mice.

Table of Tables

List of Abbreviations

AA	Arachidonic Acid
Ad	Adenovirus
ADC	Albumin Dextrose Catalase
Ag85A	Antigen 85A
Ag85B	Antigen 85B
Ahr	Aryl Hydrocarbon Receptor
AIDS	Acquired Immune Deficiency Syndrome
APC	Antigen Presenting Cell
APC	Allophycocyanin
APCe780	Allophycocyanin e780
ART	Antiretroviral Therapy
BAL	Bronchoalveolar Lavage
BCG	Bacillus Calmette Guerin
BSL	Biological Safety Level
CARD 9	Caspase Recruitment Domain-Containing Protein 9
CFP	*Mtb* Culture Filtrate Protein
CFU	Colonoy Forming Units
CHILP	Common Helper-like Innate Lymphoid Progenitor
CILP	Common Innate Lymphoid Progenitor
CLP	Common Lymphoid Progenitor
CLR	C-type Lectin Receptor
COX	Cyclo-oxygenase
CT	Computed Tomography
DC	Dendtric Cell
DNA	Deoxyribonucleic Acid

EBV	Epstein Barr Virus
ELISA	Enzyme-Linked Immunosorbent Assay
ESAT-6	6 kDa Early Secretory Antigenic Target
FCS	Foetal Calf Serum
FITC	Fluorescein Isothiocyanate Conjugate
FMO	Fluorescence Minus One
FSc	Forward Scatter
G-CSF	Granulocyte colony stimulating factor
GATA3	GATA-Binding Protein 3
GFP	Green Fluorescent Protein
GM-CSF	Granulocyte Macrophage Colony Stimulating Factor
HIV	Human Immunodeficiency Virus
i.d.	Intradermal
i.p.	Intraperitoneal
IFN	Interferon
IFNαβR	Interferon αβ Receptor
IGRA	Interferon γ Release Assay
IL-	Interleukin
IL-10R	Interleukin-10 Receptor
IL-18R	Interleukin-18 Receptor
IL-1R1	Interleukin-1 Receptor
ILC	Innate Lymphoid Cell
iNOS	Inducible Nitric Oxide Synthase
IRIS	Immune Reconstitution Inflammatory Syndrome
ISO	Isotype
KGF	Keratinocyte Growth Factor
KLRG1	Killer cell Lectin-like Receptor subfamily G member 1

LCMV	Lymphocytic Choriomeningitis Virus
Lin	Lineage
LPS	Lipopolysaccharide
LTB_4	Leukotriene B4
LTi	Lymphoid Tissue Inducer
LXA_4	Lipoxin A4
M-CSF	Macrophage Colony Stimulating Factor
M. avium	*Mycobacterium avium*
M. bovis	*Mycobacterium bovis*
M. marinum	*Mycobacterium marinum*
mAb	Monoclonal Antibody
MAC	*Mycobacterium avium* Complex
MDR-TB	Multi-Drug Resistant Tuberculosis
MDSC	Myeloid Derived Suppressor Cell
MHC	Major Histocompatibility Complex
Mincle	Macrophage-Inducible C-type Lectin
MPL	Monophosphoryl Lipid A
MSMD	Mendelian Susceptibility to Mycobacterial Diseases
Mtb	*Mycobacterium tuberculosis*
MVA	Modified Vaccinia Ankara
NHP	Non Human Primate
NK	Natural Killer
NKT	Natural Killer T
NLR	NOD Like Receptor
NLR	NOD Like Receptor
NO	Nitric Oxide
OADC	Oleic Albumin Dextrose Catalase

OD_{600}	Optical Density 600
OVA	Ovalbumin
PAMP	Pathogen Associated Molecular Pattern
PAP	Pulmonary Alveolar Proteinosis
PBMC	Peripheral Blood Mononuclear Cells
PBS	Phosphate Buffered Saline
PCR	Polymerase Chain Reaction
PD-1	Programmed Cell Death Protein 1
PE	Phycoerythrin
PE Cy7	Phycoerythrin Cy7
PerCP Cy5.5	Peridinin-chlorophyll-protein Cy5.5
PET	Positron Emission Tomography
PGE_2	Prostaglandin E2
PMA	Phorbol Myristate Acetate
PPARγ	Peroxisome Proliferator-Activated Receptor γ
PPD	Purified Protein Derivative
PRR	Pattern Recognition Receptor
RD1	Region of Difference 1
RNI	Reactive Nitrogen Species
RORα	RAR-related orphan Receptor α
RORγt	RAR-related orphan Receptor γ
ROS	Reactive Oxygen Species
RSV	Respiratory Syncytial Virus
SD	Standard Deviation
SPF	Specific Pathogen Free
SSc	Side Scatter
STAT	Signal Transducer and Activator of Transcription

Syk	Spleen Tyrosine Kinase
TAP	Transporter Associated with Antigen Processing
TB	Tuberculosis
TCR	T Cell Receptor
Th	T helper
TIR	Toll/interleukin-1 receptor
TLR	Toll Like Receptor
TNF	Tumour Necrosis Factor
TNFR	Tumour Necrosis Factor Receptor
Treg	Regulatory T cell
TSLP	Thymic stromal lymphopoietin
TST	Tuberculin Skin Test
vIL-10	Viral IL-10
WHO	World Health Organisation
XDR TB	Extensively drug resistant tuberculosis
αGM-CSF	anti-GM-CSF
αIL-10R	anti- IL-10 Receptor
αLy6G	anti-Ly6G
αLP	Alpha Lymphoid Progenitor

Chapter 1: Introduction

1.1. Tuberculosis – a global problem

Tuberculosis (TB) is caused by infection with the acid-fast bacilli *Mycobacterium tuberculosis* (*Mtb*), which was first identified by Robert Koch in 1882 (Koch, 1882)**.** Despite the knowledge of the causative pathogen for over 100 years, TB remains a considerable global health problem, being the second leading cause of death by infectious disease (WHO, 2014b). In 2013 there was an estimated 9 million new TB cases and 1.5 million deaths in 2013 (WHO, 2014b). Furthermore it is estimated that approximately one third of the world's population is infected with *Mtb* (Dye et al., 1999). Such a high burden of disease exists despite initiatives such as the Stop TB Strategy by the World Health Organisation (WHO), which aims to half the incidence of TB by 2015 compared to 1990 (which has been achieved) with the ultimate goal of achieving a TB-free world by 2050 (WHO, 2006; WHO, 2014b).

1.1.1 Clinical manifestations of Mtb infection

Mtb is transmitted predominately via aerosol droplets and most commonly leads to a pulmonary disease, although it can affect many organs (Lawn and Zumla, 2011). Following infection with *Mtb* there are several potential clinical outcomes (**Figure 1.1**). A minority of individuals will rapidly develop active disease where there is bacterial replication and clinical symptoms including weight loss, fever and in pulmonary disease haemoptysis (reviewed in O'Garra et al., 2013). Active tuberculosis is most commonly defined by the presence of symptoms and the demonstration of the bacteria through sputum (or tissue) microscopy and culture of the bacillus (Chegou et al., 2011). Due to the technical difficulties involved in acquiring sputum, the possibility that bacterial loads are below the detection limit, and the time taken to culture *Mtb*, other tests have been developed to identify the presence of bacteria such as GeneXpert. This is a PCR based test which is also able to identify whether the infecting *Mtb* strain has rifampicin resistance (Boehme et al., 2010).

The majority of those infected with *Mtb* will develop a latent infection, displaying evidence of infection through demonstration of an adaptive immune response (through a positive Tuberculin Skin Test (TST) or Interferon Gamma Release Assay (IGRA)) in the absence of clinical symptoms (Barry et al., 2009; Young et al., 2009). However, this definition of latent infection could, encompass a wide range of clinical phenotypes (Barry et al., 2009; Young et al., 2009). This definition could include those who have mounted an effective adaptive immune response and have no viable bacteria, those who are controlling infection with non-replicating bacteria or those with a subclinical disease where there is active bacterial replication but the absence of clinical symptoms (Young et al., 2009). Furthermore, it should be noted that a positive TST test and/or IGRA does not distinguish between active and latent tuberculosis and thus diagnostic tools with this capability are required (Young et al., 2009).

In addition to the heterogeneity of clinical phenotypes encompassed by a positive TST or IGRA test, definition of latent tuberculosis by the TST test is flawed as it relies on a delayed hypersensitivity response to Purified Protein Derivative (PPD), which is prepared from heat killed *Mtb* cultures (Reichman, 1979). This mixture contains multiple *Mtb* antigens but also antigens from other mycobacterial strains including the vaccine BCG and various environmental mycobacteria, which leads to false positive results for example, in BCG vaccinated individuals (Richeldi, 2006). More recently IGRAs were developed which measure IFNγ release in response to *Mtb* specific antigens present in the Region of Difference 1 (RD1) locus, which is absent in BCG (Mahairas et al., 1996) and most other environmental mycobacteria, thus avoiding the false positive results observed with the TST (Richeldi, 2006).

Individuals can remain latently infected for long periods of time or even over their entire lifetime (reviewed in O'Garra et al., 2013). However, some individuals reactivate, progressing from a latent disease state to active disease. An immunocompetent individual has an approximately 5-10% lifetime risk of reactivating to active disease, with the highest risk following infection and in early adulthood (reviewed in O'Garra et al., 2013). The risk of

reactivation is dramatically increased when an individual is immunocompromised, for example through infection with Human Immunodeficiency Virus (HIV) (Cooper, 2009; Schutz et al., 2010) or by iatrogenic means such as through anti-TNFα treatment for Rheumatoid Arthritis of Crohn's disease (Cooper, 2009; Keane et al., 2001).

It has also been postulated that some people may be able to clear *Mtb* infection utilising only the innate immune system, without the requirement to mount an adaptive immune response (reviewed in Barry et al., 2009; Young et al., 2009). Evidence for such a phenomenon is provided by the observation that a proportion of individuals in repeated, close contact with active tuberculosis patients, such as healthcare workers or household contacts, fail to convert to TST positivity (Alcais et al., 2005; Joshi et al., 2006; Morrison et al., 2008; Young et al., 2009). In such individuals innate immune mechanisms including macrophages, neutrophils and innate lymphocytes such as Natural Killer (NK) cells (discussed in more detail later) are suggested to be capable of clearing the infection before the development of an adaptive immune response (Verrall et al., 2014). However, it must also be considered that the lack of TST positivity may be due to other causes such as HIV infection where there is induced deficiency in the adaptive response (reviewed in Barry et al., 2009).

1.1.2 HIV-TB Co-infection

Co-infection with *Mtb* and HIV is common, occurring in approximately 13% of all TB cases reported in 2013 (WHO, 2014b), although the burden of HIV/TB co-infection is highest in sub-Saharan Africa constituting 79% of all global cases (Lawn et al., 2013). TB is a major cause of mortality in HIV infected individuals, accounting for approximately a quarter of such deaths (Lawn et al., 2013). HIV infection increases not only the risk of reactivation (discussed earlier) but also the risk of developing primary disease following infection (Corbett et al., 2003; Schutz et al., 2010). Thus co-infection with *Mtb* and HIV represents a major barrier to the global control of TB (WHO, 2014b).

One initiative employed to reduce mortality in HIV-TB co-infection is the initiation of Anti-Retroviral Therapy (ART) (Lawn and Zumla, 2011). ART allows immune recovery and is reported to reduced incidence rates of TB by 67% in patients co-infected with HIV (Lawn and Zumla, 2011). However, a complication of ART in co-infected patients can be the development of Immune Reconstitution Inflammatory Syndrome (IRIS) (Walker et al., 2015b). TB-IRIS results in excessive inflammation accompanied by considerable morbidity and mortality. It can occur in patients already being treated for *Mtb* infection prior to the initiation of ART (paradoxical TB-IRIS) or in those where *Mtb* infection was not diagnosed prior to the initiation of ART (unmasking TB-IRIS) (Walker et al., 2015b). Despite the risk of this complication, initiation of ART therapy is still recommended and can largely be continued if TB-IRIS develops (Schutz et al., 2010).

1.2.3 Drug resistance in tuberculosis

The emergence of Multi-Drug Resistant (MDR) (resistant to isoniazid and rifampicin) and Extensively Drug Resistant (XDR) (resistant to isoniazid, rifampicin, fluoroquinolones and any of the second line injectable drugs including capreomycin and kanamycin) tuberculosis strains represents another major threat to the global efforts to control TB (Abubakar et al., 2013). The emergence of such drug resistant strains heightens the need for novel drugs in the treatment of tuberculosis (Abubakar et al., 2013). The shortest drug treatment regime for drug susceptible TB consists of 2 months of rifampicin, isoniazid, pyrazinamide and ethambutol followed by 4 months of rifampicin and isoniazid (Dorman and Chaisson, 2007). The length of treatment and the side effects of these drugs often result in non-compliance, and this coupled with malabsorption and poor prescribing by clinicians all contribute to the development of resistant strains (Dorman and Chaisson, 2007). Globally in 2013 MDR-TB caused 3.5% of new TB cases. However, the global distribution of drug resistant TB in unequal. In Eastern Europe and central Asia in 2013 up to 35% of newly diagnosed TB cases were drug resistant and India, China and the Russian Federation account for more than 50% of MDR-TB cases (WHO,

2014a). MDR-TB is a serious risk to global health and strategies need to be put in place to combat its development and transmission as well as strategies to aid rapid diagnosis and effective treatment (WHO, 2014a).

As the second leading cause of death from infectious disease, tuberculosis represents a major global health risk (WHO, 2014b). Difficulties in diagnosis and treatment of the disease along with the development of drug resistant strains and HIV-TB co-infection are all barriers to global control of the disease. Another barrier to control of the disease is the lack of an effective vaccine (discussed in more detail below). If the aim of a TB free world by 2050 is to be met, better diagnostics, treatments and an effective vaccine are all required. A better understanding of *Mtb* infection and the host immune response is essential to achieve this target.

1.2. Models of *Mtb* infection

Several animal models have been utilised to study *Mtb* infection, including mouse, rabbit, guinea pig, zebrafish and non-human primate (NHP), and these have aided our understanding of the immune response to *Mtb* (Capuano et al., 2003; North and Jung, 2004), although the mouse, rabbit, guinea pig and NHP are not natural hosts for *Mtb* infection (Flynn, 2006). The NHP model of TB is argued to most reflect human disease. Similarly to humans, when NHPs are infected with *Mtb* a range of clinical outcomes are observed (Capuano et al., 2003). A proportion of animals develop active disease, a proportion develops a latent disease, and a proportion of latently infected animals will reactivate, developing active disease (Capuano et al., 2003). Furthermore, the heterogeneity in disease states described in humans is reflected in the NHP model, as some animals develop a subclinical disease, where there is an absence of clinical symptoms but culture positive Bronchoalveolar Lavage (BAL) (Lin et al., 2009). In addition, the structure of granulomas (a complex aggregate of immune cells characteristic of *Mtb*, discussed in detail below) in NHPs is similar to those described in humans (Flynn et al., 2015).

The guinea pig model of TB was used by Koch in his identification of *Mtb* (Koch, 1882). The guinea pig is susceptible to infection with low does of *Mtb* and develops granulomas that resemble those observed in humans, however it does not develop latent infection (Gupta and Katoch, 2005; North and Jung, 2004). The rabbit also develops granulomas that resemble those seen in the humans, and infection with clinical isolates of *Mtb* has been demonstrated to cause a progressive infection (Flynn, 2006; Subbian et al., 2012). In addition a model of latent TB infection has been described in rabbits (Flynn, 2006; Subbian et al., 2012).

The zebrafish model employs infection with *M. marinum* (Ramakrishnan, 2013). The zebrafish is a natural host for *M. marinum*, which contrasts to the other models studied for TB, as they are not natural hosts for *Mtb* or *M. bovis* (Flynn, 2006). The transparency of the zebrafish in early

life enables experiments to track cells and assess early granuloma formation, although it should be noted that at this stage in development no adaptive immune system is present (Ramakrishnan, 2013).

The most commonly used model of TB is the mouse model. Several factors of the immune response to *Mtb* known to be protective in humans including IL-12, IFNγ and TNFα (all discussed below) are also crucial to the immune response in mice, suggesting there is at least some overlap in responses (Cooper, 2009; Fortin et al., 2007; North and Jung, 2004). There are several benefits for using the mouse to study TB. Firstly, mice are relatively inexpensive and easier to maintain in BSL-3 conditions than some other models (Flynn et al., 2015). Furthermore, a wide range of reagents are available for study of the mouse immune response (North and Jung, 2004). Finally many inbred and genetically engineered mouse strains exist facilitating study of specific components of the immune response (Flynn et al., 2015); Apt and Kramnik, 2009). However, it is argued that the mouse does not reflect human disease and therefore is not an appropriate model to study (Apt and Kramnik, 2009). This argument is based on several observations. Firstly, that all mice eventually succumb to the disease, and do not develop latent infection (Flynn, 2006). Secondly, that the structure of the granuloma does not mirror that observed in the human (Apt and Kramnik, 2009). The granulomas in the most commonly used strains of mice do not develop central necrosis (Rhoades et al., 1997), in contrast to humans (Tsai et al., 2006; Ulrichs et al., 2004; Via et al., 2008). Furthermore the granulomas within these commonly studied mouse strains are not hypoxic, in contrast to humans (Tsai et al., 2006; Via et al., 2008). However, granuloma structure in human Tb patients as well as the NHP model of *Mtb* infection has been shown to be heterogeneous, with some lesions not developing a necrotic core (Barry et al., 2009). In addition, many of the observations used to suggest the mouse is not an adequate model of *Mtb* are based on mouse strains that are resistant to *Mtb* (Apt and Kramnik, 2009; Rhoades et al., 1997; Tsai et al., 2006). There are several other in-bred mouse strains that display higher susceptibility to *Mtb* infection, with different patterns of bacterial growth and pathology, which will be discussed below.

1.2.1. Resistant and susceptible mouse strains

Following aerosol infection with *Mtb*, different inbred strains of mice display different patterns of bacterial growth and survival. C57BL/6 and BALB/c mice are "resistant" mouse strains where uncontrolled bacterial growth occurs rapidly for approximately the first 3-4 weeks of infection. Following this bacterial growth is controlled and bacterial load plateaus until the mouse succumbs to infection and dies approximately 300 days post infection (Medina and North, 1998; North and Jung, 2004). In contrast, infection of "susceptible" mouse strains including DBA/2, CBA, C3H and I/St strains leads to higher bacterial loads, as these strains fail to control bacterial growth and no plateau is reached (North and Jung, 2004; Turner et al., 2001). These mice succumb to infection earlier, at approximately 100-150 days post infection (Eruslanov et al., 2005; Eruslanov et al., 2004; Medina and North, 1998; North and Jung, 2004). The immune response to infection in these susceptible mouse strains is also described to differ to resistant mouse strains, with many susceptible strains showing increased accumulation of granulocytes (Eruslanov et al., 2005; Keller et al., 2006; Marzo et al., 2014). In addition, the kinetics of the immune response are delayed in susceptible mouse strains (Chackerian et al., 2002b; Turner et al., 2001). Furthermore, the lung pathology in susceptible mouse strains also differs, with descriptions of necrotic and hypoxic granulomas forming in C3HeB/FeJ mice (Apt and Kramnik, 2009; Harper et al., 2012; Kramnik et al., 2000). Thus it is suggested that susceptible mouse strains may provide a model of TB that more resembles active human disease.

The basis for susceptibility of the different mouse strains is not completely understood. However, use of genetic approaches has identified loci that confer susceptibility to tuberculosis (North and Jung, 2004). For example, through analysis of C3HeB/FeJ x B6 F_2 mice, the *susceptibility to tuberculosis 1* (*sst1*) loci was identified (Kramnik et al., 2000). This locus was found to play a role in necrosis of granulomas (Kramnik et al., 2000). A subsequent study

showed that resistant mice expressing this susceptibility locus display necrotising granulomas and decreased survive (Pichugin et al., 2009). Furthermore C3H mice expressing the *sst1* locus from resistant mice display lower bacterial loads and their granulomas lack necrosis (Pan et al., 2005). A gene within this locus, *Intracellular pathogen resistance 1* (*Ipr1*), was found to contribute to control of intracellular growth of *Mtb* and promote apoptotic cell death of infected macrophages (Pan et al., 2005). Such analysis of susceptible mouse strains may enable identification of factors that contribute to human susceptibility to TB.

1.3 Immune response to *Mtb*

Animal models of TB have enabled investigation of events following infection with *Mtb*. They have also enabled the identification of immune factors that are protective and some that are detrimental to control of *Mtb* infection. This section will discuss the development of the immune response to infection as well as individual aspects of the immune response that are thought to be important in protection or contribute to host pathology and disease.

1.3.1 Development of the immune response to Mtb

Following infection with *Mtb* the immune response is slow to develop, with the onset of adaptive immunity not occurring until 3-4 weeks post infection in a resistant mouse model (reviewed in Cooper, 2009) and until 5-6 weeks post infection in humans (Urdahl, 2014; Wallgren, 1948). The immune response that develops is adequate to control disease but largely incapable of eradicating infection, with many individuals developing latent infection (reviewed in O'Garra et al., 2013). It is suggested that *Mtb* manipulates the host immune response to create a niche to facilitate bacterial growth and also to create a lesion that enables release of bacteria and transmission to other hosts (reviewed in

et al., 2015).

1.3.1.1 Infection of innate cells and formation of the early granuloma

Following aerosol inhalation of the *Mtb* bacillus, it is thought that the first cell to become infected is the alveolar macrophage (Srivastava et al., 2014). Other innate cells rapidly accumulate and are infected with *Mtb*, including dendritic cells (DCs), neutrophils and monocytes (Wolf et al., 2007). This aggregation of innate immune cells forms the early granuloma. Work in the zebrafish model suggests that this early granuloma is a permissive niche for mycobacterial growth (Davis and Ramakrishnan, 2009). In this model *M. marinum* promoted necrotic cell death to facilitate recruitment and infection of macrophages (Davis and

Ramakrishnan, 2009). In addition, *Mtb* has developed multiple mechanisms to avoid intracellular killing mechanisms including inhibition of phago-lysosome fusion and disruption of normal acidification of the phagosome, thus enabling growth within macrophages (Russell et al., 2010). Thus the environment within this early granuloma is suggested to allow unchecked bacterial growth and progressive infection of recruited innate cells (Ramakrishnan, 2012).

1.3.1.2 Priming of an adaptive response in the lymph node

The adaptive immune response is crucial to control of *Mtb* infection (discussed in detail below), with mice deficient in lymphocytes displaying increased susceptibility to *Mtb* infection (Orme and Collins, 1983), and HIV infection increasing the risk of active TB in humans (Geldmacher et al., 2012; Schutz et al., 2010). The onset of an adaptive immune response against *Mtb* is slow compared to other infections, even in previously BCG vaccinated hosts (Cooper, 2009; Urdahl et al., 2011). This delay in adaptive immunity prolongs the period of uncontrolled bacterial growth described above and is detrimental to the host. Indeed, a delay in the onset of an adaptive immune response has been associated with susceptibility to *Mtb* infection, with the time taken for infected DCs to traffic to the draining lymph node and initiate T cell responses being longer in the susceptible C3H mouse strain compared to the resistant C57BL/6 mice (Chackerian et al., 2002b).

A threshold of antigen availability is required in the lymph node for initiation of T cell priming, which is not reported to occur until approximately 11 days post infection in a resistant mouse model (Reiley et al., 2008; Wolf et al., 2008). This threshold of antigen availability is met through DCs and inflammatory monocytes trafficking bacteria from the lung to the lymph node (Samstein et al., 2013; Wolf et al., 2007). DC trafficking to the draining lymph node has been reported to be dependent upon the chemokines CCL19 and CCL21 (Wolf et al., 2007) and also IL-12p40 (Khader et al., 2006). Trafficking of DCs that have phagocytosed apoptotic neutrophils is suggested to facilitate priming of an adaptive response (Blomgran et al., 2012;

Blomgran and Ernst, 2011). *Mtb* is suggested to delay the onset of adaptive immunity through inhibition of apoptosis (Blomgran et al., 2012). Indeed, increasing the apoptosis of neutrophils through infection with an *Mtb* strain that promotes apoptosis accelerated the priming of an adaptive response (Blomgran et al., 2012).

The adaptive immune response is an antigen specific response and requires T cell activation by professional antigen presenting cells (APCs) such as DCs. APCs present antigen in the context of Major Histocompatibility Complex (MHC) class I or MHC class II molecules to $CD8^+$ or $CD4^+$ T cells respectively, both of which are activated in the response to *Mtb* (Behar, 2013; Flynn and Chan, 2001). *Mtb* infected DCs were shown to be inefficient at presenting antigen to naïve T cells (Wolf et al., 2007). However, recently it has been shown that infected DCs are capable of transferring antigen to DCs in the draining lymph node, facilitating antigen presentation (Srivastava and Ernst, 2014).

Depending on the context in which naïve $CD4^+$ T cells are activated they display different phenotypes, capable of producing specific cytokines. In response to mycobacterial infection $CD4^+$ T cells are polarised mostly toward a Th1 phenotype, where they express IFNγ, but also a Th17 phenotype, where they express IL-17 (discussed in more detail below) (Cruz et al., 2006). *Mtb* specific suppressive regulatory T cells (Treg) also expand in the lymph node upon infection and contribute to the delay in priming of adaptive response (Scott-Browne et al., 2007; Shafiani et al., 2010).

1.3.1.3 The adaptive immune response arrests growth of bacteria and contributes to the formation of the granuloma

Following their activation T cells are recruited to the lung and arrive at approximately 20 days post infection in resistant mouse models (reviewed in Cooper, 2009). The initiation of an adaptive immune response in the lung leads to activation of phagocytes (at least partly through

IFNγ) to restrict mycobacterial growth via mechanisms such as reactive nitrogen intermediates (RNIs) (reviewed in Nathan and Shiloh, 2000; O'Garra et al., 2013) (discussed in more detail below). Initiation of the adaptive response in the lung correlates with control of bacterial growth in resistant mouse strains reflecting the requirement for an adaptive response to control infection, despite its inability to eradicate infection (North and Jung, 2004). Initiation of the adaptive immune response leads to the formation of the mature granuloma (**Figure 1.2**).

The localisation of T cells within the infected lung is also important. Mice deficient for CXCR5, the chemokine receptor for CXCL13, are more susceptible to *Mtb* infection through poor localisation of T cells within lung parenchyma (Slight et al., 2013). Furthermore distinct T cell populations residing either within the vasculature or the lung parenchyma have recently been identified (Sakai et al., 2014). These populations are described to have different capacities to protect against *Mtb* infection when adoptively transferred into T cell deficient hosts (Sakai et al., 2014). Thus it is not only the arrival of an adaptive response, but its appropriate localisation that enables control of infection.

1.3.2 The Granuloma

The granuloma is a complex aggregate of immune cells that forms in response to persistent stimuli and granulomas are a hallmark of *Mtb* infection. In humans the classic granuloma (shown in **Figure 1.2**) has a caseous necrotic core surrounding by highly activated infected macrophages, neutrophils and DCs (Ramakrishnan, 2012; Ulrichs et al., 2004). Macrophages within the granuloma undergo specialisation into multinucleated giant cells, epitheloid cells and foamy macrophages (Russell et al., 2009). This central core of innate cells is surrounded by a lymphocytic cuff of T and B cells and also fibroblasts which produce a fibrotic capsule (Ramakrishnan, 2012). As discussed above, the resistant mouse model of TB does not form granulomas that possess all of these features (Rhoades et al., 1997; Tsai et al., 2006), although

some susceptible mouse strains, rabbits, guinea pigs and NHPs more closely resemble human granulomas (Apt and Kramnik, 2009; Flynn, 2006).

1.3.2.1 Heterogeneity in granuloma structure

Use of imaging tools such as Computer Tomography (CT) and Positron Emission Tomography (PET) has allowed visualisation of granuloma in the NHP model and human patients (Barry et al., 2009; Lin et al., 2014). Such studies have underlined the considerable heterogeneity within lesions from a single animal or patient and have demonstrated that not all lesions are necrotic (like that shown in **Figure 1.2**) (Barry et al., 2009; Lin et al., 2014). Some granulomas that are non-necrotizing and contain mainly macrophages are most commonly found in patients with active TB, and others are fibrotic, composed mainly of fibroblasts (Barry et al., 2009). Considerable overlap in the structure of lesions in latent and active patients and NHP has been observed (Gideon and Flynn, 2011; Lin et al., 2009).

1.3.2.3 Function of granuloma

The function of the granuloma is classically regarded to be a site for control of mycobacterial growth, which contains bacteria and prevents dissemination (Flynn et al., 2011). However, more recently it has been proposed to provide a niche for bacterial replication and aid dissemination. In the zebrafish model of *M. marinum* infection, macrophages were shown to be recruited to nascent granulomas where they became infected and provided a niche for bacterial growth and promoted dissemination (Davis and Ramakrishnan, 2009; Ramakrishnan, 2012).

Studies using the NHP model have shown that granulomas have distinct outcomes. Some reached sterilization whilst others were permissive to continued bacterial growth (Lin et al., 2014). This data suggests that the function of the granuloma cannot be labelled as either protective or permissive, but that the environment at the level of individual granulomas dictates this function. *In silico* modelling has suggested that the balance between pro- and anti-

inflammatory cytokines is important in determining the outcome of granulomas (Cilfone et al., 2015). In addition, assessment of the T cell responses in individual granulomas from NHPs has shown that there is inverse correlation between T cells producing pro-inflammatory cytokine (such as TNFα, IL-17 or IFNγ) and the bacterial load within the granuloma (Gideon et al., 2015). Thus, although granulomas can form a permissive niche for bacterial growth, data also suggests that they can eliminate bacteria indicating that they can be protective or contribute to pathology.

1.3.3 Multifaceted Role of Neutrophils in Mtb infection

Neutrophils are short-lived phagocytes that possess several killing mechanisms to combat infection such as the generation of reactive oxygen species (ROS), production of enzymes including lysozyme and proteases, production of antimicrobial peptides and molecules that sequester iron (Dallenga et al., 2015). The role of neutrophils during *Mtb* infection has been controversial with conflicting reports implicating them in protection through *Mtb* killing or pathogenesis through excessive inflammation (Lowe et al., 2012). These conflicting reports may reflect a dual role for neutrophils in the response to *Mtb* infection. Initially they are protective and contribute to control of infection but as inflammation and infection progresses they become detrimental facilitating pathogenesis.

1.3.3.1 Neutrophils are recruited and infected upon mycobacterial infection

Neutrophils are recruited early upon infection with several mycobacterial species (Lowe et al., 2012). In mice neutrophils are observed at the site of BCG infection as early as 4h post infection (Abadie et al., 2005). However, in contrast, in the zebrafish model of *M. marinum* infection, neutrophil recruitment was only obsevered following the death of infected macrophages within the nascent granuloma (Yang et al., 2012). Despite this finding it is thought that neutrophils are rapidly recruited to disease sites (Lowe et al., 2012). Once recruited, neutrophils are then

infected with *Mtb*. A study using a fluorescent *Mtb* strain showed that neutrophils can be infected with *Mtb* and that they were a prominent infected population following infection (Wolf et al., 2007). Furthermore in humans neutrophils were found to be the most infected phagocyte in human sputum (Eum et al., 2010).

1.3.3.2 Neutrophils can be protective in Mtb infection

A protective role for neutrophils in mycobacterial infection has been reported. Several studies show that neutrophil depletion prior to, or early in infection is detrimental to the outcome of *Mtb* infection (Lowe et al., 2012). Similarly LPS treatment in order to recruit neutrophils of rats prior to *Mtb* infection led to lower bacterial loads later in infection (Sugawara et al., 2004). In the zebrafish model of *M. marinum* neutrophils were found be important in the early control of infection and granuloma formation, as defects in their recruitment (through mutation in the chemokine receptor CXCR4) led to impaired granuloma formation and higher bacterial loads (Yang et al., 2012). In the same study a subset of neutrophils were also found to be capable of killing bacteria in a ROS dependent manner (Yang et al., 2012). Although neutrophils possess several mechanisms by which they could kill *Mtb*, whether restriction of mycobacterial growth by neutrophils takes place *in vivo,* in humans and in the mouse model, is unclear (Lowe et al., 2012).

Neutrophils are also suggested to benefit the immune response to *Mtb* infection through influencing the priming of an adaptive immune response (Blomgran et al., 2012; Blomgran and Ernst, 2011). Depletion of neutrophils at 9 days post infection increased the frequency of infected DCs, however, a decrease in DC trafficking to the draining lymph node and the initiation of an adaptive response was simultaneously observed (Blomgran and Ernst, 2011). This study suggested that phagocytosis of infected neutrophils is important in facilitating trafficking of DCs to the draining lymph node and initiating the adaptive immune response (Blomgran and Ernst, 2011). In this context DCs were suggested to acquire bacteria at least

partly from apoptotic neutrophils (Blomgran et al., 2012). Indeed augmenting apoptosis using a mutant *Mtb* strain accelerated the T cell response in a neutrophil dependent manner (Blomgran et al., 2012).

1.3.3.3 Accumulation of neutrophils is detrimental to the outcome of Mtb infection

Although protective roles for neutrophils have been described, increased neutrophil numbers have been found to correlate with poor outcome. Increased bacterial loads and delayed clearance of bacteria from sputum in human TB patients has been observed (Lowe et al., 2013; Martineau et al., 2011). Furthermore, the level of neutrophilia in the blood in HIV positive patients correlates with bacterial load in the sputum (Kerkhoff et al., 2013). Increased number of neutrophils expressing Granzyme B in NHP and human granulomas also correlated with increased bacterial load (Mattila et al., 2015). This data correlating increased numbers of neutrophils with higher bacterial loads and poor outcome of infection, and a report correlating a neutrophil driven signature with severity of disease (Berry et al., 2010), is suggestive of a negative role for neutrophils in *Mtb* infection.

In various mouse studies increased susceptibility to infection has been correlated with increased neutrophil influx. Increased recruitment of granulocytes has been observed in the susceptible DBA, C3H/FeBJ and I/St mice and suggested to contribute to susceptibility (Eruslanov et al., 2005; Keller et al., 2006; Marzo et al., 2014). In the I/St mice neutrophils were suggested to harbour large amounts of bacteria and provide a permissible environment for bacterial replication (Eruslanov et al., 2005). In addition, the increased susceptibility of mice deficient for Caspase Recruitment Domain-Containing Protein 9 (CARD9) or the micro-RNA mir-223 correlated with increased neutrophilia leading to excessive inflammation (Dorhoi et al., 2010; Dorhoi et al., 2013). IFNγ signalling has been described to negatively regulate neutrophil accumulation and survival (Desvignes et al., 2012; Nandi and Behar, 2011). Thus neutrophilia during infection may represent a response with inadequate IFNγ production.

One way in which neutrophils are suggested to play a detrimental role in *Mtb* infection is through production of immunosuppressive cytokines. Indeed, neutrophils have been identified as a source of the immunosuppressive cytokine IL-10 upon infection (Dorhoi et al., 2010; Dorhoi et al., 2013; Zhang et al., 2009). Neutrophil depletion in BALB/c mice infected with *Mtb* led to lower bacterial loads at 6 weeks following infection with a lower level of IL-10 accompanied by an increase in TNFα production (Zhang et al., 2009).

The precise role of neutrophils in *Mtb* infection is unclear and will require further investigation. Although they possess the potential to kill mycobacteria, in some circumstances it appears they contribute to immunopathology. These opposing roles for neutrophils in *Mtb* infection could potentially be explained by timing. Early in infection neutrophils are protective, killing bacteria and influencing priming of an adaptive response. As infection progresses neutrophils contribute to immunopathology, with the development of neutrophilia signifying a pathogenic immune response.

1.4 Protective factors in the immune response to *Mtb*

The immune response to *Mtb* encompasses factors that contribute to protection and factors that could contribute to pathology and maintenance of infection. The precise nature of a protective response to *Mtb* infection is not clearly understood. It is likely that a finely balanced immune response is required for protection, where the level of inflammation is adequate to combat infection but avoid host pathology (Orme et al., 2015). However, some aspects of the protective immune response to *Mtb* are known and will be discussed below. Key factors identified in experimental models and the resultant increase in susceptibility are shown in **Figure 1.3**.

1.4.1 Innate immune factors involved in the protective response to Mtb infection

1.4.1.1 Recognition of Mtb through Pattern Recognition Receptors

Pattern Recognition Receptors (PRRs) are germline encoded receptors that recognise conserved molecules expressed by pathogens termed Pathogen Associated Molecular Patterns (PAMPs). Recognition of PAMPs by PRRs can facilitate phagocytosis of the pathogen by the innate cell as well as induction of an inflammatory response (Medzhitov and Janeway, 2000). There are several classes of PRR including Toll-Like Receptors (TLRs), C-type Lectin Receptors (CLRs), NOD-Like Receptors (NLRs) and RIG-Like Receptors (Takeuchi and Akira, 2010). Several classes of PRR have been implicated in the response to mycobacteria and will be discussed below. The activation of PRRs in response to mycobacteria is thought to shape the adaptive immune response and contribute to the regulation of inflammation. Upon infection it is likely that many PRRs work in concert to initiate and shape the immune response, perhaps explaining why in some cases deficiency in single PRRs does not impact the outcome of infection, despite their ability to recognise *Mtb*.

1.4.1.1.1. NOD2

NOD2 is part of the NOD-Like Receptor (NLR) family of PRRs and is a cytoplasmic receptor. In mice a role for NOD2 is suggested through study of *Nod2* deficient mice, although its precise importance in the immune response to *Mtb* is unclear. At early time points following *Mtb* infection *Nod2* deficiency did not impact bacterial load, however, at later time points *Nod2* deficiency resulted in increased bacterial load and impaired survival (Divangahi et al., 2008). In contrast, a second study demonstrated that *Nod2* deficiency did not impact susceptibility to *Mtb* infection although a late time point was not assessed (Gandotra et al., 2007). However, *in vitro* macrophages from *Nod2* deficient mice displayed impaired production of nitric oxide (NO) and proinflammatory cytokines (Gandotra et al., 2007). The role of NLRP3, an inflammasome forming NLR, will be discussed below.

1.4.1.1.2 CLRs and CARD9

CARD9 is an adaptor molecule required for the downstream signalling of several classes of PRRs including CLRs. CARD9 deficient mice display increased susceptibility to *Mtb* infection with enhanced recruitment of neutrophils and higher levels of proinflammatory cytokines in both the lung and serum (Dorhoi et al., 2010). Neutrophils deficient in CARD9 were also observed to be incapable of producing IL-10 in response to *Mtb* infection, suggesting CARD9 has a role in regulating inflammation in response to *Mtb* infection (Dorhoi et al., 2010). In addition, another study showed that IL-10 production by neutrophils in response to BCG was dependent upon MyD88 and Syk signalling downstream of CLRs (Zhang et al., 2009).

Dectin-1 is a CLR that signals via the molecules Syk and CARD9. Dectin-1 has been demonstrated to recognise mycobacteria and was found to induce IL-12p40 expression in mouse splenic DCs (Rothfuchs et al., 2007). Dectin-1 is also suggested to be important in the induction of an IL-17 response to *Mtb* (van de Veerdonk et al., 2010; Zenaro et al., 2009). However, no impact on susceptibility to *Mtb* infection was reported in *CLEC7A* (the gene encoding dectin-1)

deficient mice (Marakalala et al., 2011). More recently a role Dectin-2 in *Mtb* infection has been suggested (Yonekawa et al., 2014). *Clec4n* (the gene encoding dectin-2) deficient dendritic cells produced lower levels of pro and anti-inflammatory cytokines in response to BCG and exhibited higher bacterial loads and lung pathology upon infection with *M. avium* complex (MAC), however, dectin-2 deficiency in virulent *Mtb* infection was not assessed (Yonekawa et al., 2014)

Another CLR that is implicated in the recognition and initiation of the response to mycobacteria is Macrophage-Inducible C-type Lectin (Mincle), which also signals via Syk and CARD9 (Philips and Ernst, 2012). Mincle expression was observed to be upregulated upon intra-tracheal BCG infection and *Mincle* deficient mice displayed higher bacterial loads in the draining lymph node and spleen throughout infection (Behler et al., 2012). Furthermore, following intravenous infection with BCG *Mincle* knockout mice displayed higher bacterial loads in the spleen and liver with reduced granuloma formation and lower TNFα and IFNγ levels in the spleen (Behler et al., 2015). In contrast, in another study *Mincle* deficient mice did not show enhanced susceptibility to *Mtb* infection, nor a defect in granuloma formation following either low or high dose aerosol infections with *Mtb* (Heitmann et al., 2013). Thus the precise importance of Mincle in the recognition of *Mtb*, and its role in *Mtb* infection remains unclear.

DC-SIGN is primarily expressed on human DCs and has been demonstrated to bind to *Mtb* (Geijtenbeek and van Kooyk, 2003; Philips and Ernst, 2012). Recognition of *Mtb* via DC-SIGN was required for optimal IL-10, IL-12p35, IL-12p40 and IL-6 mRNA expression, although this was not evident at the protein level (Gringhuis et al., 2009). Genetic susceptibility studies provide conflicting data surrounding the association of polymorphisms in DC-SIGN with susceptibility to tuberculosis (Philips and Ernst, 2012). Elucidating the precise role for DC-SIGN in the response to *Mtb* infection is hindered by the absence of a mouse ortholog (Philips and Ernst, 2012).

1.4.1.1.4 TLRs and MyD88

TLRs contain a cytoplasmic domain that is shared with IL-1 and IL-18 receptors called the Toll/IL-1R domain (TIR). MyD88 is an adaptor molecule recruited to the TIR domain which is required for the subsequent signalling cascade of TIR containing molecules including all TLRs except TLR3 (Akira and Takeda, 2004). MyD88 is also involved in the signalling downstream of the IL-1 Receptor (IL-1R) and the IL-18 Receptor (IL-18R) (Akira and Takeda, 2004). Mice deficient in MyD88 have been reported to display considerable increased susceptibility to *Mtb* infection, with higher bacterial loads and decreased survival (Bafica et al., 2005a; Fremond et al., 2004; Mayer-Barber et al., 2010; Scanga et al., 2004).

It was originally suggested that the susceptible phenotype displayed by the MyD88 deficient mice was solely due to loss of TLR signalling downstream of one or multiple TLRs. However, much conflicting data exists detailing the precise role of TLRs in susceptibility to *Mtb* infection. TLR2, TLR4 and TLR9 have been suggested to play a role in the recognition and response to *Mtb*. C3H/HeJ mice have a missense mutation in TLR4 and were shown to display increased susceptibility to low dose aerosol *Mtb* infection (Abel et al., 2002). In contrast, another study found no increase in bacterial load in low or high dose *Mtb* infection in the TLR4 mutant C3H/HeJ mice (Reiling et al., 2002). A further study suggested a protective role for TLR4 only in the immune response to infection with a more virulent *Mtb* strain of the Beijing lineage not with the lab-adapted strain H37Rv (Carmona et al., 2013). Mice deficient in TLR2 are suggested to show increased susceptibility to low and high dose *Mtb* infection (Drennan et al., 2004), although others have demonstrated a role for TLR2 only in high dose infection (Reiling et al., 2002). However, *in vitro*, TLR2 has been reported to be required for the induction of pro-inflammatory cytokines by macrophages in response to several *Mtb* strains (Carmona et al., 2013). Mice deficient in TLR9 showed increased susceptibility to *Mtb*, which is most marked with high dose infection (Bafica et al., 2005a). Mice deficient for both TLR2 and TLR9 also display increased susceptibility to *Mtb* infection (Bafica et al., 2005a), but the phenotype displayed is milder than in MyD88 deficient mice (Mayer-Barber et al., 2010). In contrast, mice

triply deficient for TLR2/4/9 did not show enhanced susceptibility to aerosol *Mtb* infection, unlike those deficient for MyD88 (Holscher et al., 2008). Although MyD88 is required for signalling downstream of TLRs, mice deficient in single or multiple TLRs do not display the increased susceptibility seen in MyD88 deficient mice.

1.4.1.2 IL-1 and the Inflammasome

As none of the TLR deficient mice discussed above displayed a consistent phenotype that mirrored the severe MyD88 deficient phenotype, a role for IL-1 in protection against *Mtb* was proposed, as IL-1 also signals via MyD88. IL-1R1 deficient mice (Sugawara et al., 2001), or those doubly deficient in IL-1α/IL-1β (Yamada et al., 2000), displayed increased susceptibility to *Mtb* infection. This increase in susceptibility of the IL-1R1 deficient mouse was similar to that observed in MyD88 deficient mice (Fremond et al., 2007). Further support for the importance of IL-1 was provided by a study that showed that the phenotype of the MyD88 deficient mouse was similar to that seen in the IL-1β deficient, IL-1R deficient or TRIF/MyD88 deficient mice (Mayer-Barber et al., 2010). Mice deficient in IL-18 were more susceptible to *Mtb* infection than wild type mice but displayed a milder phenotype in comparison to MyD88 deficient mice (Mayer-Barber et al., 2010). Subsequently, IL-1α and IL-1β were shown to have independent roles in defence to *Mtb* infection (Mayer-Barber et al., 2011). Recently IL-1 was seen to induce PGE_2 in both human and mouse macrophages and this was suggested to contribute to the protective effect of IL-1 during *Mtb* infection (Mayer-Barber et al., 2014). Furthermore, administration of exogenous IL-1 to *Mtb* infected mouse bone marrow derived macrophages reduced production of type I IFNs, which are detrimental to control of *Mtb* infection (discussed in more detail later) and led to lower bacterial loads (Mayer-Barber et al., 2014).

IL-1β is processed to its active form by the inflammasome, a complex comprising a PRR of the NLR family, the CARD domain-containing molecule ASC, and caspase-1 (Lamkanfi, 2011).

Although the role of IL-1 in *Mtb* infection is established, the role for the inflammasome remains unclear. *In vitro* infection of macrophages or macrophage cell lines or DCs with *Mtb* showed IL-1β production to largely depend upon the NLRP3 inflammasome (Abdalla et al., 2012; Dorhoi et al., 2012; Mayer-Barber et al., 2010; Mishra et al., 2010). However, *in vivo,* mice deficient in components of the inflammasome did not show defects in IL-1β production (Dorhoi et al., 2012; Mayer-Barber et al., 2010). Mice lacking NLRP3 were not more susceptible to *Mtb* infection but those lacking caspase-1 or ASC did display increased susceptibility to *Mtb* infection (Dorhoi et al., 2012; Mayer-Barber et al., 2010). Therefore the precise role of the inflammasome and its importance in mediating IL-1 production *in vivo* remains unclear.

1.4.1.3 Eicosanoids

Eicosanoids are lipid mediators derived from arachidonic acid (AA). AA can be metabolised by Cyclo-oxygenase 1 or 2 (COX1/COX2) or 5-lipoxgenase to produce a variety of lipid mediators including prostaglandins, lipoxins and leukotrienes. The balance of various lipid mediators produced from AA has been found to be important in mediating the outcome of *Mtb* infection (Mayer-Barber and Sher, 2015).

Cell death of infected cells by necrosis or apoptosis is important in determining the outcome of infection (Behar et al., 2011). Cell death by necrosis is beneficial to *Mtb*, allowing release of the bacilli from the infected cells, evasion of host defences and spread to other cells, whereas apoptosis promotes control of bacterial replication (Behar et al., 2011). PGE_2 has been found to be beneficial to the outcome of *Mtb* infection through protecting against necrotic cell death by protecting the integrity of the plasma membranes (Chen et al., 2008; Divangahi et al., 2009). In keeping with a protective role for PGE_2, *pges* knock mice (lacking the enzyme required for PGE_2 production) displayed increased susceptibility to *Mtb* infection (Chen et al., 2008; Divangahi et al., 2009). However, the production of PGE_2 is inhibited by LipoxinA4 (LXA_4), which promotes necrotic cell death and is produced at higher levels upon infection with virulent

Mtb strains (Chen et al., 2008; Divangahi et al., 2009). Mice lacking *Alox5*, the enzyme required for production of LXA_4, showed increased resistance to *Mtb* infection *in vivo* (Bafica et al., 2005b; Divangahi et al., 2009). Inhibition of apoptosis by LXA_4 also impacts the adaptive response through the prevention of cross presentation of *Mtb* antigens, and in keeping with this deficiency in *Alox5* led to earlier and increased $CD4^+$ and $CD8^+$ T cell responses (Divangahi et al., 2010).

Further support for a detrimental role of LXA_4 during mycobacterial infection is provided by study of the zebrafish. In zebrafish, a mutation in the *lta4h* locus (encoding leukotriene A4 hydrolase, which converts Leukotriene A_4 to Leukotriene B_4 (LTB_4)) led to susceptibility to *M. marinum* infection, through increased LXA_4 production accompanied by decreased LTB_4 and TNFα production (Tobin et al., 2010). This was supported by observations in humans, where polymorphisms in the *lta4h* locus correlated with susceptibility to *Mtb* infection (Tobin et al., 2010). However, modulation of the *lta4h* locus in zebrafish underlined the importance of the balance in the immune response in mycobacterial infection. Genotypes that led to high LXA_4 production were accompanied by low LTB_4 and low TNFα production with increased susceptibility to infection (Tobin et al., 2012). However, genotypes that led to low LXA_4 were accompanied by high LTB_4 and excess TNFα and also led to host susceptibility, suggesting there is an optimal level of LXA_4 to control infection (Tobin et al., 2012). This idea of balance in the level of production of LXA_4 was supported in human patients with tuberculous meningitis. Patients with genotypes at the *lta4h* locus that led to either the high or low extreme inflammatory phenotypes had poorer survival (Tobin et al., 2012).

1.4.1.4 Innate lymphocytes - NK cells, NKT cells, γδ T cells and MAIT cells

The ability of innate lymphocytes such as Natural Killer (NK) cells, Natural Killer T cells (NKT) and γδ T cells to respond rapidly to infection makes it attractive to think they may play a role in the early events following *Mtb* infection (Orme et al., 2015). Furthermore it has been

suggested such innate lymphocytes could contribute to immunity in individuals thought to have cleared *Mtb* infection without mounting an adaptive response (Young et al., 2009). However, the role of these innate lymphocytes in response to *Mtb* infection remains unclear.

γδ T cells are activated in response to *Mtb* infection and are a main source of IL-17 (Lockhart et al., 2006; Okamoto Yoshida et al., 2010). Deficiency in γδ T cells increased susceptibility to intravenous infection with *Mtb* with increased bacterial loads and decreased survival (Ladel et al., 1995). In contrast deficiency in γδ T cells did not impact control of bacterial load or survival in response to aerosol infection but did lead to increased inflammation (D'Souza et al., 1997). Thus the role of γδ T cells in the response to *Mtb* is uncertain, although it appears they can contribute to optimal control of inflammation (D'Souza et al., 1997).

NKT cells are able to recognise antigens presented in the context of CD1. Mice deficient in CD1 did not show any increased susceptibility to *Mtb* infection (Behar et al., 1999). However, activation of NKT cells through administration of the ligand α-galactosylceramide was beneficial to the outcome of infection (Chackerian et al., 2002a). Furthermore NKT cells are capable of producing IFNγ or GM-CSF to restrict mycobacterial growth *in vitro* (Rothchild et al., 2014; Sada-Ovalle et al., 2008). GM-CSF producing NKT cells have been identified upon *Mtb* infection in mice, supporting the idea they may contribute to macrophage activation in vivo (Rothchild et al., 2014).

The role of NK cells in the immune response to *Mtb* is unclear. IFNγ production by NK cells has been identified during *Mtb* infection in both wild-type mice and those lacking an adaptive immune system (Feng et al., 2006; Junqueira-Kipnis et al., 2003). In mice lacking an adaptive immune system NK cell-derived IFNγ was suggested to be important to regulate accumulation of granulocytes upon *Mtb* infection (Feng et al., 2006). In the absence of IFNγ this granulocyte accumulation was found to be protective during *Mtb* infection (Feng et al., 2006). However,

when NK cells were depleted in wild-type mice there was no impact on the outcome of infection (Junqueira-Kipnis et al., 2003). During BCG infection, IL-15 treatment decreased bacterial loads and expanded NK cell populations as well as leading to increased IFNγ production by $CD8^+$ T cells (Umemura et al., 2001). This increased resistance to infection was not seen when NK cells or $CD8^+$ T cells were depleted, suggesting NK cells are capable of providing protection (Umemura et al., 2001). In addition *Il-15* deficient mice, which lack NK cells and have defects in $CD8^+$ T cell memory populations, show slightly higher bacterial loads in chronic infection and defects in cell recruitment to the lung (Lazarevic et al., 2005). Deficiency in NK cells could contribute to this phenotype although this was not directly assessed (Lazarevic et al., 2005). In humans, NK cells have been shown to have the capacity to produce cytokines in response to infected cells and lyse *Mtb* infected cells *in vitro*, although their contribution to the immune response at the site of disease is unknown (Esin and Batoni, 2015). NK cells have also been suggested to contribute to the efficacy of BCG vaccination through IL-22 production and lysis of $Foxp3^+$ Treg cells, with depletion of $NK1.1^+$ cells at the time of vaccination leading to higher bacterial loads upon *Mtb* challenge (Dhiman et al., 2012). In addition, NK cells producing IFNγ cells have been identified in the peripheral blood of BCG vaccinated infants, suggesting these cells could contribute to BCG induced immunity (Zufferey et al., 2013).

Mucosal associated invariant T (MAIT) cells have also been implicated in the immune response to *Mtb* infection (Gold et al., 2015). MAIT cells are T cells with a semi-invariant T cell receptor (TCR) that have been described to recognise vitamin B2 metabolites in the context of MR1 (Gold et al., 2015). These cells have been identified in the human airway and are capable of producing IFNγ and TNFα in response to *Mtb* infected epithelial cells (Gold et al., 2010; Gold et al., 2015). In the context of *Mtb* infection in humans, MAIT cells were found to be enriched in the lung and decreased in peripheral blood (Gold et al., 2010; Le Bourhis et al., 2010). The ability of these cells to respond rapidly and produce cytokines in response to *Mtb* infection may

indicate they could contribute to early control of *Mtb* infection (Gold et al., 2015; Orme et al., 2015).

The possibility exists that, although such innate lymphocytes appear to play minimal roles in the optimal response to *Mtb*, augmentation of their response may be beneficial to the outcome of infection.

1.4.1.5 TNFα

Various cell types can produce TNFα including macrophages, DCs as well as T cells (Flynn and Chan, 2001). The importance of TNFα in the control of *Mtb* infection has been demonstrated by the observation that treatment of patients with TNF neutralizing agents, for diseases such as Rheumatoid Arthritis, led to reactivation of latent tuberculosis (Keane et al., 2001). Earlier it had been shown in the mouse model that mice deficient in TNFα or the 55 kDa TNF receptor (TNFR), or those where TNF was neutralized during infection, all displayed increased susceptibility to *Mtb* infection (Bean et al., 1999; Flynn et al., 1995a). These mice had decreased survival, increase bacterial loads and disrupted granuloma formation (Bean et al., 1999; Flynn et al., 1995a). Furthermore, neutralisation of TNFα in low dose chronic infection led to increased bacterial loads, disorganized granulomas and decreased survival despite maintained or increased expression of IL-12p40 and IFNγ (importance of which will be discussed later) (Chakravarty et al., 2008; Mohan et al., 2001; Scanga et al., 1999).

The above studies suggested that TNFα might act through regulation of granuloma formation and maintenance. However, this concept was challenged in the NHPs where TNFα neutralisation during acute infection led to severe disseminated disease and during latent infection led to reactivation of disease, but granuloma structure was similar to controls (Lin et al., 2010). Further support that TNFα may not contribute to protection through formation of granulomas is provided by work in the zebrafish. Knockdown of the TNFα ortholog led to

accelerated granuloma formation, increased bacterial growth and increased necrotic death of infected macrophages (Clay et al., 2008). This study suggests that TNFα may act during *Mtb* infection to regulate intracellular killing of mycobacteria, given that in the absence of TNFα macrophages have increased bacterial burdens (Clay et al., 2008). The idea that TNF can regulate the ability of macrophages to restrict mycobacterial growth is supported by observations that it can synergise with IFNγ for induction of RNIs (Chan et al., 1992; Flynn and Chan, 2001).

More recently the idea that there is an optimal level of TNFα during infection has been proposed. Zebrafish with genotypes that lead to extreme levels of TNFα (either low or high) are susceptible to *M marinum* infection (Tobin et al., 2012; Tobin et al., 2010). Excessive levels of TNFα in the zebrafish have been demonstrated to lead to ROS production and macrophage necrosis, allowing unchecked extracellular growth (Roca and Ramakrishnan, 2013). Thus it seems that whilst TNFα is essential for protection, a balanced response is vital.

1.4.2 Adaptive immune factors protective in the immune response to Mtb infection

1.4.2.1 $CD4^+$ T cells

Lymphocytes are crucial for control of *Mtb* infection, with early studies in mice showing that adoptive transfer of T cells from infected donors can confer protection against *Mtb* in T cell deficient recipients (Orme and Collins, 1983). Subsequently the importance of $CD4^+$ T cells specifically in response to *Mtb* was demonstrated and is now well established in both mice and humans. Studies using CD4 deficient mice or depletion of $CD4^+$ T cells using monoclonal antibody showed that $CD4^+$ T cells were crucial for a protective response against *Mtb* (Mogues et al., 2001; Saunders et al., 2002; Scanga et al., 2000). Furthermore, MHC II deficient mice have increased susceptibility to *Mtb* (Mogues et al., 2001). A requirement for direct interaction of $CD4^+$ T cells with infected cells to control bacterial loads has been demonstrated, with MHC

II deficient myeloid cell populations in the lung harbouring more bacteria than MHC II sufficient cells (Srivastava and Ernst, 2013). In humans, the importance of $CD4^+$ T cells in control of *Mtb* infection is supported by reports that HIV positive patients are highly susceptible to *Mtb* infection and reactivation, particularly those with low $CD4^+$ T cell counts (Cooper, 2009; Schutz et al., 2010). In addition, *Mtb* specific $CD4^+$ T cells are suggested to be preferentially depleted following HIV infection, increasing susceptibility to TB (Geldmacher et al., 2012).

Different populations of $CD4^+$ T cells have been described during *Mtb* infection based on their expression of PD-1 and KLRG1, markers that correlate with an exhausted phenotype (Reiley et al., 2010). However, during *Mtb* infection PD-1^+ $CD4^+$ T cells were not exhausted, displaying proliferative capacity, but low cytokine production (Reiley et al., 2010). Upon transfer into infected mice PD-1^+ $CD4^+$ T cells were able to give rise to $KLRG1^+$ cells which displayed higher cytokine production than $PD1^+$ cells, but lower proliferative capacity (Reiley et al., 2008). Subsequently it was found that PD-1^+ $KLRG1^-$ $CD4^+$ T cells, which were dependent upon ICOS and Bcl-6, persisted when transferred into an uninfected host, and induced a robust protective response upon *Mtb* infection (Moguche et al., 2015). PD-1 has been shown to be important in inhibiting excessive $CD4^+$ T cell responses during *Mtb* infection (Barber et al., 2011). Mice lacking PD-1 were shown to display decreased survival accompanied by increased bacterial load and immunopathology (Barber et al., 2011). Like many aspects of the immune response to *Mtb* infection, this demonstrates that a balance in the T cell response is required for optimal outcome (Barber et al., 2011).

The PD-1^+ T cells described above were found to localise to the lung parenchyma (Moguche et al., 2015). Distinct populations of T cells that localise to the lung parenchyma and populations that are retained in the vasculature have been described during *Mtb* infection (Sakai et al., 2014). The localisation of T cells within the lung is described to be important in their capability to contribute to protection during *Mtb* infection, with parenchymal $CD4^+$ T cells providing

superior protection against *Mtb* when transferred into susceptible hosts compared to those isolated from the vasculature (Sakai et al., 2014).

Although it seems that different populations of $CD4^+$ T cells have different capacities to produce cytokines and localise within the lung, $CD4^+$ T cell derived cytokines are thought to be required during *Mtb* infection to stimulate anti-mycobacterial responses in innate cells (reviewed in Cooper, 2009; O'Garra et al., 2013). As discussed above, the phenotype and cytokine production displayed by activated T cells depends on the context in which $CD4^+$ T cells are activated (reviewed in Zhu et al., 2010). Th1 cells differentiate in the presence of IL-12 and produce IFNγ, Th2 cells differentiate in the presence of IL-4 and produce IL-4, IL-5 and IL-13 and Th17 cells differentiate in the presence of IL-6, TGFβ and IL-1β and produce IL-17 (Zhu et al., 2010). In the context of *Mtb* both Th1 and Th17 cells are induced and their roles will be discussed below.

1.4.2.2 Th1 axis –IFNγ, IL-12

Th1 cells express the transcription factor T-bet, produce IFNγ and differentiate in the context of APC-derived IL-12, a dimer formed of the subunits IL-12p40 and IL-12p35 12p35 (Hsieh et al., 1993; Macatonia et al., 1995; Trinchieri, 2003). IFNγ produced by Th1 cells can activate macrophage populations (via STAT1 signalling) to increase their anti-microbial capacity through mechanisms including induction of iNOS and production of RNIs, and production of ROS (North and Jung, 2004; Zhu and Paul, 2008). Th1 cells are known to be crucial for the immune response to intracellular pathogens but their inappropriate activation can also contribute to autoimmunity (Zhu and Paul, 2008).

1.4.2.2.1 Th1 axis –IFNγ, IL-12 in Mtb infection

The Th1 axis is crucial in the immune response to *Mtb* infection. Administration of exogenous IL-12 during *Mtb* infection increased survival of mice and their resistance to *Mtb* infection (Cooper et al., 1995; Flynn et al., 1995b). Treatment with exogenous IL-12 increased production of IFNγ by splenocytes (Cooper et al., 1995) and was not protective in IFNγ deficient mice, suggesting that the protective effect of IL-12 is IFNγ dependent (Flynn et al., 1995b). Furthermore neutralisation of IL-12 using antibody treatment led to increased susceptibility to *Mtb* infection (Cooper et al., 1995).

Further support for the importance of IL-12 to induce IFNγ responses during *Mtb* infection was provided using IL-12p40 deficient mice. Mice deficient in IL-12p40 displayed increased susceptibility to *Mtb* infection, with dramatically reduced levels of IFNγ production by splenocytes and defective granuloma formation (Cooper et al., 2002; Cooper et al., 1997). However, comparison of IL-12p35 and IL-12p40 (the two subunits of IL-12 discussed above) deficient mice showed that IL-12p35 deficient mice were less susceptible to *Mtb* infection and were capable of inducing an IFNγ response, albeit at a reduced level (Cooper et al., 2002). A possible explanation for this is that IL-12p40 is also a subunit for IL-23 (discussed further below). In addition, IL-12p40 homodimers have been demonstrated to be required for optimal DC trafficking and T cell activation (Khader et al., 2006). As well as being required for the induction of Th1 immunity, IL-12 is suggested to have a role in the maintenance of the Th1 response during *Mtb* infection. IL-12p40 deficient mice treated with exogenous IL-12 for the first 4 weeks of infection, displayed increased resistance to *Mtb* infection compared to no treatment, but this was lost over time and correlated with a decrease in IFNγ producing $CD4^+$ T cells in the lung (Feng et al., 2005).

That IFNγ is crucial for the control of *Mtb* infection has been demonstrated by the observation that administration of IL-12 to IFNγ deficient mice did not increase their survival, unlike IL-12

administration in wild type mice (discussed above) (Flynn et al., 1995b). The fundamental importance of IFNγ in the immune response to *Mtb* is also demonstrated in mice deficient for IFNγ, which displayed a marked increase in susceptibility to *Mtb* infection, with development of necrotic lesions and impaired induction of inducible Nitric Oxide Synthatase (iNOS) (Cooper et al., 1993; Flynn et al., 1993).

IFNγ activates macrophages, inducing programmes that can control mycobacterial growth including iNOS, an enzyme that synthesises RNIs and NADPH-oxidase which synthesises ROS (North and Jung, 2004). Various studies provide evidence that RNIs are capable of controlling *Mtb* growth (Nathan and Shiloh, 2000). Indeed, deletion of the *Nos2* gene (encoding iNOS) in mice resulted in increased susceptibility to *Mtb* infection (Cooper et al., 2000a; MacMicking et al., 1997; Scanga et al., 2001), although the role for NO in humans is less clear (reviewed in O'Garra et al., 2013). A role for NADPH-oxidase in the mouse model of *Mtb* is less clear than that for iNOS, with conflicting reports of increased bacterial loads following *Mtb* infection and no decrease in survival compared to wild-type mice (Cooper et al., 2000b; Nathan and Shiloh, 2000; North and Jung, 2004). One mechanism by which *Mtb* survives intracellularly in macrophages is through inhibition of phagosome maturation leading to a less acidic environment (Russell et al., 2010). In addition to production of RNIs and ROS, activation of macrophages with IFNγ facilitates increased acidification of the phagosome (Russell et al., 2010).

In addition to the role for IFNγ in activating macrophages, IFNγ has also been shown to have a regulatory role protecting from immunopathology. IFNγ was shown to regulate neutrophil survival and also suppress neutrophil recruitment through suppression of IL-17 production (Nandi and Behar, 2011). In addition IFNγ mediated induction of NO inhibited IL-1β production and accumulation of neutrophils (Mishra et al., 2013).

The vital role for the IL-12/ IFNγ pathway in the response to mycobacterial infection is also demonstrated in humans. Mutations in the IL-12/IFN-γ pathway lead to Mendelian Susceptibility to Mycobacterial Disease (MSMD) (Casanova, 2001; Fortin et al., 2007). Genes mutated in such patients include *IFNGR1* and *IFNGR2* (the chains of the IFNγ receptor), *IL12B* (encoding IL-12p40), *IL12RB1* (encoding one chain of the IL-12 receptor) and *STAT1* (a molecule required for IFNγ signal transduction) (Casanova, 2001). Such patients are more susceptible to infection with weakly virulent mycobacterial infection, such as BCG and nontuberculous environmental mycobacteria, as well as to *Mtb* (Casanova and Abel, 2002; Fortin et al., 2007). The most common manifestation of such genetic mutations is disease caused by BCG (following vaccination) or nontuberculous environmental mycobacteria (Casanova and Abel, 2002). However, more recently a small proportion of patients with mutations in *IL-12Rβ1*, *IL-12B* or *IFNGR1* have been identified that were resistant to BCG infection (as evidenced by lack of disease following vaccination) and presented with severe or disseminated TB in childhood or even adulthood (Altare et al., 2001; Casanova and Abel, 2002; Tabarsi et al., 2011). The frequency of such patients and the reasons they to succumb to TB disease rather than atypical mycobacteria are unknown (Casanova and Abel, 2002).

1.4.2.3 IFNγ independent T cell mediated protection

As discussed above both $CD4^+$ T cells and IFNγ are important for protection against *Mtb* infection and it is largely accepted that $CD4^+$ T cell derived IFNγ is important (reviewed in O'Garra et al., 2013). However, IFNγ is a poor correlate of protection following vaccination (Abebe, 2012; Kagina et al., 2010; Mittrucker et al., 2007), suggesting other mechanisms may exist. Several studies suggest that $CD4^+$ T cells can mediate a protective effect independently of IFNγ. Transfer of Th1 skewed cells incapable of producing IFNγ still provided protection against *Mtb* (Gallegos et al., 2011). $CD4^+$ T cells were capable of activating macrophages to control *Mtb* growth in *IFNGR* deficient macrophages, suggesting an IFNγ independent

mechanism (Cowley and Elkins, 2003). Additionally, BCG vaccinated IFNγ deficient mice showed enhanced resistance to *Mtb* challenge compared to unvaccinated IFNγ deficient mice and this resistance was $CD4^+$ dependent (Cowley and Elkins, 2003). Furthermore, depletion of $CD4^+$ T cells using a monoclonal antibody increased bacterial loads without differences in IFNγ expression or the number of iNOS positive cells, suggesting existence of IFNγ independent functions of $CD4^+$ T cells (Scanga et al., 2000). The recent observations that T cells that localise to the lung parenchyma can provide protection upon adoptive transfer but produce low levels of IFNγ also suggests IFNγ independent mechanisms of control of *Mtb* infection (Sakai et al., 2014).

1.4.2.4 IL-17 producing Th17 cells

$CD4^+$ T cells can differentiate towards a RORγt expressing Th17 phenotype when activated in the context of IL-6, TGFβ and IL-1β (reviewed in Gaffen et al., 2014). Th17 cells produce a variety of cytokines including IL-17, IL-22 and GM-CSF and are important in the immune response to infection with extracellular bacteria and fungi (reviewed in Gaffen et al., 2014; Zhu et al., 2010). Exposure of Th17 cells to IL-23 (a dimer formed of the subunits IL-12p40 and IL-23p19 (reviewed in Trinchieri, 2003) can promote a highly inflammatory phenotype, where cells contribute to chronic inflammation following infection or autoimmunity (reviewed in Gaffen et al., 2014). IL-17, the hallmark cytokine of Th17 cells, is a pro-inflammatory cytokine that induces production of anti-microbial peptides and several chemokines that drive granulocyte accumulation and can also be produced by a variety of other cell types including γδ T cells, NKT cells and ILC3s (discussed in detail below) (reviewed in Gaffen et al., 2014).

1.4.2.4.1 IL-23, Th17 cells and other sources of IL-17 during Mtb infection

In addition to IFNγ producing Th1 cells, IL-17 producing Th17 cells are also induced following mycobacterial infection (Cruz et al., 2006). In addition to Th17 cells, other cellular sources of

IL-17 during mycobacterial infection are also described including γδ T cells and non $CD4^+/CD8^+$ cells (Lockhart et al., 2006; Okamoto Yoshida et al., 2010; Umemura et al., 2007), and it is thought that γδ T cells are the major source of IL-17 upon *Mtb* infection (Lockhart et al., 2006). The role of IL-17 in primary *Mtb* infection is unclear, although it is suggested to be important in vaccination against *Mtb* (discussed in more detail below). IL-17 was proposed to play a role in granuloma formation and Th1 enhancement following BCG infection (Umemura et al., 2007); (Okamoto Yoshida et al., 2010), although IL-17 deficiency was not reported to impact control of infection (Umemura et al., 2007). In the context of *Mtb* infection, IL-17 is suggested to be required for control of hyper-virulent HN878 infection, through CXCL13 induction and localisation of T cells within the granuloma (Gopal et al., 2014). However, the same study reported that IL-17 was dispensable for protection against the lab-adapted *Mtb* strain H37Rv and a less virulent clinical isolate CDC1551 (Gopal et al., 2014). In contrast, IL-17 was required for control of bacterial loads following intra-tracheal infection with H37Rv (Okamoto Yoshida et al., 2010). In addition *IL17RA* deficient mice (mice deficient for the IL-17 receptor) show increased susceptibility to intra-tracheal H37Rv infection at chronic time points (Freches et al., 2013). Thus it seems IL-17 can contribute to protection to mycobacterial infections in some settings but the precise role of IL-17 in *Mtb* infection is unclear.

The balance between Th1 and Th17 subsets is thought to influence immunopathology upon mycobacterial infection (Cruz et al., 2006). Excessive IL-17 responses have been demonstrated to be detrimental to control of mycobacterial infection. Mice deficient in IFNγ exhibited enhanced Th17 generation, accumulation of neutrophils and immunopathology in the lung upon BCG infection (Cruz et al., 2006) and also *Mtb* infection (Nandi and Behar, 2011). Furthermore increased IL-17 contributed to the granulocyte influx and immunopathology observed in *Mtb* infected mice that were repeatedly BCG vaccinated (Cruz et al., 2010).

As mentioned above, IL-23 is a heterodimeric cytokine, composed of 2 subunits IL-12p40 and IL-23p19 and is required for inflammatory Th17 responses (Gaffen et al., 2014). IL-23p19 is suggested to be required for IL-17 production by $CD4^+$ T cells following *Mtb* infection, but IL-23p19 deficiency did not impact control of infection (Khader et al., 2005). In addition, IL-12p40 was also shown to be required for induction of IL-17 production by γδ T cells (Lockhart et al., 2006). However, another study showed that IL-17 producing $CD4^+$ T cells are induced following BCG vaccination in IL-12p40 deficient mice, which lack both IL-12 and IL-23 (Wozniak et al., 2006). Thus the importance of IL-23 for induction of IL-17 following mycobacterial infection is unclear.

In the absence of IL-12, IL-23 can compensate in the induction of Th1 responses to some extent following *Mtb* infection (Khader et al., 2005). IL-23 is required for a residual Th1 response to *Mtb* infection in mice lacking IL-12p35, a subunit of bioactive IL-12p70 (Khader et al., 2005). In addition, immunization of IL-12p40 deficient mice with a DNA vaccine encoding a mycobacterial antigen and a plasmid expressing IL-23 leads to induction of a Th1 response in the lung, again suggesting IL-23 can induce a Th1 response to mycobacterial antigens, in the absence of IL-12 (Wozniak et al., 2006).

1.4.2.5 Granulocyte – Macrophage Colony Stimulating Factor (GM-CSF)

GM-CSF (also known as Csf-2) was identified due to its ability to induce proliferation and differentiation of both macrophage and granulocyte populations from precursors (Burgess and Metcalf, 1980). Given its ability to induce differentiation of myeloid populations, it was surprising when it was found that mice deficient for GM-CSF had no obvious defects in myeloid cell numbers in peripheral blood in the steady state (Dranoff and Mulligan, 1994; Stanley et al., 1994). It was suggested that other cytokines could compensate for the lack of GM-CSF resulting in normal myeloid cell development (Dranoff and Mulligan, 1994). However, more recently GM-CSF has been found to be required for development of alveolar

macrophages through induction of PPARγ in precursors (Guilliams et al., 2013; Schneider et al., 2014) and mice deficient for GM-CSF show deficiency in alveolar macrophage populations (Becher et al., 2014; Guilliams et al., 2013). Furthermore, GM-CSF is suggested to be required for the development of non-lymphoid $CD103^+$ DC subsets, although there are opposing reports concerning this (Bogunovic et al., 2009; Hamilton, 2015; King et al., 2010). GM-CSF deficiency has also been shown to impact the function of NKT cells (Bezbradica et al., 2006). Thus, although not as dramatic as originally expected given the capability of GM-CSF to differentiate bone marrow precursors, GM-CSF deficient mice do have perturbations in myeloid populations as well as NKT cells.

GM-CSF is vital for lung homeostasis (Trapnell and Whitsett, 2002). Mice deficient in GM-CSF or the βc subunit of the GM-CSF receptor (also shared with IL-3 and IL-5) develop lung pathology that resembles the human disease Pulmonary Alveolar Proteinosis (PAP) (Dranoff et al., 1994; Nishinakamura et al., 1996; Stanley et al., 1994). This results from altered surfactant catabolism by alveolar macrophages (Dranoff 1994). PAP is a disease characterised by accumulation of surfactant and proteins within the alveolar space, which leads to progressive dyspnoea and impaired gas exchange (Trapnell and Whitsett, 2002). In humans causes of PAP can be genetic or acquired. Acquired causes are more common; accounting for more than 90% of cases (Seymour and Presneill, 2002). The majority of patients with an acquired cause of PAP have autoantibodies against GM-CSF (Seymour and Presneill, 2002). Patients with mutations in CSF2RA or CSF2RB, the two subunits of the GM-CSF receptor, or in surfactant protein B or C or the transporter ABCA3 account for genetic causes of PAP (Whitsett et al., 2015). Patients with PAP have increased susceptibility to various infections, with reports of infection with *Nocardia, Pneumocystis, Acinetobacter, Aspergillus, Cladosporium, Mtb* and other atypical mycobacteria (Borie et al., 2011; Seymour and Presneill, 2002).

In addition to a role in myeloid development, GM-CSF has pro-inflammatory roles in activation of myeloid populations. GM-CSF pre-treatment of bone marrow macrophages differentiated with Macrophage Colony Stimulating Factor (M-CSF) increased their production of pro-inflammatory cytokines upon LPS stimulation (Fleetwood et al., 2007). Furthermore, GM-CSF increased the capacity of both $CD8^+$ and CD8- DCs to present antigen and induced upregulation of costimulatory molecules (Min et al., 2010; Zhan et al., 2012). Further support for a pro-inflammatory role of GM-CSF is provided by the observation that GM-CSF is crucial for the induction of experimental autoimmune encephalitis (Codarri et al., 2011; El-Behi et al., 2011), and also for the development of disease in a collagen induced model of arthritis (Campbell et al., 1998; Hamilton, 2008).

1.4.2.5.1 GM-CSF in Mtb infection

Mice deficient in GM-CSF showed enhanced susceptibility to aerosol infection with both Erdman (Gonzalez-Juarrero et al., 2005) and H37Rv lab-adapted strains of *Mtb* and BCG (Szeliga et al., 2008). Deficiency in GM-CSF impaired granuloma formation in response to *Mtb*, ultimately leading to large necrotic lesions (Gonzalez-Juarrero et al., 2005; Szeliga et al., 2008). Furthermore, a decrease in recruitment of IFNγ producing $CD4^+$ T cells to the lung was observed in mice lacking GM-CSF upon *Mtb* infection (Gonzalez-Juarrero et al., 2005). However, these studies are difficult to interpret owing to the developmental defects in alveolar macrophage populations and the resultant lung pathology.

A role for GM-CSF in activation of APCs and subsequent priming of the adaptive immune response is supported the observation that a BCG strain expressing GM-CSF, increased the number of antigen presenting cells in the lymph nodes and their expression of costimulatory molecules (Nambiar et al., 2010; Ryan et al., 2007). Vaccination with BCG expressing GM-CSF also increased the number of IFNγ producing $CD4^+$ T cells in the lymph node following

vaccination and lowered bacterial loads systemically upon *Mtb* challenge, compared to vaccination with the parental BCG strain (Nambiar et al., 2010; Ryan et al., 2007).

A direct anti-mycobacterial role for GM-CSF is suggested by the ability of iNKT-derived GM-CSF to restrict *Mtb* growth in mouse bone marrow derived macrophages *in vitro* (Rothchild et al., 2014). Furthermore treatment of *Mtb* infected mice with Keratinocyte Growth Factor (KGF), either throughout infection or after infection is established, is suggested to induce GM-CSF production and lead to restriction of bacterial growth (Pasula et al., 2015). The proposed mechanism for this was through enhancing phagolysosome fusion in macrophages (Pasula et al., 2015). In human macrophages GM-CSF has also been described to restrict growth of *Mtb* (Denis and Ghadirian, 1990), *M. avium* complex (Bermudez and Young, 1990) and *M. avium* (Denis, 1991).

Higher and sustained levels of GM-CSF in the lung over infection in IL-10 knock-out mice correlates with increased resistance to *Mtb* infection, suggesting a protective role for GM-CSF in *Mtb* infection (Redford et al., 2010). However, the balance of GM-CSF levels is important as mice engineered to overexpress GM-CSF in the lung also demonstrate enhanced susceptibility to *Mtb* infection (Gonzalez-Juarrero et al., 2005; Szeliga et al., 2008).

1.4.2.6 $CD8^+$ T cells

A role for $CD8^+$ T cells during *Mtb* infection was suggested from studies where β2m, a component of MHC class I (MHC I) was deleted. These mice displayed increased susceptibility to *Mtb* infection and succumbed to disease faster than controls (Flynn et al., 1992); (Mogues et al., 2001). MHC I is required to present antigen to $CD8^+$ T cells thus it was inferred the increased susceptibility to *Mtb* infection in β2m deficient mice was due deficiency in $CD8^+$ T cells (Behar, 2013). However, other β2m associated proteins exist including non-classical class I molecules such as CD1 and HFE, which complicates the interpretation of the above studies.

HFE is an MHC class I-like molecule with an important role in iron homeostasis (Schaible et al., 2002). β2m deficient mice suffer from iron overload, normalisation of which recuses their increased susceptibility to *Mtb* infection, suggesting that the susceptibility of β2m deficient mice is not solely due to defects in $CD8^+$ T cell responses (Schaible et al., 2002).

A role for $CD8^+$ T cells during *Mtb* was subsequently supported by the study of mice deficient in Transporter Associated with Antigen Processing (TAP). Antigen presentation via MHC class I requires translocation of antigens into the endoplasmic reticulum via the protein TAP (Behar, 2013). TAP deficient mice displayed increased susceptibility to *Mtb* with reduced survival and increased bacterial loads, suggesting $CD8^+$ T cells have a protective role in *Mtb* infection (Behar et al., 1999). Furthermore, depletion of $CD8^+$ cells using a monoclonal antibody increases susceptibility of mice to *Mtb* infection (Mogues et al., 2001).

$CD8^+$ T cells could contribute to protective immunity in *Mtb* infection through cytokine production or lysis of infected cells (Behar, 2013). *In vitro*, *Mtb* specific $CD8^+$ T cells from mice and humans have been demonstrated to lyse infected cells (Behar, 2013). In the mouse, *Mtb* specific $CD8^+$ T cells are recruited to the lung upon *Mtb* infection (Kamath et al., 2004) and require perforin to lyse target cells and provide protection upon adoptive transfer (Woodworth et al., 2008). Cytotoxic activity has also been detected in $CD8^+$ T cells specific for other *Mtb* antigens (Woodworth et al., 2008). IFNγ production by $CD8^+$ T cells has been described, although the relative importance of this is unclear (Behar, 2013). IFNγ production by $CD8^+$ T cells depends on the presence of $CD4^+$ T cells and thus in $CD4^+$ T cell deficient models, the contribution of $CD8^+$ T cells to protective immunity may be underestimated (Bold and Ernst, 2012).

Augmenting $CD8^+$ T cell mediated immunity is thought to be an avenue by which vaccination against *Mtb* can be improved. For example, boosting BCG vaccination using an adenovirus encoding antigen 85A from *Mtb* has shown that increased $CD8^+$ T cell responses correlated with increased protection to subsequent *Mtb* infection (Forbes et al., 2008). Furthermore, the vaccine candidate VPM1002 (discussed in further detail below) is suggested to increase cross-presentation, thus augmenting $CD8^+$ T cell immunity and provide increased protection against *Mtb* challenge (Grode et al., 2005).

1.4.2.7 B cells

Although the protective immune response to *Mtb* is classically regarded not to be antibody dependent, more recently a role for B cells in the immune response to *Mtb* has begun to be appreciated (Kozakiewicz et al., 2013; Maglione and Chan, 2009). Aggregates of B cells are described at the periphery of granulomas in mouse models, NHP models of *Mtb* infection and human TB patients (Gonzalez-Juarrero et al., 2001; Phuah et al., 2012; Ulrichs et al., 2004). However, reports of the impact of B cell deficiency on the outcome *Mtb* infection have been variable. For example, one study showed B cell deficiency did not impact early control of CDC1551 (a clinical isolate of *Mtb*) bacterial load in the lung but delayed inflammation in the lung and dissemination (Bosio et al., 2000). In contrast another study showed B cell deficient mice infected with the *Mtb* strain Erdman, displayed decreased survival accompanied by increased bacterial load, IL-10 levels and neutrophil infiltration upon *Mtb* infection (Maglione et al., 2007). B cells could impact the immune response to *Mtb* in multiple ways, for example, through antibody dependent mechanisms or through antigen presentation and cytokine production (Kozakiewicz et al., 2013; Maglione and Chan, 2009). A role for antibodies has been suggested by use of mice deficient in antibody receptors. Mice deficient in the inhibitory receptor FcγRII were more resistant to *Mtb* infection, whereas those deficient in activating receptors were more susceptible (Maglione et al., 2008). The precise role for B cells in the

immune response to *Mtb* is currently incompletely understood. Better understanding of their role could aid development of novel vaccine regimes that harness the B cell response.

Overall there are many aspects of the immune response that contribute to protective immunity to *Mtb* infection. However, it is becoming clearer that a balanced response is required, as situations where there is too little or too much inflammation both lead to poor outcomes following infection (Orme et al., 2015). Increasing our understanding of a protective response will aid the design of novel vaccine regimes.

1.5 Factors detrimental to control of *Mtb* infection

1.5.1 IL-10, a suppressive cytokine

IL-10 is an immunosuppressive cytokine first identified in 1989 (Fiorentino et al., 1989). Although it was initially found to be produced by Th2 cells (Fiorentino et al., 1989), IL-10 is produced by many cell types from both the innate and adaptive arms of the immune system including macrophages, dendritic cells, other T cell subsets and B cells (Moore et al., 2001). IL-10 signals via STAT3 and primarily acts on macrophages and dendritic cells which express the highest level of the IL-10 Receptor (IL-10R) (Murray, 2006). IL-10 inhibits production of pro-inflammatory cytokines such as IL-12, suppresses antigen presentation and suppresses DC migration to the draining lymph node and thus supresses a subsequent adaptive immune response (Demangel et al., 2002; Moore et al., 2001; Redford et al., 2011). IL-10 can act directly on certain T cell subsets such as Th17 cells, where it suppresses their function (Huber et al., 2011) or on $Foxp3^+$ Tregs to maintain their regulatory phenotype (Chaudhry et al., 2011; Murai et al., 2009).

Although IL-10 is largely suppressive, it can also have stimulatory effects on B cells, increasing humoral responses (Moore et al., 2001). It can also increase $CD8^+$ T cell and NK cell responses in some conditions (reviewed in O'Garra et al., 2008). These stimulatory properties of IL-10 could be important in survival of some cancers and are thought to contribute to the pathogenesis of the autoimmune disease Systemic Lupus Erythematosus (reviewed in Moore et al., 2001; O'Garra et al., 2008).

1.5.2 Role of IL-10 in infectious diseases

A successful immune response is one that clears the invading pathogen but does not lead to immunopathology in the host (**Figure 1.4**). A delicate balance is required to achieve this perfect

scenario, allowing sufficient inflammation to control infection without this becoming excessive and detrimental to the host. In the response to many pathogens such a scenario is not achieved. IL-10 plays an important role in mediating the delicate balance of the immune response following infection, being able to constrain the immune response, avoiding pathology. However, the levels of IL-10 produced are sometimes inappropriate with high levels of IL-10 promoting chronic infection and low levels of IL-10 allowing an excessive immune response and host pathology.

Studies using mice deficient for IL-10 have identified several infections where IL-10 is required to control the excessive inflammation and pathology. Such pathogens include *Toxoplasma gondii* (Gazzinelli et al., 1996), *Plasmodium chabaudi chabaudi* (Li et al., 1999), *Trypanosoma cruzi* (Hunter et al., 1997), and Respiratory Syncytial Virus (RSV) (Loebbermann et al., 2012), where an absence of IL-10 during infection leads to death and pathology without affecting pathogen load. Interestingly the source of IL-10 in *T. gondii* and *P. chabaudi chabaudi* infection was found to be Th1 cells (do Rosario et al., 2012; Jankovic et al., 2007). This was also largely found to be the case during RSV infection (Loebbermann et al., 2012). This suggests that IL-10 is a mechanism by which Th1 cells self-regulate.

In contrast, infection of *Il10* deficient mice or treatment with an IL-10 receptor blocking antibody with some pathogens can enhance their clearance, without increased pathology. These pathogens include *Listeria monocytogenes* (Dai et al., 1997; Silva and Appelberg, 2001), lymphocytic choriomeningitis virus (LCMV) (Brooks et al., 2006; Ejrnaes et al., 2006) and *Leishmania major* (Belkaid et al., 2001) and demonstrate how IL-10 can contribute to the establishment and maintenance of chronic infection. Both $CD4^+$ $Foxp3^-$ Th1 cells and $Foxp3^+$ Treg cells have been described to produce IL-10 and influence the establishment of chronic Leishmania infection, the different sources may be explained by the use of different Leishmanial substrains (Anderson et al., 2007; Belkaid et al., 2002).

Further support for the ability of IL-10 to contribute to the establishment and maintenance of chronic infection, is the observation that several viruses encode homologues of IL-10. Several herpes viruses and pox viruses encode viral IL-10 (vIL-10), displaying varying amounts of sequence identity to the human IL-10 (Slobedman et al., 2009). Epstein Barr Virus (EBV) also encodes a vIL-10. EBV vIL-10 has retained much of the immunosuppressive activity and is able to suppress the production of inflammatory cytokines, reduce macrophage activation and suppress antigen presentation (Hsu et al., 1990). However, it has lost many of the immunostimulatory properties of mammalian IL-10 (Hsu et al., 1990). Acquisition and maintenance of vIL-10 genes within the viral genome suggests this is beneficial to the virus, and could suggest a mechanism of immune evasion and which contributes to the ability to persist (Moore et al., 2001).

1.5.3 The role of IL-10 during Mtb infection

The role of IL-10 during *Mtb* infection has been controversial, with many conflicting studies. Reasons for these inconclusive results could include differences in the genetic background of the mice, strain of *Mtb* used for infection and also differences in microflora in mice from difference sources (Redford et al., 2011). Early studies suggested IL-10 deficiency in mice had no effect on bacterial load (North, 1998), and was not responsible for suppressing a Th1 response, although early increases in IFNγ and iNOS mRNA were reported (Jung et al., 2003). Another study suggested that IL-10 only suppressed a protective response early in infection (Roach et al., 2001).

The level of IL-10 production has been linked with susceptibility of different mouse strains to *Mtb* infection, with the susceptible CBA/J mice expressing higher levels of IL-10 in foamy macrophages than C57BL/6 mice at days 50 and 150 post infection (Turner et al., 2002). Genetic modification of the resistant mouse strain C57BL/6 such that IL-10 is expressed as a transgene under control of the IL-2 promoter enhanced its susceptibility (Turner et al., 2002).

Subsequently it was shown that resistant mice (C57BL/6 and BALB/c) or susceptible mice (CBA/J) either deficient in IL-10 or treated with monoclonal antibody to block IL-10 action had enhanced protection against *Mtb* (Beamer et al., 2008; Redford et al., 2010). This was accompanied by an earlier and enhanced Th1 immune response to aerosol *Mtb* infection (Redford et al., 2010). Subsequent work comparing CBA/J mice deficient in IL-10 or those treated with αIL-10R early in infection, demonstrated that IL-10 within the first month of infection was detrimental to control of *Mtb* infection (Cyktor et al., 2013b). Furthermore, IL-10 inhibited the formation of mature, fibrotic granulomas capable of containing infection in the susceptible CBA/J (Cyktor et al., 2013b). It has also been found that CBA/J mice display a clonal accumulation of IL-10 producing $CD8^+$ T cells during chronic *Mtb* infection, however, depletion of these cells did not enhance protection against *Mtb*, which was suggested to be because these cells also produced IFNγ (Cyktor et al., 2013a).

Recently using *in silico* modelling based on data from NHPs, a role for IL-10 at the level of individual granuloma has been suggested (Cilfone et al., 2015). IL-10 was suggested to be detrimental to sterilisation of the granuloma but at the expense of caseation, with models of IL-10 deficiency leading to increased sterilisation (Cilfone et al., 2015). In this model macrophage-derived IL-10 was implicated as the important source of IL-10, with models of macrophage specific deletion increasing levels of TNFα within the granuloma and increasing lesion sterilisation (Cilfone et al., 2015).

Further support for a detrimental role for IL-10 during *Mtb* infection is provided by the observation that more virulent *Mtb* strains induce higher levels of IL-10. The lab *Mtb* strain H37Rv and the clinical isolate CH, have been demonstrated to have different capacities to induce IL-10 upon infection of human monocyte derived macrophages (Newton et al., 2006). CH induced higher levels of IL-10 and lower levels of the protective IL-12p40, suggesting CH can induce an anti-inflammatory environment to further its survival (Newton et al., 2006). *In*

vivo, the hyper virulent *Mtb* strain HN878 induced higher levels of IL-10 producing Foxp3$^+$ T cells upon aerosol infection in mice, which may contribute to its virulence (Ordway et al., 2007).

A role for IL-10 in contributing to the pathogenesis of *Mtb* infection is also suggested by studies in humans (Redford et al., 2011). In active TB patients elevated levels of IL-10 are seen in the lungs (Barnes et al., 1993), serum (Verbon et al., 1999) and sputum (Almeida et al., 2009) and reviewed in (Redford et al., 2011). CD4$^+$ T cells isolated from BAL more frequently produce both IFNγ and IL-10 in active TB patients compared to CD4$^+$ T cells from healthy controls or inactive subjects (Gerosa et al., 1999). Furthermore, IL-12p40 and IFNγ production by PBMCs from TB patients cultured with *Mtb,* was enhanced when IL-10 was neutralised, suggesting a suppressive role for IL-10 (Gong et al., 1996). The level of IL-10 expression has been correlated with bacterial load in TB patients, with the level of the *Mtb* antigen CFP32, correlating with IL-10 in active TB patients (Huard et al., 2003). Furthermore, IL-10 production by CD8$^+$ T cells correlated with bacterial load in the sputum (Silva et al., 2014).

There are conflicting reports on the association of polymorphisms in the *Il10* gene at -1082, -819 and -592 and susceptibility to *Mtb* infection (reviewed in (Redford et al., 2011). A meta-analysis employing 8 studies to assess association of polymorphism in the *Il10* gene at -1082, showed that there was a trend towards association with susceptibility to pulmonary TB, but this did not reach significance (Pacheco et al., 2008). A subsequent meta-analysis evaluated the association of IL-10 polymorphisms at -1082, -819 and -592 (Liu et al., 2015). Analysis in all ethnic groups suggested that there is no association between IL-10 polymorphisms and susceptibility to TB (Liu et al., 2015). However, assessment within specific ethnic groups demonstrated that polymorphism at -1082 were associated with TB susceptibility in Caucasians, polymorphism at -819 were associated with TB susceptibility in Asians, and those at -592 were associated with TB susceptibility in Asians, Caucasians and Europeans (Liu et al., 2015). In

agreement with this, a second meta-analysis reported no association between IL-10 polymorphisms at -1082, -819 and -592 and susceptibility to TB (Gao et al., 2015). When specific ethnic groups were assessed, polymorphism at -819 was associated with susceptibility to TB in Asians, and polymorphism at -592 associated with susceptibility to TB in Europeans (Gao et al., 2015). Thus the association of *Il10* gene polymorphisms with susceptibility to TB remains unclear, and data suggests it is dependent upon ethnicity.

1.5.4 Regulatory T cells in the suppression of the immune response to Mtb infection

Regulatory T cells (Treg) are a subset of $CD4^+$ T cells that express Forkhead box P3 (Foxp3) and suppress the immune response with the aim of avoiding immunopathology (Josefowicz et al., 2012). Numbers of $Foxp3^+$ Tregs expand in the lung and spleen of *Mtb* infected mice over the course of *Mtb* infection (Kursar et al., 2007). Further work has shown that pathogen specific Tregs expand in the pulmonary lymph node following *Mtb* infection, but subsequently diminish following IL-12 induced expression of T-bet (Shafiani et al., 2013). Tregs are suggested to be detrimental to protective immunity to *Mtb*. Indeed, *Rag* deficient mice reconstituted with $CD4^+$ $CD25^-$ T cells together with Tregs defined as $CD4^+$ $CD25^+$ show higher bacterial loads than those reconstituted with $CD4^+$ $CD25^-$ T cells alone (Kursar et al., 2007). However, it should be noted that CD25 can also be expressed on activated T cells (Josefowicz et al., 2012). Use of $Foxp3^-$GFP reporter mice (where cells expressing Foxp3 also express the green fluorescent protein (GFP)) showed that Tregs expand in the pulmonary lymph nodes and accumulate in the lung (Scott-Browne et al., 2007). Depletion of $Foxp3^+$ Tregs reduced bacterial loads following *Mtb* infection (Scott-Browne et al., 2007). In addition, *Mtb*-specific Tregs in the lymph node were capable, even at low numbers, of delaying T cell priming and suppressing a protective immune response upon *Mtb* infection (Shafiani et al., 2010). Furthermore, the hyper-virulent *Mtb* strain HN878, induced higher numbers of IL-10 producing $Foxp3^+$ Tregs in the lung

compared to virulent H37Rv, which may contribute to the waning Th1 response and impaired survival observed following infection with this strain (Ordway et al., 2007).

1.5.5 Type 1 IFNs

A detrimental role for type I IFNs during *Mtb* infection is suggested by the observation that infection with virulent clinical isolates of *Mtb*, such as HN878, induces high levels of type I IFNs (Manca et al., 2001; Manca et al., 2005). Furthermore, mice deficient for the type I IFN receptor (IFNαβR) displayed increased survival following infection with these clinical isolates (Manca et al., 2005). However, in contrast another study showed that IFNαβR deficient mice displayed lower bacterial loads in the lung when infected with several different strains of *Mtb* but that there was no impact upon survival (Ordway et al., 2007). A possible explanation for the differences observed in these studies is the different mouse strains assessed (McNab et al., 2015). In humans a pathogenic role for type I IFNs was suggested by the identification of an IFN inducible gene profile has been seen in patients with active TB but not latent or healthy controls (Berry et al., 2010).

Augmentation of type I IFNs during infection either through exogenous application of type I IFNs, or through administration of an agent that induces type I IFN (Poly IC) exacerbated bacterial load and disease in mice (Antonelli et al., 2010; Manca et al., 2001; Mayer-Barber et al., 2014). In addition, mice deficient for a negative regulator of type I IFN expression, TPL2, display increased susceptibility to *Mtb* infection in a type I IFN dependent manner (McNab et al., 2013). These mice also displayed increased susceptibility to *Listeria monocytogenes* infection, which was accompanied by increased IL-10 levels and decreased IL-12 levels (McNab et al., 2013). Furthermore co-infection with influenza A and *Mtb* resulted in a type I IFN dependent increase in bacterial loads in the lung (Redford et al., 2014).

The mechanism for the detrimental role for type I IFN is multifactorial (McNab et al., 2015). Type I IFNs have been demonstrated to suppress IL-1 production and promote IL-10 production *in vivo* (Mayer-Barber et al., 2011). This is supported by *in vitro* findings in mouse bone-marrow derived macrophages, where induction of type I IFN using PolyIC decreased IL-1α and IL-1β expression (Mayer-Barber et al., 2011). This was shown to be at least partially dependent upon IL-10 (Mayer-Barber et al., 2011). Type I IFN was found to induce IL-10 expression in mouse bone marrow-derived macrophages in an IL-27 independent fashion and suppress TNFα and IL-12 production in a manner at least partially dependent upon IL-10 (McNab et al., 2014). Type I IFNs have also been shown to regulate the production of IL-1 in human macrophages and DCs (Mayer-Barber et al., 2011; Novikov et al., 2011).

Inhibition of IL-1 production by type I IFN is suggested to result in uncontrolled bacterial growth, at least in part, through decreased PGE_2 production and disruption of the eicosanoid balance (Mayer-Barber et al., 2014). Modulation of the eicosanoid balance by increasing PGE_2 in *Mtb* infected mice treated with PolyIC, increased their survival (Mayer-Barber et al., 2014). Furthermore, PGE_2 suppresses type I IFN production contributing to control of infection (Mayer-Barber et al., 2014). This counter regulation of IL-1, PGE_2 and type I IFN is suggested to influence outcome of infection (**Figure 1.5**). Situations where there is excessive type I IFN lead to low IL-1 and PGE_2 levels compromising control of infection. Restoration of PGE_2 levels decreases type I IFN levels and facilitates control of infection (Mayer-Barber et al., 2014).

Type I IFNs have also been shown to inhibit the response to IFNγ, providing another way in which they are detrimental to control of *Mtb* infection. It has been shown that IFNβ can inhibit IFNγ induced antimicrobial activity in an IL-10 dependent manner in human monocytes infected with *Mycobacterium leprae* (Teles et al., 2013). Suppression of the response to IFNγ by type I IFNs has also been seen in mouse macrophages infected with *Mtb* (McNab et al., 2014).

However, it has also been suggested that in some circumstances type I IFNs could provide some level of protection. In the absence of type II IFN signalling, type I IFNs could act to limit the recruitment of myeloid cells permissible to *Mtb* infection (Desvignes et al., 2012). In support of a protective role for type I IFNs, patients with mutations in ISG15, a type I IFN inducible protein, are more susceptible to mycobacterial infection, due to a defect in induction of IFNγ (Bogunovic et al., 2012). However, ISG15 has also been shown to be a negative regulator of type I IFNs in patients with ISG15 deficiency (Zhang et al., 2015). Further investigation is required to determine whether the increased susceptibility to mycobacterial infections observed in patients with ISG15 mutations could also result from excessive type I IFN production.

1.5.6 Myeloid suppressor cells as a marker of susceptibility to Mtb

Myeloid derived suppressor cells (MDSC) were originally identified in tumours and have the capability to suppress T cell responses (Gabrilovich and Nagaraj, 2009). In mice they are defined based on their expression of Gr-1 and CD11b (Gabrilovich and Nagaraj, 2009). In humans they are most commonly defined as $CD14^{-}$ $CD11b^{+}$ but also as $CD33^{+}$ but lacking markers of mature lymphoid or myeloid populations (Gabrilovich and Nagaraj, 2009). MDSC are suggested to play a detrimental role during *Mtb* infection. Recently an increase in the level of Gr-1^{dim} $CD11b^{+}$ cells (suggested to represent a MDSC population) upon *Mtb* infection in mice was suggested to be a marker of severe infection (Tsiganov et al., 2014). These cells were capable of suppressing T cell proliferation and IFNγ production *in vitro* but did not affect bacterial loads *in vivo* when adoptively transferred (Tsiganov et al., 2014). Furthermore, numbers of both $Ly6G^{+}$ Gr-1^{int} and $Ly6G^{-}$ $Gr1^{hi}$ MDSCs were increased upon *Mtb* infection in susceptible 129S2 mice to a greater extent than in C57BL/6 mice (Knaul et al., 2014). These cells were capable of suppressing IFNγ production by splenocytes (Knaul et al., 2014). These cells were also capable of being infected with *Mtb* and specific depletion of these cells using all-trans retinoic acid (an active form of vitamin A) decreased bacterial loads (Knaul et al., 2014), although all-trans retinoic acid may have also have other effects on the immune response. A

detrimental role for MDSC is also suggested in humans where increased frequencies of MDSCs have been identified in the blood and lungs of active TB patients, compared to healthy controls (El Daker et al., 2015).

1.6 Vaccination against *Mtb*

In order to achieve the target set out by WHO to eradicate TB infection by 2050, an effective vaccine against *Mtb* is required. The BCG vaccine is one of the most widely administered vaccines, with over 4 billion children BCG vaccinated since 1974 (Abebe, 2012). Although it provides protection against childhood TB meningitis (Trunz et al., 2006), the efficacy it provides in protecting adults against a pulmonary disease is variable (Fine, 1995) (discussed in more detail below) and therefore improved vaccines or vaccine regimes are required. There are several issues that complicate the development of a new vaccine against TB. Firstly, there is an incomplete understanding of the protective immune response to *Mtb* infection and therefore there is a lack of correlates of protection that can predict vaccine efficacy. It was suggested that the presence of IFNγ producing $CD4^+$ T cells correlated with protection against *Mtb* infection (Chackerian et al., 2001), although more recently this concept has been challenged (Abebe, 2012; Kagina et al., 2010; Mittrucker et al., 2007). Subsequently it was suggested that the presence of $IFN\gamma^+$ $TNF\alpha^+$ $IL\text{-}2^+$ multifunctional T cells in the lung correlated with protection following vaccination (Forbes et al., 2008). More recently multifunctional T cells expressing IL-17, TNFα and IL-2 in the lung are suggested to correlate with protection (Cruz et al., 2015). However, in human infants no expression profile of IFNγ, IL-17, IL-2 or TNFα following BCG vaccination in $CD4^+$, $CD8^+$ or γδ T cells correlated with protection (Kagina et al., 2010). However, this was in peripheral blood rather than a disease site (Kagina et al., 2010). Without the knowledge of what guarantees a protective response the rational design and assessment of putative vaccines is hindered.

Secondly, unlike other infectious diseases, the immune response to *Mtb* is not sterilizing. Indeed re-infection of mice with *Mtb* following clearance through drug treatment induces an earlier control of bacterial growth and reduced bacterial load but not sterilising immunity (Jung et al., 2005). This phenomenon is also seen in humans where individuals successfully treated for *Mtb*

infection remain susceptible to reinfection (Verver et al., 2005). In addition, latently infected individuals, assumed to display an adequate immune response to prevent disease, can reactivate and develop disease. The change in the immune response that facilitates this reactivation in immunocompetent individuals is not understood. Such observations suggest that the boosting the natural immune response is insufficient to provide protective immunity and suggest targeting of other aspects on immunity, not naturally induced to *Mtb* infection, should be considered.

Furthermore, use of appropriate animals models and *Mtb* strains in pre-clinical trials to assess vaccine efficacy is important (McShane and Williams, 2014). As discussed earlier there are several animal models of *Mtb* infection, some bearing more resemblance to human disease than others (Flynn, 2006). The responses to a vaccine and the efficacy of the vaccine will differ between these models and most likely will differ to humans (McShane and Williams, 2014). Therefore it is difficult to use preclinical models to assess vaccine efficacy. Further work is required to evaluate the capacity of various animal models to predict efficacy of vaccine candidates in humans (McShane and Williams, 2014). Methods that assess the restriction of mycobacterial growth in humans following vaccination may also aid the assessment of vaccine efficacy. For example, a BCG challenge model has been developed where patients are given an intradermal challenge with BCG following vaccination, and the restriction of BCG bacterial growth is assessed (Minassian et al., 2012). Alternatively the restriction of mycobacterial growth by whole blood or PBMCs *in vitro* following vaccination could be used assess vaccine efficacy (Fletcher et al., 2013).

Finally, most vaccines currently in pre-clinical trials have been evaluated for their ability to protect against lab-adapted strains of *Mtb* such as H37Rv (McShane and Williams, 2014). However, such strains may not reflect the virulence of the clinical isolates infecting humans, against which these vaccines will have to protect. The importance of testing the ability of a vaccine to protect against clinical isolates is underlined by the observation that the protection

afforded by BCG in terms of control of bacterial load is more transient when mice are challenged with the hyper-virulent HN878 compared to the lab-adapted strain H37Rv (Grode et al., 2005; Ordway et al., 2011).

1.6.1 BCG vaccination

BCG is a live vaccine originally derived from serial passage of *Mycobacterium bovis*, a mycobacterial strain that causes bovine tuberculosis and can infrequently cause disease in humans (Pitt et al., 2012a). This serial passage resulted in loss of the virulence associated RD1 locus (Mahairas et al., 1996). The RD1 locus encodes proteins important for virulence of mycobacteria and also for T cell responses including early secretory antigenic 6 kDa (ESAT-6) and culture filtrate protein 10 (CFP-10) (Andersen and Kaufmann, 2014).

Despite BCG being a widely administered vaccine, there is considerable variation in reports of the efficacy it provides in protecting against adult pulmonary tuberculosis, with estimates ranging between 0-80% (Fine, 1995). Highest rates of efficacy are reported at higher latitudes for example in North America or Europe and low to no efficacy is reported in the tropics (Fine, 1995; Rowland and McShane, 2011). Several reasons for the variation in the efficacy of BCG vaccination have been proposed. Firstly, exposure to environmental mycobacteria, which is higher in areas where efficacy is lowest, is suggested to mask any additional benefit of BCG vaccination or to inhibit the induction of a protective response by BCG vaccination (Brandt et al., 2002; Fine, 1995; Rowland and McShane, 2011). Another proposed reason for the variation in efficacy is due to differences in the immune responses induced by different BCG strains leading to different levels of protection (Rowland and McShane, 2011). There are 4 main BCG strains used for vaccination: Pasteur 1173 P2 strain, Danish SSI 1331 strains, Glaxo 1077 strain and Japanese Tokyo 172 strain (Rowland and McShane, 2011). It has been shown that the induction of an immune response differs between BCG strains and this is suggested to impact vaccine efficacy (Ritz et al., 2012; Ritz et al., 2008).

Although BCG is suboptimal for protection against an adult pulmonary disease, BCG does prove a much better vaccine in protecting infants from disseminated forms of tuberculosis such as TB meningitis (Trunz et al., 2006). However, there are limitations in the safety of BCG. Immunodeficiency is a contraindication for BCG vaccination in infants. For example BCG vaccination of infants with HIV, can lead to a disease caused by BCG itself termed BCG-osis (Hesseling et al., 2006).

1.6.2 Prophylactic Vaccines in clinical trials

As a result of the limitations of the BCG vaccine there are several new pre-exposure, prophylactic vaccine candidates in clinical trials, which are summarised in **Figure 1.6**. These vaccine candidates aim to improve immunity to *Mtb* and prevent TB disease. Other post-exposure vaccines are also being developed that either aim to prevent reactivation from latent TB to active TB or act as therapeutic vaccines to aid chemotherapy of active TB patients (Andersen and Kaufmann, 2014).

Broadly two different strategies to improve prophylactic vaccination have been taken. Firstly, to boost pre-existing BCG immunity using vectors expressing *Mtb* antigens or protein antigens delivered in adjuvant. Secondly, to replace BCG vaccination with recombinant BCG strains or genetically modified *Mtb* strains.

1.6.2.1 Viral vectors

Viral vectors employ replication deficient viruses to deliver *Mtb* antigens in order to boost an immune response. Candidates in clinical trials include MVA85A, AERAS 402, Ad35/MVA85A, and Ad5 Ag85A and have employed either adenoviruses or a modified vaccinia virus as a delivery vector **(Figure 1.6)**.

MVA85A is a modified vaccinia virus Ankara, expressing antigen 85A (Ag85A) given as a boost to pre-existing BCG immunity. MVA85A was the first vaccine candidate to enter phase IIb clinical trials. Disappointingly it failed to show efficacy in prevent TB disease over BCG alone in both infants in South Africa and HIV^{+} adults in South Africa and Senegal (Ndiaye et al., 2015; Tameris et al., 2013). This lack of efficacy occurred despite evidence that MVA85A can induce long term, multifunctional T cell responses (Tameris et al., 2014). However, variation in the response to MVA85A vaccination has been described, with low responses correlating with increased Treg frequency following vaccination (Matsumiya et al., 2013) and increased basal levels of Indoleamine 2,3-dioxygenase activity (which suppresses T cell function) prior to vaccination (Tanner et al., 2014). This variation in response to MVA85A could have contributed to the observed lack of efficacy (Matsumiya et al., 2013; Tameris et al., 2013).

Aeras 402 and Ad5 Ag85A both employ replication deficient adenovirus as their delivery systems. Aeras 402 employs Ad35 as its delivery system for the following antigens: Ag85A, Ag85B and TB10.4 (Andersen and Kaufmann, 2014). It has been seen to induce a polyfunctional immune response in both adults and infants and has entered phase IIa trials (Abel et al., 2010; Kagina et al., 2014). In addition, Aeras 402 has entered clinical trials in combination with MVA85A (Andersen and Kaufmann, 2014).

Ad5 Ag85A utilises adenovirus 5 to deliver antigen 85A in order to boost pre-existing BCG immunity (Andersen and Kaufmann, 2014). Concern surrounding the use of adenovirus 5 exists due to the high prevalence of neutralising antibodies to this adenovirus serotype in TB endemic areas (Andersen and Kaufmann, 2014). Despite this, Ad5 Ag85A has shown immunogenicity in healthy adults and the magnitude of the response did not correlate with the level of neutralising antibodies in the serum (Smaill et al., 2013). However, failure of the STEP trial, where vaccination with recombinant adenovirus 5 expressing HIV antigens increased HIV infection,

questions the use of adenoviruses as TB vaccine candidates given the endemics for *Mtb* and HIV largely overlap (Andersen and Kaufmann, 2014; Hanke, 2008).

1.6.2.2 Proteins in adjuvant as TB vaccines

Protein *Mtb* antigens delivered in adjuvant are also designed to boost pre-existing BCG immunity. Most of the vaccines in clinical trials combine multiple fused antigens. Candidates in clinical trials include H1, H4, H56, M72 and ID93 (Andersen and Kaufmann, 2014).

H1 consists of a fusion of Ag85B and ESAT-6 given in adjuvant IC31, which is an agonist for TLR9. This vaccine induces a robust Th1 response and is currently in phase IIa trials (Andersen and Kaufmann, 2014). H1 has also been tested in the context of the adjuvant CAF01, which is a liposome base adjuvant. This formulation has completed phase I clinical trials (Andersen and Kaufmann, 2014). H4 is similar to H1 but contains Ag85B fused with TB10.4 given in IC31 and has also completed phase I trials (Andersen and Kaufmann, 2014).

H56 is based on the H1 backbone, but includes the antigen Rv2660c (Aagaard et al., 2011). This antigen is induced under nutrient stress conditions and is termed a "late stage" antigen, as opposed to Ag85B and ESAT-6, which are acute antigens (Aagaard et al., 2011). Inclusion of a late stage antigen is suggested to enhance the immune response throughout infection. As well as serving as a prophylactic vaccine, inclusion of the late stage antigen in H56 is designed to prevent reactivation (Andersen and Kaufmann, 2014). Indeed in the NHP model, vaccination with BCG and H56, prevented reactivation of disease following αTNF treatment (Lin et al., 2012). A phase I trial of H56 has recently been completed, demonstrating that it is safe and immunogenic in healthy adults with or without *Mtb* infection (Luabeya et al., 2015).

M72 is a fusion of Rv1196 and Rv0125 given in the adjuvant AS01, which comprises monophosphryl lipid A (MPL) and QS21 in liposomes. This vaccine is currently undergoing

phase IIb clinical trials, having successfully shown safety and immunogenicity in *Mtb* infected and uninfected adults (Day et al., 2013) and infants in South Africa (Idoko et al., 2014).

ID93 is the latest protein in adjuvant vaccine to be developed. It consists of the antigens Rv2608, Rv3619, Rv3620 and Rv1831 given in GLA-SE, an adjuvant composed of a synthetic MPL in a lipid stable emulsion (Bertholet et al., 2010). ID93 vaccination was able to protect mice against challenge with the lab strain of *Mtb* H37Rv and also a multi-drug resistant strain (TN5904) (Bertholet et al., 2010). Furthermore ID93 boost of BCG vaccination in a guinea pig model increased survival upon *Mtb* challenge (Bertholet et al., 2010). This vaccine is now undergoing phase I clinical trials (Andersen and Kaufmann, 2014).

1.6.2.3 Live vaccines to replace BCG

Currently two live candidates are in clinical development. These are VPM1002 and *MTB*VAC. VPM1002 is a recombinant BCG strain expressing listeriolysin from *Listeria monocytogenes,* which is a pore forming enzyme. This allows egress of *Mtb* antigens into the cytosol and increases cross presentation and apoptosis of macrophages, increasing the immunogenicity of BCG (Grode et al., 2005). Listeriolysin functions at an acidic pH, and to allow optimal function, Urease C has also been deleted in the VPM1002 vaccine to facilitate optimal acidification of the phagosome (Grode et al., 2005). This vaccine has successfully completed phase I trials, displaying safety in adults in Germany and South Africa, and is currently undergoing phase IIa trials in infants in South Africa (Kaufmann et al., 2014).

*MTB*VAC is a genetically modified *Mtb* strain with deletion of *PhoP* and *Fad26*, which has progressed to phase I clinical trials. PhoP is a key transcription factor for *Mtb* virulence and Fad26 is required for synthesis of complex lipids also vital for virulence (Arbues et al., 2013).

1.6.2.4 Mucosal delivery of vaccine candidates

As *Mtb* mainly infects via the aerosol route, it is argued that vaccination via this route may be superior, inducing local responses at the site of infection (Belyakov and Ahlers, 2009; Manjaly Thomas and McShane, 2015). Indeed, in mice, intranasal administration of BCG vaccination led to increased protection against *Mtb* challenge compared to subcutaneous BCG vaccination (Chen et al., 2004; Goonetilleke et al., 2003). In guinea pigs, aerosol vaccination with a spray dried BCG vaccine led to lower bacterial loads in the lung upon *Mtb* challenge, in a dose dependent manner compared to subcutaneous BCG vaccination (Garcia-Contreras et al., 2008). Furthermore boosting BCG vaccination using an adenovirus expressing Ag85A (Ad5 Ag85A) was only effective in controlling lung bacterial loads upon *Mtb* challenge, if the vaccine was administered intranasally (Forbes et al., 2008). Intranasal boosting with Ad5 Ag85A induced higher levels of multifunctional $CD4^+$ and $CD8^+$ T cells in the lung following vaccination, which were suggested to correlate with protection (Forbes et al., 2008). In addition, in a mouse model intranasal MVA85A as a boost to intranasal BCG vaccination led to lower bacterial loads upon *Mtb* challenge compared to intranasal BCG alone (Goonetilleke et al., 2003). In UK adults, aerosol administration of MVA85A led to greater induction of T cell responses in the BAL compared to parental administration of MVA85A (Satti et al., 2014), suggesting this could be a beneficial way to improve efficacy. However, a recent study in the NHP model, showed that although aerosolised Aeras-402, alone or following BCG vaccination, induced T cell responses in BAL, this did not lead to protection upon *Mtb* challenge (Darrah et al., 2014). Although this lack of protection was suggested to be due to the high bacterial load in challenge (Darrah et al., 2014), this could indicate that even aerosol administration of boosting vaccines will not be sufficient to increase the efficacy of BCG alone.

1.6.3 IL-23 and IL-17 as protective factors in Mtb vaccination.

Although the role of IL-17 during primary infection is unclear, in the context of vaccination, IL-17 is thought to be required for optimal vaccine responses. IL-17 is suggested to be required for recruitment of IFNγ producing $CD4^+$ T cells upon *Mtb* challenge (Khader et al., 2007). IL-17 neutralisation during *Mtb* challenge, following vaccination with a peptide epitope in adjuvant, led to decreased production of the chemokines CXCL9, 10 and 11 and lower recruitment of IFN-γ producing cells to the lung (although the effect of IL-17 neutralisation upon control of bacterial load was not assessed) (Khader et al., 2007). In a mucosal vaccination regime IL-17 has also been shown to induce CXCL13 important for localising T cells mediating vaccine induced protection (Gopal et al., 2013). Adoptive transfer of Th17 cells into naïve hosts can also mediate protection. Indeed, in the absence of IL-12p40, BCG vaccinated mice induced robust Th17 responses and transfer of these Th17 cells into a *Rag* deficient host provided some protection against *Mtb* challenge (Wozniak et al., 2006; Wozniak et al., 2010). Furthermore, transfer of ESAT-6 specific, *in vitro* differentiated, Th17 cells into mice prior to *Mtb* challenge led to better control of *Mtb* bacterial load in an IL-23 dependent manner (Monin et al., 2015).

IL-23 is also suggested to contribute to vaccine-mediated immunity. IL-23 dependent IL-17 is suggested to be required for induction of a protective Th1 response to *Mtb* challenge, following BCG vaccination (Gopal et al., 2012). Furthermore, co-immunization of mice deficient in IL-12p40 (unable to produce IL-12 or IL-23) with a plasmid containing Ag85B and IL-23 led to induction of an antigen specific IFNγ response (although not an IL-17 response), which provided partial protection against *Mtb* challenge (Wozniak et al., 2006). However IL-17 and IL-23 have been reported to mediate immune pathology in *Mtb* infected mice subsequently vaccinated repeatedly with BCG, so attempts to boost IL-17 production may require caution (Cruz et al., 2010).

1.6.4 IL-10 and its role in vaccination

IL-10 can suppress the immune response to a vaccine and therefore use of IL-10 or IL-10R blockade could enhance vaccination response and efficacy (reviewed in O'Garra et al., 2008). IL-10R blockade during vaccination with a viral vector expressing leishmanial proteins increased the Th1 response and protection against *Leishmania* infection (Darrah et al., 2010). Furthermore, therapeutic vaccination in LCMV infection was only effective at increasing the anti-viral immune response and clearing persistent infection in the context of IL-10R blockade (Brooks et al., 2008). In the context of mycobacterial infection, IL-10 neutralisation during vaccination with CFP increases protection against *M. avium* infection (Silva et al., 2001). During BCG vaccination IL-10 is suggested to suppress induction of an optimal Th1 response (Gopal et al., 2012). In addition, BCG vaccination of *Il10* deficient mice increased their protection upon *Mtb* challenge at an early time point (Gopal et al., 2012). This increased protective effect of BCG vaccination in *Il10* deficient mice was also shown at later time points (Pitt et al., 2012b). However, *Il10* deficient mice have been shown to display increased resistance to primary *Mtb* infection (Redford et al., 2010). Thus it is difficult to determine whether the protective affects of BCG vaccination in the *Il10* deficient mouse is a result of an absence of IL-10 during vaccination or during *Mtb* infection. The role of IL-10 specifically during BCG vaccination was assessed using IL-10R blockade during BCG vaccination. Anti-IL-10 Receptor (αIL-10R) monoclonal antibody (mAb) treatment, during BCG vaccination, lowered bacterial load following *Mtb* infection and enhanced the IFNγ and IL-17 responses in the resistant C57BL/6 and susceptible CBA/J mice (Pitt et al., 2012b).

1.7 Innate Lymphoid cells

Innate lymphoid cells (ILCs) are a family of recently described cells that are lymphoid in morphology, lack markers of myeloid lineages but express surface markers and cytokines associated with differentiated T cells (reviewed in Serafini et al., 2015). However, in contrast to T cells, ILCs develop independently of RAG recombinase (which is required for antigen specific receptor rearrangement) (reviewed in Spits et al., 2013). NK cells were the first described but the family of ILCs has expanded considerably to include subsets of cytokine producing ILCs referred to as ILC1, ILC2 and ILC3 (reviewed in Spits et al., 2013). Multiple roles for these cells have been described in response to infection, in allergy, autoimmunity and inflammatory bowel disease and also in metabolic regulation, although discussion will focus on their role in infection (reviewed in Artis and Spits, 2015)

1.7.1 Development of ILCs

ILC development is incompletely understood, although some progress has been made in determining how different lineages of ILC develop. **Figure 1.7** summarises a model for their development.

ILCs develop from the common lymphoid progenitor, which also gives rise to T and B cells (reviewed in Diefenbach et al., 2014). It is suggested that downstream of the CLP there is a precursor capable of giving rise to all ILC lineages including NK cells and this precursor has been termed Common Innate Lymphoid Progenitor (CILP) or α Lymphoid Precursor (αLP) (reviewed in Artis and Spits, 2015; Diefenbach et al., 2014; Yu et al., 2014). The transcription factors Tox and Nfil3 are suggested to be required for this early differentiation of ILCs and NK cells (reviewed in Artis and Spits, 2015). Nfil3 deficient mice have deficiencies in NK cells (Gascoyne et al., 2009), ILC2s and ILC3s (Geiger et al., 2014; Seillet et al., 2014; Yu et al., 2014) and ILC1s (Klose et al., 2014; Yu et al., 2014). Although *Nfil3* deficient mice had a defect in Peyer's Patch formation, peripheral lymph nodes were unaffected suggesting some

functional LTi cells were still present (Seillet et al., 2014). More recently it has been described that Nfil3 is upregulated in response to the common γ chain cytokine IL-7 and is required for subsequent Id2 expression in the Common Helper-like Innate Lymphoid Progenitor (CHILP), which is downstream of these early ILC precursors (**Figure 1.7**) (Xu et al., 2015). Nfil3 has also been described to directly bind to the Tox promoter and regulate its expression, thus regulating subsequent ILC development (Yu et al., 2014). Tox deficiency led to a defect in the development of all ILC subsets, including NK cells (Seehus et al., 2015). In addition *Tox* deficient mice have a complete block in lymph node organogenesis (Seehus et al., 2015).

A CHILP has been described in the bone marrow which expressed high levels of the transcription factor Id2 as well as the IL-7 receptor and the integrin $\alpha_4\beta_7$ (Klose et al., 2014). These cells were suggested to be downstream of the CILP (αLP) as they had a more restricted potential, giving rise to all defined ILC subsets with the exception of NK cells (Klose et al., 2014). The transcription factor Id2 is required for development of NK cells and other ILC subsets (Cherrier et al., 2012; Moro et al., 2010; Serafini et al., 2015; Yokota et al., 1999). Using Id2 fate reporter mice it was shown that all ILC subsets, including conventional NK cells expressed Id2 (Carotta et al., 2011; Hoyler et al., 2012). However, the observation that NK cell precursors are Id2 negative suggests Id2 expression does not occur at the CILP (αLP) stage, but later in ILC development (Klose et al., 2014).

GATA3 is another transcription factor that has been found to be required for development of ILCs. Deletion of GATA3 in the haematopoietic compartment leads to defects in the development of all IL-7Rα expressing ILCs, but not IL-7Rα negative NK cells (Yagi et al., 2014). Another study supporting this showed that GATA3 deficient foetal liver precursors were unable to generate ILC3s in the gut (Serafini et al., 2014). Although GATA3 is required for the development of all ILC subsets, only ILC2s require GATA3 for their maintenance following development (Hoyler et al., 2012; Yagi et al., 2014).

Another ILC progenitor, suggested to be downstream of the CHILP, has been identified based on the expression of the transcription factor PLZF. Using a fate-mapping approach it was found that most ILC subsets were positive for PLZF fate map, suggesting a $PLZF^+$ precursor existed (Constantinides et al., 2014). The $PLZF^+$ precursor identified was able to give rise to all ILC subsets with the notable exception of NK cells and Lymphoid Tissue inducer (LTi) cells (Constantinides et al., 2014).

1.7.2 Subsets and effector functions of ILCs

ILCs have been divided into different subsets: ILC1, ILC2 and ILC3 based on their transcription factor requirements and the cytokines they produce, which have many similarities with those of Th1, Th2 and Th17 cells respectively (**Figure 1.7**) (reviewed in Serafini et al., 2015; Spits et al., 2013).

1.7.1.1 ILC1

ILC1s, like Th1 cells, produce IFNγ and are dependent on the transcription factor T-bet. ILC1s are reported to produce cytokines in response to IL-12, IL-15 and IL-18 (reviewed in Artis and Spits, 2015). Although NK cells are included in the ILC1 subset, there are differences between NK cells and other ILC1 subsets (Robinette et al., 2015). NK cells are cytotoxic as well as having the capacity to produce cytokines, whereas other ILC1s are not cytotoxic (reviewed in Serafini et al., 2015). Furthermore, it has been suggested that ILC1 subsets can be differentiated based on their expression of Eomes, with cytotoxic NK cells expressing Eomes and other ILC1 subsets being Eomes negative (Klose et al., 2014; Serafini et al., 2015).

Several ILC1 subsets distinct from Eomes positive NK cells have been described. In the mouse an ILC1 subset has been described in the gut (Klose et al., 2014). These cells are Lin^- $NK1.1^+$

NKp46^{+} CD127^{+} CD27^{+} and are dependent upon IL-15 and T-bet but not Eomes for development and/or maintenance (Klose et al., 2014). In addition, distinct IL-15 and T-bet dependent subset of "tissue resident" NK cells have been described in the mouse liver, which are T-bet positive and express TRAIL but Eomes are negative (Daussy et al., 2014; Sojka et al., 2014). An intraepithelial ILC1 which is implicated the pathology of a mouse model of colitis and is enriched in patients with Crohn's disease has been described in humans and mice (Fuchs et al., 2013). These cells expressed NKp44, T–bet and Eomes, and produced IFNγ in response to IL-12 and IL-15 and were partly IL-15R independent (Fuchs et al., 2013). An additional ILC1 subset has been described in the human tonsil and in the inflamed gut (Bernink et al., 2013). These cells expressed T-bet, lacked NK cell markers including granzyme B and perforin and produced IFNγ in response to IL-12 (Bernink et al., 2013). ILCs with an ILC1 type phenotype have also been described to develop from ILC3s. These cells upregulate T-bet and downregulate RORγt to acquire the ability to produce IFNγ in response to IL-12 (Bernink et al., 2013; Klose et al., 2014; Klose et al., 2013; Vonarbourg et al., 2010). Recently this plasticity from an ILC3 phenotype to an ILC1 phenotype has been reported to be reciprocal, with human ILC1 capable of differentiating towards an ILC3 phenotype in the context of IL-23, IL-1β and retinoic acid (Bernink et al., 2015)

In the context of infection, ILC1s (that are not NK cells) are implicated in the response to the intracellular parasite *Toxoplasma gondii* and also in colitis. In response to *T. gondii* infection ILC1s in the gut have been described to produce IFNγ and TNFα, which was important for the outcome of infection (Klose et al., 2014). ILC1s that were derived from RORγt expressing ILC3s and produced IFNγ were described to contribute to resistance to infection with Salmonella species through mucus release but can also contribute to enterocolitis (Klose et al., 2013). In mice, IFNγ production from a RORγt dependent ILC also contributes to intestinal pathology following *Helicobacter hepaticus* infection (Buonocore et al., 2010). Conventional

NK cells have a well-described role in the response to viral infections and to other intracellular pathogens (Bancroft, 1993; Biron et al., 1999). Their role in *Mtb* infection was discussed above.

1.7.1.2 ILC2

ILC2 express high levels of GATA3 and produce cytokines associated with a T helper 2 (Th2) response (reviewed in Spits et al., 2013). They respond to a variety of cytokines including IL-25, IL-33, TSLP, IL-2 and IL-9 with production of IL-4, IL-5, IL-9 and IL-13 as well as other factors such as amphiregulin (reviewed in Spits et al., 2013). An IL-25 responsive non- T non-B cell capable of producing IL-5 and IL-13 cell was suggested to exist in 2001 (Fort et al., 2001). Subsequently such cells were shown to also respond to IL-33 and identified as natural helper cells (Moro et al., 2010), nuocytes (Neill et al., 2010) and innate helper 2 cells (Price et al., 2010), now referred to as ILC2s. ILC2s have been identified in a variety of organs including fat associated lymphoid tissue (Moro et al., 2010), adipose tissue (Brestoff et al., 2015; Hams et al., 2013; Molofsky et al., 2013), lungs (Chang et al., 2011; Fort et al., 2001; Monticelli et al., 2011), mesentertic lymph nodes (Neill et al., 2010; Price et al., 2010) and intestine (Hoyler et al., 2012).

ILC2s depend upon GATA3 for their function and maintenance in both mice and humans (Hoyler et al., 2012; Klein Wolterink et al., 2013; Yagi et al., 2014); (Mjosberg et al., 2012). ILC2s also depend on RORα for development. Deficiency in RORα leads to deficiency of ILC2s systemically and impaired induction of an allergic immune response and immunity to helminths (Halim et al., 2012; Wong et al., 2012). In addition, ILC2s depend upon the transcription factor TCF-1 (encoded by *Tcf7*). Deletion of *Tcf7* leads to a defect in ILC2 development and an impaired response to helminth infection (Mielke et al., 2013; Yang et al., 2013). The transcription factor Gfi1 is also required in ILC2 development to suppress expression of ILC3 specific genes (Spooner et al., 2013), similarly to that described in Th2 cells

where Gfi1 suppresses non-Th2 cell lineages (Zhu et al., 2010). Recently Bcl11b was found to be required for ILC2 development (Walker et al., 2015a; Yu et al., 2015).

ILC2s are an important source of type 2 cytokines in the immune response to helminth infections. In response to *Nippostrongylus brasiliensis* ILC2s production of IL-13 is required for protective immunity (Moro et al., 2010; Neill et al., 2010; Price et al., 2010). ILCs have been shown to interact with T cells via MHC class II and in the context of *N. brasiliensis* infection (Oliphant et al., 2014). This interaction is required for optimal Th2 responses and the ability of transferred ILC2s to reduce worm burden in IL-13 deficient mice (Oliphant et al., 2014). In addition ILC2s are required to promote tissue repair to the lung stages of *N. brasiliensis* infection (Turner et al., 2013). In this context ILC2 accumulation, promotion of tissue repair and amphiregulin expression was dependent upon IL-9 signalling (Turner et al., 2013). In the context of influenza infection ILC2s are described to induce airway hyper-reactivity (Chang et al., 2011). In contrast to this detrimental role during influenza infection, ILC2-derived amphiregulin was required to the restoration of tissue homeostasis following infection (Monticelli et al., 2011).

1.7.1.3 ILC3

ILC3s have many developmental and functional similarities with Th17 cells. ILC3s express RORγt and respond to IL-1β, IL-23 and in some cases IL-12 and produce, IL-22, IL-17, IFNγ and GM-CSF (reviewed in Artis and Spits, 2015; Mortha et al., 2014; Spits et al., 2013; Vonarbourg et al., 2010). Several different subtypes of ILC3 have been described: $CCR6^+$ LTi cells, $CCR6^-$ $NKp46^+$ ILC3s and $CCR6^-$ $NKp46^-$ ILC3s, each having different capabilities to produce the cytokines described above (reviewed in Artis and Spits, 2015; Serafini et al., 2015; Spits et al., 2013). All ILC3 subtypes are dependent upon RORγt for development, with RORγt deficient mice lacking lymph nodes (Artis and Spits, 2015; Eberl et al., 2004; Satoh-Takayama et al., 2008). ILC3s also require Ahr for development, with *Ahr* deficient mice showing defects

in development of ILC3s, decreased IL-22 production and increased susceptibility to *Citrobacter rodentium* infection (Lee et al., 2012; Qiu et al., 2012). Transfer experiments have shown that NKp46^{+} ILC3s develop from NKp46^{-} cells (Vonarbourg et al., 2010). Furthermore, this differentiation was accelerated by IL-12 (Vonarbourg et al., 2010) and required upregulation of T-bet (Klose et al., 2013; Rankin et al., 2013). In addition Notch signalling and the Notch target TCF-1, downstream of T-bet, was shown to be required for the differentiation of NKp46^{+} ILC3s (Mielke et al., 2013; Rankin et al., 2013).

ILC3s are important in the immune response to bacterial and fungal infection. ILC3 derived IL-22 is crucial for the response to both intestinal and respiratory pathogens. ILC3 derived IL-22, and its appropriate localisation, has been seen to be required for the innate response to *C. rodentium* infection (Qiu et al., 2012; Satoh-Takayama et al., 2014; Satoh-Takayama et al., 2008; Sonnenberg et al., 2011). In *Streptococcus pneumoniae* infection ILC3 derived IL-22 is also important to the immune response (Van Maele et al., 2014). IL-17 production by ILC3s has also been shown to be protective in the innate response to *Candida albicans* (Gladiator et al., 2013).

ILC3s also have an important role in maintaining intestinal homeostasis. IL-22 producing ILC3s were seen to be required for anatomical containment of commensal bacteria (Sonnenberg et al., 2012). Furthermore, ILC3-derived GM-CSF production in response to commensal bacteria, was essential to promote Tregs and for intestinal homeostasis (Mortha et al., 2014). More recently, ILC3s have been described to possess the capability to process and present antigen to T cells and this function has been shown to be required to maintain intestinal homeostasis (Hepworth et al., 2013). ILC3s were subsequently shown to induce death of T cells specific for commensal bacteria (Hepworth et al., 2015).

1.7.5 Innate lymphoid cells in Mtb infection?

The response of innate lymphoid cells, other than NK cells (discussed above), to *Mtb* infection is unknown. Cytokine production by an "innate like", Thy1.2^{+} CD3^{-} CD4^{-} CD8^{-} γδ TCR^{-} population upon *Mtb* challenge has been described in mice vaccinated with BCG in the context of IL-10R blockade but these were not characterised further (Pitt et al., 2012b). Furthermore the response of ILCs to primary infection is unknown. It is possible they could impact the immune response to *Mtb* at several stages. They could provide an early source of cytokine influencing the development of the granuloma in lung and/or they could provide some level of protection when T cell immunity is failing to control infection.

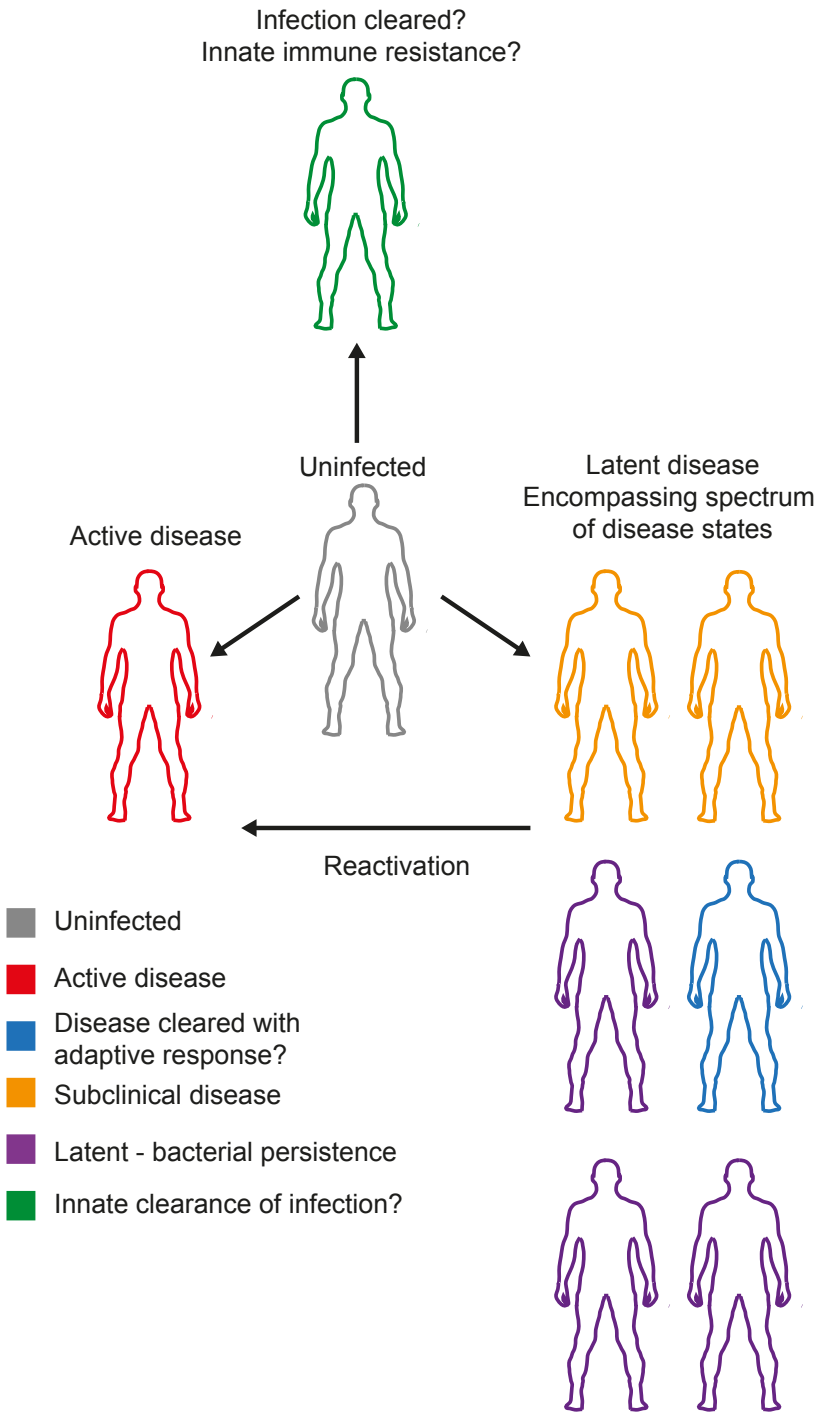

Figure 1.1 Clinical outcomes following infection with Mtb

Following infection with *Mtb* there are several possibility clinical outcomes. An individual can develop a primary active disease (red), displaying symptoms including fever, night sweats and haemoptysis. The majority of individuals will develop latent disease, where there is evidence of infection through demonstration of an adaptive response but lack of clinical symptoms. This latent state could encompass different diverse responses from those controlling infection but with bacterial persistence (purple) to those who may have eradicated the bacteria (Molofsky et al.) or to those with subclinical disease (yellow). An individual with latent disease can progress to active disease in a process termed reactivation. An additional scenario is suggested to exist where an individual is capable of eradicating infection without initiating an adaptive response (green), although this is difficult to prove. Figure based on O'Garra et al., 2013.

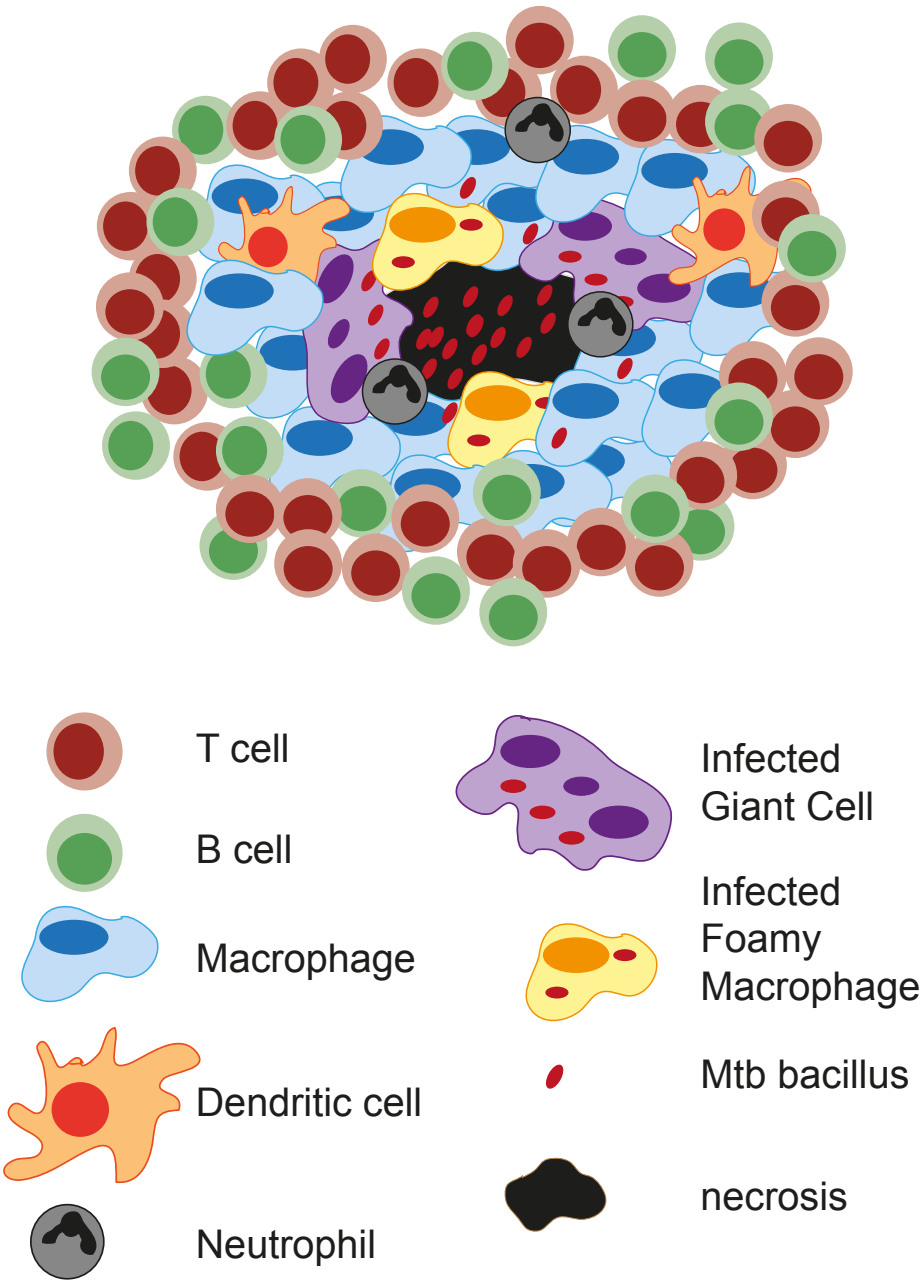

Figure 1.2 The structure of the tuberculous granuloma

Following aerosol inhalation of *Mtb*, alveolar macrophages are thought to be the first cell type infected. Subsequently other phagocytic cells are recruited including DCs and neutrophils, which may also become infected with *Mtb*. *Mtb* creates a niche within this early collection of cells where uncontrolled growth occurs. Following migration of DCs to the draining lymph node and priming of an adaptive immune response bacterial growth can be controlled. T and B cells form a lymphocytic cuff surrounding infected and activated macrophages. The centre of the granuloma contains the majority of bacteria and can become necrotic. Macrophages can differentiate into foamy macrophages or fuse to form giant cells. DCs and neutrophils are also found within the granuloma. Figure based on Ramakrishnan, 2012.

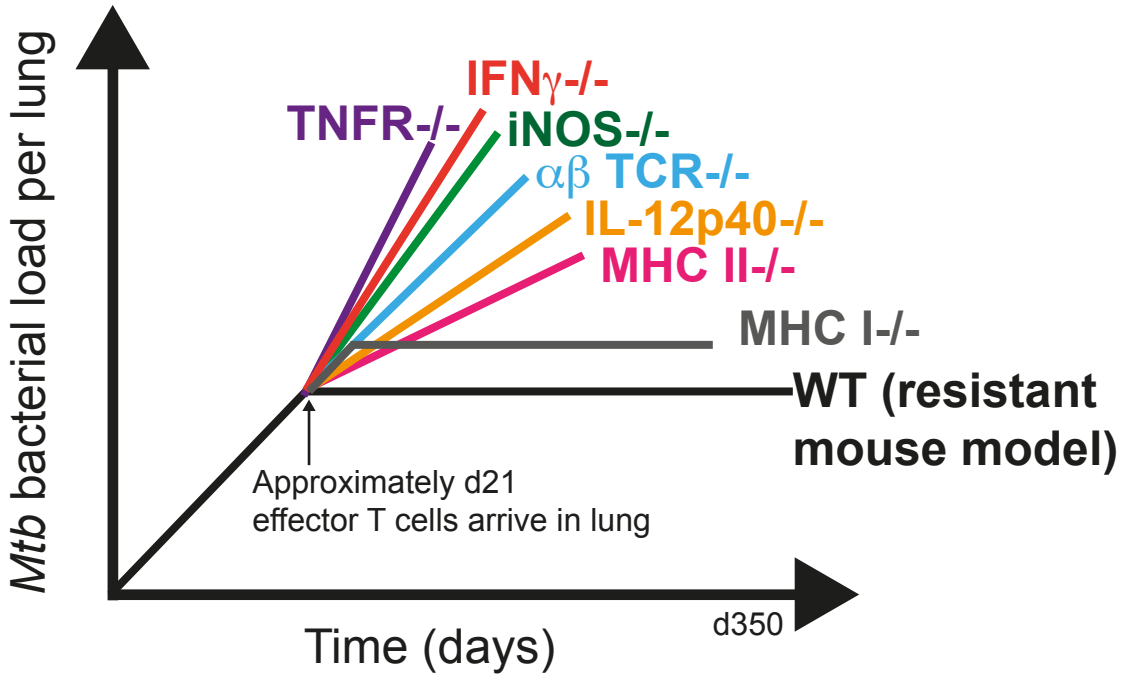

Figure 1.3 Factors of the immune response known to be protective from studies in mice.

In a "resistant" mouse strain bacterial growth occurs exponentially until 3-4 weeks post infection where a plateau in bacterial load is observed. Mice deficient in the 55 kDa TNRα receptor (TNFR), IFNγ, inducible nitric oxide synthase (iNOS), αβ T cell receptor (αβTCR), IL-12p40 or MHC class II (MHC II) all fail to obtain this plateau and display increased bacterial loads past 3-4 weeks and succumb to infection earlier than wild-type mice. Mice deficient in MHC class I (MHC I) are able to control infection, albeit at higher bacterial loads. Modified from North and Jung, 2004.

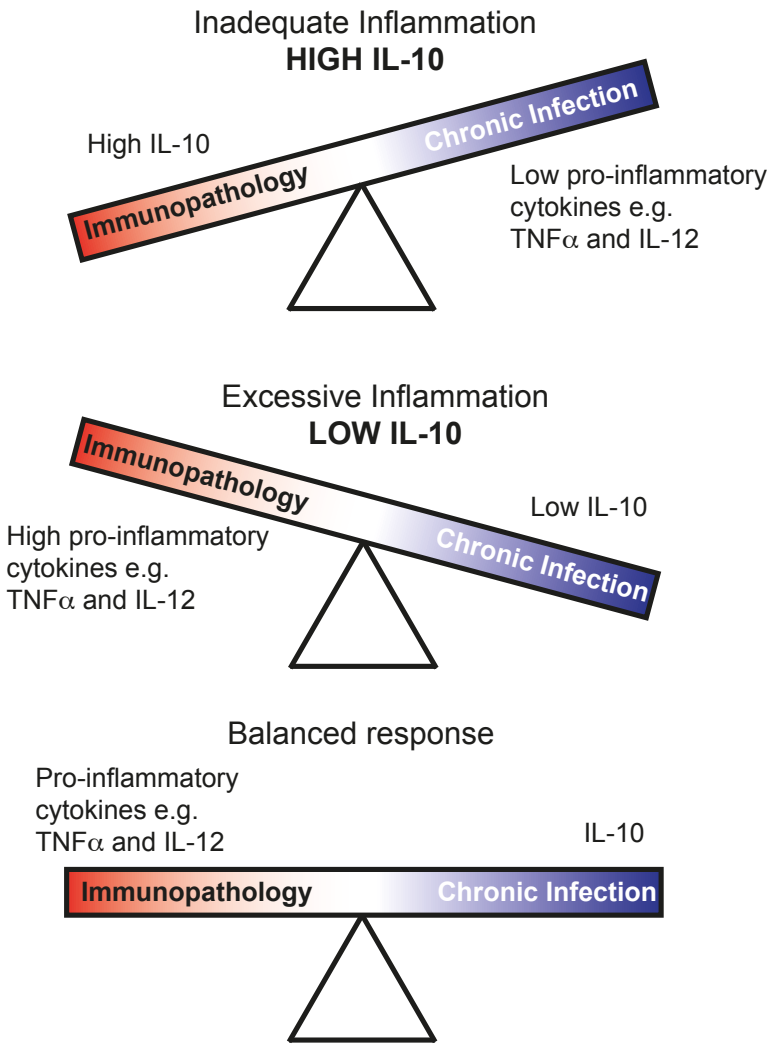

Figure 1.4 IL-10 regulates the balance of the immune response

The level of IL-10 production is important in controlling the balance of an immune response. Too much IL-10 leads to low production of pro-inflammatory cytokines and can contribute to the establishment of chronic infection. In contrast, too little IL-10 leads to excessive production of pro-inflammatory cytokines, including TNFα and IL-12, and results in immunopathology. A balance between production of pro-inflammatory cytokines and IL-10 is required to control infection but avoid immunopathology

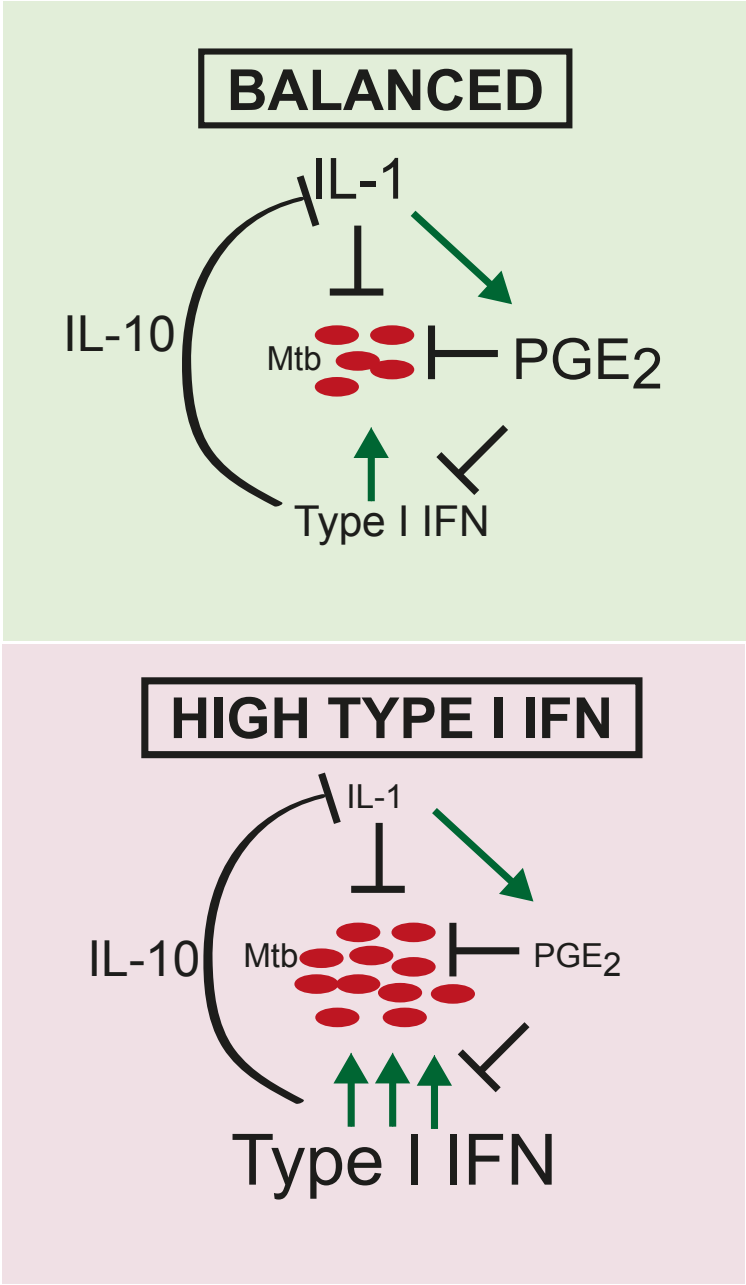

Figure 1.5 Counter regulation of IL-1, PGE_2 and type I IFN influences outcome of Mtb infection

A balance between IL-1, PGE_2 and type I IFN levels is required for containment of bacterial growth and avoidance of immunopathology. When high levels of type I IFN are present during *Mtb* infection this suppresses IL-1 production, at least partially via IL-10, leading to low PGE_2 levels and exacerbated bacterial growth. Figure based on Mayer-Barber et al., 2014.

Name	Antigen(s)	Delivery system	Description	Phase in clinical trials
Recombinant mycobacterial strains				
MTBVAC	N/A	Live vaccine	Genetic deletion of PhoP and fad26	Phase Ia
VPM 1002	N/A	Live vaccine	BCG strain expressing listeriolysin with urease deletion	Phase IIa
Viral vectors				
MVA85A	Ag85A	Modified vaccinia virus Ankara	Viral vector expressing Ag85A	Phase IIb
Ad5 Ag85A	Ag85A	Adenovirus 5	Viral vector expressing Ag85A	Phase I
Ad35/ MVA85A	Ag85A, Ag85B, TB10.4 Ag85A	Adenovirus 35 Modified vaccinia virus Ankara	Viral vectors expressing Ag85A, Ag85B and TB10.4	Phase I
AERAS 402	Ag85A, Ag85B, TB10.4	Adenovirus 35	Viral vector expressing Ag85A, Ag85B and TB10.4	Phase IIa
Protein in Adjuvant				
H1	Ag85B, ESAT-6	Adjuvant IC31		Phase IIa
H4	Ag85B, TB10.4	Adjuvant IC31		Phase I
H56	Ag85B, ESAT-6, Rv2660c	Adjuvant IC31	Also designed to prevent reactivation of latent infection	Phase I
M72	Rv1196, Rv0125	Adjuvant AS01		Phase IIa
ID93	Rv2608, Rv3619, Rv3620, Rv1813	Adjuvant GLA-SE		Phase I

Figure 1.6 Prophylactic vaccine candidates currently in clinical trials

Novel vaccine candidates broadly fall into 3 categories: 1. Recombinant mycobacterial strains designed to replace BCG. 2. Viral vectors capable of expressing *Mtb* antigens designed to boost pre-existing BCG immunity. 3. Protein antigens from *Mtb* given in adjuvant to boost pre-existing BCG immunity. Phase I clinical trials assess the safety of the vaccine candidate. Phase IIa clinical trials determine the dose and/or route of administration. Phase IIb clinical trials assess the immunogenicity of the vaccine and provide the first evidence vaccine efficacy. Finally candidate vaccines are assessed in Phase III clinical trials, which assess vaccine efficacy. Figure based on Andersen and Kaufmann, 2014.

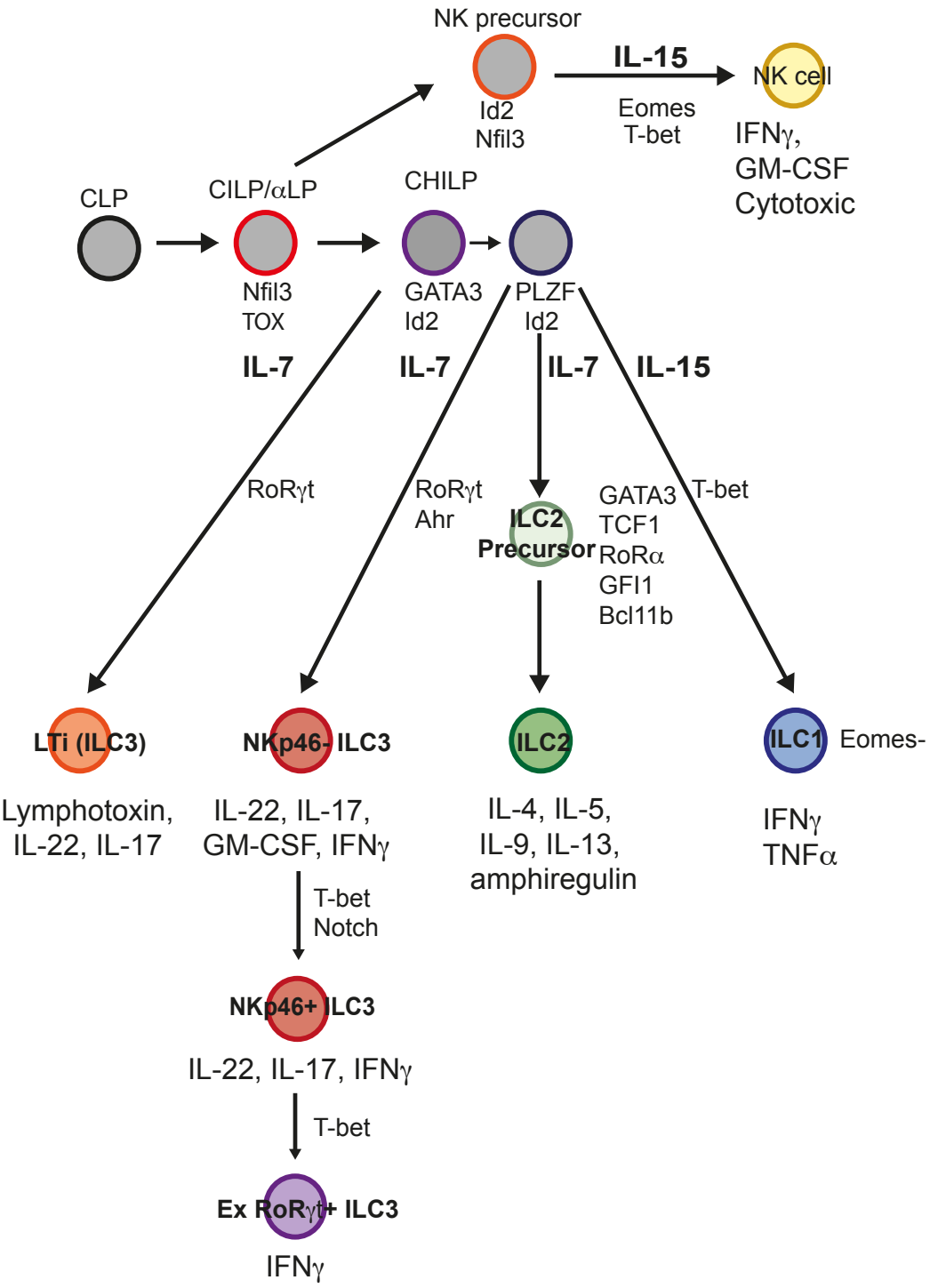

Figure 1.7 Model of the development of innate lymphoid cells

ILCs develop from the Common Lymphoid Progenitor (CLP) via the Common Innate Lymphoid Progenitor (CILP) also referred to as the α Lymphoid Progenitor (αLP), capable of giving rise to all ILC subsets including NK cells. The Common Helper-like Innate Lymphoid Progenitor (CHILP) is downstream of the CILP/αLP and can give rise to all non-cytotoxic ILCs. The expression of the transcription factor PLZF confers more restricted potential. ILCs are divided into ILC1, ILC2 and ILC3 subsets based on their requirements for various transcription factors and the cytokines they produce. A precursor with further restricted potential has also been described, capable of giving rise to ILC2s only (Hoyler et al., 2012). Figure based on Artis and Spits, 2015 and Diefenbach et al., 2014.

Chapter 2: Materials and Methods

2.1 Mice

All mice were kept under Specific Pathogen Free conditions at the Francis Crick Institute Mill Hill Laboratories in accordance with UK Home Office regulations and the Animals (Scientific Procedures) Act 1986. C57BL/6, B6.129S7-*Rag1*^{tm1MOM}, B6.129S7-*Rag1*^{tm1MOM} x B6;129X1-*Il15ra*^{tm1Ama}, B6.129S7-*Rag1*^{tm1MOM} x C57BL/6J-*Il7*^{hlb368} and B6.129-*Rag2*^{tm1Fwa} x 129Ola.BALB/c.B6 *Il2rg*^{tm1Cgn} (only mice homozygous for mutated alleles were used in experiments) mice were bred under Specific Pathogen Free (SPF) conditions at the Francis Crick Institute Mill Hill Laboratories. CBA/J mice were either bred at the Francis Crick Institute Mill Hill Laboratories in SPF conditions or purchased from Jackson Laboratories (Bar Harbour, USA) as indicated. Female mice were appropriately age matched between 8 and 18 weeks for all *in vivo* experiments.

2.2 Growth of Bacteria

2.2.1 Mtb

The *Mtb* strain H37Rv was originally obtained from The London School of Hygiene and Tropical Medicine. Hyper-virulent *Mtb* strain HN878 was obtained from Barry Kreisworth at the Public Health Research Institute, Newark,USA.

To grow stock batches of both strains of *Mtb,* they were plated on solid 7H11 (BD Middlebrook) supplemented with 10% albumin dextrose catalase (ADC; BD, Middlebrook) plates. Up to 10 colonies from these cultures were used to inoculate fast rolling (rotation at 25rpm) 10ml cultures of 7H9 media (BD, Middlebrook) supplemented with 10% oleic albumin dextrose catalase (OADC; BD, Middlebrook) and 0.5% glycerol and 0.05% Tween (Sigma). The optical density at 600nm (OD_{600}) was used to monitor bacterial growth. When an OD_{600} of 1 was reached, 1ml was used to inoculate a 50ml slow rolling culture (rotation at 2.5 rpm) of fresh 7H9 media (supplemented as above). The OD_{600} was again monitored and at OD_{600} of 1 the

culture was split into two 50ml tubes and centrifuged at 3000rpm for 20mins. HN878 pellets were washed once with PBS supplemented with 0.05% Tween-80 (Sigma) then in PBS and centrifuged at 800rpm to remove clumps. The supernatant was the collected and made up to 100ml in PBS and aliquots of 1ml were frozen at -80°C until use. H37Rv pellets were washed once with PBS supplemented with 0.05% Tween-80 (Sigma) then twice in PBS. H37Rv pellets were then resuspended in PBS + 10% glycerol before being centrifuged at 600rpm to remove clumps. The supernatant was made to 100ml in PBS + 10% glycerol and aliquots of 1ml were frozen at -80°C until use.

To determine stock concentrations for both strains, 2-3 vials were thawed and serially diluted in PBS. Dilutions were plated on solid 7H11 (BD, Middlebrook) supplemented with 10% OADC (BD, Middlebrook) and incubated at 37°C for 2-3 weeks before colonies were counted and concentrations calculated. In order to ensure stocks were not contaminated, they were also plated on blood agar plates (10% sheep's blood) and incubated for up to 5 days.

2.2.2 BCG

BCG strain Danish 1331 was obtained from Statens Serum Institute, Denmark. Stock batches of BCG were grown in 7H9 media (BD, Middlebrook) supplemented with 0.5% glycerol, 0.05% Tween-80 (Sigma) and 10% ADC (BD Middlebrook). 10ml fast cultures were inoculated with approx. 4 colonies of BCG, previously plated on solid 7H11 (BD, Middlebrook) supplemented with OADC (BD, Middlebrook). The OD_{600} was monitored and when this reached 1, 1ml was used to inoculate a 90ml slow rolling culture of fresh supplemented 7H9 media. The OD_{600} was again monitored. At OD_{600} of 1 the culture was split into two 50ml tubes and centrifuged at 2500rpm for 25mins. Pellets were washed in PBS supplemented with 5% glycerol and 0.1% Tween-80 (Sigma) and spun again at 2500rpm for 25 minutes. The two pellets were then combined, resuspended in PBS supplemented as above and spun again. The pellet was

resuspended in 50-75ml PBS supplemented as above and aliquoted into 1ml aliquots. These were frozen at -80°C until use.

As for *Mtb* strains, stock concentrations were determined by thawing 2-3 vials and serially diluting them in PBS. Dilutions were plated on solid 7H11 (BD, Middlebrook) supplemented with 10% OADC (BD, Middlebrook) and incubated at 37°C for 2-3 weeks before colonies were counted and concentrations calculated. In order to ensure stocks were not contaminated, they were also plated on blood agar plates (10% sheep's blood) and incubated for up to 5 days.

2.3 Reagents

2.3.1 Monoclonal antibodies used for injections in vivo

2.3.1.1 anti-IL-10 Receptor

Anti-IL-10 Receptor (αIL-10R) monoclonal antibody (clone 1B1.3A, rat IgG1) and isotype control (clone GL113, rat IgG1) were gifts from DNAX (now Merck, USA). These were grown up and purified by Harlan Laboratories, USA, and contained less than 0.5 EU/mg endotoxin. The required concentrations were obtained through dilutions in PBS (Gibco). For *in vivo* vaccination experiments mice were injected intraperitoneally with 300μl containing 1mg of either αIL-10R antibody or isotype control the day prior to vaccination. Subsequently they received a total of 6 300μl intraperitoneal (i.p.) injections weekly containing 0.35mg αIL-10R antibody or isotype control.

2.3.1.2 anti-GM-CSF

anti-GM-CSF (αGM-CSF) monocloncal antibody (clone MP1-22E9) and isotype control (clone GL117, rat IgG2a) were gifts from DNAX (now Merck, USA). These were grown up and purified by Harlan Laboratories, USA and contained 0.5EU/mg endotoxin or less. The required

concentrations were obtained through dilutions in PBS (Gibco). For *in vivo* experiments mice were injected intraperitoneally with 300μl containing 1mg of either αGM-CSF antibody or isotype control the day prior to *Mtb* infection. Subsequently they received twice weekly i.p. injections of 300μl containing 0.3mg αGM-CSF antibody or isotype control for the course of the experiment.

2.3.1.3 anti-Ly6G

anti-Ly6G (αLy6G) monoclonal antibody (clone 1A8) was purchased from BioXCell and contained less than 0.76EU/mg endotoxin. Isotype (Rat IgG2a clone GL117) was a gift from DNAX (now Merck, USA) and was grown up and purified by Harlan Laboratories, USA and contained 0.5EU/mg endotoxin. Required concentrations of αLy6G or isotype control were acquired by dilution in PBS. For *in vivo* experiments mice received a total of 5 i.p. injections containing 0.2mg of αLy6G or isotype control on days 10, 12, 14, 16 and 18 post *Mtb* infection.

2.3.2 Media for cell culture

Cell were cultured in RPMI 1640 (BioWhittaker, Lonza) complemented with 5 or 10% heat-inactivated FCS (BioWhittaker, Lonza), 0.05mM 2-ME (Sigma-Aldrich), 10mM HEPES buffer (BioWhittaker, Lonza), 100U/ml penicillin (BioWhittaker, Lonza), 100U/ml streptomycin (BioWhittaker, Lonza), 2mM L-glutamine (BioWhittaker, Lonza), 1mM sodium pyruvate (BioWhittaker, Lonza).

2.4 BCG Vaccination

Vaccination was carried out under Biological Safety Level-2 (BSL) or BSL-3 conditions. Mice received 2 intradermal (i.d.) injections of 5μl in the thigh containing approximately $5x10^5$ CFU of BCG in PBS (Gibco) or PBS (Gibco) as a control.

2.5 Aerosol *Mtb* Infection

All experiments using *Mtb* were carried out under BSL-3 conditions. Mice were exposed to approximately $5x10^6$ *Mtb* CFU aerosolised using a 3-jet Collision nebulizer unit (BGI, USA) for a period of 30mins. This delivered approximately 100-200 CFU to the lung. Delivery of bacteria to the lung was determined by plating homogenised lung on 7H11 (BD Middlebrook) media supplemented with 10% OADC (BD Middlebrook) and BBl MIGIT PANTA antibiotic cocktail (BD, Middlebrook which contains the following antibiotics: Polymyxin B 6,000 units/L, Amphotericin B 600 g/L, Nalidixic acid 2,400g/L, Trimethroprim 600 g/L, and Azlocillin 600 g/L, plates were produced at NIMR) on the day of infection. Visible colonies were counted 4 weeks later and bacterial load per lung determined.

In experiments that required BCG vaccination, aerosol challenge with *Mtb* was performed 6-9 weeks following BCG vaccination.

2.6 Harvest of *Mtb* infected organs for cell culture and CFU determination

Lung and spleens from infected animals were aseptically dissected and placed into 5ml RPMI (BioWhittaker, Lonza) or 2ml of collagenase D at 1mg/ml (Roche) as indicated. Organs placed into collagenase D were incubated at 37°C 5% CO_2 for 45 minutes. Organs were homogenised by passage through a 70μm filter with the piston of a 2ml syringe. 3ml RPMI (BioWhittaker, Lonza) were added to organs digested with collagenase.

Serial dilutions were made of the cell suspensions and streaked onto 7H11 media (BD Middlebrook) supplemented with OADC (BD Middlebrook) and BBl MIGIT PANTA antibiotic cocktail (see above; plates produced at NIMR). Plates were incubated for 2-3 weeks before colonies were counted and bacterial load per lung calculated.

2.7 Restimulation of cell cultures with PPD

For cell culture 0.83% ammonium chloride (produced at the Francis Crick Institute Mill Hill Laboratories) or ACK lysis buffer (Life technologies, Thermo Fischer Scientific) was used to lyse red cells. Numbers of live cells were determined using trypan blue exclusion. $1x10^6$ lung cells and $5x10^6$ spleen cells were cultured with 20μg/ml PPD (Statens Serum Institute, Denmark) and 2μg/ml anti-CD28 (αCD28, clone 37.51, Harlan Laboratories, USA) for 16 hours at 37°C, 5% CO_2. Supernatants were harvested before addition of 10μg/ml Brefeldin A for a further 4 hours to allow cytokine assessment by intra-cellular cytokine staining (total stimulation time=20hrs).

2.8 Restimulation of cell cultures with PMA and Ionomycin

For cell culture 0.83% ammonium chloride (produced at the Francis Crick Institute Mill Hill Laboratories) or ACK lysis buffer (Life technologies, Thermo Fischer Scientific) was used to lyse red cells. Numbers of live cells were determined using trypan blue exclusion. $5x10^5$ cells were cultured with 50ng/ml PMA (Sigma-Aldrich) and 500ng/ml ionomycin (Calbiochem) and 10μg/ml Brefeldin A (Sigma-Aldrich) at 37°C, 5% CO_2 for 2h as indicated.

2.9 Flow cytometry and intracellular staining

Direct *ex vivo* cell suspensions or cells harvested following restimulation were aliquoted into capped polystyrene 5 ml tubes (BD Falcon) and washed with 2ml PBS (Gibco) and incubated with 2μg anti-FcγRI/FcγRII (24G2, National Institute for Medical Research, now Francis Crick Institute Mill Hill Laboratories). To identify live cells, cells were stained with a red LIVE/DEAD cell stain kit (Invitrogen), according to manufacturer's instructions. Cells were then resuspended in 100μl of a cocktail of antibodies against extracellular markers as indicated and incubated for 20 minutes. For details of antigens and fluorochromes used see table 2.1.

Cells were then washed with 2ml PBS and, if intracellular staining was not required, resuspended in 250µl BD stabilising fix (BD Biosciences).

Intracellular staining for transcription factors was carried out using the Foxp3 staining kit (eBioscience) in line with the manufacturer's instructions. Intracellular staining for cytokines was carried out using Cytofix/Cytoperm kit (BD Biosciences) according to the manufacturer's instructions. Following fixation and permeabilisation cells were resuspended in 100µl of a cocktail of antibodies against intracellular antigens for 30mins. For details of antigens and fluorochromes used see table 2.1. Cells were then washed and resuspended in 250µl BD stabilising fix (BD Biosciences). Samples were incubated overnight at 4°C before acquisition a nine-colour CyAN ADP analyzer (Dako, Ely, UK) using Summit software (Cytomation), under BSL-3 conditions. Analysis was carried out using Flow Jo version 9.4.11 (Treestar). Gates for CD127, CD25 and T1/ST2 were set using Fluorescence Minus One (FMO) controls. Gates for cytokine staining were set using isotype controls. Gates for transcription factor staining were set using either isotype or FMO controls.

Table 2.1 Antibodies used for flow cytotometry

Antigen	Fluorochrome	Clone	Species and Isotype	Source	Concentration used
Extracellular					
B220	PerCP Cy5.5	RA3-6B2	Rat IgG2a k	eBiosciences	1µg
B220	APC	RA3-6B2	Rat IgG2a k	eBiosciences	1µg
CD115	APC	AFS98	Rat IgG2a k	eBiosciences	1µg
CD11b	PerCP Cy5.5	M1/70	Rat IgG2b k	eBiosciences	0.5µg
CD11b	PE Cy7	M1/70	Rat IgG2b k	eBiosciences	1µg
CD11b	APC	M1/70	Rat IgG2b k	eBiosciences	1µg
CD11b	v500	M1/70	Rat IgG2b k	BD Horizon	1µg
CD11c	PE	HL3	Armenian Hamster IgG1	BD Horizon	1µg
CD11c	v450	HL3	Armenian Hamster IgG1	BD Horizon	1µg
CD11c	PerCP Cy5.5	N418	Armenian Hamster IgG	eBiosciences	1µg
CD11c	APC	HL3	Armenian Hamster IgG1	BD Horizon	1µg
CD127	PE	A7R34	Rat IgG2a k	eBiosciences	2µg
CD25	APC e780	PC61.5	Rat IgG1 l	eBiosciences	2µg
CD27	PerCP Cy5.5	LG.3A10	Armenian Hamster IgG	BioLegend	1µg
CD27	APC	LG.7F9	Armenian Hamster IgG	eBiosciences	1µg
CD3	APC	145-2C11	Armenian Hamster IgG1	eBiosciences	1µg
CD3	APC e780	17A2	Rat IgG2b	eBiosciences	2ug
CD3	PerCP Cy5.5	145-2C11	Armenian Hamster IgG1	eBiosciences	1µg
CD4	e450	RM4-5	Rat IgG2a k	eBiosciences	1µg
CD4	v500	RM4-5	Rat IgG2a k	BD Horizon	1µg
CD49b	PerCP Cy5.5	DX5	Rat IgM k	eBiosciences	2µg
CD49b	APC	DX5	Rat IgM k	eBiosciences	2µg
CD5	APC	53-7.3	Rat IgG2a k	eBiosciences	0.5µg
CD5	PerCP Cy5.5	53-7.3	Rat IgG2a k	eBiosciences	0.5µg
CD8	PerCP e710	53-6.7	Rat IgG2a k	eBiosciences	1µg
CD8	v500	53-6.7	Rat IgG2a k	BD Horizon	1µg
CD86	Brilliant Violet 421	GL-1	Rat IgG2a k	BioLegend	2.5µg
F4/80	PE Cy7	BM8	Rat IgG2a k	eBiosciences	1µg
F4/80	APC	BM8	Rat IgG2a k	eBiosciences	1µg
γδ TCR	FITC	eBioGL3	Armenian Hamster IgG	eBiosciences	2.5µg
Ly6C	PerCP Cy5.5	HK1.4	Rat IgG2c	eBiosciences	0.5µg
Ly6G	FITC	1A8	Rat IgG2a k	BD Pharmingen	2.5µg
MHC II (I-A/I-D)	APCe780	M5/114.15	Rat IgG2b k	eBiosciences	1µg
NK1.1	PE	PK136	Mouse IgG2a k	eBiosciences	1µg
NK1.1	PerCP Cy5.5	PK136	Mouse IgG2a k	eBiosciences	1µg
NK1.1	APC	PK136	Mouse IgG2a k	eBiosciences	1µg
NKp46	PE	29A1.4	Rat IgG2a k	eBiosciences	4µg
Sca-1	v500	D7	Rat IgG2a k	BD Horizon	2µg
T1/ST2	FITC	DJ8	Rat IgG1	MD Bioproducts	5µg
TCR β	PerCP Cy5.5	H57-597	Armenian Hamster IgG	eBiosciences	0.5µg
TCR β	APC	H57-597	Armenian Hamster IgG	eBiosciences	0.5µg
Thy1.2 (CD90)	PE Cy7	53-2.1	Rat IgG2a k	eBiosciences	1µg
Isotypes					
Rat IgG1	e450	eBRG1	n/a	eBiosciences	2µg
Rat IGg2a	APC	eBR2a	n/a	eBiosciences	2µg
Rat IGg2a	PE	eBR2a	n/a	eBiosciences	2µg
Rat IGg2a	FITC	eBR2a	n/a	eBiosciences	2µg
Mouse IgG1	Pacfic Blue	MOPC-21	n/a	BioLegend	5µg
Rat IgG1k	PerCP e710	eBRG1	n/a	eBiosciences	2µg
Rat IGg2ak	Brilliant Violet 421	RTK2758	n/a	BioLegend	2.5µg
Rat IgG1k	Brillian Violet 510	RTK2071	n/a	BioLegend	5µg
Intracellular					
GM-CSF	PE	MP1-22E9	Rat IGg2a	eBiosciences	2µg
GM-CSF	FITC	MP1-22E9	Rat IGg2a	eBiosciences	2µg
IFNγ	e450	XMG1.2	Rat IgG1	eBiosciences	2µg
IL-17	Brilliant Violet 510	TC11-18H	Rat IgG1k	BioLegend	4µg
IL-17	APC	eBio17B7	Rat IGg2a	eBiosciences	2µg
IL-22	APC	IL22JOP	Rat IGg2a	eBiosciences	2µg
RoRγt	PerCP e710	B2D	Rat IgG1k	eBiosciences	2µg
T-bet	Pacific Blue	4B10	Mouse IgG1	BioLegend	5µg

2.10 Enzyme Linked Immunosorbent Assay (ELISA)

Cell free supernatants from restimulated cultures were assessed by ELISA for cytokines following sterilisation by gamma-irradiation (20kGrays, Synergy Health, UK). IL-17 and GM-CSF levels were assessed using commercially available kits from eBiosciences. A sandwich ELISA was used to assess IFNγ levels (capture: R46A2 detection: AN-18).

Table 2.2 Reagents used for ELISAs, their concentrations and sources

Cytokine	**Capture Antibody (concentration used)**	**Standard (top concentration)**	**Detection antibody (concentration used)**	**HRP-strepdavidin**	**Developing substrate**	**Source**
GM-CSF	Kit	Recombinant GM-CSF (10ng/ml)	kit	kit	TMB	eBiosciences
IL17A	Kit	Recombinant IL-17A (10ng/ml)	kit	kit	TMB	eBiosciences
IFNγ	R46A2 (2.72 μg/ml)	HDK1 Recombinant IFNγ (50ng/ml, DNAX)	AN-18 (1 μg/ml)	1ug/ml (Jackson Immunoresearch)	ABTS	The Francis Crick Institute Mill Hill Laboratories

2.11 Statistical Analysis

Data was analysed using GraphPad Prism software. A 2–way ANOVA with Tukey's post test analysis or an unpaired Student's t-test was performed as indicated in the figure legends. Differences were considered significant when $p<0.05$. * $p<0.05$, ** $p<0.01$, *** $p<0.001$, **** $p<0.0001$

Chapter 3: Determining whether IL-10 during BCG vaccination influences the early cytokine response to *Mtb* challenge in susceptible mice.

3.1 Does αIL-10R mAb treatment during BCG vaccination impact early cytokine production in susceptible CBA/J mice? Aims of the investigation

To determine how IL-10 during BCG vaccination impacts the early immune response upon *Mtb* challenge in susceptible CBA/J mice, we aimed to investigate:

1) Whether BCG vaccination in the context of IL-10R blockade impacted early control of bacterial load

2) If there was earlier recruitment of T cells to the lung upon *Mtb* challenge

3) Whether differences in the early T cell cytokine response to *Mtb* challenge, which could contribute to increased control of infection, correlated with increased protection in mice vaccinated with BCG in the context of IL-10R blockade

3.2 Background

Although BCG vaccination is one of the most widely given vaccines and the only licensed vaccine against tuberculosis, the efficacy it provides against adult pulmonary disease is variable with reports ranging from 0-80% (Fine, 1995). As a result, better vaccines or vaccine regimes are required. Development of such vaccines is complicated by several factors including lack of correlates of protection, and an incomplete understanding of what constitutes a protective immune response to *Mtb* infection (Andersen and Kaufmann, 2014).

Immunosuppressive mechanisms, including regulatory T cells, can negatively impact the immune response to vaccination and impair the level of protection they provide (Boer et al.,

2015). The immunosuppressive cytokine IL-10 has also been shown to negatively impact the protective capacity of vaccines in various scenarios. Indeed, vaccination against Leishmaniasis using leishmanial proteins was improved by blockade of IL-10 signalling (Darrah et al., 2010). Furthermore, DNA vaccination during chronic LCMV infection was only effective in the context of IL-10R blockade (Brooks et al., 2008). With respect to mycobacterial infection, the protective effect of vaccination with CFP-10 against subsequent *M. avium* challenge was enhanced in the absence of IL-10 signalling (Silva et al., 2001).

IL-10 is also able to suppress the immune response to BCG with IL-10 deficient mice displaying superior control of BCG bacterial loads (Murray and Young, 1999). IL-10 can also negatively impact the ability of BCG to provide protection towards subsequent *Mtb* challenge. Indeed, BCG vaccination in IL-10 deficient mice led to better control of *Mtb* bacterial loads upon challenge compared to wild type controls (Gopal et al., 2012). This higher control of bacterial load following BCG vaccination of IL-10 deficient mice, has also been shown at later time points (Pitt et al., 2012b). However, the specific role for IL-10 in vaccination rather than infection is difficult to delineate when using an *Il10* deficient mouse. It is unclear whether effects in the BCG vaccinated mouse are a result of an absence of IL-10 during vaccination, or a result of the absence of IL-10 during *Mtb* infection, as IL-10 deficient mice also display lower bacterial loads upon primary infection (Redford et al., 2010).

The suppressive role of IL-10 specifically during BCG vaccination has been addressed using treatment with anti-IL-10R monoclonal antibody (αIL-10R mAb) throughout vaccination in both resistant C57BL/6 and susceptible CBA/J mouse models (Pitt et al., 2012b). αIL-10R mAb treatment during BCG vaccination led to lower bacterial loads upon *Mtb* challenge at late time points (day 63 (C57BL/6 and CBA/J) and day 112 post infection (CBA/J only)) and was accompanied by increased and sustained IL-17 and IFNγ production in both mouse strains (Pitt et al., 2012b).

Different strains of mice display different levels of susceptibility to *Mtb* infection (North and Jung, 2004). Resistant strains include C57BL/6 and BALB/c mice, which succumb to primary infection approximately 300 days post infection (Medina and North, 1998). Susceptible mouse strains include CBA, DBA, C3H and I/St mouse strains (Eruslanov et al., 2005; Medina and North, 1998). These strains display higher bacterial loads than resistant mouse strains (from approximately 4 weeks post *Mtb* infection) and succumb to infection earlier at approximately 150 days post infection (Eruslanov et al., 2005; Medina and North, 1998; Turner et al., 2001). It is argued that susceptible mouse strains may provide a model more representative of human tuberculosis disease than the more commonly used resistant strains (Apt and Kramnik, 2009), suggesting that they may represent a better model in which to test the efficacy of vaccine regimes.

The susceptibility of the CBA/J strains to *Mtb* infection has been linked to increased levels of IL-10 production compared to resistant C57BL/6 mice (Beamer et al., 2008; Turner et al., 2002), suggesting this is a good model in which to study the suppressive effects of IL-10. Indeed, BCG vaccination in the context of αIL-10R mAb treatment led to a greater protective effect in the susceptible CBA/J mouse than in the resistant C57BL/6 mouse (Pitt et al., 2012b).

In the resistant C57BL/6 mouse model, IL-10R blockade during BCG vaccination led to an accelerated and enhanced Th1 response, with IFNγ producing T cells evident in the lung at day 20 post infection, however this was not assessed in the susceptible CBA/J model (Pitt et al., 2012b). Given that the immune response to *Mtb* is slow to develop in comparison to other infectious diseases (reviewed in Cooper, 2009; Robinson et al., 2015) and that the delayed onset of adaptive immune responses is linked to susceptibility to *Mtb* infection (Beamer et al., 2011; Chackerian et al., 2002b), this acceleration in the onset of the immune response could be an important mechanism by which protection in increased. The idea that acceleration in the onset

of an adaptive immune response can positively impact outcome of infection is supported by the observation that transfer of activated *Mtb* specific Th1 cells prior to infection is beneficial to control of bacterial load (Gallegos et al., 2011).

IL-10R blockade during BCG vaccination had a large effect upon control of bacterial load late in infection in the susceptible CBA/J mouse (Pitt et al., 2012b). One way in which this increased protection could occur is through the acceleration of the development of the adaptive immune response, as discussed above. As this was not assessed, further investigation is required to determine whether the development of an adaptive immune response is accelerated in the same way as in the resistant mouse strain. Furthermore, although it is known that IFNγ and $CD4^+$ T cells are crucial for the immune response to *Mtb* infection (Cooper, 2009; Cooper et al., 1993; Flynn et al., 1993; Flynn et al., 1992; Mogues et al., 2001), studies in both mouse models and humans have demonstrated that IFNγ production by $CD4^+$ T cells does not correlate with protection against *Mtb* (Abebe, 2012; Kagina et al., 2010; Mittrucker et al., 2007; Pitt et al., 2012a). Therefore, investigation of other aspects of the immune response may also provide insight into how IL-10R blockade during BCG vaccination could increase protection upon *Mtb* challenge.

3.3 Assessing the impact of IL-10R blockade during BCG vaccination on the early events in the lung following *Mtb* challenge

3.3.1 BCG vaccination in the context of αIL-10R mAb enhances control of Mtb bacterial load in chronic infection but this does not manifest early following challenge

Blockade of IL-10R signalling during BCG vaccination in susceptible CBA/J mice, enhances control of bacterial load in chronic infection (Pitt et al., 2012b), however the impact on the early control of bacterial load was not assessed. In order to determine whether this increased control of bacterial load begins early following infection we assessed bacterial loads at day 14, day 21 and day 28 post *Mtb* challenge. CBA/J mice received 1mg αIL-10R mAb or an isotype control antibody (clone 1B1.3A or GL113 respectively) via intraperitoneal (i.p.) injection one day prior to receiving intradermal BCG or PBS (PBS vaccinated mice are described as "unvaccinated"). Mice then received weekly i.p. injections containing 0.35mg αIL-10R mAb or the isotype control antibody for 6 weeks. Three weeks after the final i.p. injection, mice were challenged with aerosol *Mtb* infection and tissues harvested at 14, 21, 28 or 112 days following *Mtb* challenge, as shown in **Figure 3.1**.

Bacterial loads were determined in the lung and spleens as described in Materials and Methods and are shown in **Figure 3.2**. As expected we found that BCG vaccination alone led to lower bacterial loads in the lung compared to unvaccinated controls from day 14 post *Mtb* challenge and this was also evident at day 21 and day 28 (**Figure 3.2A**) (day 14 $p<0.001$, day 21 $p<0.0001$, day 28 $p<0.001$ BCG vaccination compared to unvaccinated controls). However we found that blockade of IL-10R through mAb treatment during vaccination did not increase this control of *Mtb* bacterial load any further than BCG vaccination alone at day 14, 21 or 28 post infection (**Figure 3.2A**). We did however find, as described by Pitt et al 2012, that BCG

vaccination in the context of αIL-10R mAb treatment led to better control of bacterial load at day 112 post *Mtb* challenge (**Figure 3.2A**) ($p<0.01$ BCG vaccination alone compared to BCG vaccination in the context of IL-10R mAb).

In the spleen we did not detect bacteria at day 14 or day 21 post *Mtb* challenge in vaccinated or unvaccinated mice (Figure 3.2B). At day 28 post *Mtb* challenge BCG vaccination alone led to lower *Mtb* bacterial loads in the spleen compared to unvaccinated mice. We did not find any additional benefit of αIL-10R mAb treatment during BCG vaccination upon the bacterial load in the spleen following *Mtb* challenge (**Figure 3.2B**). At day 112 post infection, BCG vaccination alone led to a strong trend towards lower bacterial loads in the spleen compared to no vaccination ($p=0.07$ BCG vaccination compared to no vaccination) but there was no additional control in mice vaccinated with BCG in the context of αIL-10R mAb (**Figure 3.2B**).

3.3.2 Early and enhanced production of IL-17 and GM-CSF upon Mtb challenge in mice vaccinated with BCG in the context of αIL-10R mAb

Although BCG vaccination in the context of αIL-10R blockade did not impact early control of *Mtb* bacterial load, it did impact control of *Mtb* bacterial load in chronic infection. We hypothesised that differences in the early immune response in the lung, as a result of IL-10R blockade during vaccination, could impact the control of *Mtb* bacterial load in chronic infection following challenge. We therefore assessed how IL-10R blockade during vaccination impacts the cytokine response in the lung at early time points following *Mtb* challenge.

Mice were vaccinated as shown in **Figure 3.1**. At days 14, 21 and 28 post infection lungs were harvested, homogenised and cultured for 16 hours with Purified Protein Derivative (PPD), which is an assortment of *Mtb* antigens, as described in the Materials and Methods. Supernatants from these cultures were harvested and levels of IFNγ, IL-17A and GM-CSF were

assessed by ELISA. We chose to assess levels of IFNγ, because it is well established that this cytokine is crucial for control of *Mtb* infection (Cooper et al., 1993; Flynn et al., 1993). Although the role of IL-17 in primary *Mtb* infection is unclear, IL-17 is suggested to be important in *Mtb* vaccination so levels of IL-17 were assessed (Gopal et al., 2012; Khader et al., 2007). We additionally chose to assess levels of GM-CSF, as this cytokine is also important for control of *Mtb* infection (Gonzalez-Juarrero et al., 2005; Szeliga et al., 2008) and is elevated throughout infection in IL-10 deficient mice, suggesting its expression is regulated by IL-10 (Redford et al., 2010).

At day 14 post *Mtb* challenge IFNγ, IL-17 and GM-CSF were undetectable following restimulation (**Figure 3.3A**). At day 21 post *Mtb* challenge IFNγ, IL-17 and GM-CSF were also undetectable in unvaccinated mice. Low, but elevated levels of IFNγ, IL-17 and GM-CSF were detected at day 21 post *Mtb* challenge in mice vaccinated with BCG in the context of IL-10R mAb, compared to those vaccinated with BCG alone (**Figure 3.3B**). By day 28 post infection IFNγ, IL-17A and GM-CSF protein was produced by all groups (**Figure 3.3C**). Levels of IFNγ, IL-17A and GM-CSF were higher in vaccinated groups compared to unvaccinated groups. In mice vaccinated with BCG in the context of αIL-10R mAb, levels of IL-17A and GM-CSF were higher in the lung at d28 post infection than in mice vaccinated with BCG alone (GM-CSF $p<0.05$, IL-17A $p<0.001$ BCG vaccination with αIL-10R mAb compared to BCG vaccination alone). αIL-10R mAb treatment during vaccination did not significantly impact IFNγ production at day 28 post infection (**Figure 3.3C**).

3.3.3 BCG vaccination in the context of αIL-10R mAb does not impact early recruitment of $CD4^+$ and $CD8^+$ T cells to the lung

We next investigated whether BCG vaccination in the context of αIL-10R mAb influenced the recruitment of total T cell populations to lung, as this could indicate an acceleration in the kinetics of the immune response. In order to assess T cell recruitment to the lung, mice were vaccinated as described in **Figure 3.1**. At days 14, 21 and 28 post *Mtb* challenge lungs were harvested and processed to achieve single cell suspensions. These were stained to identify $CD4^+$, $CD8^+$ and γδ T cells by flow cytometry and a gating strategy for their identification is shown in Appendix 1.

At every time point assessed there was no significant difference in recruitment of total $CD4^+$ or $CD8^+$ T cell populations between mice vaccinated with BCG or with BCG in the context of αIL-10R mAb, either in their percentage or number (**Figure 3.4A and 3.4B**). There was a small but consistent increase in the percentage of γδ T cells present in the lung at day 21 post *Mtb* challenge in mice vaccinated with BCG in the context of IL-10R mAb compared to BCG vaccination alone (**Figure 3.4C**) ($p<0.05$ BCG vaccination with αIL-10R mAb compared to BCG vaccination alone). However, there was not a significant increase in the number of γδ T cells present in the lung in mice vaccinated with BCG in the context of IL-10R blockade compared to BCG vaccination alone. This increase in the percentage of γδ T cells present appeared to be transient as no significant differences were observed at day 14 or 28 post infection.

3.3.4 BCG vaccination in the context of αIL-10R mAb does not significantly impact early IL-17 or IFNγ production by $CD4^+$ T cells in the lung but accelerates and enhances their production of GM-CSF

Although no large differences in the early recruitment of T cells to the lung following vaccination with BCG in the context of αIL-10R mAb were found, there were differences in the

levels of cytokine production early after *Mtb* challenge. We therefore aimed to assess T cell function by assessing cytokine production to determine whether vaccination in the context of αIL-10R mAb impacted this, in an attempt to explain the differences in total cytokine levels. Mice were vaccinated as described in **Figure 3.1**. Single cell suspensions were generated from the lungs at days 14, 21 and 28 post *Mtb* challenge and were restimulated with PPD and anti-CD28 (αCD28) for 16 hours before the addition of Brefeldin A for a further 4 hours. Cells were then harvested and intra-cellular cytokine staining was performed in order to identify IFNγ, IL-17A and GM-CSF production by T cells. The gating strategy to identify cytokine-producing populations is shown in Appendix 2.

We first assessed IFNγ and IL-17A production by $CD4^+$ T cells. In keeping with the total cytokine levels in the culture supernatant, we could not detect cytokine production by $CD4^+$ T cells at day 14 post *Mtb* challenge in any group (**Figure 3.5A** (flow cytometry plots) **Figure 3.6A** (percentage and number graphs)). At day 21 post *Mtb* challenge there was no difference in the proportion of IL-17A producing $CD4^+$ T cells between mice vaccinated with BCG in the context of αIL-10R mAb compared to BCG vaccination alone. IFNγ producing $CD4^+$ T cells were detected in both BCG vaccinated groups and, although there was a strong trend towards an increase in IFNγ producing $CD4^+$ T cells in mice vaccinated with BCG in the context of αIL-10R mAb compared to BCG vaccination alone, this did not reach significance (**Figure 3.5B** (flow cytometry plots) **Figure 3.6B** (percentage and number graphs)). By day 28 post *Mtb* challenge, IFNγ producing $CD4^+$ T cells were detected in all groups, but the proportion and number were higher in both BCG vaccinated groups compared to unvaccinated groups (**Figure 3.5C** (flow cytometry plots) **Figure 3.6C** (percentage and number graphs)). Compared to BCG vaccination alone, αIL-10R mAb treatment during vaccination did not significantly enhance IFNγ production by $CD4^+$ T cells at this time point (**Figure 3.5C** (flow cytometry plots) **Figure 3.6C** (percentage and number graphs)). IL-17A production by $CD4^+$ T cells was only detected in BCG vaccinated mice and, similarly to IFNγ production, αIL-10R mAb treatment did not

impact this (**Figure 3.5C** (flow cytometry plots) **Figure 3.6C** (percentage and number graphs)). At all time points assessed we found that $CD4^+$ T cells largely produced either IFNγ or IL-17A and comparatively few were producing both IFNγ and IL-17A.

No significant differences in the proportions, numbers or timing of IFNγ or IL-17A producing $CD4^+$ T cells were found in mice vaccinated with BCG in the context of αIL-10R mAb compared to mice vaccinated with BCG alone. Having found that total GM-CSF levels are elevated in the lung when mice are vaccinated with BCG in the context of IL-10R blockade, we assessed production of GM-CSF by $CD4^+$ T cells. Similarly to IFNγ and IL-17A, we did not detect GM-CSF producing $CD4^+$ T cells at day 14 post *Mtb* challenge in any group (**Figure 3.7A** (flow cytometry plots) **Figure 3.8A** (percentage and number graphs)). In keeping with the total protein levels of GM-CSF, at day 21 post *Mtb* challenge, GM-CSF producing by $CD4^+$ T cells were detected only in mice vaccinated with BCG in the context of αIL-10R mAb (**Figure 3.7B** (flow cytometry plots) **Figure 3.8B** (percentage and number graphs)). Furthermore, some of these cells co-produced IFNγ (**Figure 3.7B** (flow cytometry plots) **Figure 3.8B** (percentage and number graphs)). GM-CSF production by $CD4^+$ T cells was also increased at day 28 post *Mtb* challenge when vaccination occurred in the context of IL-10R blockade compared to BCG vaccination alone. Similarly to day 21 post infection, we identified $CD4^+$ T cells co-producing IFNγ and GM-CSF (**Figure 3.7C** (flow cytometry plots) **Figure 3.8C** (percentage and number graphs)). GM-CSF producing CD4 T cells were only detected in mice that had been BCG vaccinated (**Figure 3.7C** (flow cytometry plots) **Figure 3.8C** (percentage and number graphs)), although as discussed above were increased in mice vaccinated with BCG in the context of αIL-10R mAb.

3.3.5 BCG vaccination in the context of αIL-10R mAb enhances IL-17 production by γδ T cells at day 21 and by CD8$^+$ T cells at day 28 post infection in the lung

In addition to cytokine production by CD4$^+$ T cells, CD8$^+$ T cells and γδ T cells can be sources of cytokines during *Mtb* infection (Behar, 2013; Bold and Ernst, 2012; Lockhart et al., 2006; Okamoto Yoshida et al., 2010). We therefore also assessed cytokine production by these T cell subsets.

Similar to CD4$^+$ T cells, we did not detect significant cytokine production by γδ T cells at day 14 post *Mtb* challenge (**Figure 3.9A** (flow cytometry plots) **Figure 3.10A** (percentage and number graphs)). However, at day 21 post infection there was a higher proportion ($p<0.001$) and number ($p<0.01$) of IL-17A producing γδ T cells in mice vaccinated with BCG in the context of αIL-10R mAb compared to BCG vaccination alone (**Figure 3.9B** (flow cytometry plots) **Figure 3.10B** (percentage and number graphs)). By day 28 post *Mtb* challenge IL-17A producing γδ T cells were detected in all groups, although this was considerably higher in BCG vaccinated groups (**Figure 3.9C** (flow cytometry plots) **Figure 3.10C** (percentage and number graphs)). In contrast to day 21 post *Mtb* challenge, there was no difference in the proportion or number of γδ T cells producing IL-17A between mice vaccinated with BCG in the context of αIL-10R mAb and BCG vaccination alone at day 28 post *Mtb* challenge (**Figure 3.9C** (flow cytometry plots) **Figure 3.10C** (percentage and number graphs)). Low levels of IFNγ production by γδ T cells were detected in vaccinated mice at day 28 post *Mtb* challenge but αIL-10R mAb treatment did not significantly impact this (**Figure 3.9C** (flow cytometry plots) **Figure 3.10C** (percentage and number graphs)).

Cytokine production by CD8$^+$ T cells was undetectable in any unvaccinated or vaccinated group at day 14 post *Mtb* challenge (**Figure 3.11A** (flow cytometry plots) **Figure 3.12A** (percentage and number graphs)). At day 21 post *Mtb* challenge low and variable production of IFNγ

production was detected by $CD8^+$ T cells in mice vaccinated with BCG in the context of αIL-10R mAb (**Figure 3.11B** (flow cytometry plots) **Figure 3.12B** (percentage and number graphs)). At day 28 post *Mtb* challenge IFNγ production by $CD8^+$ T cells was higher in BCG vaccinated groups but there was no impact of αIL-10R mAb treatment (**Figure 3.11C** (flow cytometry plots) Figure **3.12C** (percentage and number graphs)). In contrast, we found a small but significant increase in the percentage ($p<0.05$) and number ($p<0.01$) of IL-17 producing $CD8^+$ T cells at day 28 post *Mtb* infection in mice vaccinated with BCG in the context of αIL-10R mAb compared to BCG vaccination alone (**Figure 3.11C** (flow cytometry plots) **Figure 3.12C** (percentage and number graphs)). However the significance of such a small population of IL-17 producing $CD8^+$ T cells is unclear.

3.4 Determining how IL-10R blockade during BCG vaccination impacts the splenic response to *Mtb* challenge

3.4.1 Early and increased GM-CSF and IL-17 production in the spleen following BCG vaccination in the context of αIL-10R mAb

Having identified differences in early cytokine production in the lung upon *Mtb* challenge of mice vaccinated with BCG in the context of IL-10R blockade, we next assessed whether these differences in cytokine production were also evident systemically by assessing the response in the spleen. Mice were vaccinated as described in **Figure 3.1** and single cell suspensions from the spleen generated at days 14, 21 and 28 post *Mtb* challenge. *Ex vivo* splenocytes were restimulated with PPD and αCD28 for 16 hours as described in Materials and Methods and levels of IFNγ, IL-17A and GM-CSF in the culture supernatants were determined.

IFNγ, IL-17A and GM-CSF levels were low to undetectable in all groups at day 14 post *Mtb* challenge and no significant differences were seen in mice vaccinated with BCG in the context of IL-10R blockade as compared to BCG vaccination alone (**Figure 3.13A**). Similarly to the lung, increased amounts of IFNγ, IL-17A and GM-CSF were detected in mice vaccinated with BCG in the context of IL-10R blockade at day 21 post *Mtb* compared to BCG vaccination alone (**Figure 3.13B**). By day 28 post *Mtb* challenge IFNγ, IL-17A and GM-CSF were detectable in all groups but we did not observe differences in IFNγ production between any of the groups. In contrast levels of both GM-CSF and IL-17 were significantly elevated in mice vaccinated with BCG in the context of αIL-10R mAb compared to BCG vaccination alone (**Figure 3.13C**).

3.4.2 BCG vaccination in the context of αIL-10R mAb does not significantly impact early IL-17 or IFNγ production by CD4$^+$ T cells in the spleen but enhances the proportion producing GM-CSF

We next aimed to assess the T cell sources of IFNγ, IL-17A and GM-CSF in the spleen following *Mtb* challenge. Splenocyte cultures, as for lung cultures, were restimulated with PPD for 16 hours before the addition of brefeldin A and culture for a further 4 hours. Cells were then harvested and intracellular cytokine staining was performed to identify IFNγ, IL-17A and GM-CSF producing CD4$^+$, CD8$^+$ and γδ T cells, with the gating strategy shown in Appendix 2.

We first assessed cytokine production by CD4$^+$ T cells. In contrast to the lung, at day 14 post *Mtb* challenge we detected IFNγ producing CD4$^+$ T cells in BCG vaccinated mice, however, BCG vaccination in the context of αIL-10R did not increase this production over BCG vaccination alone. We could not detect IL-17A production by CD4$^+$ T cells at this time point (**Figure 3.14A** (flow cytometry plots) **Figure 3.15A** (percentage and number graphs). At day 21 post *Mtb* challenge we identified IFNγ producing CD4$^+$ T cells in BCG vaccinated groups, and in some cases unvaccinated groups, although there was considerable variation within the groups (**Figure 3.14B** (flow cytometry plots) **Figure 3.15B** (percentage and number graphs). There was a trend towards an increased proportion of IFNγ producing CD4$^+$ T cells in the spleens of those mice vaccinated with BCG in the context of αIL-10R compared to BCG vaccination alone but this did not reach significance. IL-17A producing CD4$^+$ T cells were not detected in any group. (**Figure 3.14B** (flow cytometry plots) **Figure 3.15B** (percentage and number graphs). By day 28 post *Mtb* infection, similarly to the lung, IFNγ producing CD4$^+$ T cells were identified in both vaccinated and unvaccinated groups. However, in contrast to the lung, the proportion of IFNγ producing CD4$^+$ T was equivalent between vaccinated and unvaccinated groups (**Figure 3.14C** (flow cytometry plots) **Figure 3.15C** (percentage and number graphs). We found a small

increase in the percentage of IL-17A producing $CD4^+$ T cells in mice vaccinated with BCG in the context of IL-10R mAb compared to BCG vaccination alone, although there was no difference in the number of IL-17A producing $CD4^+$ T cells (**Figure 3.14C** (flow cytometry plots) **Figure 3.15C** (percentage and number graphs). Like in the lung, $CD4^+$ T cells largely produced either IFNγ or IL-17A and few IFNγ, IL-17A double producing T cells were detected at any time point (**Figure 3.14** (flow cytometry plots) **Figure 3.15** (percentage and number graphs).

GM-CSF levels were elevated in the spleen at days 21 and 28 post infection **(Figure 3.13B and 3.13C)**. As GM-CSF producing $CD4^+$ T cells were identified in the lung, we also assessed $CD4^+$ T cell production of GM-CSF in the spleen. At day 14 post *Mtb* challenge variable proportions and numbers of GM-CSF producing $CD4^+$ cells were detected in mice vaccinated with BCG in the context of αIL-10R mAb. No significant difference in the proportion or number of GM-CSF producing $CD4^+$ T cells between mice vaccinated with BCG in the context of αIL-10R compared to BCG vaccination alone was detected at this time point (**Figure 3.16A** (flow cytometry plots) **Figure 3.17A** (percentage and number graphs). In contrast, at day 21 post infection an increase in percentage and number of GM-CSF producing $CD4^+$ T cells was found in mice vaccinated with BCG in the context of αIL-10R blockade, compared to BCG vaccination alone (**Figure 3.16B** (flow cytometry plots) **Figure 3.17B** (percentage and number graphs). Like in the lung, more cells co-produced both IFNγ and GM-CSF than only GM-CSF, although both patterns of GM-CSF expression were higher in mice vaccinated with BCG in the context of αIL10R compared to BCG vaccination alone (**Figure 3.16B** (flow cytometry plots) **Figure 3.17B** (percentage and number graphs). This pattern of GM-CSF producing $CD4^+$ T cells was also largely maintained at day 28 post infection, although no significant increase in the number of GM-CSF single producing $CD4^+$ T cells was found (**Figure 3.16C** (flow cytometry plots) **Figure 3.17C** (percentage and number graphs).

3.4.4 BCG vaccination in the context of αIL-10R mAb minimally impacts cytokine production by γδ T cells and by CD8$^+$ T cells in the spleen

CD8$^+$ T cells and γδ T cells were also sources of cytokines in the lung early following *Mtb* challenge and thus we also assessed their cytokine production in the spleen. At day 14 post *Mtb* challenge IFNγ and IL-17A producing γδ T cells in the spleen were not detected (**Figure 3.18A** (flow cytometry plots) **Figure 3.19A** (percentage and number graphs). There was a trend towards an increase in IFNγ producing by γδ T cells in mice vaccinated with BCG in the context of IL-10R blockade in the spleen at day 21 post *Mtb* challenge, although this did not reach significance. We did observe a significant increase in the number of IL-17 producing γδ T cells in mice vaccinated with BCG in the context of IL-10R blockade, although there was no significant difference in the percentage of IL-17A producing γδ T cells (**Figure 3.18B** (flow cytometry plots) **Figure 3.19B** (percentage and number graphs). At day 28 post infection we did not observe any significant differences in percentage of IFNγ or IL-17A producing γδ T cells in mice vaccinated with BCG alone compared to those vaccinated with BCG in the context of αIL-10R mAb. Although there was a significant increase in the number of IL-17A producing γδ T cells, this varied between experiments (**Figure 3.18C** (flow cytometry plots) **Figure 3.19C** (percentage and number graphs).

CD8$^+$ T cells producing IFNγ or IL-17A were barely detectable in the spleen at day 14 post infection, although very low levels of IFNγ production by CD8$^+$ T cells was evident in some mice vaccinated with BCG in the context of αIL-10R (**Figure 3.20A** (flow cytometry plots) **Figure 3.21A** (percentage and number graphs). The percentage and number of IFNγ producing CD8$^+$ T cells was also low at day 21 post *Mtb* challenge in the spleen and no significant difference was found between mice vaccinated with BCG and those vaccinated with BCG in the

context of αIL-10R mAb. (**Figure 3.20B** (flow cytometry plots) **Figure 3.21B** (percentage and number graphs). At day 28 post *Mtb* challenge we observed IFNγ producing $CD8^+$ T cells in unvaccinated and vaccinated mice and there was no significant difference between mice vaccinated with BCG in the context of αIL-10R and those that received BCG alone (**Figure 3.20C** (flow cytometry plots) **Figure 3.21C** (percentage and number graphs). In the lung we identified a small population of $CD8^+$ T cells producing IL-17A in mice vaccinated with BCG in the context of αIL-10R mAb, in the spleen however, this population was not evident (**Figure 3.20C** (flow cytometry plots) **Figure 3.21C** (percentage and number graphs).

3.5 Establishing a role for GM-CSF in the immune response to *Mtb* challenge following BCG vaccination

3.5.1 GM-CSF is crucial for optimal protection upon Mtb challenge following BCG vaccination

We have observed early and enhanced production of IL-17A and GM-CSF upon *Mtb* challenge in both the lung and spleen of mice vaccinated with BCG in the context of αIL-10R compared to BCG vaccination alone. IL-17A is known to be important in recruiting Th1 cells following a vaccination regime with an ESAT-6 epitope in adjuvant (Khader et al., 2007). Furthermore, transfer of *in vitro* differentiated ESAT-6 specific Th17 cells are capable of controlling bacterial loads upon *Mtb* challenge (Monin et al., 2015).

Augmentation of GM-CSF expression at the time of BCG vaccination suggests that GM-CSF is beneficial to the outcome of vaccination. Indeed, augmentation of GM-CSF expression at the time of BCG vaccination either through genetic modification of BCG strains (Nambiar et al., 2010; Ryan et al., 2007) or administration of GM-CSF expressing viral vectors along with BCG vaccination (Dou et al., 2010; Wang et al., 2002) led to lower bacterial loads systemically upon mycobacterial challenge compared to controls. Furthermore, vaccination using a plasmid expressing Ag85A and GM-CSF led to increased induction of $CD4^+$ and $CD8^+$ T cell responses compared to Ag85A alone (Kamath et al., 1999; Zhang et al., 2007). However the role of GM-CSF in the recall response to *Mtb* challenge following BCG vaccination in unknown. We were therefore interested in determining how GM-CSF expression upon *Mtb* challenge impacted the protective affect of BCG vaccination. In order to address this, susceptible CBA/J mice were intradermally vaccinated with BCG or PBS (PBS vaccinated mice described as unvaccinated) and rested for at least 6 weeks. The day prior to *Mtb* infection they received an i.p. injection

containing 1mg of αGM-CSF mAb or isotype control (clone MP1-22E9 or GL117 respectively). After *Mtb* infection, mice received twice weekly i.p. injections containing 0.3 mg of αGM-CSF mAb or isotype before being sacrificed at day 63 post *Mtb* challenge. Bacterial loads in the lung were then determined as described in the materials and methods.

Neutralisation of GM-CSF during *Mtb* challenge in unvaccinated mice led to a dramatic increased in bacterial load (**Figure 3.22**). As expected BCG vaccination led to lower bacterial loads in the lung at day 63 post *Mtb* challenge. In BCG vaccinated mice, GM-CSF neutralisation during *Mtb* challenge led to higher bacterial loads compared to isotype controls (**Figure 3.22**).

3.6 Discussion

BCG vaccination is currently the only licensed vaccination against TB, and provides inadequate levels of protection against adult pulmonary disease (Fine, 1995). Improved vaccines or vaccine regimes are therefore required. IL-10 suppresses the response to BCG vaccination, with blockade of the IL-10R during BCG vaccination in both resistant and susceptible mouse models leading to lower *Mtb* bacterial chronic infection (Pitt et al., 2012b). As the immune response to *Mtb* is slow to develop (reviewed in Cooper, 2009), acceleration of the onset of adaptive immunity is one potential way in which to improve vaccination. In a resistant mouse model, IFNγ production by $CD4^+$ T cells was accelerated in mice vaccinated with BCG in the context of αIL-10R mAb (Pitt et al., 2012b). However, acceleration of the immune response in susceptible mice vaccinated with BCG and αIL-10R mAb was not assessed. As susceptible mouse strains are proposed to better reflect human disease (Apt and Kramnik, 2009), determination of how IL-10R blockade during BCG vaccination impacts the early immune response could provide insight into improving vaccination against TB.

3.6.1 Enhanced control of pulmonary Mtb bacterial load in mice vaccinated with BCG in the context αIL-10R mAb does not manifest at early time points

The data in this thesis confirms that BCG vaccination of susceptible CBA/J mice in the context of αIL-10R mAb leads to lower bacterial loads in the lung compared to BCG alone at day 112 post *Mtb* challenge, suggesting IL-10 suppresses BCG vaccination (Pitt et al., 2012b). A suppressive role for IL-10 during vaccination has also been demonstrated in other vaccine platforms. Protection against Leishmaniasis through vaccination with leishmanial proteins is enhanced in the absence of IL-10 signalling (Darrah et al., 2010). In addition, therapeutic DNA vaccination led to clearance of chronic LCMV infection only in the absence of IL-10 signalling (Brooks et al., 2008).

Increased control of bacterial load in the lung in mice vaccinated with BCG in the context of αIL-10R mAb, compared to BCG vaccination alone is not evident early following *Mtb* challenge. At these early time points following infection, BCG vaccination alone was sufficient to lower bacterial loads in the lung, with no additional benefit of IL-10R blockade during vaccination observed. In the spleen *Mtb* bacterial loads were not detectable until day 28 post infection and BCG vaccination alone decreased bacterial loads with no additional effect of αIL-10R mAb treatment, even in chronic infection. This suggests that the beneficial effect of this vaccine regime is local to the lung.

The reasons for the delayed increased control of pulmonary *Mtb* bacterial loads when mice are vaccinated with BCG in the context of αIL-10R mAb are unclear. A similar pattern of delayed control of bacterial load compared to BCG vaccination was also evident for the novel vaccine VPM1002, a recombinant BCG strain (Grode et al., 2005). Increased control of *Mtb* bacterial load when vaccinated with VPM1002 compared to BCG was not evident in the lung until day 90 post infection when challenged with the lab-adapted strain H37Rv, or day 200 when challenged with a clinically relevant Beijing/W strain (Grode et al., 2005). Control of pulmonary *Mtb* bacterial loads following BCG vaccination has been shown to wane over the course of infection, which may be somewhat dependent upon the length of time between vaccination and challenge (Cruz et al., 2015; Kamath and Behar, 2005). A possible explanation for our findings is that when BCG vaccination is administered in the context of αIL-10R mAb, control of bacterial load is maintained through chronic infection unlike BCG vaccination alone, thus improving the outcome of infection.

Further investigation into how BCG vaccination in the context of αIL-10R affects the immune response in chronic infection will further our understanding of protective vaccine strategies. Recently it has been demonstrated that IL-2 producing $KLRG1^{-}$ $CD4^{+}$ T cells, that retain proliferative capacity, are induced following boosting of BCG immunity with H1 (fusion of

antigen85B and ESAT-6) with the adjuvant CAF01, or vaccination with cryptic ESAT-6 epitopes (Lindenstrom et al., 2013; Woodworth et al., 2014). This increase in IL-2^+ KLRG1^- $CD4^+$ T cells in mice vaccinated with BCG and H1 CAF01 correlated with maintained control of *Mtb* bacterial load upon challenge, compared to BCG vaccination alone (Lindenstrom et al., 2013). Investigation into whether cells with this phenotype are also induced in BCG vaccination in the context of αIL-10R and correlate with increased protection could provide a possible explanation for the maintenance of the immune response and control of bacterial loads.

3.6.2 IL-10R blockade during BCG vaccination impacts early cytokine responses upon Mtb challenge

Although maintenance of the immune response is a possible explanation for the observation that increased control of pulmonary bacterial loads in mice vaccinated with BCG in the context of αIL-10R, another possibility is that early changes in the immune response influence the events in chronic infection. Indeed, in resistant C57BL/6 mice BCG vaccinated in the context of αIL-10R mAb there was accelerated recruitment of IFNγ producing $CD4^+$ T cells, but increased control of bacterial load was not evident until day 63 post *Mtb* challenge (Pitt et al., 2012b). In addition, early elevation of cytokine responses following *Mtb* challenge of mice vaccinated with the recombinant BCG strain VPM1002 were observed (Desel et al., 2011), but increased control of *Mtb* bacterial load was not evident until 90 days post infection (when challenged with the lab-adapted *Mtb* strain H37Rv) (Desel et al., 2011; Grode et al., 2005).

3.6.2.1 Early IFNγ production upon Mtb challenge following BCG vaccination in the context of αIL-10R mAb

IFNγ activates macrophages to control mycobacterial growth and is crucial for control of *Mtb* infection, so could be important for mediating enhanced control of bacterial load (Cooper et al.,

1993; Flynn et al., 1993; North and Jung, 2004). Furthermore, IFNγ is important in regulating immunopathology and thus influencing the outcome of infection (Nandi and Behar, 2011). We found that IL-10R blockade during BCG vaccination led to accelerated production of IFNγ at 21 days post *Mtb* challenge, but at day 28 post *Mtb* challenge IFNγ production was equivalent in BCG vaccinated groups. Although we saw a strong trend towards an increase in IFNγ producing $CD4^+$ T cells in CBA/J mice vaccinated with BCG in the context of αIL-10R mAb at day 21 post *Mtb* challenge, this did not reach significance. This contrasts to resistant C57BL/6 mice where there was accelerated recruitment of IFNγ producing $CD4^+$ T cells in mice vaccinated with BCG in the context of αIL-10R mAb (Pitt et al., 2012b). This finding highlights the differences in the immune responses between susceptible and resistant mouse models of *Mtb,* and the importance of assessing the immune response in susceptible mouse strains. CBA/J mice have been reported to have defects in the upregulation of adhesion molecules on T cells compared to C57BL/6 mice (Turner et al., 2001), which is not overcome by BCG vaccination (Gruppo et al., 2002). An inability to upregulate adhesion molecules on T cells, even when mice are vaccinated with BCG in the context of αIL-10R mAb, may explain the difference in recruitment of IFNγ producing T cells between CBA/J and C57BL/6 mice.

Given that we did not find significant differences in the presence of IFNγ producing $CD4^+$ T cells at day 21 post *Mtb* challenge, it is possible there are other cellular sources of IFNγ contributing to the accelerated production of IFNγ we observed at this time point when mice were vaccinated with BCG in the context of αIL-10R mAb. Indeed NK cells and other ILCs can produce IFNγ in response to activation by myeloid or epithelial-derived cytokines (reviewed in Artis and Spits, 2015). An "innate-like" source of IFNγ was described in CBA/J mice vaccinated with BCG in the context of αIL-10R mAb at day 112 post *Mtb* infection (Pitt et al., 2012b). Furthermore, IFNγ production by NK cells has been reported in the peripheral blood of BCG vaccinated infants, suggesting these cells could contribute to BCG induced immunity

(Zufferey et al., 2013). Further investigation would be required to determine whether BCG vaccination in the context of αIL-10R impacts the ability of NK cells or other ILCs to respond early upon *Mtb* challenge in CBA/J mice.

3.6.2.2 IL-10R blockade during BCG vaccination leads to early and enhanced IL-17A production upon Mtb challenge

We show that in both the lung and the spleen there is earlier IL-17A production, beginning at day 21 post *Mtb* challenge, and increased production of IL-17A at day 28 post *Mtb* challenge, in mice vaccinated with BCG in the context on αIL-10R mAb. These results correlating increased, early production of IL-17 with increased control of bacterial load in chronic infection are in keeping with a report where early, increased production of IL-17 correlated with increased protection later after *Mtb* challenge following vaccination with the recombinant BCG strain VPM1002 (Desel et al., 2011).

We did not identify increased proportions or numbers of IL-17A producing $CD4^+$ T cells in mice vaccinated with BCG in the context of αIL-10R at any time point, however we did identify increases in the percentage and number of other cell populations producing IL-17A. In the lung at day 21 post *Mtb* challenge there was an increase in γδ T cells producing IL-17A. The role of γδ T cells during primary *Mtb* infection is unclear, with reports of mice deficient in γδ T cells displaying increased susceptibility to intravenous but not aerosol *Mtb* infection (D'Souza et al., 1997; Ladel et al., 1995). γδ T cells are reported to be a major source of IL-17 following *Mtb* infection (Lockhart et al., 2006). In the context of vaccination against *Mtb* little is known about the role of γδ T cells, although it has been suggested that they could participate in a protective response (Andersen and Kaufmann, 2014). γδ T cells producing IL-17 have been identified in mice vaccinated with the recombinant BCG strain VPM1002 (Desel et al., 2011), although the significance of this is not known. In addition, γδ T cells have been described to

produce IFNγ in BCG vaccinated infants (Kagina et al., 2010; Zufferey et al., 2013), supporting the idea they could be involved in protection following vaccination.

At day 28 post infection we found a small population of $CD8^+$ T cells producing IL-17A in the lung only in mice vaccinated with BCG in the context of IL-10R blockade. IL-17 production by $CD8^+$ T cells has been described in the blood of TB patients (Silva et al., 2014), although not in mice. Vaccination in the context of IL-10R blockade may change the quality of the CD8 T cell response, leading to their production of IL-17 upon *Mtb* challenge.

Increased production of IL-17 could contribute to increased protection in mice vaccinated with BCG in the context of αIL-10R mAb. Although the role of IL-17 in primary infection is unclear, IL-17 has been described to be protective in recall responses (Freches et al., 2013; Gopal et al., 2014; Khader and Cooper, 2008). For example, transfer of *in vitro* differentiated ESAT-6 specific $CD4^+$ T cells producing IL-17, into naive hosts leads to enhanced control of bacterial load upon *Mtb* challenge (Monin et al., 2015). Furthermore $CD4^+$ T cells producing IL-17, primed in an IL-12p40 deficient mouse in response to BCG, are capable of mediating protection when transferred into *Rag* deficient mice in response to intravenous *Mtb* challenge (Wozniak et al., 2010).

The protective consequence of increased IL-17 production following vaccination in the context of IL-10R blockade could be through induction of chemokines. Indeed, IL-17 was required for optimal expression of CXCL9, CXCL10 and CXCL11, required to recruit CXCR3 expressing T cells, following vaccination with ESAT-6 peptide in adjuvant (Khader et al., 2007). In a mucosal vaccination model, IL-17 is required for induction of CXCL13, a CXCR5 ligand, which is required for appropriate localisation of T cells within lymphoid structures (Gopal et al., 2013). CXCR5 deficient mice show increased susceptibility to *Mtb* infection, which is associated with poor localisation of T cells within ectopic lymphoid structures and poor

macrophage activation (Slight et al., 2013). Assessment of the induction of chemokines early following *Mtb* challenge in mice vaccinated with BCG in the context of αIL-10R mAb, as well as the location of T cells within the lung, could provide further information as to how this vaccine regime increases protection against *Mtb* challenge.

In addition to increased production of IL-17, its timing is also suggested to be important, with an early Th17 response proposed to be required for expression of a subsequent Th1 response (Khader et al., 2007). Following vaccination with an ESAT-6 epitope in adjuvant, early Th17 responses were observed, and IL-17 was required for induction of chemokines to recruit IFNγ producing T cells upon *Mtb* challenge (although the importance of this in terms of control of infection was not assessed) (Khader et al., 2007). However, in contrast to this study, we identified IL-17 producing T cells at a later time point and this did not appear to precede IFNγ production by $CD4^+$ T cells. There are several possible reasons for this. Firstly, we conducted this study in a susceptible mouse strain as opposed to the resistant C57BL/6. As discussed above, CBA/J mice have been shown to have a defect in the upregulation of adhesion molecules on lymphocytes which affects their recruitment to the lung (Turner et al., 2001). This could be an important explanation to the different kinetics of the response. Secondly, we are assessing the T cell response to multiple *Mtb* antigens, through PPD restimulation, rather than to ESAT-6 in isolation. Finally we use a different vaccine regime.

Although we have identified early increased IL-17 to correlate with subsequent control of infection, excessive levels of IL-17 can also have detrimental affects on the outcome of *Mtb* infection. For example, IL-17 driven neutrophilia leading to host pathology is described following repeated BCG vaccination of *Mtb* infected mice (Cruz et al., 2010). In addition, IFNγ has been demonstrated to control IL-17 production and subsequent neutrophil accumulation (Nandi and Behar, 2011). Thus a balanced immune response is required for optimal control of *Mtb* infection.

3.6.2.3 Early and enhanced GM-CSF production upon Mtb challenge in mice vaccinated with BCG in the context of αIL-10R mAb

In addition to early production of IFNγ in the lung and early and increased production of IL-17A in the lung and spleen, we also show early and increased production of GM-CSF in the lung and spleen in mice vaccinated with BCG in the context of IL-10R blockade. Thus we identify early and increased production of GM-CSF, as well as IL-17A, to correlate with increased control of bacterial load in chronic infection. Such a pattern of increased cytokine production was also demonstrated early in *Mtb* challenge in mice vaccinated with the recombinant BCG strain VPM1002 and correlated with increased control of bacterial loads in chronic infection (Desel et al., 2011).

Although GM-CSF was originally described as a factor capable of directing the differentiation of haematopoietic cells towards macrophages and granulocytes (Burgess and Metcalf, 1980), and is crucial for the development of alveolar macrophages from foetal monocytes (Guilliams et al., 2013; Schneider et al., 2014), it also has roles in inflammation (Hamilton, 2008). Indeed in the context of *Mtb* infection, GM-CSF plays a protective role with mice deficient for this cytokine displaying increased susceptibility to infection with disorganised granulomas and reduced recruitment of IFNγ producing Th1 cells to the lung through lower levels of chemokine induction (Gonzalez-Juarrero et al., 2005; Szeliga et al., 2008). However, a caveat of these studies utilising GM-CSF deficient mice is that these mice develop lung pathology resembling Pulmonary Alveolar Proteinosis (PAP) (Dranoff et al., 1994; Stanley et al., 1994; Trapnell and Whitsett, 2002), which complicates interpretation of results (discussed in more detail in Chapter 4). Despite this it is possible that the accelerated and enhanced GM-CSF production observed in mice vaccinated with BCG in the context of αIL-10R mAb could contribute to increased protection later following *Mtb* challenge through induction of chemokines with the capacity to recruit Th1 cells. Although we identified GM-CSF$^+$ IFNγ$^+$ co-producing CD4$^+$ T cells,

suggesting that Th1 cells are already recruited, GM-CSF could act to promote further or continued recruitment of IFNγ producing T cells.

GM-CSF has also been described to directly activate macrophages to restrict growth of mycobacteria (Denis and Ghadirian, 1990; Pasula et al., 2015; Rothchild et al., 2014). It is possible that increased levels of GM-CSF at early time points in mice vaccinated with BCG in the context of αIL-10R, following *Mtb* infection could influence the function of macrophages at leading to lower bacterial loads in chronic infection.

Although GM-CSF is protective in the immune response to *Mtb* infection, mice overexpressing GM-CSF in the lung are also susceptible to *Mtb* infection, suggesting there is an optimal level of GM-CSF upon infection (Gonzalez-Juarrero et al., 2005; Szeliga et al., 2008). Despite this, mice vaccinated with a the recombinant BCG strain VPM 1002 were more protected against *Mtb* challenge compared to parental BCG vaccination and expressed higher levels of GM-CSF, along with other cytokines, including IL-17 (Desel et al., 2011). Furthermore, as mentioned above, IL-10 deficient mice, which are more resistant to *Mtb* infection, also have an increased level of GM-CSF in the lung through *Mtb* infection (Redford et al., 2010). It is possible that augmented GM-CSF expression in the context of increased expression of other cytokines does not lead to the increase in susceptibility or alternatively, the mouse overexpressing GM-CSF does so at higher non-physiological levels.

3.6.4 GM-CSF is required for optimal BCG mediated protection upon Mtb challenge

Subcutaneous or intranasal vaccination with a recombinant BCG strain engineered to express GM-CSF led to increased activation of APC populations in the draining lymph node and decreased bacterial loads in the spleen upon *Mtb* challenge (Nambiar et al., 2010; Ryan et al., 2007). Furthermore boosting of BCG vaccination using a viral vector expressing GM-CSF or

the *Mtb* antigen, antigen 85A (Ag85A), and GM-CSF led to lower mycobacterial loads following challenge (Dou et al., 2010; Wang et al., 2002). In addition, vaccination using a plasmid expressing Ag85A and GM-CSF led to increased induction of $CD4^+$ and $CD8^+$ T cell responses compared to vaccination with Ag85A alone (Kamath et al., 1999; Zhang et al., 2007). This suggests that vaccines or vaccine regimes against *Mtb* where GM-CSF expression is increased at the time of vaccination are beneficial to the protective effect of vaccination.

However, the role of GM-CSF in the recall response to *Mtb* infection is unknown. Having identified that early, increased production of GM-CSF correlated with increased protection in chronic infection, we investigated the impact of GM-CSF neutralisation during *Mtb* challenge upon the protection afforded by BCG vaccination in a susceptible mouse model. We show that GM-CSF during *Mtb* challenge following BCG vaccination is required for the protective effect of BCG in chronic infection. We also show that in primary infection neutralisation of GM-CSF leads to a much higher level of susceptibility to *Mtb* infection.

Further investigation will be required to determine the function of GM-CSF in the recall response and how, if at all, this differs to the primary response. Studies using BCG strains that express GM-CSF suggest that it could function to activate APCs (Nambiar et al., 2010; Ryan et al., 2007) and thus loss of this function could lead to inadequate priming of a T cell response. In BCG vaccinated mice, such priming events have already occurred and thus the function of GM-CSF to activate APCs may be less important. This could explain the smaller increase in bacterial load upon GM-CSF neutralisation in BCG vaccinated mice compared to unvaccinated mice. In GM-CSF deficient mice a defect in the recruitment of Th1 cells was reported (Gonzalez-Juarrero et al., 2005). A defect in the recruitment of Th1 cells could explain the increased susceptibility of mice when GM-CSF is neutralised in both vaccinated and unvaccinated mice, although in vaccinated mice other factors induced by BCG vaccination such as IL-17, could at least partially compensate for the defect in GM-CSF. Another possibility is that GM-CSF is required for optimal activation and function of macrophages to restrict

mycobacterial growth (Denis and Ghadirian, 1990; Pasula et al., 2015; Rothchild et al., 2014) as well as for APC function. These functions of GM-CSF are not mutually exclusive, and it is likely that several mechanisms contribute to the increase in susceptibility of both vaccinated and unvaccinated mice when GM-CSF is neutralised.

3.6.3 Summary

We show that IL-10R blockade during BCG vaccination leads to increased control of pulmonary bacterial loads at late time points following *Mtb* challenge, but this is not evident at early time points. We also show that lower pulmonary bacterial load at late time points following *Mtb* challenge correlate with early and enhanced production of IL-17 and GM-CSF and early production of IFNγ in susceptible CBA/J mice. We highlight the difference in the immune response between resistant and susceptible mouse strains as in contrast to resistant C57BL/6 mice (Pitt et al., 2012b) there was no significant acceleration in the recruitment of IFNγ producing $CD4^+$ T cells in susceptible CBA/J mice. We suggest the mechanism for increased control of pulmonary bacterial loads upon *Mtb* challenge in CBA/J mice vaccinated with BCG in the context of αIL-10R could be twofold. Firstly, accelerated and increased production of protective cytokines limits the ability of *Mtb* to manipulate the lung environment, potentially through chemokine induction and localisation of the T cell response. Secondly, maintenance of the immune response, as shown by much higher IL-17A and IFNγ production by $CD4^+$ at day 112 post *Mtb* challenge in CBA/J mice vaccinated with BCG in the context of αIL-10R mAb (Pitt et al., 2012b), leads to lower bacterial loads late in infection.

We also show that GM-CSF is required for optimal protection following BCG vaccination. This finding suggests that augmentation of GM-CSF production upon *Mtb* challenge could be a beneficial strategy to improve vaccination. Further investigation is required to determine

whether enhanced levels of GM-CSF, in mice vaccinated with BCG in the context of αIL-10R mAb, are important for mediating increased control of bacterial loads.

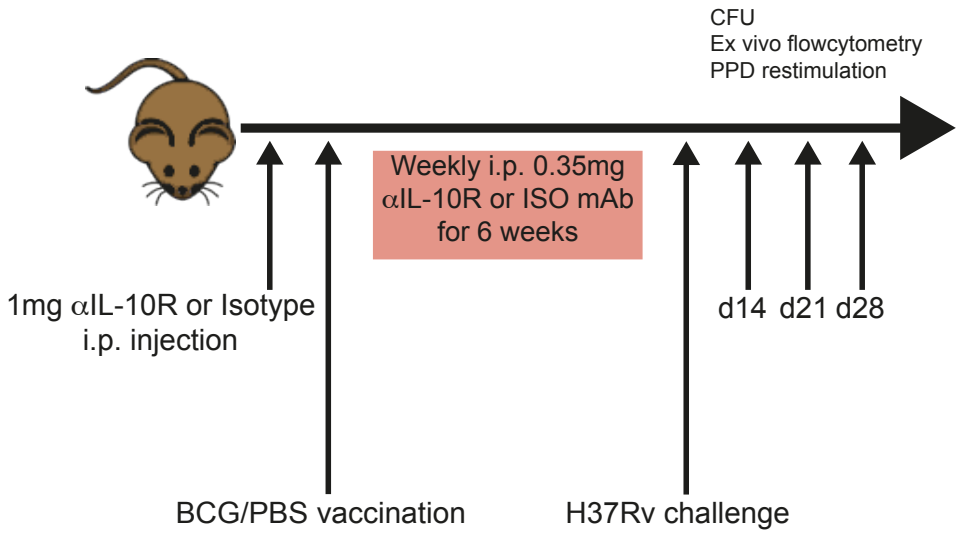

Figure 3.1 Experimental design

CBA/J mice received an intraperitoneal (i.p.) injection containing 1mg isotype (ISO) or anti-IL-10R (αIL-10R) the day prior to intradermal vaccination with approximately $5x10^5$ CFU BCG or PBS. Mice then received weekly i.p. injections containing 0.35mg ISO or αIL-10R monoclonal antibody (mAb) for 6 weeks. Mice were then rested for 3 weeks before aerosol challenge with approx. 100-200 CFU of the *Mtb* strain H37Rv. Mice were sacrificed at indicated time points post *Mtb* challenge.

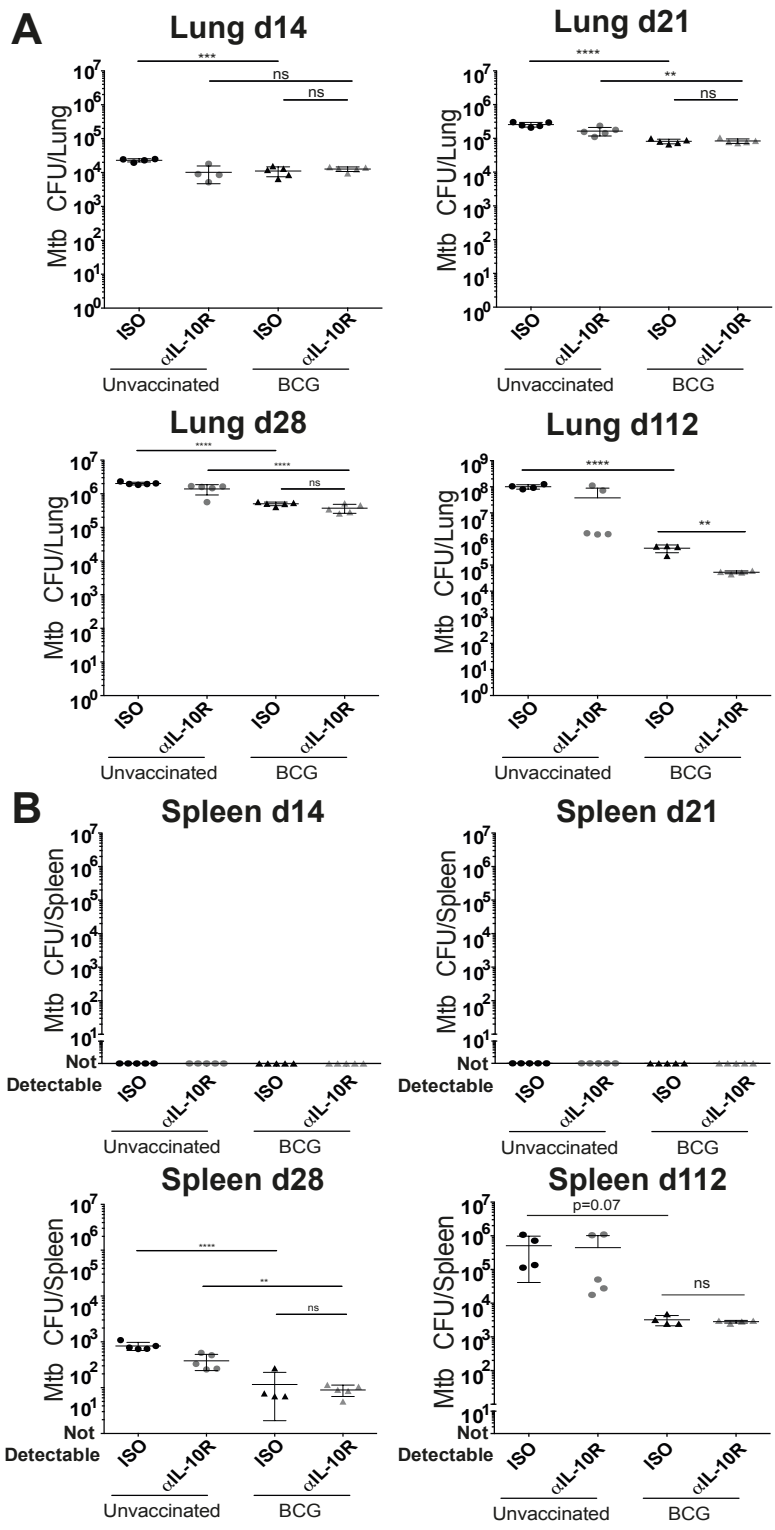

Figure 3.2 Increased control of bacterial load upon Mtb infection in mice BCG vaccinated in the context of αIL-10R mAb does not manifest until chronic infection

CBA/J mice were BCG vaccinated and challenged with *Mtb* as shown in **Figure 3.1.** Mice were sacrificed at 14, 21, 28 and 112 days post *Mtb* challenge and the lungs and spleens harvested. Bacterial loads in the lung **(A)** and spleen **(B)** were determined as described in Materials and Methods. Time points shown are from independent experiments and are representative of 2 (d14 and d112) or 3 (d21 and d28) identical experiments. 4-5 mice per group. Graphs show mean ± SD. ns – not significant *p<0.05, **p<0.01, **p<0.001, ****p<0.0001 by unpaired students t test.

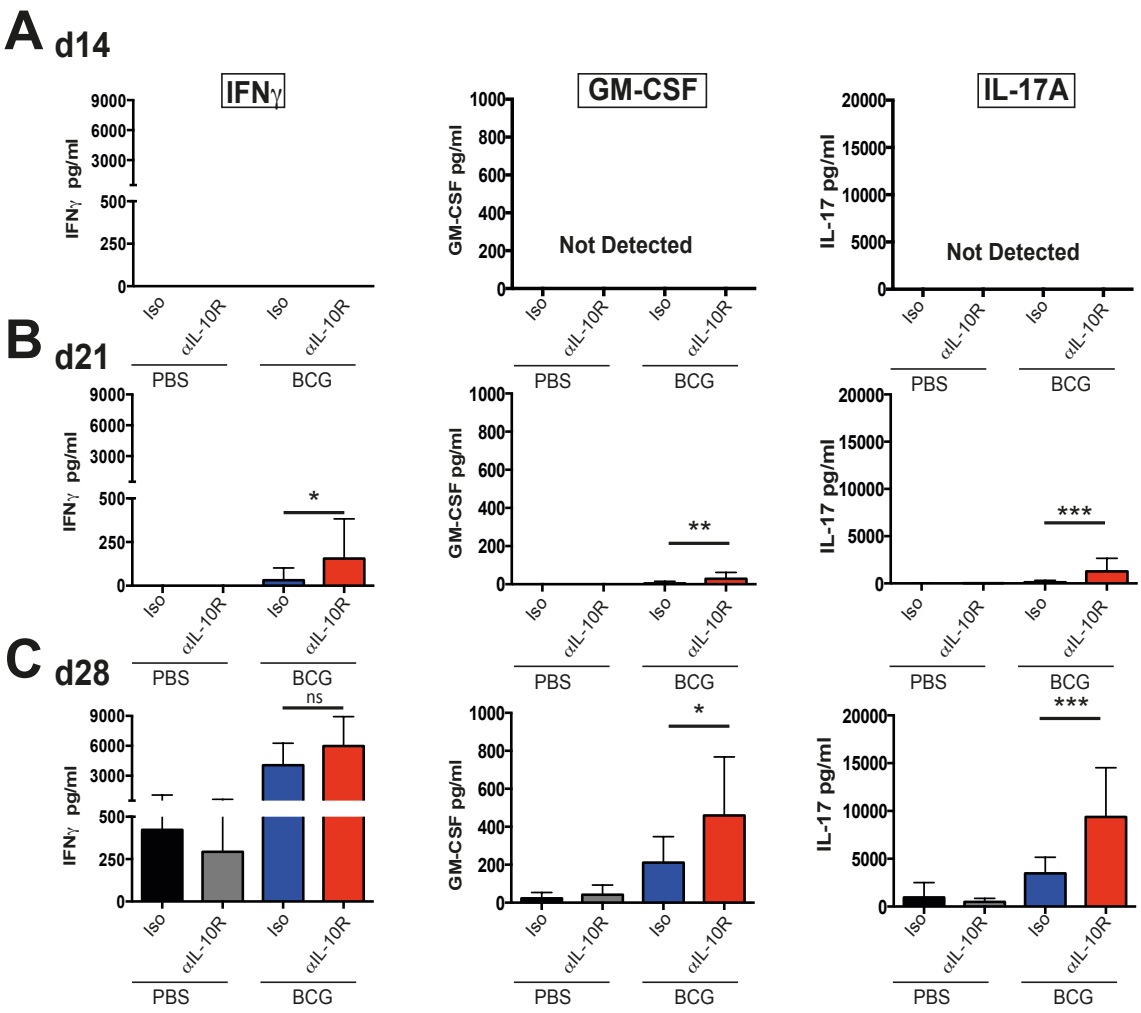

Figure 3.3 Early and enhanced IL-17 and GM-CSF production in the lung upon Mtb challenge following BCG vaccination in the context of αIL-10R mAb

CBA/J mice were BCG vaccinated and challenged with *Mtb* as shown in **Figure 3.1**. Mice were sacrificed and lungs harvested at 14, 21 and 28 days post *Mtb* challenge. Lung cell suspensions were restimulated with 20μg PPD and 2μg αCD28 for 16h after which supernatants were harvested. Enzyme Linked Immunosorbent Assays (ELISA) were performed for IFNγ, IL-17 and GM-CSF in supernatants from cultures at day 14 **(A)**, day 21 **(B)** and day 28 **(C)** post infection. Data pooled from 2 (d14 and d28) or 3 (d21) independent experiments. 9-15 mice per group. Graphs show mean ± SD. ns – not significant *p<0.05, **p<0.01, ***p<0.001, by 2-way ANOVA with Tukey post test.

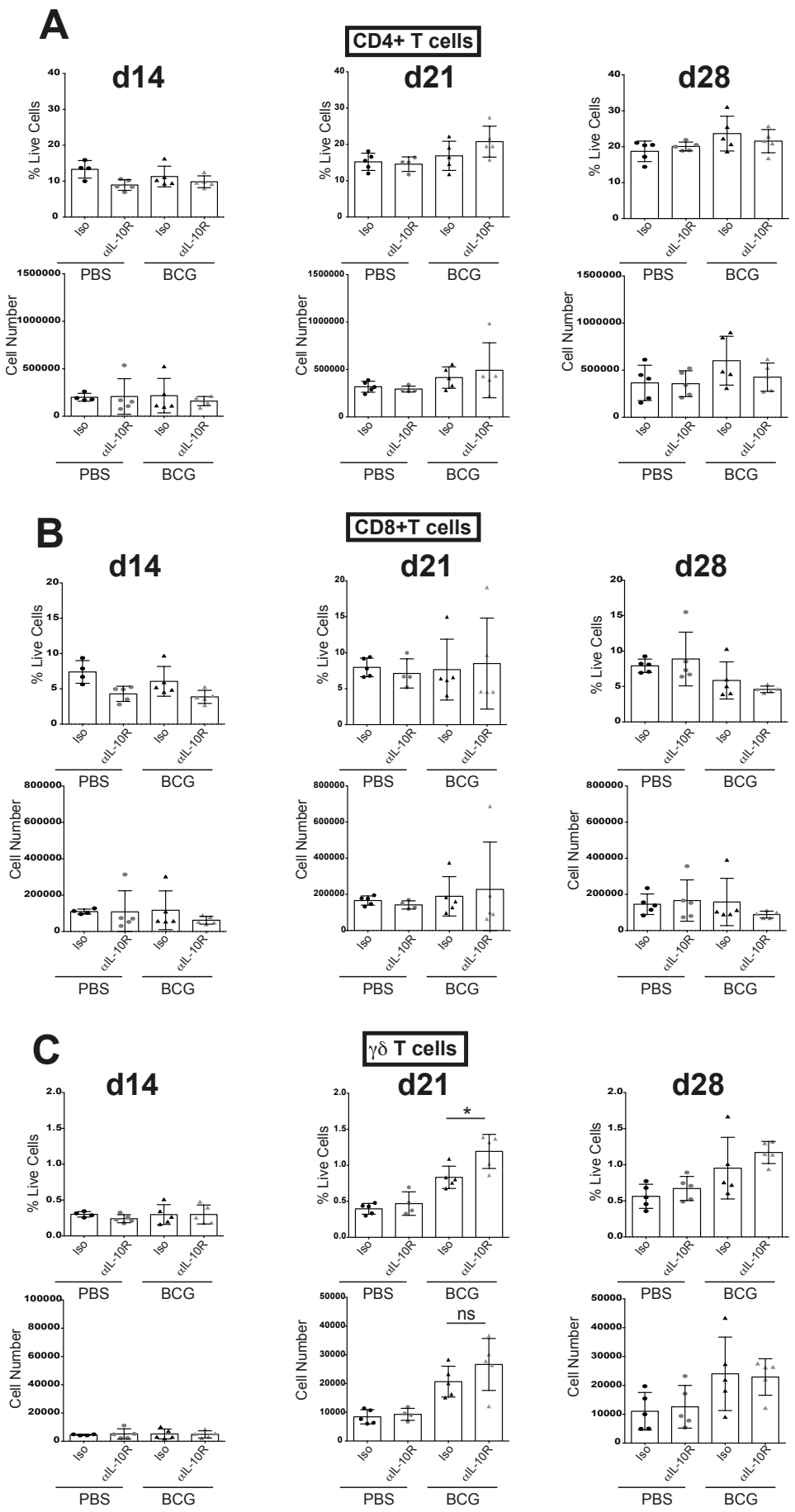

Figure 3.4 BCG vaccination in the context of αIL-10R mAb does not significantly impact the early recruitment of CD4$^+$ or CD8$^+$ T cells to the lung

CBA/J mice were BCG vaccinated and challenged with *Mtb* as shown in **Figure 3.1**. Mice were sacrificed and lungs harvested at 14, 21 and 28 days post *Mtb* challenge. Lungs were homogenized by passage through a 70μm filter. Samples were stained with the following antibodies to assess percentages and calculate numbers of lymphoid populations by flow cytometry: γδ TCR FITC, Thy1.2 PECy7, CD4 e450, CD8 v500 and CD3 APC. Percentage and number of CD4+ T cells defined as $CD3^+$ $Thy1.2^+$ $CD4^+$ at day 14, 21 and 28 post infection **(A)**. Percentage and number of $CD8^+$ T cells defined as $CD3^+$ $Thy1.2^+$ $CD8^+$ at day 14, 21 and 28 post infection **(B).** Percentage and number of γδ T cells defined as $CD3^+$ $Thy1.2^+$ $CD4^-$ $CD8^-$ $\gamma\delta TCR^+$ at day 14, 21 and 28 post infection **(C).** Time points shown are from independent experiments and data is representative of 2 (d14) or 3 (d21 and d28) independent experiments. 4-5 mice per group. Graphs show individual mice with mean ± SD. ns – not significant *$p<0.05$, by 2-way ANOVA with Tukey post test.

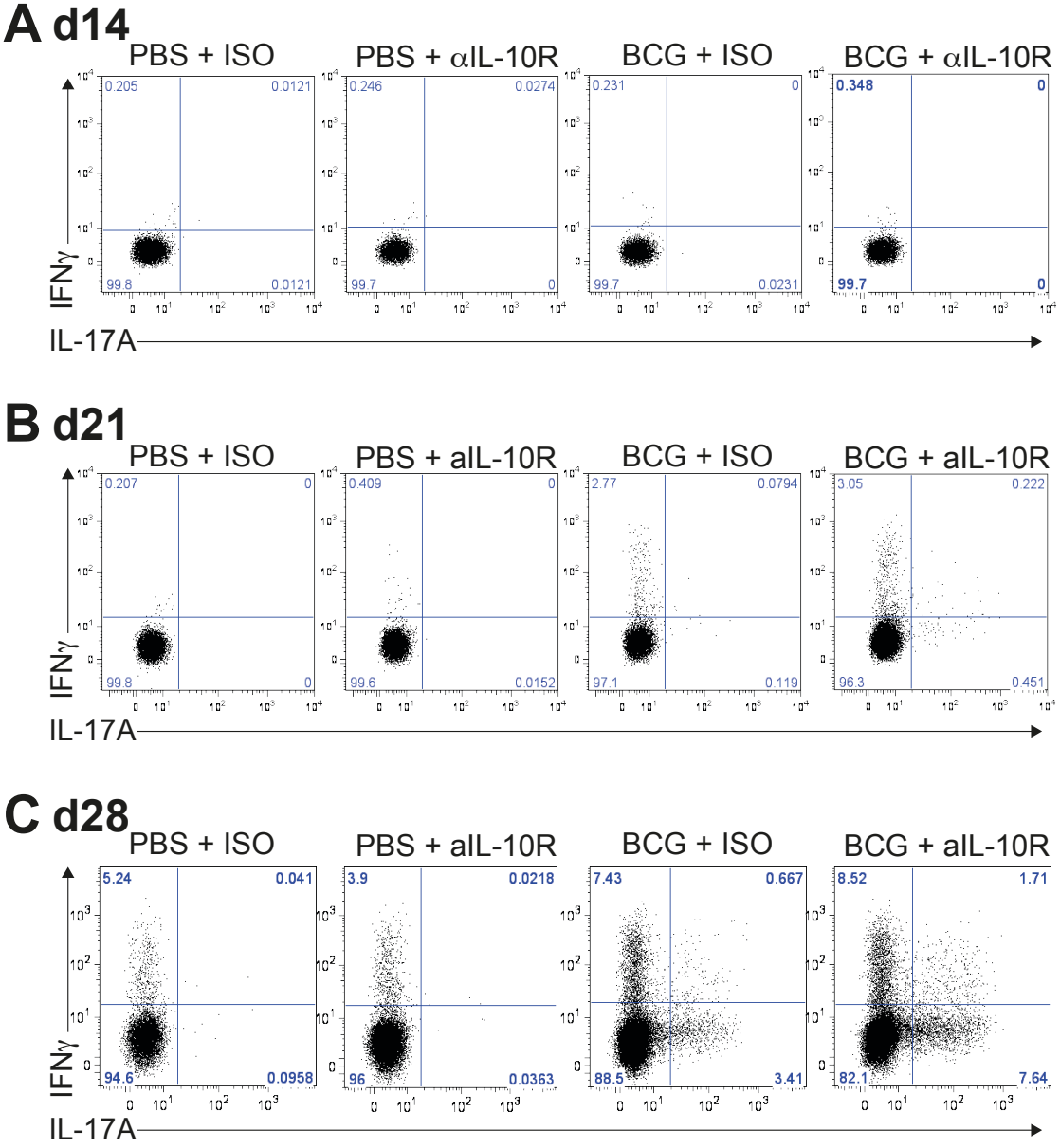

Figure 3.5 BCG vaccination in the context of αIL-10R mAb does not significantly accelerate recruitment of IFNγ or IL-17 producing CD4$^+$ T cells to the lung upon Mtb challenge. (Flow cytometry plots)

CBA/J mice were BCG vaccinated and challenged with *Mtb* as shown in **Figure 3.1**. Mice were sacrificed and lungs harvested at 14, 21 and 28 days post *Mtb* challenge. Lungs were homogenized by passage through a 70μm filter. 1x10^6 cells were restimulated with 20μg PPD and 2μg αCD28 mAb for 16h before the addition of BFA for a further 4h. Cells were then harvested and stained with the following to assess cytokine production: γδ TCR FITC, GM-CSF PE, CD8 PerCP e710, Thy1.2 PE Cy7, IFNγ e450, CD4 v500, IL-17A APC, CD3 APCe780. CD4$^+$ T cells were identified as CD3$^+$ Thy1.2$^+$ CD4$^+$. Representative flow cytometry plots from day 14 **(A)**, day 21 **(B)** or day 28 post infection **(C)** are shown. Individual time points are from independent experiments. Data representative of 2 (d14 and d28) or 3 (d21) independent experiments. 4-5 mice per group.

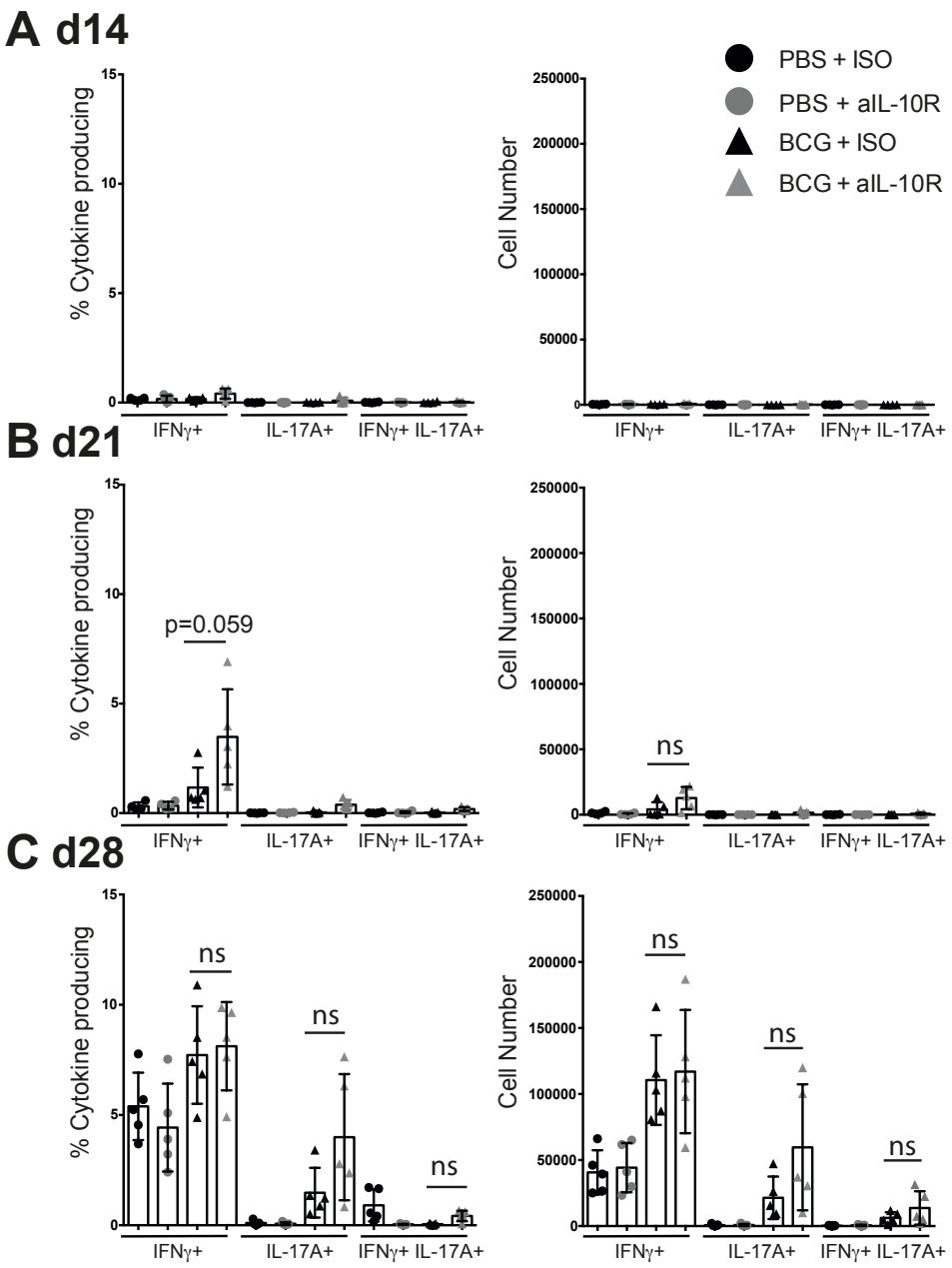

Figure 3.6 BCG vaccination in the context of αIL-10R mAb does not significantly accelerate recruitment of IFNγ or IL-17 producing CD4$^+$ T cells (percentage and number cytokine producing) to the lung upon Mtb challenge

CBA/J mice were BCG vaccinated and challenged with *Mtb* as shown in **Figure 3.1**. Mice were sacrificed and lungs harvested at 14, 21 and 28 days post *Mtb* challenge. Lungs were homogenized by passage through a 70μm filter. 1x10^6 cells were restimulated with 20μg PPD and 2μg αCD28 mAb for 16h before the addition of BFA for a further 4h. Cells were then harvested and stained with the following to assess cytokine production: γδ TCR FITC, GM-CSF PE, CD8 PerCP e710, Thy1.2 PE Cy7, IFNγ e450, CD4 v500, IL-17A APC, CD3 APCe780. CD4$^+$ T cells were identified as CD3$^+$ Thy1.2$^+$ CD4. Percentage and number of cytokine producing CD4$^+$ T cells at day 14 **(A)**, day 21 **(B)** or day 28 post infection **(C).** Graphs show individual mice with mean ± SD. Individual time points are from independent experiments. Data representative of 2 (d14 and d28) or 3 (d21) independent experiments. 4-5 mice per group. ns – not significant by 2-way ANOVA with Tukey post test.

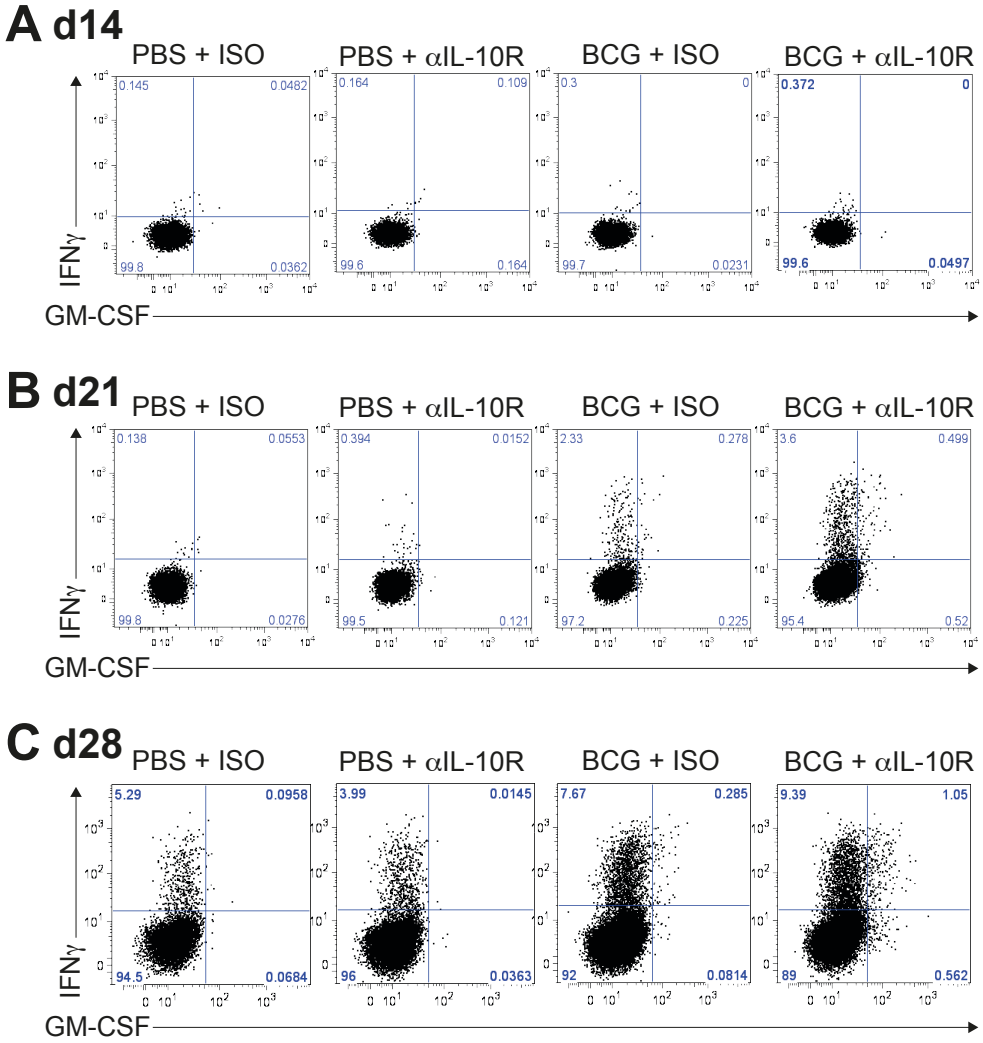

Figure 3.7 Production of GM-CSF by CD4$^+$ T cells in the lung upon Mtb challenge is accelerated and enhanced by BCG vaccination in the context of αIL-10R mAb. (Flow cytometry plots)

CBA/J mice were BCG vaccinated and challenged with *Mtb* as shown in **Figure 3.1**. Mice were sacrificed and lungs harvested at 14, 21 and 28 days post *Mtb* challenge. Lungs were homogenized by passage through a 70µm filter. 1x10^6 cells were restimulated with 20µg PPD and 2µg αCD28 mAb for 16h before the addition of BFA for a further 4h. Cells were then harvested and stained with the following to assess cytokine production: γδ TCR FITC, GM-CSF PE, CD8 PerCP e710, Thy1.2 PE Cy7, IFNγ e450, CD4 v500, IL-17A APC, CD3 APCe780. CD4$^+$ T cells were identified as CD3$^+$ Thy1.2$^+$ CD4$^+$. Representative flow cytometry plots from day 14 **(A)**, day 21 **(B)** or day 28 post infection **(C)** are shown. Individual time points are from independent experiments. Data representative of 2 (d14 and d28) or 3 (d21) independent experiments. 4-5 mice per group

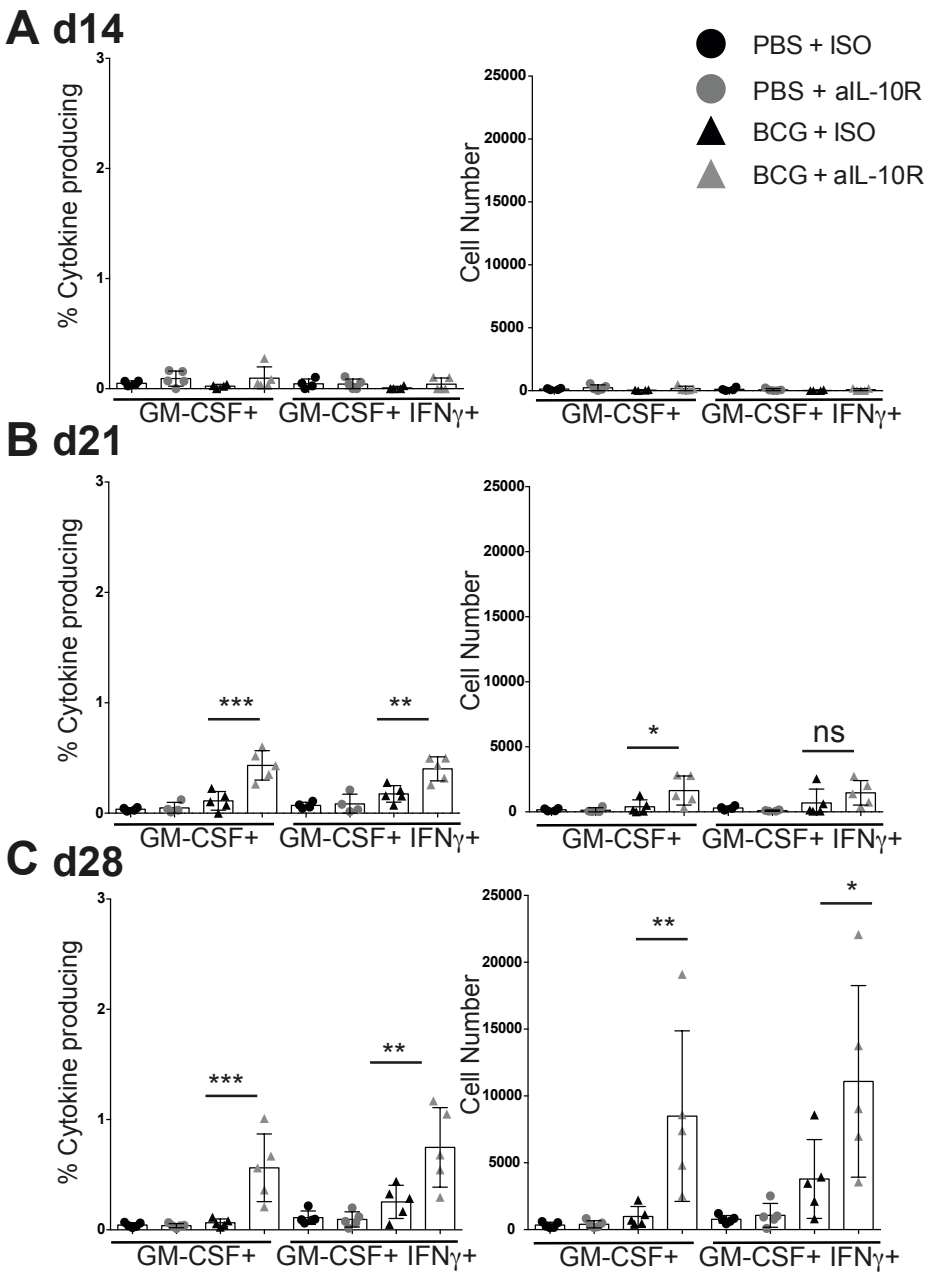

Figure 3.8 Production of GM-CSF by CD4$^+$ T cells (percentage and number cytokine producing) in the lung upon Mtb challenge is accelerated and enhanced by BCG vaccination in the context of αIL-10R mAb.

CBA/J mice were BCG vaccinated and challenged with *Mtb* as shown in **Figure 3.1**. Mice were sacrificed and lungs harvested at 14, 21 and 28 days post *Mtb* challenge. Lungs were homogenized by passage through a 70μm filter. 1x10^6 cells were restimulated with 20μg PPD and 2μg αCD28 mAb for 16h before the addition of BFA for a further 4h. Cells were then harvested and stained with the following to assess cytokine production: γδ TCR FITC, GM-CSF PE, CD8 PerCP e710, Thy1.2 PE Cy7, IFNγ e450, CD4 v500, IL-17A APC, CD3 APCe780. CD4$^+$ T cells were identified as CD3$^+$ Thy1.2$^+$ CD4$^+$. Percentage and number of cytokine producing CD4$^+$ T cells at day 14 **(A)**, day 21 **(B)** or day 28 post infection **(C).** Data representative of 2 (d14 and d28) or 3 (d21) independent experiments. 4-5 mice per group. Graphs show mean ± SD. ns – not significant *p<0.05, **p<0.01, ***p<0.001 by 2-way ANOVA with Tukey post test.

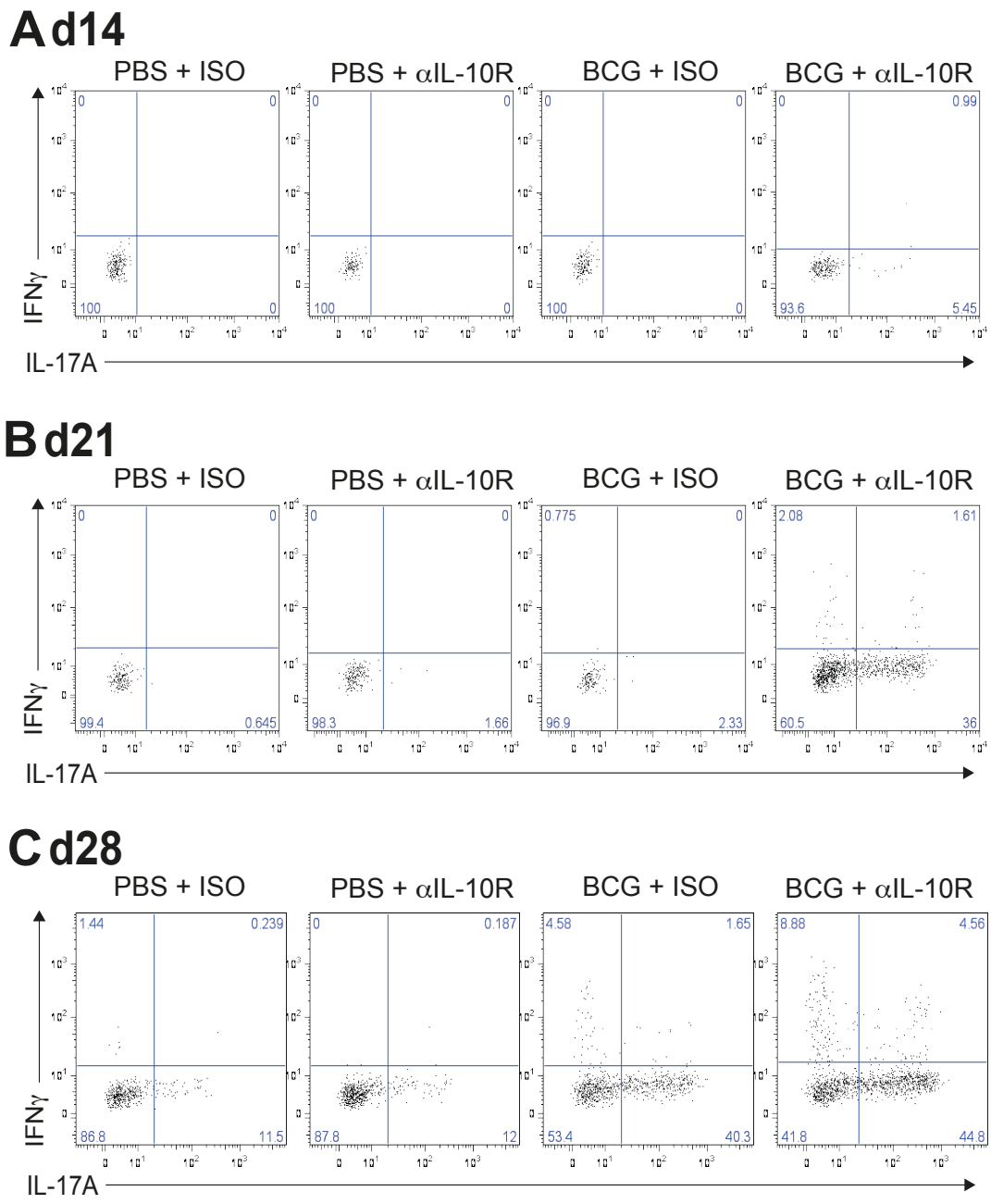

Figure 3.9 Increased production of IL-17 by gamma delta T cells in the lung in mice BCG vaccinated in the context of αIL-10R mAb (Flow cytometry plots)

CBA/J mice were BCG vaccinated and challenged with *Mtb* as shown in **Figure 3.1**. Mice were sacrificed and lungs harvested at 14, 21 and 28 days post *Mtb* challenge. Lungs were homogenized by passage through a 70µm filter. $1x10^6$ cells were restimulated with 20µg PPD and 2µg αCD28 mAb for 16h before the addition of BFA for a further 4h. Cells were then harvested and stained with the following to assess cytokine production: γδ TCR FITC, GM-CSF PE, CD8 PerCP e710, Thy1.2 PE Cy7, IFNγ e450, CD4 v500, IL-17A APC, CD3 APCe780. γδ T cells were identified as $CD3^+$ $Thy1.2^+$ γδ TCR^+. Representative flow cytometry plots from day 14 **(A)**, day 21 **(B)** or day 28 post infection **(C)** are shown are shown. Individual time points are from independent experiments. Data representative of 2 (d14 and d28) or 3 (d21) independent experiments. 4-5 mice per group.

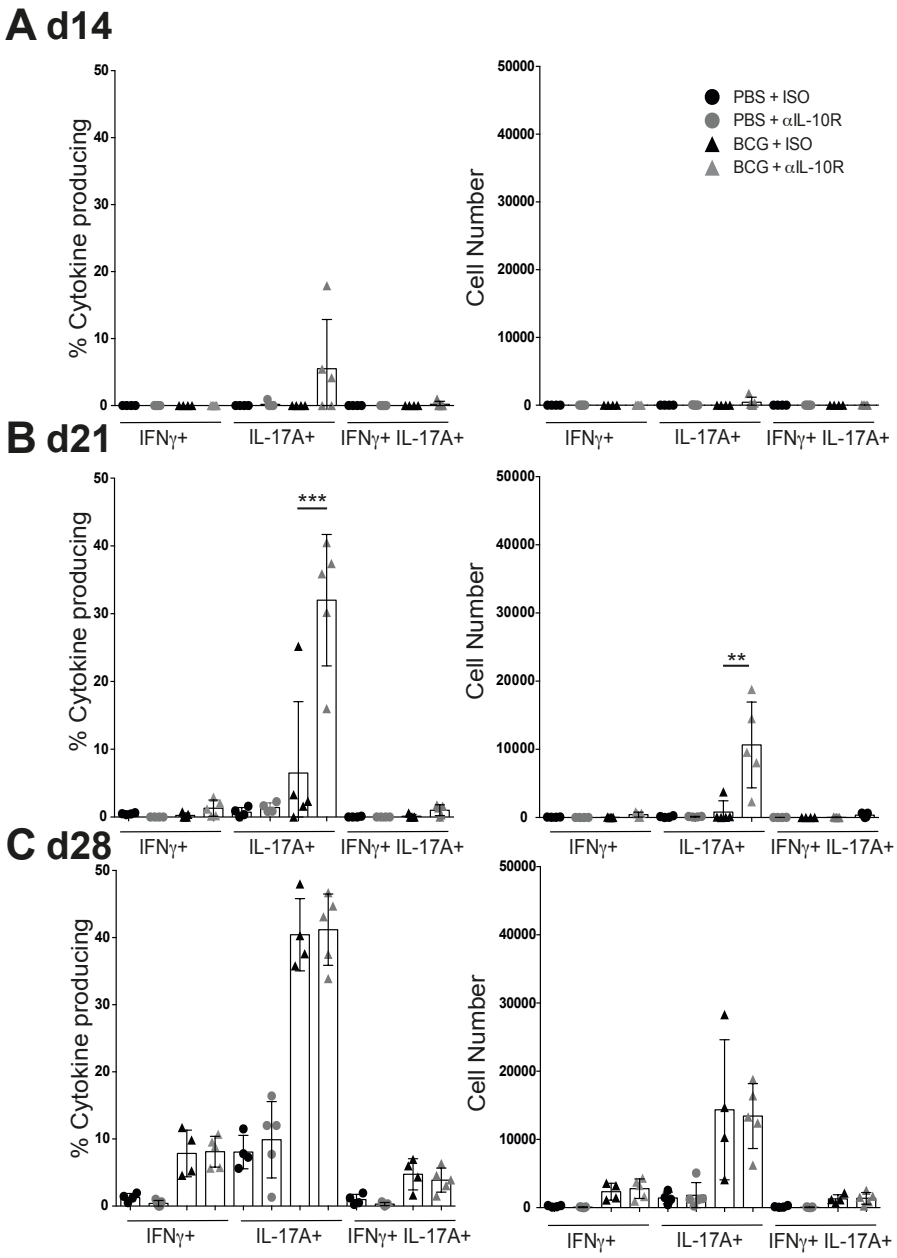

Figure 3.10 Increased production of IL-17 by gamma delta T cells (percentage and number cytokine producing) in the lung in mice BCG vaccinated in the context of αIL-10R mAb.

CBA/J mice were BCG vaccinated and challenged with *Mtb* as shown in **Figure 3.1**. Mice were sacrificed and lungs harvested at 14, 21 and 28 days post *Mtb* challenge. Lungs were homogenized by passage through a 70μm filter. $1x10^6$ cells were restimulated with 20μg PPD and 2μg αCD28 mAb for 16h before the addition of BFA for a further 4h. Cells were then harvested and stained with the following to assess cytokine production: γδ TCR FITC, GM-CSF PE, CD8 PerCP e710, Thy1.2 PE Cy7, IFNγ e450, CD4 v500, IL-17A APC, CD3 APCe780. γδ T cells were identified as $CD3^+$ $Thy1.2^+$ γδ TCR^+. Percentage and number of cytokine producing γδ T cells at day 14 **(A)**, day 21 **(B)** or day 28 post infection **(C).** Data representative of 2 (d14 and d28) or 3 (d21) independent experiments. 4-5 mice per group. Graphs show mean ± SD. ns – not significant *p<0.05, **p<0.01, ***p<0.001 by 2-way ANOVA with Tukey post test.

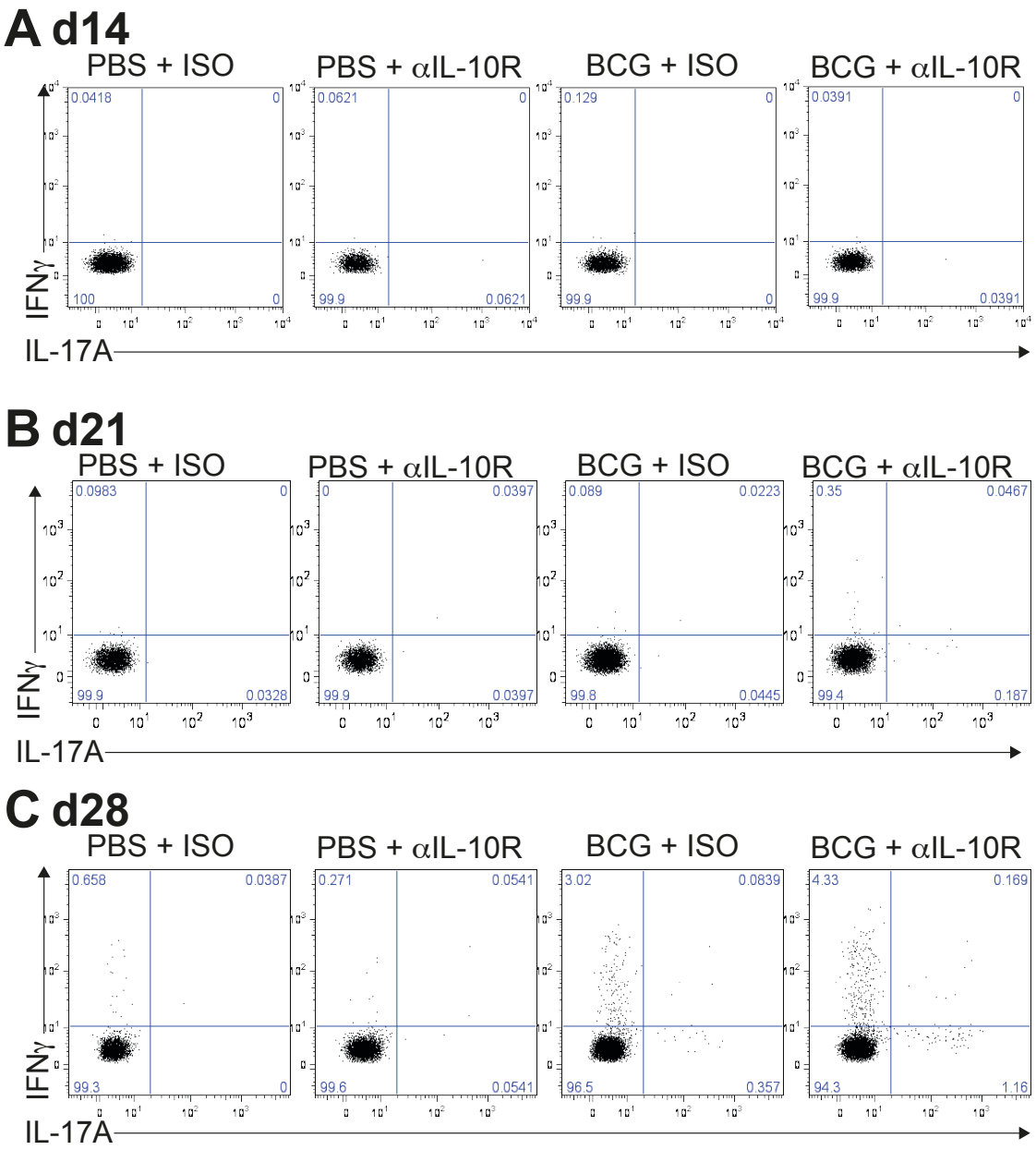

Figure 3.11 Increased IL-17 production by CD8$^+$ T cells in the lung in mice BCG vaccinated in the context of αIL-10R mAb (Flow cytometry plots)

CBA/J mice were BCG vaccinated and challenged with *Mtb* as shown in **Figure 3.1**. Mice were sacrificed and lungs harvested at 14, 21 and 28 days post *Mtb* challenge. Lungs were homogenized by passage through a 70μm filter. 1x10^6 cells were restimulated with 20μg PPD and 2μg αCD28 mAb for 16h before the addition of BFA for a further 4h. Cells were then harvested and stained with the following to assess cytokine production: γδ TCR FITC, GM-CSF PE, CD8 PerCP e710, Thy1.2 PE Cy7, IFNγ e450, CD4 v500, IL-17A APC, CD3 APCe780. CD8$^+$ T cells were identified as CD3$^+$ Thy1.2$^+$ CD8$^+$. Representative flow cytometry plots from day 14 **(A)**, day 21 **(B)** or day 28 post infection **(C)** are shown are shown. Individual time points are from independent experiments. Data representative of 2 (d14 and d28) or 3 (d21) independent experiments. 4-5 mice per group.

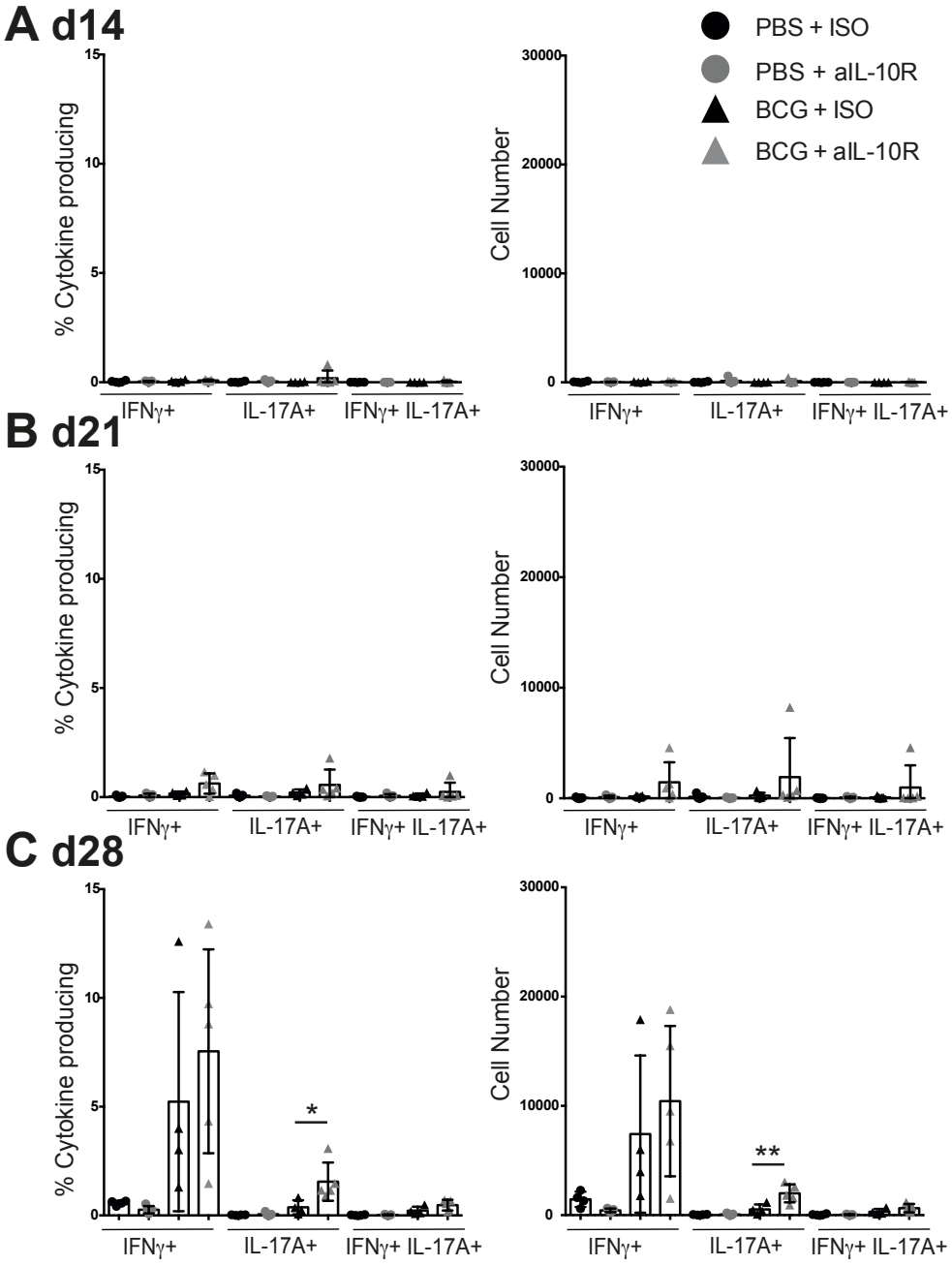

Figure 3.12 Increased IL-17 production by CD8$^+$ T cells (percentage and number cytokine producing) in the lung in mice BCG vaccinated in the context of αIL-10R mAb.

CBA/J mice were BCG vaccinated and challenged with *Mtb* as shown in **Figure 3.1**. Mice were sacrificed and lungs harvested at 14, 21 and 28 days post *Mtb* challenge. Lungs were homogenized by passage through a 70μm filter. 1x10^6 cells were restimulated with 20μg PPD and 2μg αCD28 mAb for 16h before the addition of BFA for a further 4h. Cells were then harvested and stained with the following to assess cytokine production: γδ TCR FITC, GM-CSF PE, CD8 PerCP e710, Thy1.2 PE Cy7, IFNγ e450, CD4 v500, IL-17A APC, CD3 APCe780. CD8$^+$ T cells were identified as CD3$^+$ Thy1.2$^+$ CD8$^+$. Percentage and number of cytokine producing γδ T cells at day 14 **(A)**, day 21 **(B)** or day 28 post infection **(C).** Data representative of 2 (d14 and d28) or 3 (d21) independent experiments. 4-5 mice per group. Graphs show mean ± SD. ns – not significant *p<0.05, **p<0.01 by 2-way ANOVA with Tukey post test.

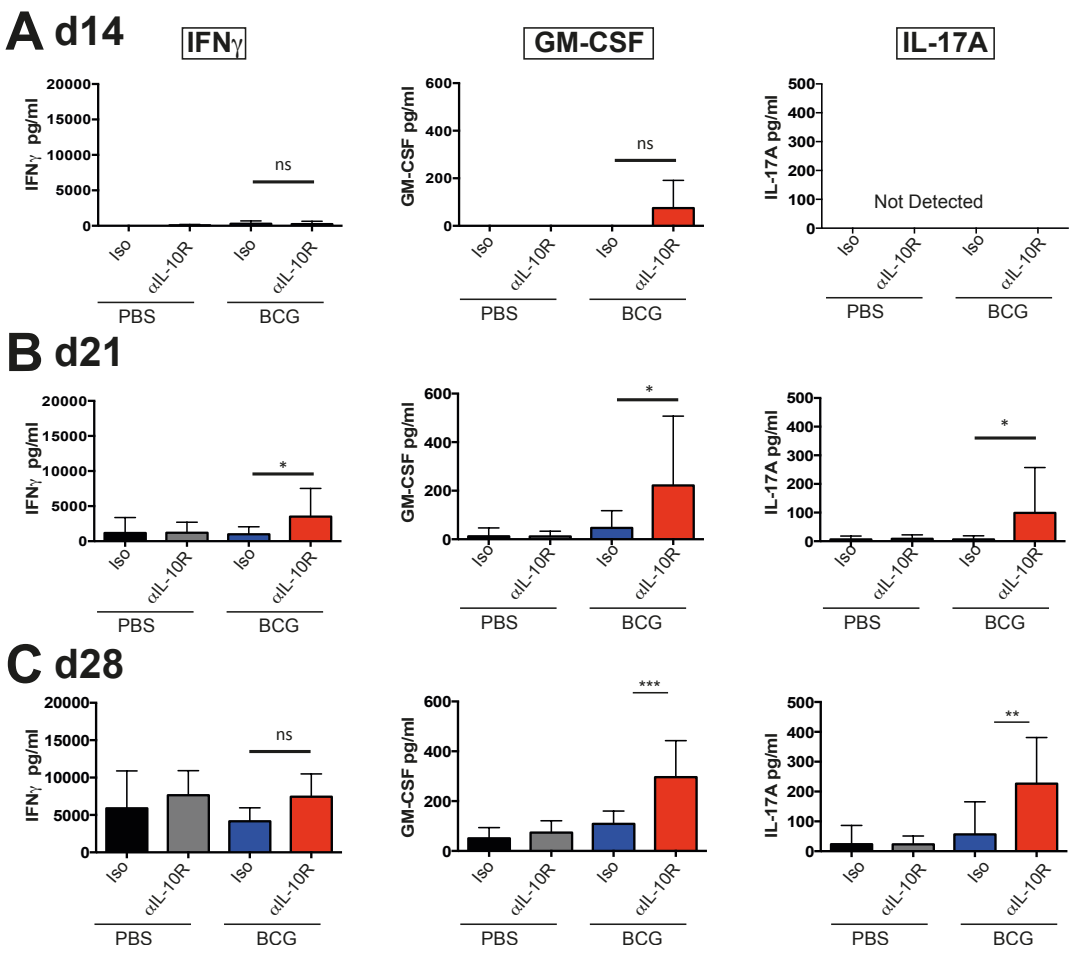

Figure 3.13 Increased GM-CSF and IL-17 production in the spleen upon Mtb challenge following BCG vaccination in the context of αIL-10R mAb

CBA/J mice were BCG vaccinated and challenged with *Mtb* as shown in **Figure 3.1**. Mice were sacrificed and lungs harvested at 14, 21 and 28 days post *Mtb* challenge. $5x10^6$ cells were restimulated with 20μg PPD and 2μg αCD28 for 16h after which supernatants were harvested. ELISAs were performed for IFNγ, IL-17 and GM-CSF in supernatants from cultures at day 14 **(A)**, day 21 **(B)** and day 28 **(C)** post infection. Data pooled from 2 (d14 and d28) or 3 (d21) independent experiments. 5-15 mice per group. Graphs show mean ± SD. ns – not significant *p<0.05, **p<0.01, ***p<0.001 by 2-way ANOVA with Tukey post test.

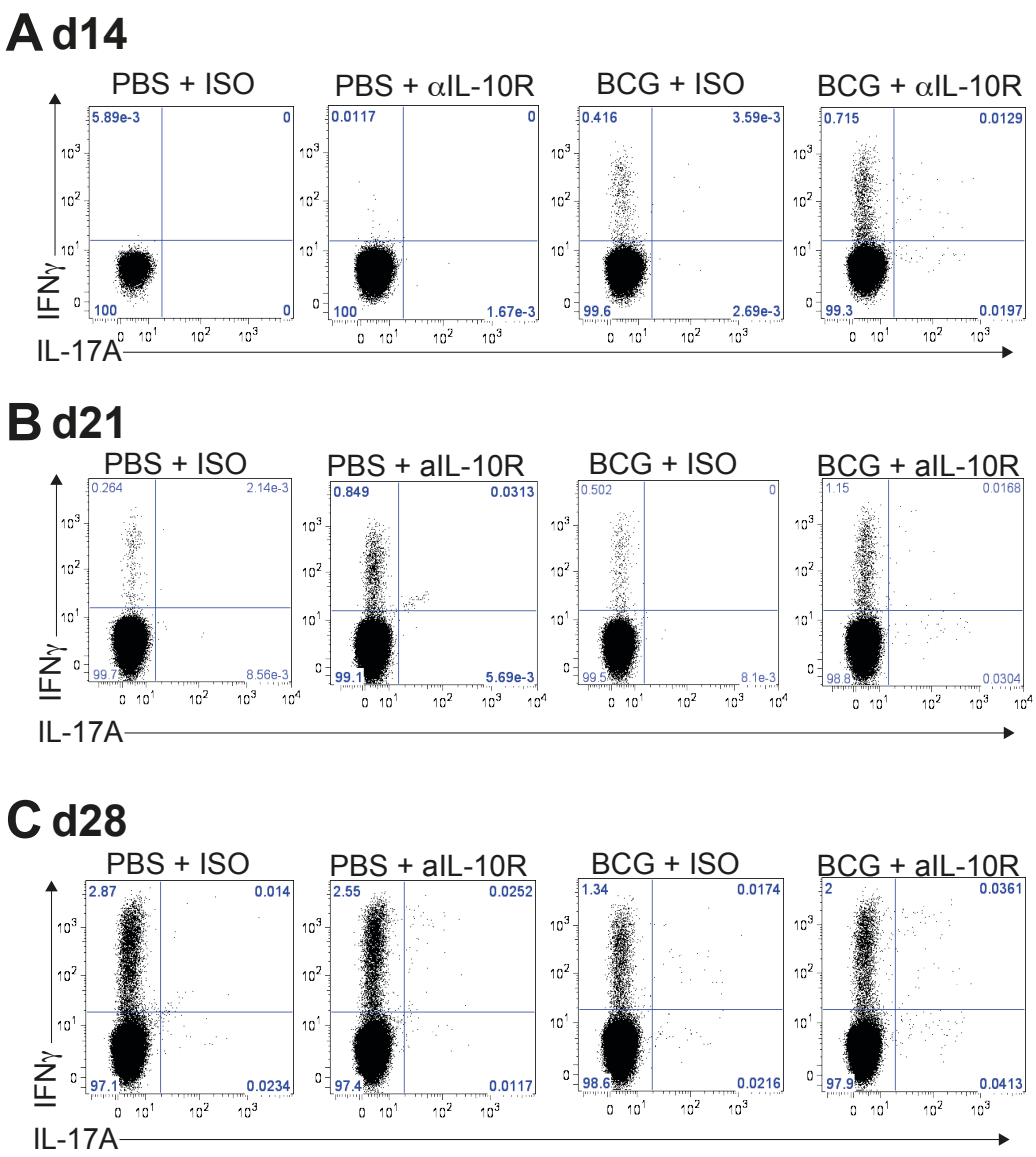

Figure 3.14 BCG vaccination in the context of αIL-10R mAb does not significantly affect IFNγ or IL-17 production by CD4$^+$ T cells in the spleen upon Mtb challenge. (Flow cytometry plots)

CBA/J mice were BCG vaccinated and challenged with *Mtb* as shown in **Figure 3.1**. Mice were sacrificed and lungs harvested at 14, 21 and 28 days post *Mtb* challenge. Spleens were homogenized by passage through a 70μm filter. 5x10^6 cells were restimulated with 20μg PPD and 2μg αCD28 mAb for 16h before the addition of BFA for a further 4h. Cells were then harvested and stained with the following to assess cytokine production: γδ TCR FITC, GM-CSF PE, CD8 PerCP e710, Thy1.2 PE Cy7, IFNγ e450, CD4 v500, IL-17A APC, CD3 APCe780. CD4$^+$ T cells were identified as CD3$^+$ Thy1.2$^+$ CD4$^+$. Representative flow cytometry plots from day 14 **(A)**, day 21 **(B)** or day 28 post infection **(C)** are shown are shown. Individual time points are from independent experiments. Data representative of 2 independent experiments at each time point. 2-5 mice per group.

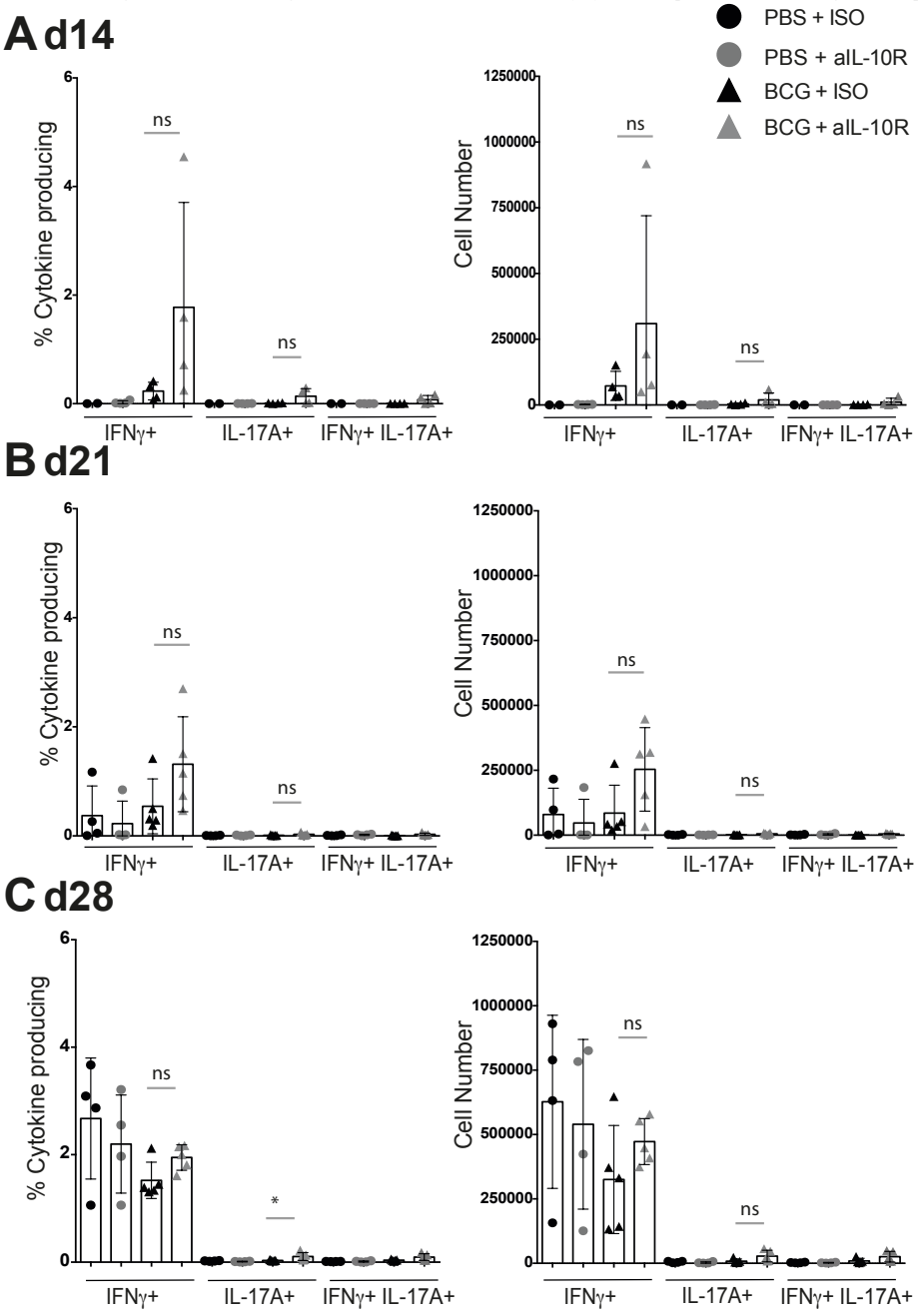

Figure 3.15 BCG vaccination in the context of αIL-10R mAb does not significantly affect IFNγ or IL-17 production by CD4$^+$ T cells (percentage and number cytokine producing) in the spleen upon Mtb challenge.

CBA/J mice were BCG vaccinated and challenged with *Mtb* as shown in **Figure 3.1**. Mice were sacrificed and lungs harvested at 14, 21 and 28 days post *Mtb* challenge. Spleens were homogenized by passage through a 70μm filter. 5x10^6 cells were restimulated with 20μg PPD and 2μg αCD28 mAb for 16h before the addition of BFA for a further 4h. Cells were then harvested and stained with the following to assess cytokine production: γδ TCR FITC, GM-CSF PE, CD8 PerCP e710, Thy1.2 PE Cy7, IFNγ e450, CD4 v500, IL-17A APC, CD3 APCe780. CD4$^+$ T cells were identified as CD3$^+$ Thy1.2$^+$ CD4$^+$. Percentage and number of cytokine producing CD4$^+$ T cells at day 14 **(A)**, day 21 **(B)** or day 28 post infection **(C).** Data representative of 2 independent experiments at each time point. 2-5 mice per group. Graphs show mean ± SD. ns – not significant *p<0.05, **p<0.01 by 2-way ANOVA with Tukey post test.

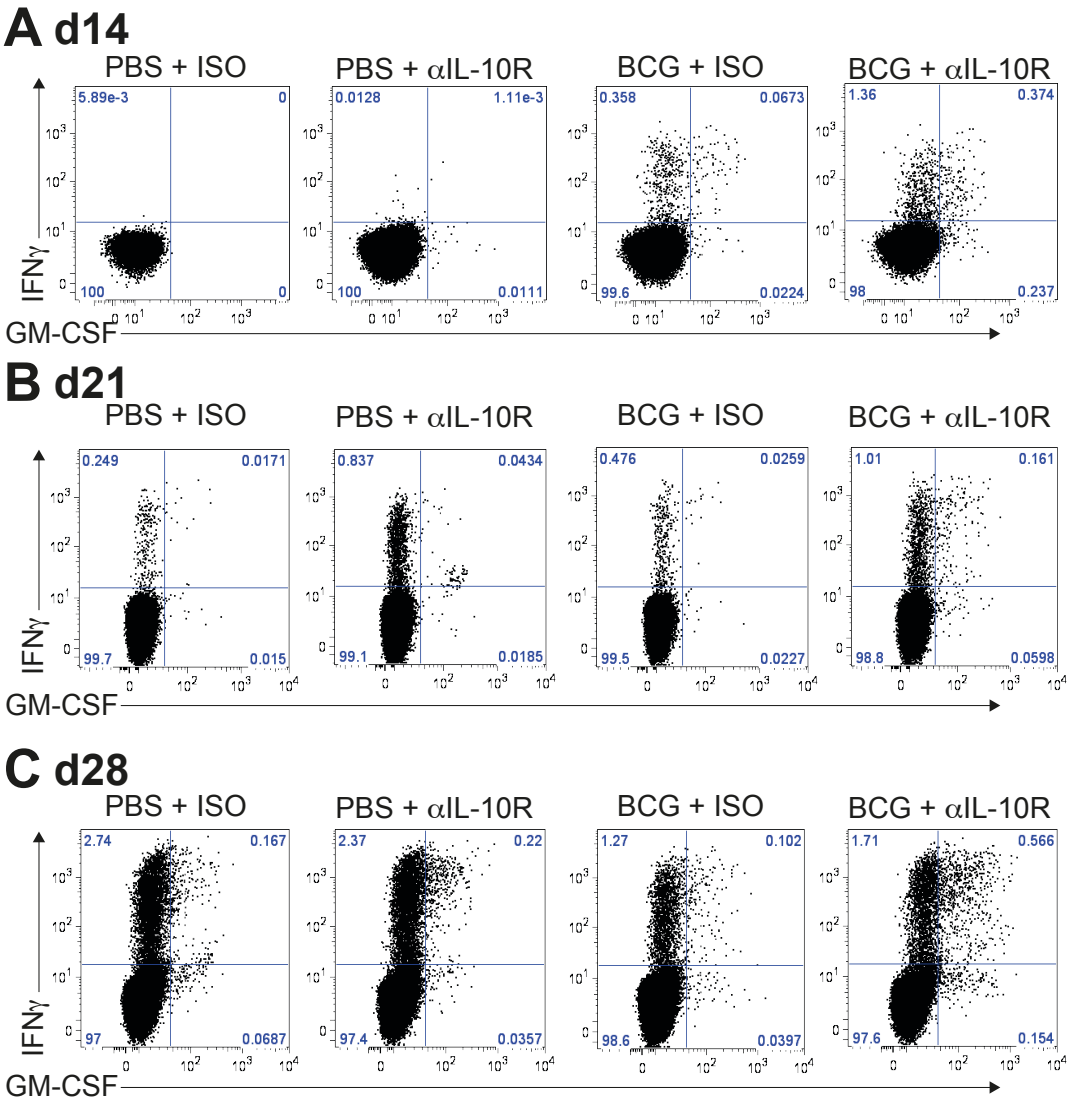

Figure 3.16 GM-CSF production by CD4$^+$ T cells is increased in the spleen upon Mtb challenge in mice vaccinated with BCG in the context of αIL-10R mAb. (Flow cytometry plots)

CBA/J mice were BCG vaccinated and challenged with *Mtb* as shown in **Figure 3.1**. Mice were sacrificed and lungs harvested at 14, 21 and 28 days post *Mtb* challenge. Spleens were homogenized by passage through a 70μm filter. 5x10^6 cells were restimulated with 20μg PPD and 2μg αCD28 mAb for 16h before the addition of BFA for a further 4h. Cells were then harvested and stained with the following to assess cytokine production: γδ TCR FITC, GM-CSF PE, CD8 PerCP e710, Thy1.2 PE Cy7, IFNγ e450, CD4 v500, IL-17A APC, CD3 APCe780. CD4$^+$ T cells were identified as CD3$^+$ Thy1.2$^+$ CD4$^+$. Representative flow cytometry plots from day 14 **(A)**, day 21 **(B)** or day 28 post infection **(C)** are shown are shown. Individual time points are from independent experiments. Data representative of 2 independent experiments at each time point. 2-5 mice per group.

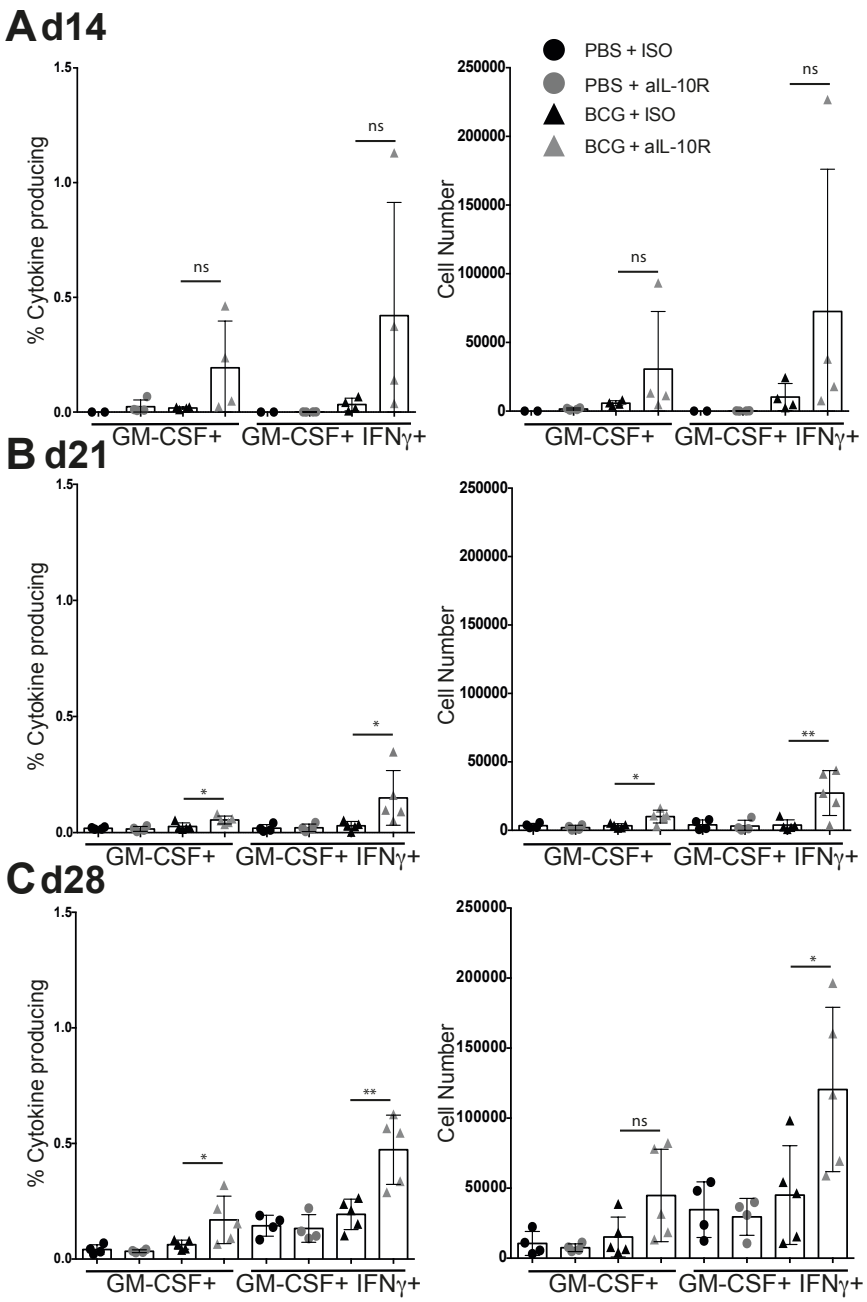

Figure 3.17 GM-CSF production by CD4$^+$ T cells (percentage and number cytokine producing) is increased in the spleen upon Mtb challenge in mice vaccinated with BCG in the context of αIL-10R mAb

CBA/J mice were BCG vaccinated and challenged with *Mtb* as shown in **Figure 3.1**. Mice were sacrificed and lungs harvested at 14, 21 and 28 days post *Mtb* challenge. Spleens were homogenized by passage through a 70μm filter. 5x10^6 cells were restimulated with 20μg PPD and 2μg αCD28 mAb for 16h before the addition of BFA for a further 4h. Cells were then harvested and stained with the following to assess cytokine production: γδ TCR FITC, GM-CSF PE, CD8 PerCP e710, Thy1.2 PE Cy7, IFNγ e450, CD4 v500, IL-17A APC, CD3 APCe780. CD4$^+$ T cells were identified as CD3$^+$ Thy1.2$^+$ CD4$^+$. Percentage and number of cytokine producing CD4$^+$ T cells at day 14 **(A)**, day 21 **(B)** or day 28 post infection **(C).** Data representative of 2 independent experiments at each time point. 2-5 mice per group. Graphs show mean ± SD. ns – not significant *p<0.05, **p<0.01 by 2-way ANOVA with Tukey post test.

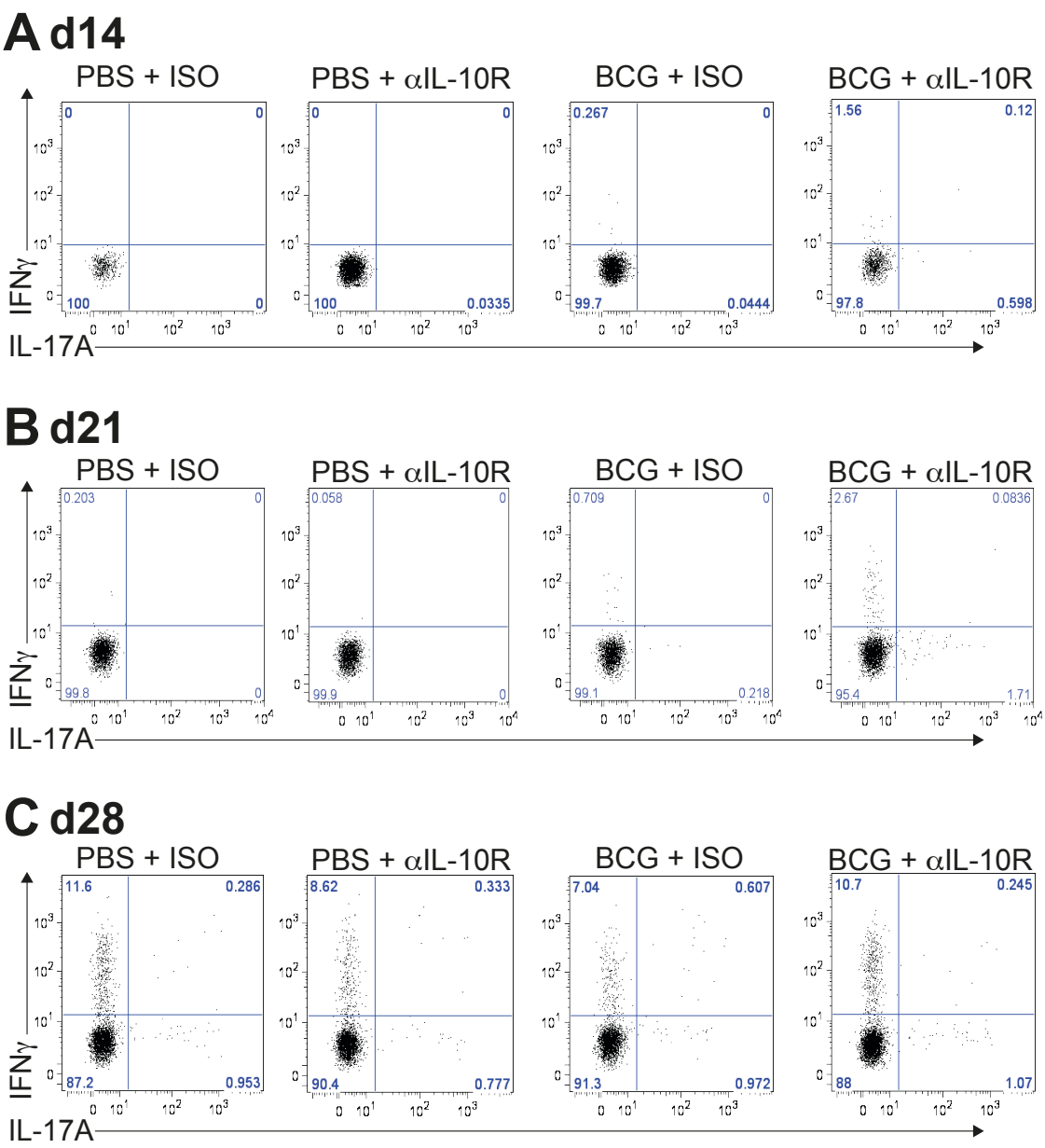

Figure 3.18 BCG vaccination in the context of αIL-10R mAb does not impact cytokine production by γδ T cells in the spleen upon Mtb challenge. (Flow cytometry plots)

CBA/J mice were BCG vaccinated and challenged with *Mtb* as shown in **Figure 3.1**. Mice were sacrificed and lungs harvested at 14, 21 and 28 days post *Mtb* challenge. Spleens were homogenized by passage through a 70μm filter. $5x10^6$ cells were restimulated with 20μg PPD and 2μg αCD28 mAb for 16h before the addition of BFA for a further 4h. Cells were then harvested and stained with the following to assess cytokine production: γδ TCR FITC, GM-CSF PE, CD8 PerCP e710, Thy1.2 PE Cy7, IFNγ e450, CD4 v500, IL-17A APC, CD3 APCe780. γδ T cells were identified as $CD3^+$ $Thy1.2^+$ γδ TCR^+. Representative flow cytometry plots from day 14 **(A)**, day 21 **(B)** or day 28 post infection **(C)** are shown are shown. Individual time points are from independent experiments. Data representative of 2 independent experiments at each time point. 2-5 mice per group.

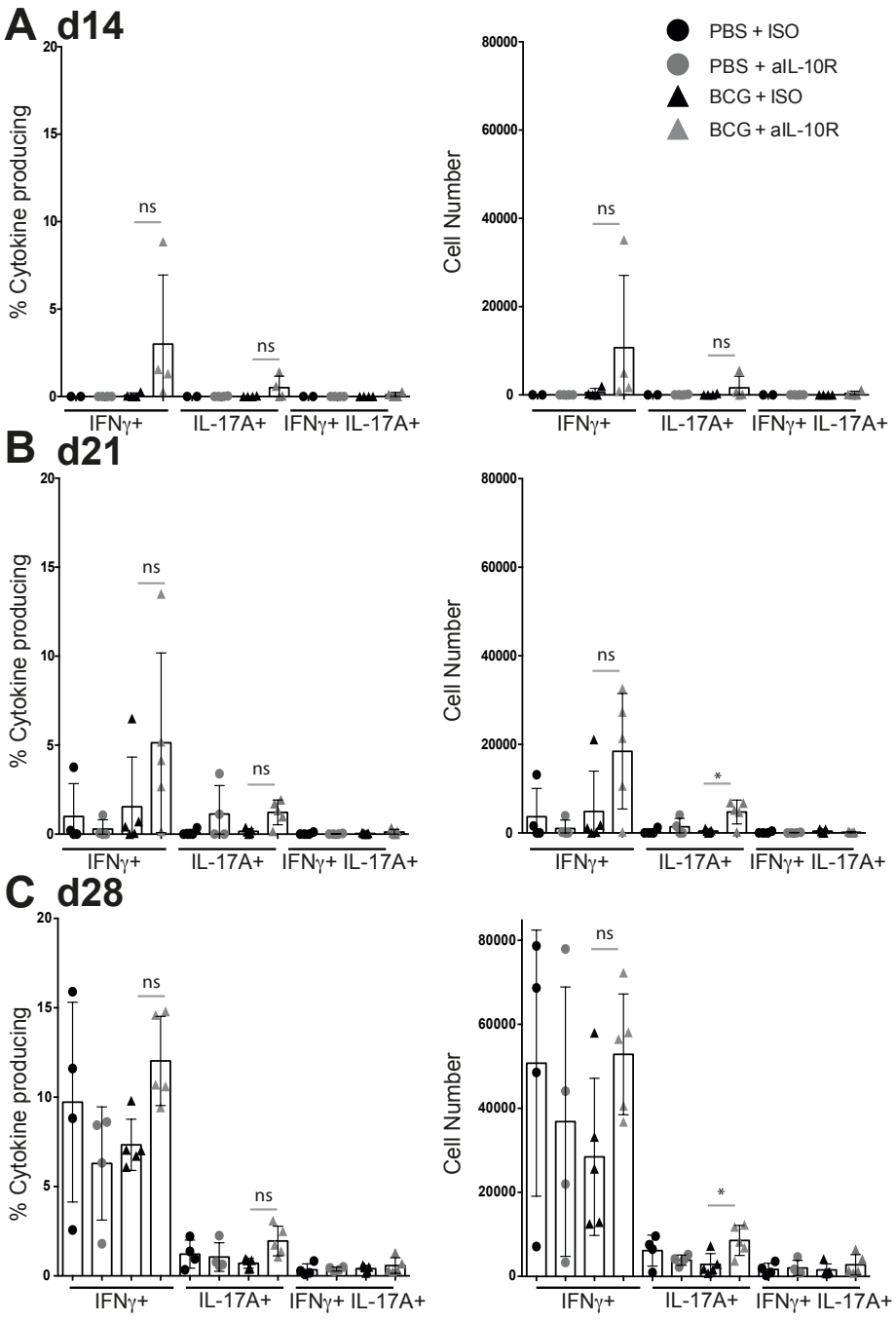

Figure 3.19 BCG vaccination in the context of αIL-10R mAb does not impact cytokine production by γδ T cells (percentage and number cytokine producing) in the spleen upon Mtb challenge.

CBA/J mice were BCG vaccinated and challenged with *Mtb* as shown in **Figure 3.1**. Mice were sacrificed and lungs harvested at 14, 21 and 28 days post *Mtb* challenge. Spleens were homogenized by passage through a 70μm filter. $5x10^6$ cells were restimulated with 20μg PPD and 2μg αCD28 mAb for 16h before the addition of BFA for a further 4h. Cells were then harvested and stained with the following to assess cytokine production: γδ TCR FITC, GM-CSF PE, CD8 PerCP e710, Thy1.2 PE Cy7, IFNγ e450, CD4 v500, IL-17A APC, CD3 APCe780. γδ T cells were identified as $CD3^+$ $Thy1.2^+$ γδ TCR^+. Percentage and number of cytokine producing γδ T cells at day 14 **(A)**, day 21 **(B)** or day 28 post infection **(C).** Data representative of 2 independent experiments at each time point. 2-5 mice per group. Graphs show mean ± SD. ns – not significant *$p<0.05$ by 2-way ANOVA with Tukey post test.

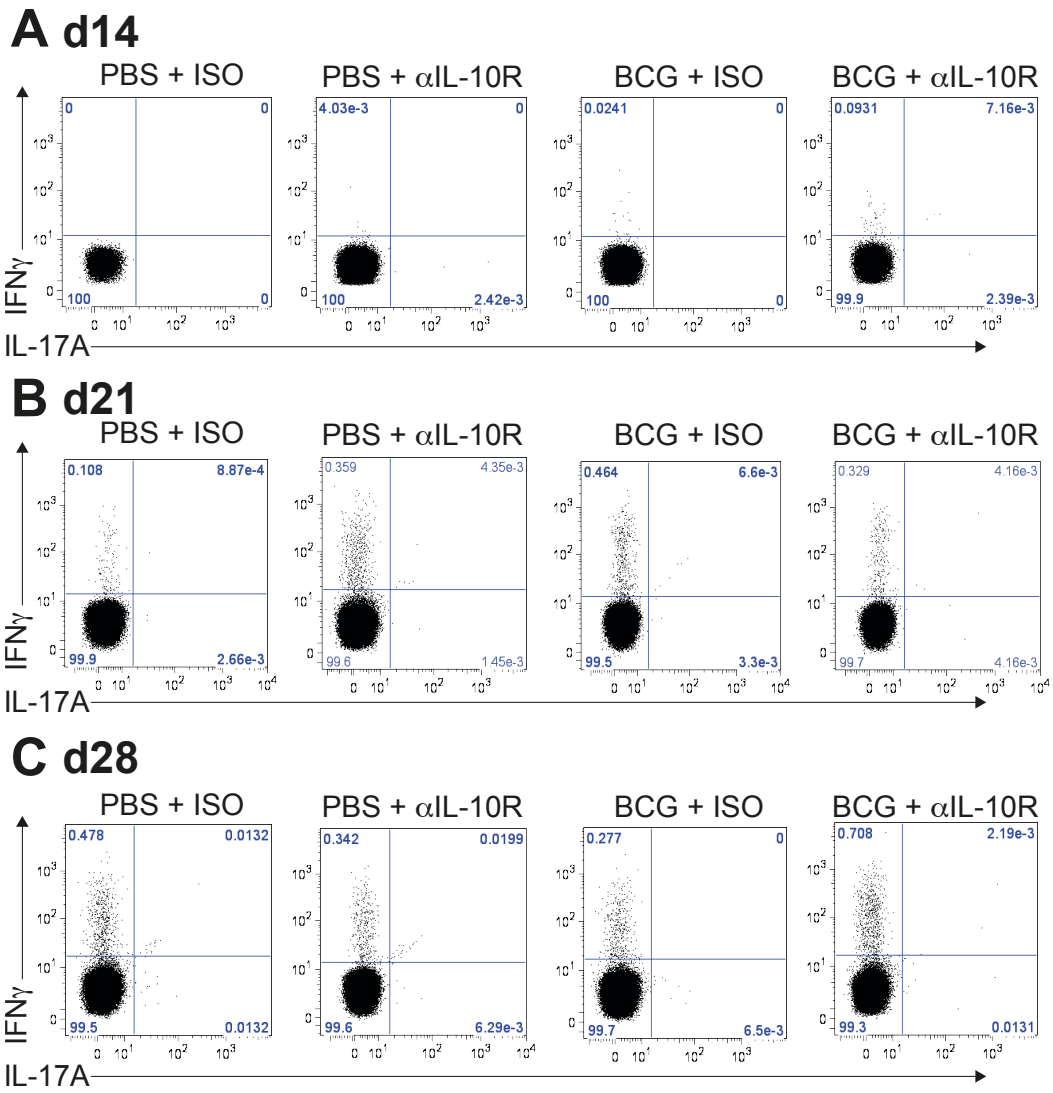

Figure 3.20 BCG vaccination in the context of αIL-10R mAb does not impact cytokine production by CD8$^+$ T cells in the spleen upon Mtb challenge. (Flow cytometry plots)

CBA/J mice were BCG vaccinated and challenged with *Mtb* as shown in **Figure 3.1**. Mice were sacrificed and lungs harvested at 14, 21 and 28 days post *Mtb* challenge. Spleens were homogenized by passage through a 70μm filter. 5x10^6 cells were restimulated with 20μg PPD and 2μg αCD28 mAb for 16h before the addition of BFA for a further 4h. Cells were then harvested and stained with the following to assess cytokine production: γδ TCR FITC, GM-CSF PE, CD8 PerCP e710, Thy1.2 PE Cy7, IFNγ e450, CD4 v500, IL-17A APC, CD3 APCe780. CD8$^+$ T cells were identified as CD3$^+$ Thy1.2$^+$ CD8$^+$. Representative flow cytometry plots from day 14 **(A)**, day 21 **(B)** or day 28 post infection **(C)** are shown are shown. Individual time points are from independent experiments. Data representative of 2 independent experiments at each time point. 2-5 mice per group.

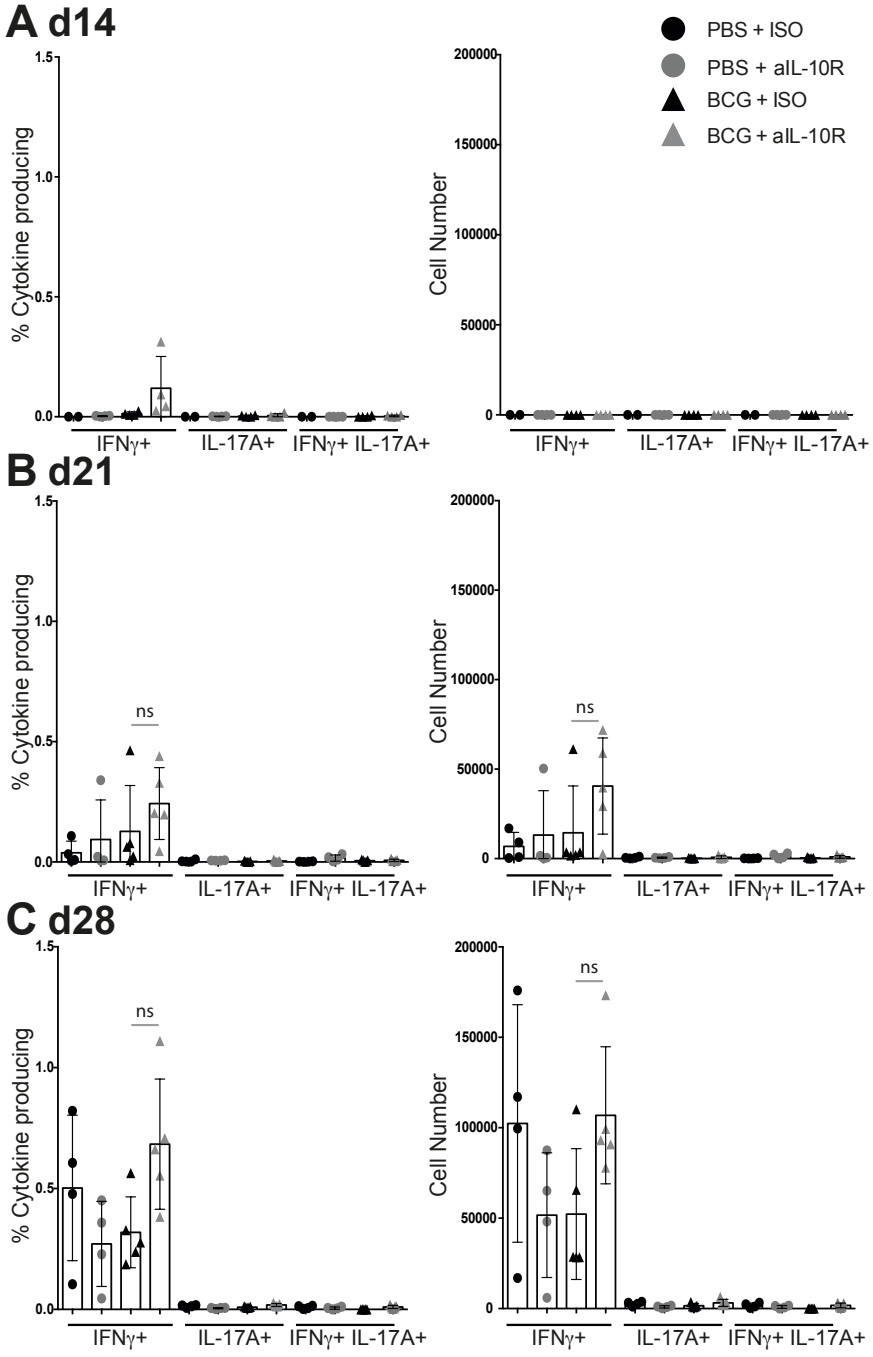

Figure 3.21 BCG vaccination in the context of αIL-10R mAb does not impact cytokine production by CD8$^+$ T cells (percentage and number cytokine producing) in the spleen upon Mtb challenge.

CBA/J mice were BCG vaccinated and challenged with *Mtb* as shown in **Figure 3.1**. Mice were sacrificed and lungs harvested at 14, 21 and 28 days post *Mtb* challenge. Spleens were homogenized by passage through a 70μm filter. 5x10^6 cells were restimulated with 20μg PPD and 2μg αCD28 mAb for 16h before the addition of BFA for a further 4h. Cells were then harvested and stained with the following to assess cytokine production: γδ TCR FITC, GM-CSF PE, CD8 PerCP e710, Thy1.2 PE Cy7, IFNγ e450, CD4 v500, IL-17A APC, CD3 APCe780. CD8$^+$ T cells were identified as CD3$^+$ Thy1.2$^+$ CD8$^+$. Percentage and number of cytokine producing CD8$^+$ T cells at day 14 **(A)**, day 21 **(B)** or day 28 post infection **(C).** Data representative of 2 independent experiments at each time point. 2-5 mice per group. Graphs show mean ± SD. ns – not significant by 2-way ANOVA with Tukey post test.

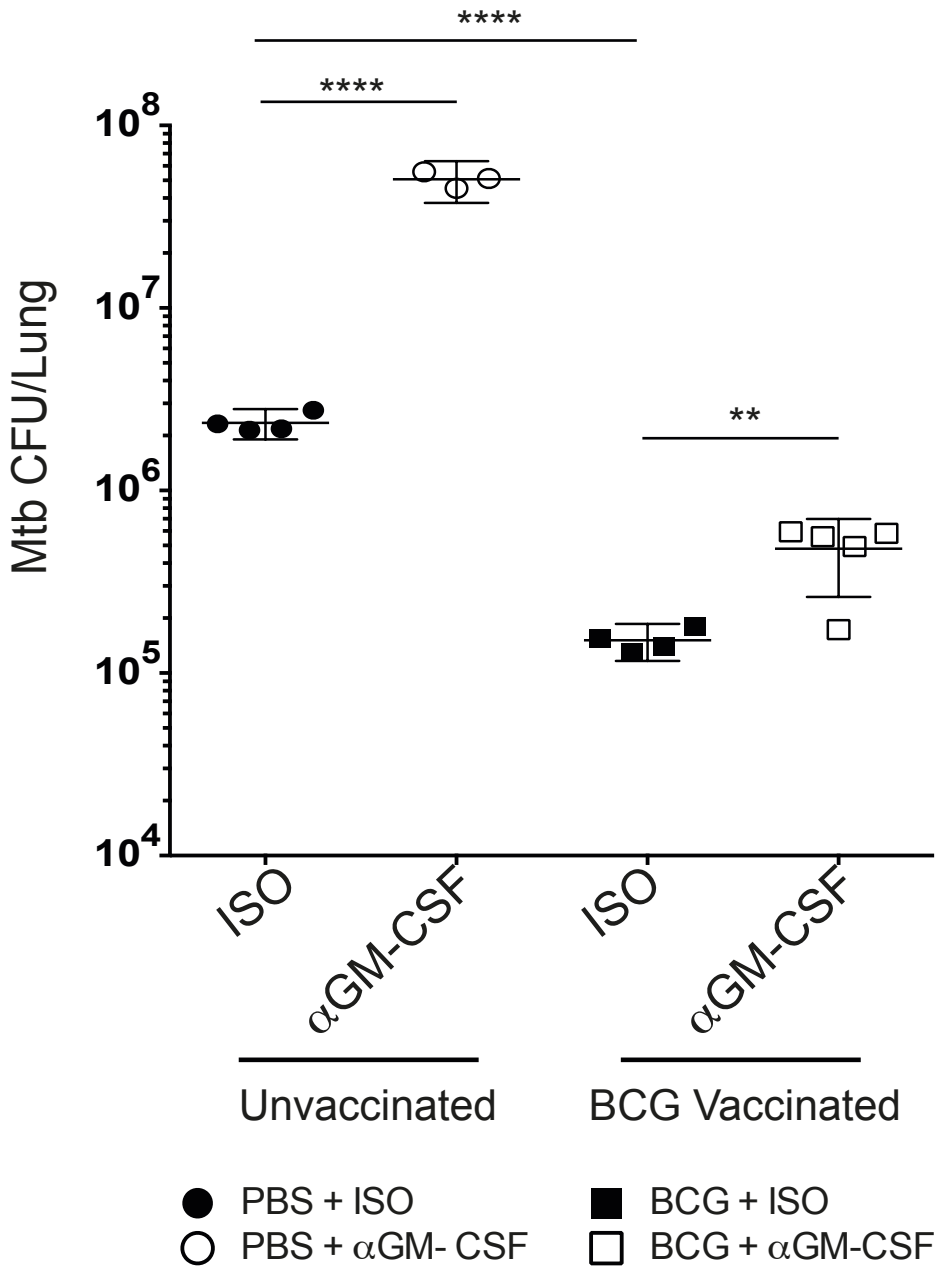

Figure 3.22 GM-CSF is required for optimal protection during Mtb challenge following BCG vaccination

CBA/J mice were intradermally vaccination with approximately $5x10^5$ CFU BCG or PBS. 6 weeks after BCG vaccination mice received 1mg i.p. injection with αGM-CSF or isotype (GL117; ISO) control. The following day mice were challenged with approx. 100-200 CFU of the *Mtb* strain H37Rv, via aerosol route. Twice weekly i.p. injections containing 0.3mg or αGM-CSF or ISO (GL117) were given. Mice were sacrificed and lungs harvested at 9 weeks post infection and bacterial load was determined. Graphs show mean ± SD. Data representative of 2 independent experiments (experiment not shown performed with mice purchased from Jackson Laboratories). **p<0.01, ****p<0.0001 by students t-test.

Chapter 4 Evaluating the importance of GM-CSF during primary *Mtb* infection

4.1 Evaluating the importance of GM-CSF during primary *Mtb* infection: aims of the investigation

In order to determine the role of GM-CSF specifically during primary *Mtb* infection, we aimed to investigate:

1) The impact of GM-CSF neutralisation during *Mtb* infection upon the control of bacterial load in *Mtb* resistant C57BL/6 and *Mtb* susceptible CBA/J mouse strains

2) How GM-CSF neutralisation impacts the onset and magnitude of an adaptive immune response in both these mouse strains

3) Whether GM-CSF neutralisation impacts myeloid populations upon *Mtb* infection

4.2 Background

4.2.1 Functions of GM-CSF

GM-CSF is produced by multiple cell types including: T cells, macrophages, endothelial cells and fibroblasts (Gasson, 1991). It was originally named due to its ability to differentiate bone marrow progenitors to macrophages and granulocytes (Burgess and Metcalf, 1980). Given this role in myeloid development it was surprising when GM-CSF deficient mice did not display overt defects in blood myeloid populations, possibly because other cytokines can compensate for the absence of GM-CSF (Dranoff et al., 1994; Stanley et al., 1994). Subsequently, however, GM-CSF was found to be crucial for the development of alveolar macrophages from foetal monocytes via induction of PPARγ (Guilliams et al., 2013; Schneider et al., 2014). Thus GM-CSF deficient mice lack mature alveolar macrophages (Becher et al., 2014; Guilliams et al., 2013; Schneider et al., 2014). GM-CSF stimulated induction of the transcription factor PU.1 is suggested to be required for maturation of alveolar macrophages and forced expression of PU.1

in GM-CSF deficient alveolar macrophages can rescue defects in cytokine production, surfactant metabolism and bacterial killing (Shibata et al., 2001).

GM-CSF deficient mice develop a lung disease resembling the human disease pulmonary alveolar proteinosis (PAP) (Dranoff et al., 1994; Stanley et al., 1994). In humans PAP can either be caused by acquired or genetic factors (Seymour and Presneill, 2002). Those with genetic causes of PAP account for less than 10% or all PAP cases, and can result from mutations in the genes encoding either subunit of the GM-CSF receptor: CSFRA or CSFRB (Seymour and Presneill, 2002; Whitsett et al., 2015). Mutations in the genes encoding surfactant protein B, C or the transporter ABCA3 can also result in PAP (Seymour and Presneill, 2002; Whitsett et al., 2015). More than 90% of PAP cases are acquired and the majority of these patients have autoantibodies against GM-CSF, although PAP can also occur following exposure to various environmental agents (Seymour and Presneill, 2002). PAP is characterised by accumulation of surfactant and proteinaceous material within the alveolar space, resulting in dyspnoea and compromised gas exchange (Trapnell and Whitsett, 2002). This build up of surfactant is due to the inadequate clearance of surfactant by alveolar macrophages (Dranoff et al., 1994; Trapnell and Whitsett, 2002). PAP patients are more susceptible to infections with opportunistic pathogens including *Nocardia, Pneumocystis, Acinetobacter, Aspergillus, Cladosporium, Mtb* and atypical mycobacteria, with reports of systemic infections, rather than localised containment (Borie et al., 2011; Seymour and Presneill, 2002). Neutrophils from patients with PAP, as well as GM-CSF deficient mice, display basal functional defects, as well as defects in bacterial killing, which could contribute to the increased susceptibility to infections (Uchida et al., 2007).

In addition to its role in the development of alveolar macrophages, GM-CSF has also been implicated in the development of other cell subsets. *In vitro* GM-CSF can induce the differentiation of DCs, in addition to macrophages and granulocytes, from bone marrow precursors (Inaba et al., 1992). *In vivo* GM-CSF is suggested to be required for the development of $CD103^+$ DCs in non-lymphoid tissue such as skin and lamina propria, although there are

some conflicting reports (Bogunovic et al., 2009; Hamilton, 2015; King et al., 2010). The role for GM-CSF in the differentiation of inflammatory DCs is controversial, with several conflicting reports (Hamilton, 2015). NKT cells have also been shown to be dependent upon GM-CSF for their functional development, with NKT cells from GM-CSF deficient mice exhibiting defects in cytokine secretion in response to αGalCer (Bezbradica et al., 2006).

GM-CSF can also act as a pro-inflammatory cytokine to activate myeloid populations (Hamilton, 2008). GM-CSF is suggested to prime macrophages to enhance pro-inflammatory cytokine production in response to LPS (Hamilton, 2002). Indeed, stimulation of GM-CSF derived bone marrow macrophages with LPS induces production of pro-inflammatory cytokines such as TNFα and IL-12p70 *in vitro*. Pre-treatment of M-CSF derived macrophages with GM-CSF, before LPS stimulation, increases production of pro-inflammatory cytokines compared to no pre-treatment (Fleetwood et al., 2007). Cross presentation by $CD8^+$ DCs is enhanced by GM-CSF (Zhan et al., 2012), as is antigen presentation by $CD8^-$ DCs (Min et al., 2010). GM-CSF treatment of DC subsets is also accompanied by upregulation of co-stimulatory molecules (Min et al., 2010). Therefore, in addition to the role of GM-CSF in the development of cell populations such as alveolar macrophages and NKT cells, GM-CSF is also crucial for maintenance of pulmonary homeostasis and has pro-inflammatory functions, influencing cytokine production by and activation status of myeloid populations.

4.2.2 The role of GM-CSF in Mtb infection

In the context of *Mtb* infection, studies using GM-CSF deficient mice have demonstrated a protective role for GM-CSF (Gonzalez-Juarrero et al., 2005; Szeliga et al., 2008). GM-CSF deficient mice show reduced survival, increased bacterial loads and disorganised granulomas in response to *Mtb* infection compared to wild-type controls (Gonzalez-Juarrero et al., 2005; Szeliga et al., 2008). However, due to the developmental defects in alveolar macrophage populations and the development of a PAP like disease, studies using GM-CSF deficient mice

are difficult to interpret. Indeed alveolar macrophages are thought to be one of the first cell types to become infected with *Mtb* following inhalation (Srivastava et al., 2014), and therefore changes in these populations could significantly impact the subsequent sequelae of infection. Furthermore, the developmental defects in other cell populations, such as NKT cells could also confound the interpretation of these results, as NKT cells are suggested to be involved in the response to *Mtb* infection through production of cytokines (Rothchild et al., 2014; Sada-Ovalle et al., 2008).

GM-CSF, produced by NKT cells, can also act directly upon mouse macrophages to restrict *Mtb* growth (Rothchild et al., 2014). Although the mechanism for this growth restriction is unknown, it was shown to be independent of iNOS (Rothchild et al., 2014). Treatment of infected mice with KGF is suggested to induce GM-CSF production, leading to restriction of bacterial growth through increased macrophage activation and phagolysosome fusion (Pasula et al., 2015). In human monocyte derived macrophages, GM-CSF is capable of restricting *Mtb* growth and also other mycobacterial species (Bermudez and Young, 1990; Denis, 1991; Denis and Ghadirian, 1990). These studies suggest a pro-inflammatory role for GM-CSF during *Mtb* infection.

In the previous chapter we correlated increased protection in chronic infection following vaccination, with earlier and elevated production of GM-CSF. We then demonstrated that GM-CSF neutralisation during *Mtb* infection, in the susceptible CBA/J mice, was detrimental to control of infection in both BCG vaccinated and unvaccinated mice. Given the difficulties in interpreting studies using GM-CSF deficient mice, we were interested in further investigating the role of GM-CSF in primary *Mtb* infection through GM-CSF neutralisation where developmental abnormalities would be avoided. In addition, as this strategy does not rely on genetic modification, the role of GM-CSF in both resistant and susceptible mice could be assessed, which is beneficial given that susceptible mouse strains are argued to better reflect human disease (Apt and Kramnik, 2009).

4.3 Assessing the importance of GM-CSF during *Mtb* infection

4.3.1 GM-CSF is required to control bacterial load in both resistant C57BL/6 and susceptible CBA/J mice

To assess the role of GM-CSF during primary *Mtb* infection, resistant C57BL/6 mice and susceptible CBA/J mice, were infected with the lab strain of *Mtb*, H37Rv, in the context of αGM-CSF treatment as shown in **Figure 4.1A**. Mice received an i.p. injection containing 1mg of αGM-CSF (clone MP1-22E9) or isotype control antibody (GL117) the day prior to *Mtb* infection and following infection mice received twice weekly i.p. injections of 0.3mg αGM-CSF or isotype control antibody. Mice were sacrificed at days 21, 28, 41 (CBA/J only) and 55 and bacterial loads in the lung were determined as described in Materials and Methods.

In resistant C57BL/6 mice, we found there was no difference in *Mtb* bacterial load in the lung at day 21 post infection. At day 28 and day 55 post infection we found a significant increase in lung bacterial load in mice treated with αGM-CSF as compared to those treated with the isotype control (**Figure 4.1B**) (day 28 $p<0.05$, day 55 $p<0.0001$). In contrast, in susceptible CBA/J mice, no difference in bacterial load between isotype treated and αGM-CSF treated mice was evident at days 21 or 28 post infection. At days 41 and 55 post infection there was an increase in bacterial load in mice treated with αGM-CSF, although at day 41 this did not quite reach significance (**Figure 4.1C**) (day 41 $p=0.07$, day 55 $p<0.001$).

4.3.2 GM-CSF marginally impacts recruitment of T cells to the lung upon Mtb infection in resistant mice but not susceptible mice

Having shown that GM-CSF is crucial for the control of bacterial load upon *Mtb* infection, we next investigated whether this correlated with a reduction in the presence of an adaptive immune response, as has been suggested at day 21 post *Mtb* infection in the GM-CSF deficient mouse (Gonzalez-Juarrero et al., 2005). We first assessed total T cell populations present in the lung at day 21 and 28 post infection, time points which should capture the onset of an adaptive immune response (reviewed in Cooper, 2009). Resistant and susceptible mice were infected and treated with αGM-CSF or isotype control as described above and as shown in **Figure 4.1A**. At days 21, 28 single cell suspensions generated from the lung were stained to identify $CD4^+$, $CD8^+$ and γδ T cells with the gating strategy shown in Appendix 1.

We found that αGM-CSF mAb treatment of resistant mice during *Mtb* infection had a small impact on T cell populations present early following infection. At day 21 and day 28 post infection, in resistant C57BL/6 mice we found no difference in the percentage of $CD4^+$ or $CD8^+$ T cells present in the lung but found significantly lower numbers of these T cells, between mice treated with αGM-CSF or isotype control (**Figure 4.2A** and **Figure 4.2B**). Numbers of $CD4^+$ and $CD8^+$ T cells were equivalent between the two groups at day 28 post infection (**Figure 4.2A** and **Figure 4.2B**). At day 21 post infection the percentage and number of γδ T cells in the lung was lower in mice treated with αGM-CSF, while at day 28 post infection the percentage of γδ T cells was higher in mice treated with αGM-CSF but there was no difference in numbers (**Figure 4.2C**).

In contrast to resistant C57BL/6 mice, GM-CSF neutralisation during *Mtb* infection in susceptible CBA/J mice, did not impact $CD4^+$, $CD8^+$ or γδ T cell populations in the lung at days 21 or 28 post infection (**Figure 4.3A, Figure 4.3B and Figure 4.3C**).

4.3.3 GM-CSF does not impact IFNγ or IL-17 production by CD4$^+$ T cells in resistant or susceptible mice

Although we found only minimal or no differences in the total T cell populations when GM-CSF was neutralised, the function of the T cells present could be impaired in the absence of GM-CSF. We therefore assessed the production of IFNγ and IL-17A by different T cell populations upon infection. Single cell suspensions were obtained from the lungs of mice infected and administered mAb as described in **Figure 4.1**. These were restimulated with PPD and αCD28 for 16 hours before addition of Brefeldin A for a further 4 hours, as described in Materials and Methods. Cells were harvested and intracellular cytokine staining was performed to identify cytokine producing CD4$^+$, CD8$^+$ and γδ T cells, with the gating strategy for identification shown in Appendix 2. We began by assessing cytokine production by CD4$^+$ T cells due to the known importance of these cells in the immune response to *Mtb* infection (reviewed in O'Garra et al., 2013).

In resistant C57BL/6 mice we found that CD4$^+$ T cells produced IFNγ, but not IL-17A, at day 21 post infection but neutralisation of GM-CSF did not impact this. Similarly at day 28 we found equivalent production of IFNγ by CD4$^+$ T cells in mice treated with αGM-CSF or isotype control and could not detect IL-17A production (**Figure 4.4A** and **Figure 4.4B**). In contrast to resistant C57BL/6 mice, at day 21 post infection we could not detect IFNγ or IL-17 production by CD4$^+$ T cells in susceptible CBA/J mice under any treatment condition. At day 28 post infection IFNγ production by CD4$^+$ T cells was equivalent in isotype treated and αGM-CSF treated susceptible CBA/J mice (**Figure 4.5A** and **Figure 4.5B**).

Our results show that GM-CSF is important in control of bacterial load during the immune response to *Mtb* infection and we were interested in defining the cellular source of GM-CSF upon infection. As CD4$^+$ T cells can produce GM-CSF, we assessed whether CD4$^+$ T cells were

a source of GM-CSF upon *Mtb* infection. Single cell suspensions were obtained from antibody treated, infected mice and restimulated with PPD and αCD28 as described in Materials and Methods and intracellular cytokine staining was performed to identify GM-CSF (and IFNγ) producing T cells. The gating strategy to identify $CD4^+$ T cells producing GM-CSF is shown in Appendix 2. Only extremely low proportions and numbers of GM-CSF producing $CD4^+$ T cells were detected at day 21 or day 28 post infection in resistant or susceptible mouse strains (**Figure 4.6A** and **Figure 4.6B**). GM-CSF is reported to be produced by many other cell types including macrophages, fibroblast and type II pneumocytes (Gasson, 1991) and it is likely that there are other cellular sources of GM-CSF upon *Mtb* infection.

4.3.4 Neutralisation of GM-CSF decreases IFNγ production by $CD8^+$ T cells and IL-17 production by γδ T cells in resistant but not susceptible mice.

It is established that $CD8^+$ T cells and γδ T cells can produce cytokines upon *Mtb* infection, which could influence the outcome of infection (Behar, 2013; Bold and Ernst, 2012; Lockhart et al., 2006; Okamoto Yoshida et al., 2010). We therefore assessed whether cytokine production by these cell types was affected by GM-CSF neutralisation.

In resistant C57BL/6 mice at day 21 post infection we detected very little production of IFNγ by $CD8^+$ T cells in either mice treated with αGM-CSF mAb or isotype control (**Figure 4.7A** and **Figure 4.7B**). At day 28 we found a small percentage and number of $CD8^+$ T cells produced IFNγ, and this production was decreased when GM-CSF was neutralised throughout infection (**Figure 4.7A** and **Figure 4.7B**). IL-17A production by $CD8^+$ T cells was not found at either time point.

In susceptible CBA/J mice, as for resistant C57BL/6 mice, we did not detect IFNγ production by $CD8^+$ T cells at day 21 post infection (**Figure 4.8A** and **Figure 4.8B**). At day 28 post infection, there was low IFNγ production by $CD8^+$ T cells, with considerable variation within the groups. Neutralisation of GM-CSF throughout infection did not impact IFNγ production by $CD8^+$ T cells at day 28 post infection. Similarly to resistant C57BL/6 mice, no IL-17A production by $CD8^+$ T cells was detected at either time point (**Figure 4.8A** and **Figure 4.8B**).

As shown earlier the total γδ T cell population was lower, both in percentage and in number, at day 21 post *Mtb* infection when GM-CSF was neutralised throughout infection in resistant C57BL/6 mice (**Figure 4.2C**). In addition, GM-CSF neutralisation during *Mtb* infection significantly decreased the percentage and number of IL-17A producing γδ T cells at day 21 post *Mtb* challenge (**Figure 4.9A** and **Figure 4.9B)** (percentage $p<0.05$, number $p<0.05$). At day 28 post infection, there was a strong trend towards lower percentage of γδ T cells producing IL-17A in mice treated with αGM-CSF mAb, but this did not reach significance ($p=0.051$). There was no difference in the number of IL-17 producing γδ T cells at this time point (**Figure 4.9A** and **Figure 4.9B**).

In contrast to resistant C57BL/6 mice, in susceptible CBA/J mice no cytokine production by γδ T cells was detected at day 21 post infection (**Figure 4.10A** and **Figure 4.10B**). At day 28 post infection, IL-17A production was detected by γδ T cells but this was unaffected by GM-CSF neutralisation (**Figure 4.10A** and **Figure 4.10B**).

4.3.5 GM-CSF neutralisation impacts myeloid populations in Mtb infection

Thus far we have shown that GM-CSF is protective during *Mtb* infection in both resistant and susceptible mouse strains. A study using the GM-CSF deficient mouse, suggested that GM-CSF

is required for recruitment of IFNγ producing T cells to the lung at day 21 post *Mtb* infection (Gonzalez-Juarrero et al., 2005). Although there are small differences in the total T cell populations and cytokine production by other T cell populations in resistant mice, we did not find differences in IFNγ producing $CD4^+$ T cells at day 21 or 28 post infection. As GM-CSF is required for the differentiation, proliferation and activation of myeloid populations (Hamilton, 2008) we investigated how GM-CSF neutralisation impacts myeloid populations present during *Mtb* infection.

We first assessed the impact of GM-CSF neutralisation upon myeloid populations present in the lung in naïve mice, as GM-CSF deficiency is known to affect these populations (Becher et al., 2014; Gonzalez-Juarrero et al., 2005). Resistant C57BL/6 and susceptible CBA/J mice were i.p. injected with 1mg αGM-CSF (clone MP1-22E9) or isotype control (ISO) and subsequently received twice weekly i.p. injection containing 0.3mg of appropriate mAb for 3 or 4 weeks. Lungs were then harvested and single cell suspensions generated. These were stained to identify myeloid populations using the gating strategy shown in Appendix 3. We found that 3 weeks of αGM-CSF treatment of resistant C57BL/6 mice led to a decrease in the percentage and number of a $CD11c^+$ $CD11b^{lo}$ (MHC II^{int}, $F4/80^+$) population we define as alveolar macrophages (Becher et al., 2014) (**Figure 4.11A**). However, after 4 week of αGM-CSF treatment, we found no significant difference in the percentage or number of alveolar macrophages, although there was a trend towards a decrease (**Figure 4.11B**). We did not find any differences in neutrophils ($Ly6G^+$ $CD11b^+$), $CD11b^+$ $CD11c^+$ DCs at either time point, and found an increase in the number (but not percentage) of monocytes ($CD11b^+$ $Ly6G^-$ Ly6C hi) after 4 weeks of αGM-CSF treatment (data not shown).

Similarly to resistant C57BL/6 mice we found that 3 weeks of treatment with αGM-CSF mAb led to a decrease in the percentage and number of $CD11c^+$ $CD11b^{lo}$ (MHC II^{int}, $F4/80^+$) alveolar macrophages present in the lungs (**Figure 4.12A**). This decrease was not evident following 4

weeks of treatment, although there was a slight trend towards a decrease (**Figure 4.12B**). We did not find any differences in neutrophils ($Ly6G^+$ $CD11b^+$), $CD11b^+$ $CD11c^+$ DCs or monocytes ($CD11b^+$ Ly6C hi) at either time point (data not shown). The observed decrease in $CD11c^+$ $CD11b^{lo}$ alveolar macrophages in the steady state is in keeping with the requirement of GM-CSF for alveolar macrophage maintenance (Hashimoto et al., 2013; Shibata et al., 2001).

In order to assess the impact of GM-CSF neutralisation upon myeloid populations present in the lung during *Mtb* infection, resistant and susceptible mice were treated with αGM-CSF mAb or isotype control antibody and infected as described in **Figure 4.1A**. Lungs were harvested at days 21, 28 and 55 post infection and single cell suspensions stained to identify myeloid populations as shown in Appendix 3.

In resistant C57BL/6 mice, we found small differences in neutrophil and monocyte populations when GM-CSF was neutralised during infection (**Figure 4.13A** and **Figure 4.13B**). GM-CSF neutralisation through infection led to a small increase in the percentage of neutrophils ($Ly6G^+$ $CD11b^+$) present at day 21 and day 28 post infection but this was not evident in terms of numbers. At day 55 post infection there was a small increase in the number of neutrophils in the lung when GM-CSF was neutralised (Figure 4.13A). At day 21 post infection we detected a small decrease in the number of monocytes present in the lung in mice treated with αGM-CSF, although their percentage was not affected (**Figure 4.13B**). There was no difference in the percentage or number of monocytes present at day 28 between isotype or αGM-CSF treated mice, and a small decrease in the percentage of monocytes present in αGM-CSF treated mice at day 55 post infection (**Figure 4.13B**).

In contrast to the small impact GM-CSF neutralisation had on the presence of neutrophils and monocytes during *Mtb* infection, we found that in resistant C57BL/6 mice, neutralisation of GM-CSF dramatically reduced both the percentage and number of $CD11c^+$ $CD11b^{lo}$ (MHC II^{int}

, F4/80^{+}) alveolar macrophages throughout infection at day 21, 28 and 55 post infection (**Figure 14.13C**). Such a finding is in keeping with the importance of GM-CSF in the differentiation, maintenance and function of alveolar macrophages (Hashimoto et al., 2013; Shibata et al., 2001).

In resistant C57BL/6 mice, there was no effect on the percentage of CD11b^{+} CD11c^{+} DCs present in the lung at day 21 and 28 post infection however, the number of CD11b^{+} CD11c^{+} DCs was lower when GM-CSF was neutralised (**Figure 4.14A**). As GM-CSF can impact activation state and antigen presentation capacity of APCs, we assessed the levels of expression of MHC class II and the co-stimulatory molecule CD86 using the mean fluorescence intensity (MFI). We did not find any consistent impact of GM-CSF neutralisation, at any time point assessed, upon expression levels of MHC class II (**Figure 4.14B**) or CD86 (**Figure 4.14C**).

In susceptible CBA/J mice, GM-CSF neutralisation led to a small increase in the percentage and number of neutrophils in the lung at day 21 post infection (**Figure 4.15A**). However, this increase was not evident at day 28 or 55 post infection (**Figure 4.15A**). We did not detect any differences in the percentage or number of monocytes present in the lung between isotype and αGM-CSF treated mice at any of the time points assessed (**Figure 4.15B**). In contrast to resistant C57BL/6 mice, αGM-CSF treatment did not affect the number or percentage of CD11c^{+} CD11b^{lo} (MHC II^{int}, F4/80^{+}) alveolar macrophages at days 21 or 28 post infection (**Figure 4.15C**). A significant decrease in the percentage and number of CD11c^{+} CD11b^{lo} (MHC II^{int} F4/80^{+}) alveolar macrophages in susceptible mice treated with αGM-CSF was only evident at day 55 post infection (**Figure 4.15C**).

CD11b^{+} CD11c^{+} DC populations were unaffected by GM-CSF neutralisation in susceptible CBA/J mice at days 21 and 28 post *Mtb* infection (**Figure 4.16A**). However, at day 55 post infection there was a significant increase in the percentage and number of these cells in the lung

in mice treated with αGM-CSF mAb (**Figure 4.16A**). The impact of GM-CSF neutralisation on expression levels of MHC class II and CD86 on $CD11b^+$ $CD11c^+$ DCs was also assessed. No consistent impact of GM-CSF neutralisation upon the MFI of MHC class II (**Figure 4.16B**) or CD86 (**Figure 4.16C**) was observed.

4.4 Discussion

Work in this thesis has shown that early and elevated production of GM-CSF, following BCG vaccination in the context of αIL-10R, correlated with increased control of bacterial load in chronic infection (see Chapter 3). Indeed studies using GM-CSF deficient mice have shown that GM-CSF is crucial for the immune response to *Mtb* infection (Gonzalez-Juarrero et al., 2005; Szeliga et al., 2008). However, GM-CSF deficient mice suffer from a lung pathology resembling PAP, leading to accumulation of surfactant in the lung (Dranoff et al., 1994; Stanley et al., 1994; Trapnell and Whitsett, 2002). These mice are also deficient in mature alveolar macrophages (Becher et al., 2014; Guilliams et al., 2013; Schneider et al., 2014). As a result, it is difficult to interpret whether GM-CSF itself is important during *Mtb* infection or whether the lack of mature alveolar macrophages and surfactant accumulation result in increased susceptibility to *Mtb* infection. Thus, in order to assess the role of GM-CSF during *Mtb* infection, without initial perturbation in the lung environment, we administered neutralising antibody throughout infection. As this approach does not rely on genetic manipulation we were also able to assess the function of GM-CSF in susceptible CBA/J mice. This is beneficial because susceptible mice have been proposed to better reflect human TB pathology and thus provide a better model of *Mtb* infection (Apt and Kramnik, 2009).

4.4.1 GM-CSF neutralisation during Mtb infection exacerbates bacterial load in the lung

Neutralisation of GM-CSF throughout *Mtb* infection increased *Mtb* bacterial loads in the lung in both resistant C57BL/6, and susceptible CBA/J mice. The increase in bacterial loads is in keeping with studies using the GM-CSF deficient mice (Gonzalez-Juarrero et al., 2005; Szeliga et al., 2008). However, these studies showed that GM-CSF knock mice all succumbed to infection by approximately 5 weeks post infection (Gonzalez-Juarrero et al., 2005; Szeliga et al., 2008). This did not occur when GM-CSF is neutralised throughout infection and all mice

survived until the end of the experiment at day 55 post infection. This suggests that the phenotype in the GM-CSF deficient mouse is more severe than when GM-CSF is neutralised during infection. One possibility is that there was incomplete neutralisation of GM-CSF, resulting in some level of residual function. Another possibility is that the basal defects in lung homeostasis in GM-CSF deficient mice (Dranoff et al., 1994; Gonzalez-Juarrero et al., 2005; Stanley et al., 1994), lead to significant impairment of the control of *Mtb* bacterial load, to a much greater extent that in mice treated with αGM-CSF, where these basal defects are not present.

4.4.2 GM-CSF neutralisation minimally impacts T cell recruitment and cytokine production in resistant C57BL/6 mice but not susceptible CBA/J mice

GM-CSF deficient mice have been shown to display impaired recruitment of an adaptive immune response to the lung upon *Mtb* infection, which was suggested to contribute to its increased susceptibility (Gonzalez-Juarrero et al., 2005). We therefore assessed whether there were similar defects in mice treated with αGM-CSF throughout infection, which could contribute to the increased susceptibility observed. In resistant C57BL/6 mice we found small decreases in the number of total $CD4^+$, $CD8^+$ and γδ T cells present in the lung at day 21 post infection when GM-CSF was neutralised. A similar decrease in $CD4^+$ T cells at day 21 post infection was found in GM-CSF deficient mice (Gonzalez-Juarrero et al., 2005). However, we found the effect on T cell recruitment was transient as by day 28 post infection there were no differences in $CD4^+$ or $CD8^+$ T cell populations in the lungs of C57BL/6 mice treated with αGM-CSF. One possible way in which GM-CSF could influence the adaptive response is through induction of lymphocyte attracting chemokines. In GM-CSF deficient mice a defect in expression of chemokines such as CCL5 in the lung was suggested to underlie their susceptibility (Gonzalez-Juarrero et al., 2005). Measurement of chemokines such as CCL5 could provide more information on how GM-CSF influences T cell recruitment.

Although the numbers of total $CD4^+$ T cells were slightly decreased at day 21 post infection in resistant C57BL/6 mice treated with αGM-CSF, equivalent percentages and number of $CD4^+$ T cells produced IFNγ at days 21 and 28 post infection in resistant mice, and no IL-17A production was detected under any condition. This contrasts with the GM-CSF knock mice which display lower numbers of IFNγ producing $CD4^+$ T cells at day 21 post infection (Gonzalez-Juarrero et al., 2005). Although IFNγ is crucial for the immune response to *Mtb* infection (Cooper et al., 1993; Flynn et al., 1993), $CD4^+$ T cells can produce other factors such as TNFα, which is also crucial for control of *Mtb* infection (Bean et al., 1999; Flynn et al., 1995a). It is possible that GM-CSF neutralisation is impacting the production of another factor such as TNFα from $CD4^+$ T cells that could impact the outcome of infection. In contrast to $CD4^+$ T cells, IFNγ production by $CD8^+$ T cells was reduced at day 28 post infection by αGM-CSF treatment, although, very few $CD8^+$ T cell produced IFNγ during *Mtb* infection in isotype control treated mice, and it is likely that $CD4^+$ T cells are the major source. Thus this small decrease in $CD8^+$ T cell derived IFNγ may not impact the outcome of infection. However, $CD8^+$ T cells can also be cytotoxic and lyse target cells. Indeed perforin expression is required for their capacity to protect against *Mtb* infection when adoptively transferred (Woodworth et al., 2008). A possibility is that this function of $CD8^+$ T cells is impaired in the absence of GM-CSF which would require further investigation in future studies.

In resistant C57BL/6 mice, in addition to lower total γδ T cell numbers in the lung, we also observed a decrease in γδ T cell derived IL-17 at day 21 post infection. Although the role of IL-17 in primary *Mtb* infection is unclear, IL-17 is suggested to be required for the formation of granulomas following BCG infection and for localisation of the T cell response within the granulomas through CXCL13 induction following infection with hyper-virulent HN878 (Gopal et al., 2014). Thus it is possible that lower IL-17 production in mice treated with αGM-CSF

could be detrimental to early granuloma formation and/or detrimental to the localisation of T cells within the granuloma contributing to increased bacterial loads. Thus although GM-CSF does not appear to influence the functions of T cells we have assessed it may impact their ability to localise appropriately, impacting control of bacterial load. Appropriate localisation could be important given recent data showing direct recognition of infected cells by $CD4^+$ T cells is required for control of bacterial growth (Srivastava and Ernst, 2013).

In contrast to resistant C57BL/6 mice, we did not detect an impact of GM-CSF neutralisation on the presence of T cell populations in the lung in susceptible CBA/J mice. Furthermore we did not find any effect of αGM-CSF treatment on cytokine production by $CD4^+$, $CD8^+$ or γδ T cell populations at any time point assessed in susceptible CBA/J mice. The reasons for these differences are unclear. It is known that CBA/J mice have defects in the ability to upregulate adhesion molecules on T cells, which impacts the recruitment of lymphocytes to the lung, leading to a delayed response (Gruppo et al., 2002; Turner et al., 2001). Perhaps, in the context of a slower adaptive immune response in CBA/J mice, the transient effect of GM-CSF neutralisation to delay T cell recruitment observed in resistant C57BL/6 mice may not be evident. Alternatively, the kinetics of a delay in T cell recruitment may differ in susceptible mice, with an intermediate time point, between day 21 and 28, being required to identify such an effect. However, it is unclear whether such transient, small differences in T cell numbers in resistant mice will impact the outcome of infection.

4.4.3 GM-CSF neutralisation impacts myeloid populations throughout Mtb infection

As discussed above only small and transient defects in the adaptive immune response in resistant C57BL/6 mice were identified and no such defects were evident in susceptible CBA/J mice. These results in isolation are unlikely to explain the increased bacterial loads observed throughout infection in resistant mice treated with αGM-CSF and do not explain the increased

bacterial loads in susceptible mice treated with αGM-CSF. However, in both resistant and susceptible mouse strains treated with αGM-CSF, the increase in bacterial load was not evident until after the onset of adaptive immunity. This could suggest that there is a defect in the interaction between the adaptive response and myeloid populations leading to a defect in their activation and thus restriction of bacterial growth. Furthermore, as GM-CSF deficient mice displayed differences in myeloid populations during *Mtb* infection (Gonzalez-Juarrero et al., 2005) we assessed how GM-CSF neutralisation during infection impacted myeloid populations in the lung.

4.4.3.1 GM-CSF neutralisation decreases CD11c^{+} CD11b^{lo} alveolar macrophages during Mtb infection and in the steady-state

During *Mtb* infection we found a dramatic and sustained decrease in the presence of alveolar macrophages in resistant C57BL/6 mice throughout *Mtb* infection when mice were treated with αGM-CSF. In susceptible mice, this decrease was not evident until day 55 post infection. It is possible that the timing of a decrease in alveolar macrophages could contribute to the kinetics of increased bacterial load in in mice treated with αGM-CSF. Indeed, in resistant C57BL/6 mice increased bacterial load in mice treated with αGM-CSF was observed earlier than in CBA/J mice and this was reflected in the decrease in alveolar macrophages. In resistant mice, alveolar macrophages decreased in αGM-CSF treated mice prior to the detection of an increase in bacterial load. Assessment of alveolar macrophage levels in susceptible mice after day 28 but prior to day 41 (when we first observe an increase in bacterial load) will provide further insight into the correlation between alveolar macrophages and *Mtb* bacterial loads. A decrease in alveolar macrophages could result from the requirement for GM-CSF for maintenance of alveolar macrophages in the steady state as indicated by our results neutralising GM-CSF in naïve mice and published literature (Hashimoto et al., 2013). This requirement could be exacerbated during infection due to death of infected cells and the need to replenish the population.

The functional consequence of a decrease in alveolar macrophages is unclear. A study depleting alveolar macrophages prior to *Mtb* infection, using clodronate containing liposomes suggested that alveolar macrophages were detrimental to control of infection, although granuloma formation was impaired (Leemans et al., 2001). However it has subsequently been shown that treatment with clodronate recruits DCs to the lung and thus confounds interpretation of these results (Srivastava et al., 2014). Alveolar macrophages were decreased in GM-CSF deficient mice during *Mtb* infection and impaired granuloma formation was observed (Gonzalez-Juarrero et al., 2005). Assessment of granuloma structure in mice treated with αGM-CSF may provide further insight into the consequence of reduced alveolar macrophages we observed in αGM-CSF treated mice.

4.4.3.2 Could GM-CSF neutralisation impact the functional capacity of macrophages leading to increased in Mtb bacterial loads?

As well as influencing the differentiation and maintenance of alveolar macrophages, GM-CSF can impact function of macrophage populations (Fleetwood et al., 2007; Hamilton, 2008; Shibata et al., 2001). Such functional defects could contribute to the enhanced bacterial load observed when GM-CSF is neutralised throughout infection in both C57BL/6 and CBA/J mice. Indeed, *in vitro* GM-CSF is described to directly restrict mycobacterial growth in both human (Denis and Ghadirian, 1990) and mouse macrophages, possibly through increased phagolysosome fusion (Pasula et al., 2015; Rothchild et al., 2014). In addition, studies using GM-CSF deficient mice have shown that alveolar macrophage function is impaired in response to *Pneumocysitis carinii* (Paine et al., 2000), *Pseudomonas aeruginosa* (Ballinger et al., 2006) and group B streptococcal infection (LeVine et al., 1999), resulting in increased susceptibility to these infections. *In vitro,* alveolar macrophages isolated from GM-CSF deficient mice display impaired killing of *E.coli* and group B *Streptococcus* (Shibata et al., 2001). GM-CSF treatment of macrophages can also restrict *Histoplasma capsulatum* growth through sequestration of Zn^{2+}

to the Golgi and superoxide production (Subramanian Vignesh et al., 2013). Thus assessment of macrophage function following GM-CSF neutralisation, for example through assessing expression of iNOS, will provide further information regarding how GM-CSF influences macrophage function *in vivo*.

In addition to influencing intracellular killing by macrophages, GM-CSF is reported to influence cytokine production. Indeed pre-treatment of macrophages with GM-CSF increases their production of TNFα in response to the TLR-4 ligand LPS, or the TLR-2 ligand Pam_3CSK_4 (Fleetwood et al., 2007; Heidenreich et al., 1989; Sorgi et al., 2012). Investigation of TNFα levels in the lungs of mice treated with αGM-CSF as well as assessment of how GM-CSF affects cytokine production by macrophages in response to *Mtb* infection, will provide insight into the impact of GM-CSF upon cytokine production during *Mtb* infection.

4.4.3.3 GM-CSF neutralisation leads to a small increase in the number of neutrophils present but could it impact their function?

In both resistant and susceptible mice there was a small increase in the number of neutrophils present at day 21 post infection in mice treated with αGM-CSF. This increase was not sustained throughout infection in susceptible CBA/J mice. The role of neutrophils during *Mtb* infection is unclear (Lowe et al., 2012). Increased numbers of neutrophils have been linked with susceptibility to *Mtb* infection, as suggested by studies using susceptible mouse strains (Eruslanov et al., 2005; Marzo et al., 2014) or mice deficient in CARD9 or mir-223 (Dorhoi et al., 2010; Dorhoi et al., 2013). However, in these scenarios where neutrophils correlate with susceptibility, there are large increases in the numbers of neutrophils present, which is not what is observed when GM-CSF is neutralised. Neutrophils are reported to have the capacity to restrict bacterial growth (Yang et al., 2012). Thus increased numbers of neutrophils could reflect an attempt to control bacterial replication. However, neutrophils from GM-CSF deficient mice and patients with PAP display defects in their functional capacity to restrict bacterial

growth (Uchida et al., 2007). Dysfunction of neutrophils in the absence of GM-CSF, rather than a dramatic change in their abundance, could contribute to increased susceptibility to *Mtb*.

4.4.3.4 GM-CSF neutralisation does not impact activation status of $CD11b^+$ $CD11c^+$ DCs

GM-CSF can enhance antigen presenting capabilities of APCs (Min et al., 2010; Zhan et al., 2012). Indeed recombinant BCG strains expressing GM-CSF increase APC numbers and activation, as measured by CD80 and CD86 expression, in draining lymph nodes. This increased activation was suggested to lead to increased induction of IFNγ producing T cells (Ryan et al., 2007). However, based on expression of MHC class II and the co-stimulatory molecule CD86, we did not find evidence to suggest that GM-CSF neutralisation impacted DC function during *Mtb* infection. This is in keeping with little or no change in the adaptive immune response that we observed in resistant and susceptible mice respectively.

4.4.6 What is the source of GM-CSF during Mtb infection?

An outstanding question from our investigation is what the cellular source(s) of GM-CSF are during *Mtb* infection. In primary infection we detected very low percentages and numbers of GM-CSF producing $CD4^+$ T cells in susceptible or resistant mouse strains. Multiple cell types have been reported to have the capacity to produce GM-CSF including myeloid cells, pneumocytes, NK cells and other ILCs (Daussy et al., 2014; Gasson, 1991; Moro et al., 2010; Mortha et al., 2014; Robinette et al., 2015; Sojka et al., 2014). During *Mtb* infection NKT cells have been found to produce GM-CSF, although whether there are other sources was not addressed (Rothchild et al., 2014). Further investigation of the source and timing of GM-CSF in resistant and susceptible mouse strains during *Mtb* infection could provide further insights into when and how this cytokine is important during *Mtb* infection.

Overall we show that GM-CSF neutralisation is detrimental to control of *Mtb* bacterial load in resistant and susceptible mouse strains. Increased *Mtb* bacterial loads were observed after the onset of adaptive immunity in both resistant and susceptible mouse strains, although no major perturbation in the adaptive immune response was observed. GM-CSF neutralisation led to a substantial decrease in $CD11c^{+}$ $CD11b^{lo}$ alveolar macrophages in both resistant and susceptible mice, which could have important consequence for granuloma structure and control of infection. We suggest that GM-CSF impacts the activation of myeloid populations following the onset of adaptive immunity and their ability to restrict bacterial growth, potentially impacting their survival. Further investigation is necessary to provide insight into the mechanism by which GM-CSF is protective during *Mtb* infection.

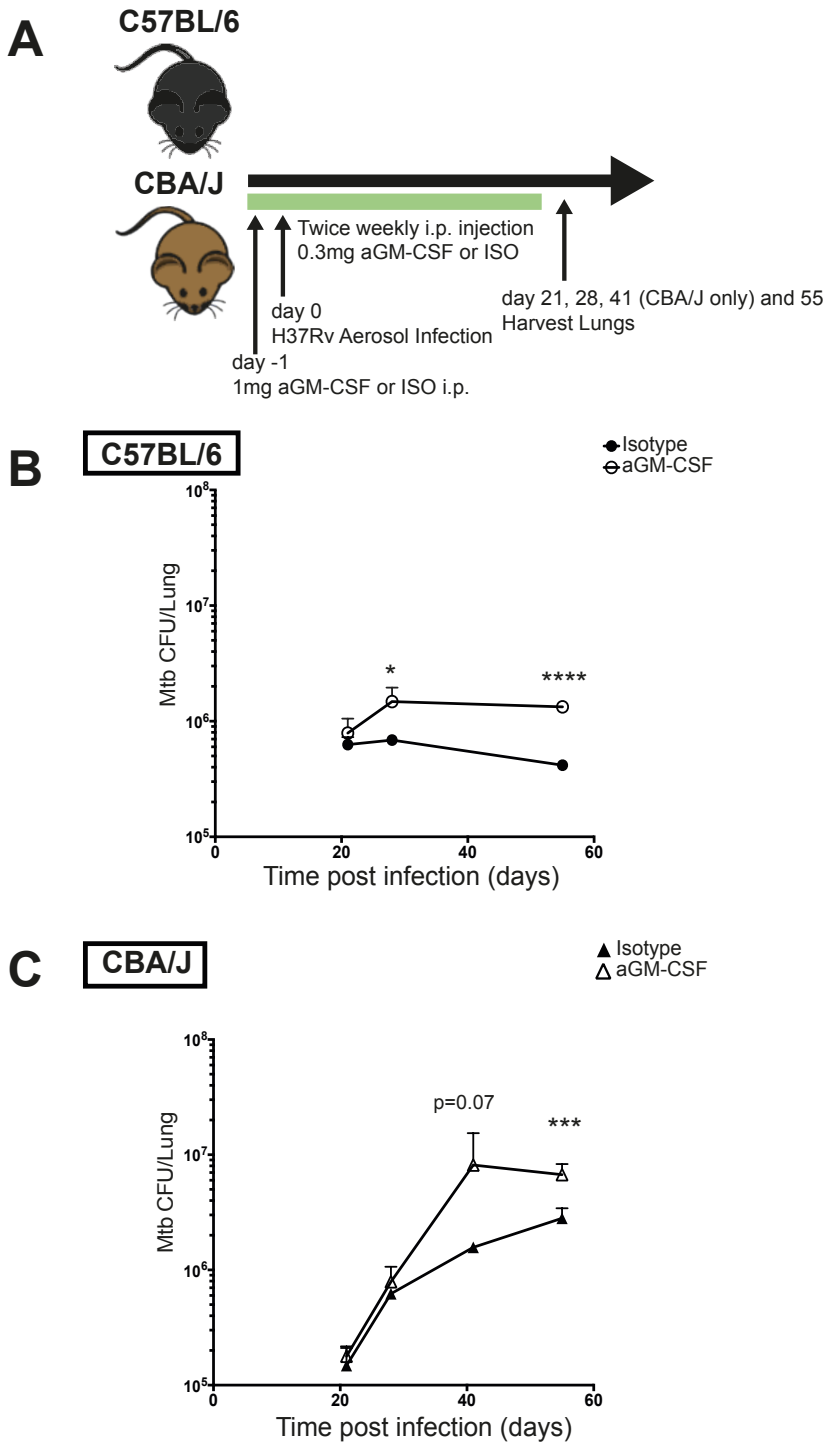

Figure 4.1 GM-CSF is protective in the primary immune response to Mtb infection in resistant and susceptible mice

Outline of experiment **(A)**. C57BL/6 and CBA/J mice were i.p. injected with 1mg anti-GM-CSF (αGM-CSF) or Isotype (ISO) control the day prior to infection with approx. 100-200 CFU of the *Mtb* strain H37Rv, via aerosol route. Mice then received twice weekly i.p. injections of aGM-CSF or ISO. Mice were sacrificed at days 21, 28, 41 (CBA/J only) and 55 post infection. Lung homogenates were serially diluted and plated to determine bacterial load in C57BL/6 mice **(B)** and CBA/J mice **(C)**. Graphs show mean ± SD. p=0.07, *p<0.5, ***p<0.001, ****p<0.0001 by student's unpaired t-test. Data representative of two independent experiments.

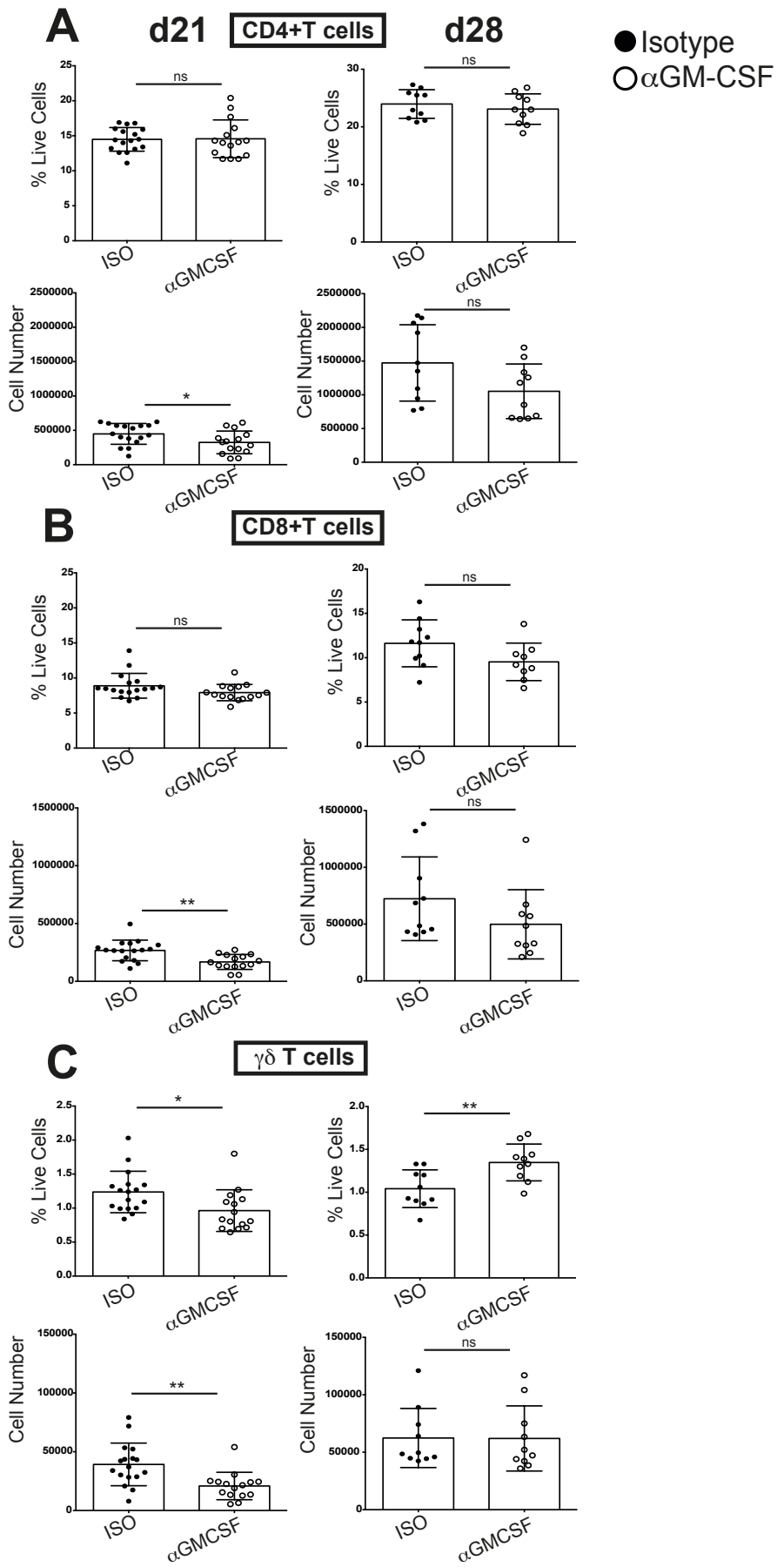

Figure 4.2 GM-CSF neutralisation during Mtb infection leads to lower numbers of T cells in the lung early post infection in resistant C57BL/6 mice

C57BL/6 mice were infected and treated with αGM-CSF or ISO as shown in Figure 4.1. Mice were sacrificed at day 21 and 28 post infection. Lungs were homogenized by passage through a 70μm filter. Single cell suspensions were stained with the following antibodies to assess percentages and calculate numbers of lymphoid populations by flow cytometry: γδ TCR FITC, Thy1.2 PECy7, CD4 e450, CD8 v500 and CD3 APC. Percentage and number of $CD4^+$ T cells (defined as $CD3^+$ $Thy1.2^+$ $CD4^+$) at day 21 and 28 post infection **(A)**. Percentage and number of $CD8^+$ T cells (defined as $CD3^+$ $Thy1.2^+$ $CD8^+$) at day 21 and 28 post infection **(B)**. Percentage and number of γδ T cells (defined as $CD3^+$ $Thy1.2^+$ $CD4^-$ $CD8^-$ $\gamma\delta TCR^+$ at day 21 and 28 post infection **(C)**. Data pooled from 2 (d28) or 3 (d21) independent experiments. 10-17 mice per group. Graphs show individual mice with mean ± SD. ns – not significant *$p<0.05$, **$p<0.01$ by unpaired student's t-test.

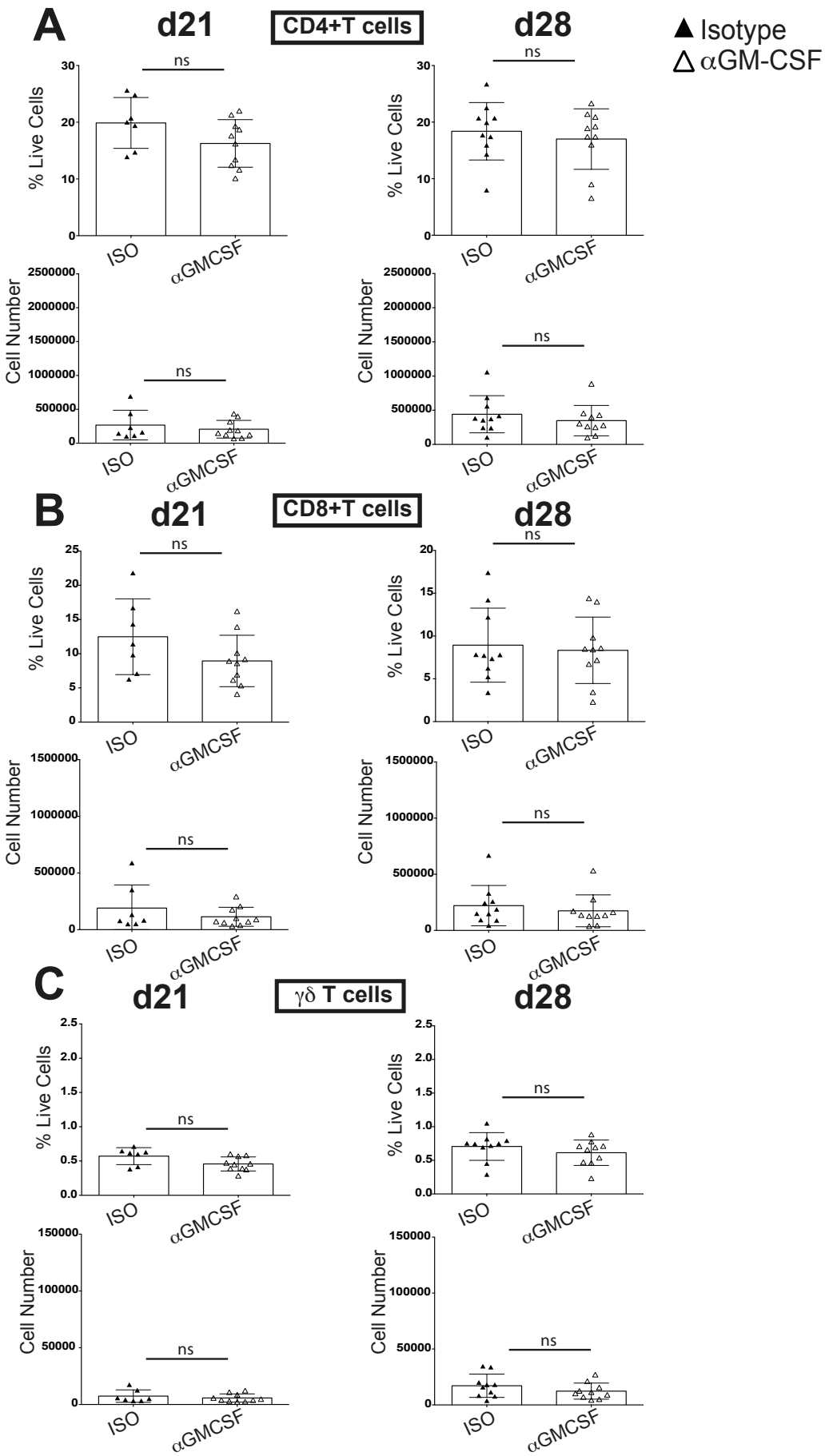

Figure 4.3 GM-CSF neutralisation during Mtb infection does not impact T cell populations in the lung in susceptible CBA/J mice.

CBA/J mice were infected and treated with αGM-CSF or ISO as shown in Figure 4.1. Mice were sacrificed at day 21 and 28 post infection. Lungs were homogenized by passage through a 70μm filter. Single cell suspensions were stained with the following antibodies to assess percentages and calculate numbers of lymphoid populations by flow cytometry: γδ TCR FITC, Thy1.2 PECy7, CD4 e450, CD8 v500 and CD3 APC. Percentage and number of $CD4^+$ T cells (defined as $CD3^+$ $Thy1.2^+$ $CD4^+$) at day 21 and 28 post infection **(A)**. Percentage and number of $CD8^+$ T cells (defined as $CD3^+$ $Thy1.2^+$ $CD8^+$) at day 21 and 28 post infection **(B)**. Percentage and number of γδ T cells (defined as $CD3^+$ $Thy1.2^+$ $CD4^-$ $CD8^-$ $\gamma\delta TCR^+$ at day 21 and 28 post infection **(C)**. Data pooled from 2 independent experiments. 7-10 mice per group. Graphs show individual mice with mean ± SD. ns – not significant by unpaired student's t-test.

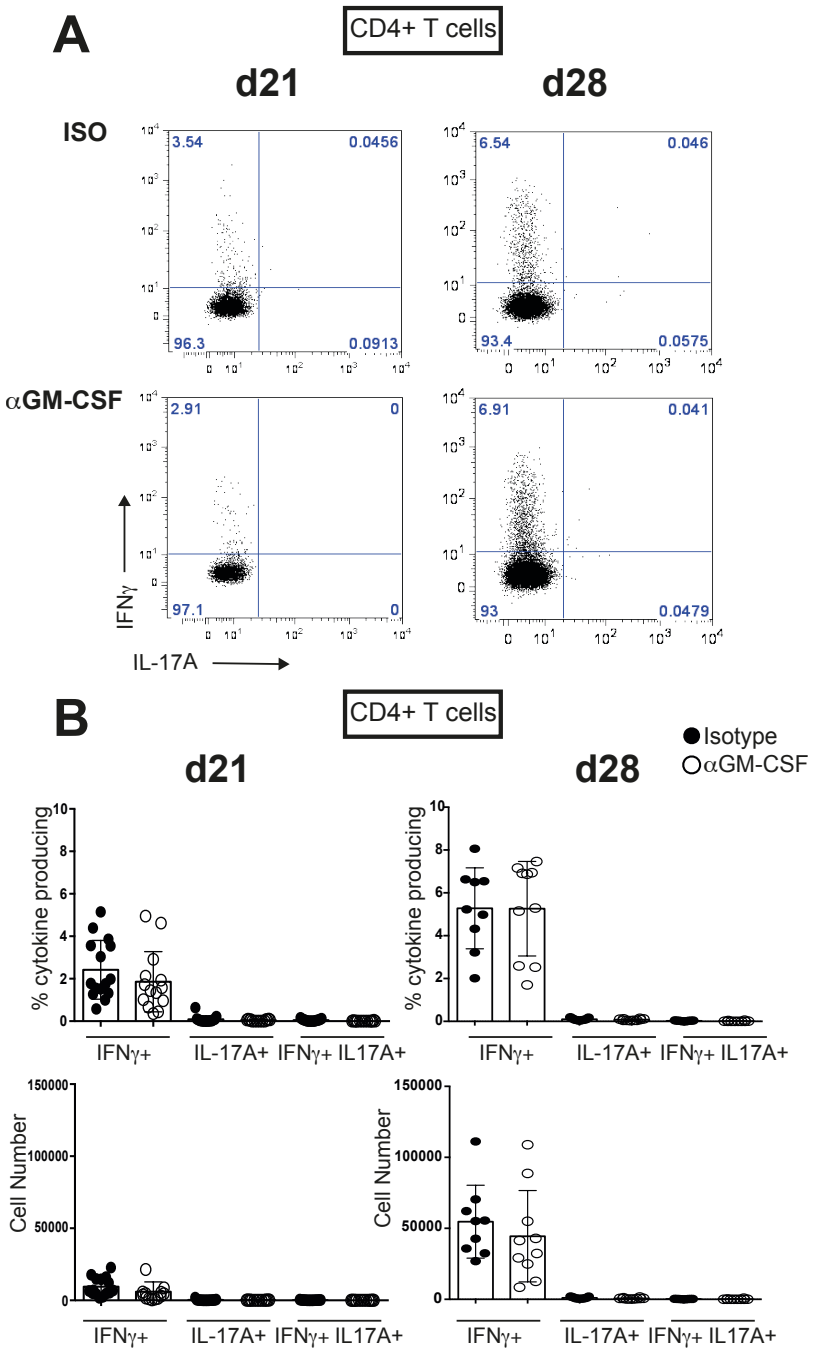

Figure 4.4 GM-CSF neutralisation during Mtb infection does not impact IFNγ or IL-17 production by CD4$^+$ T cells in resistant C57BL/6 mice.

C57BL/6 mice were infected and treated with αGM-CSF or ISO as shown in Figure 4.1. Mice were sacrificed at day 21 and 28 post infection. Lungs were homogenized by passage through a 70μm filter. 1x10^6 cells were restimulated with 20μg PPD and 2μg αCD28 mAb for 16h before the addition of BFA for a further 4h. Cells were then harvested and stained with the following to assess cytokine production: γδ TCR FITC, GM-CSF PE, CD8 PerCP e710, Thy1.2 PE Cy7, IFNγ e450, CD4 v500, IL-17A APC, CD3 APCe780. CD4$^+$ T cells were identified as CD3$^+$ Thy1.2$^+$ CD4$^+$. Representative flow cytometry plots from individual mice at day 21 or 28 post infection are shown **(A)**. Percentage and number of cytokine producing CD4$^+$ T cells at day 21 or 28 post infection **(B)**. Data pooled from 2 (d28) or 3 (d21) independent experiments. 9-15 mice per group. Graphs show individual mice with mean ± SD.

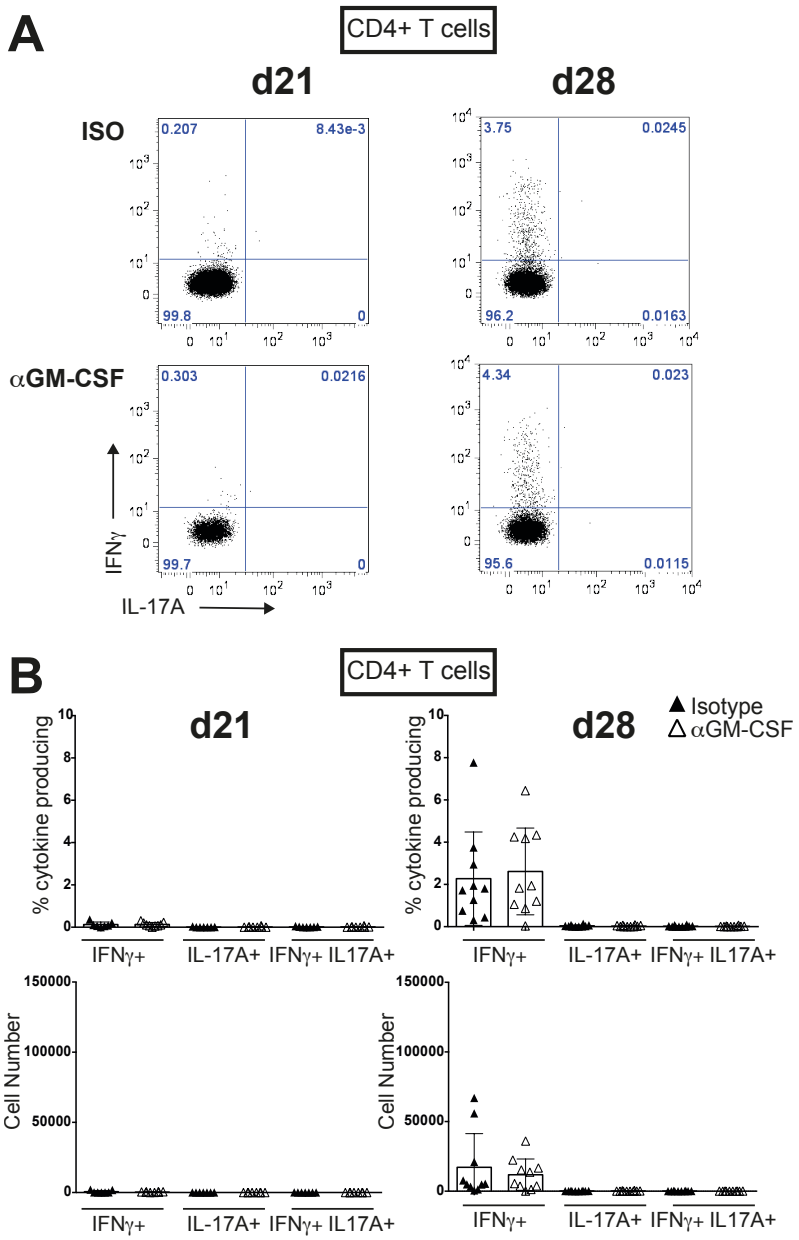

Figure 4.5 GM-CSF neutralisation during Mtb infection does not impact IFNγ or IL-17 production by CD4$^+$ T cells in susceptible CBA/J mice

CBA/J mice were infected and treated with αGM-CSF or ISO as shown in Figure 4.1. Mice were sacrificed at day 21 and 28 post infection. Lungs were homogenized by passage through a 70μm filter. 1x10^6 cells were restimulated with 20μg PPD and 2μg αCD28 mAb for 16h before the addition of BFA for a further 4h. Cells were then harvested and stained with the following to assess cytokine production: γδ TCR FITC, GM-CSF PE, CD8 PerCP e710, Thy1.2 PE Cy7, IFNγ e450, CD4 v500, IL-17A APC, CD3 APCe780. CD4$^+$ T cells were identified as CD3$^+$ Thy1.2$^+$ CD4$^+$. Representative flow cytometry plots from individual mice at day 21 or 28 post infection are shown **(A)**. Percentage and number of cytokine producing CD4$^+$ T cells at day 21 or 28 post infection **(B)**. Graphs show individual mice with mean ± SD. Data pooled from 2 independent experiments. 7-10 mice per group. Graphs show individual mice with mean ± SD.

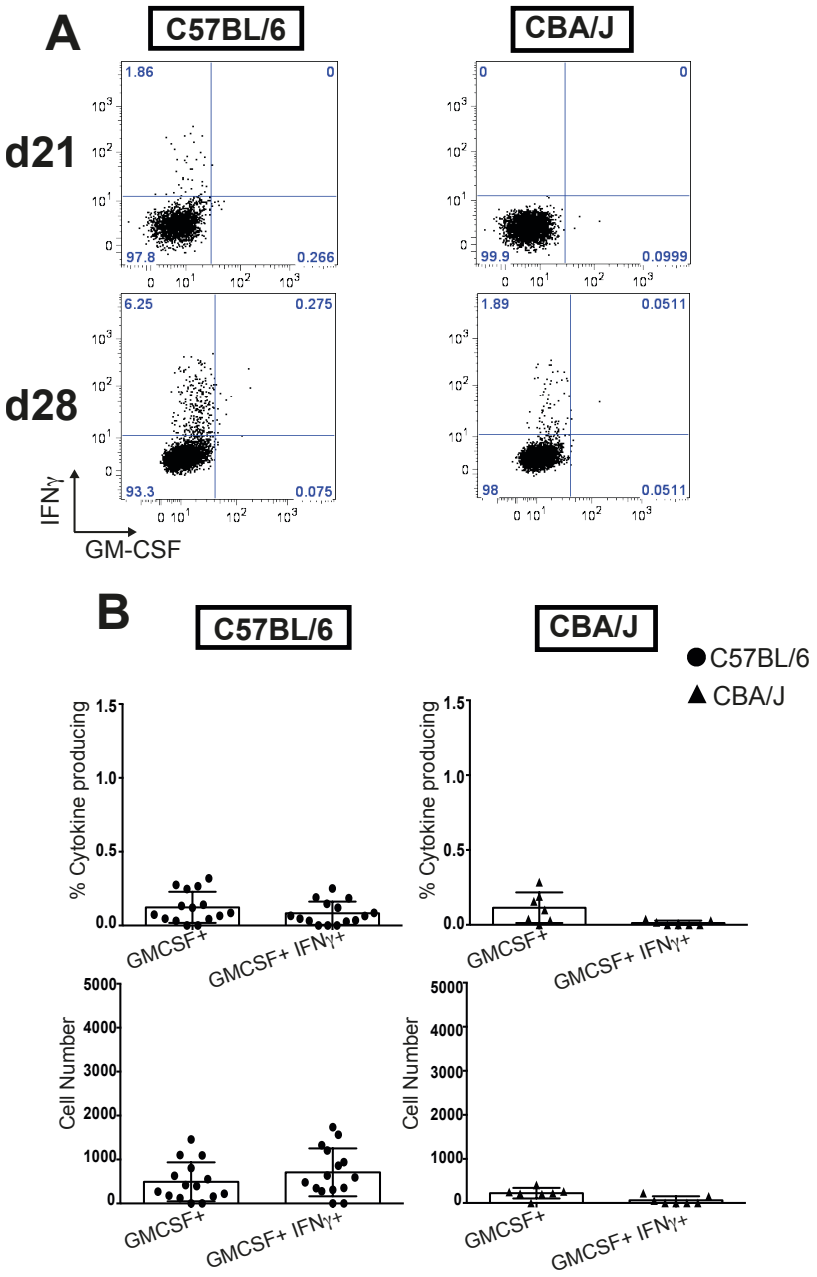

Figure 4.6 GM-CSF producing CD4$^+$ T cells are barely detectable in the lung during primary Mtb infection in resistant C57BL/6 or susceptible CBA/J mice

C57BL/6 and CBA/J mice were infected and treated with αGM-CSF or ISO as shown in Figure 4.1. Mice were sacrificed at day 21 and 28 post infection. Lungs were homogenized by passage through a 70μm filter. 1x10^6 cells were restimulated with 20μg PPD and 2μg αCD28 mAb for 16h before the addition of BFA for a further 4h. Cells were then harvested and stained with the following to assess cytokine production: γδ TCR FITC, GM-CSF PE, CD8 PerCP e710, Thy1.2 PE Cy7, IFNγ e450, CD4 v500, IL-17A APC, CD3 APCe780. CD4$^+$ T cells were identified as CD3$^+$ Thy1.2$^+$ CD4$^+$. Representative flow cytometry plots from individual mice at day 21 or 28 post infection are shown **(A)**. Percentage and number of cytokine producing CD4$^+$ T cells at day 21 or 28 post infection **(B)**. Data pooled from 2 (C57BL/6 d28, CBA/J d21, d28) or 3 (C57BL/6 d21) independent experiments. 7-15 mice per group. Graphs show individual mice with mean ± SD.

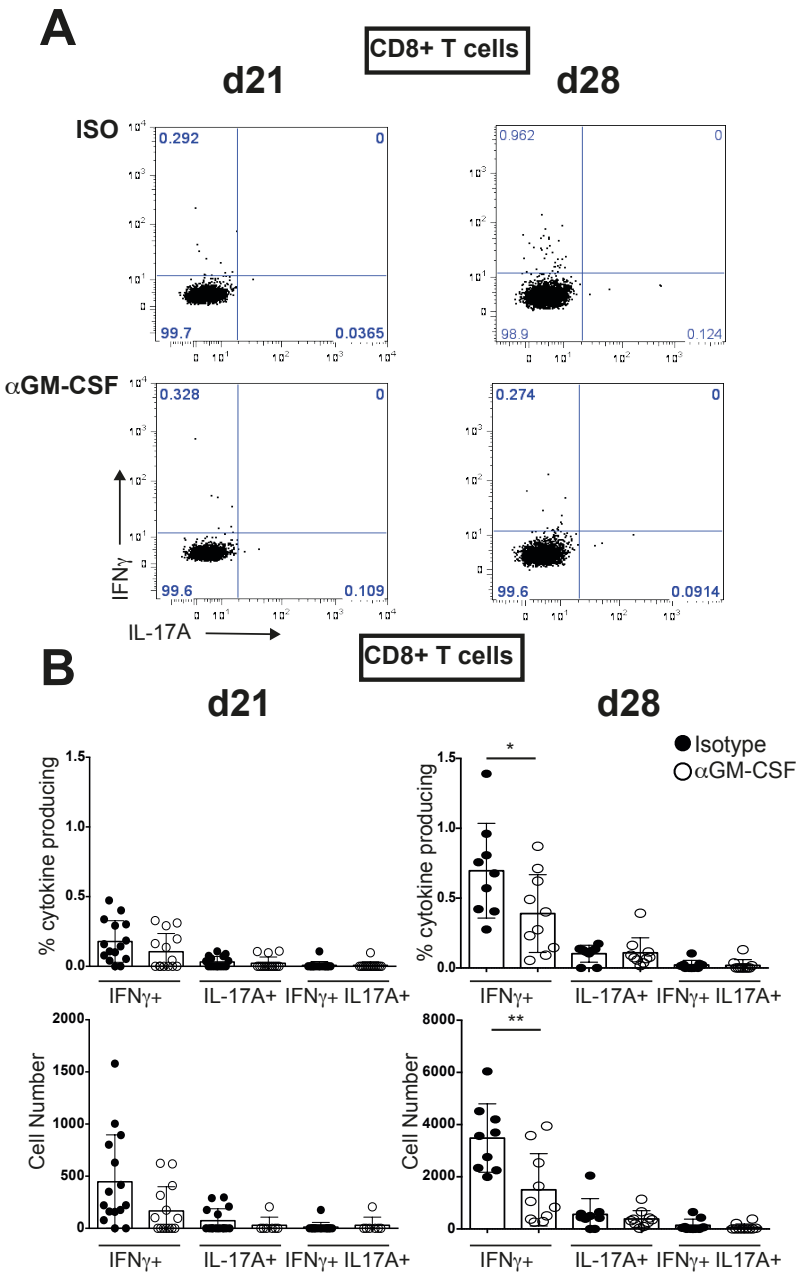

Figure 4.7 GM-CSF neutralisation during Mtb infection decreases IFNγ production by CD8$^+$ T cells in resistant C57BL/6 mice

C57BL/6 mice were infected and treated with αGM-CSF or ISO as shown in Figure 4.1. Mice were sacrificed at day 21 and 28 post infection. Lungs were homogenized by passage through a 70μm filter. 1x10^6 cells were restimulated with 20μg PPD and 2μg αCD28 mAb for 16h before the addition of BFA for a further 4h. Cells were then harvested and stained with the following to assess cytokine production: γδ TCR FITC, GM-CSF PE, CD8 PerCP e710, Thy1.2 PE Cy7, IFNγ e450, CD4 v500, IL-17A APC, CD3 APCe780. CD8$^+$ T cells were identified as CD3$^+$ Thy1.2$^+$ CD8$^+$. Representative flow cytometry plots from individual mice at day 21 or 28 post infection are shown **(A)**. Percentage and number of cytokine producing CD8$^+$ T cells at day 21 or 28 post infection **(B)**. Data pooled from 2 (d28) or 3 (d21) independent experiments. 9-15 mice per group. Graphs show individual mice with mean ± SD. ns – not significant *p<0.05, **p<0.01 by unpaired student's t-test.

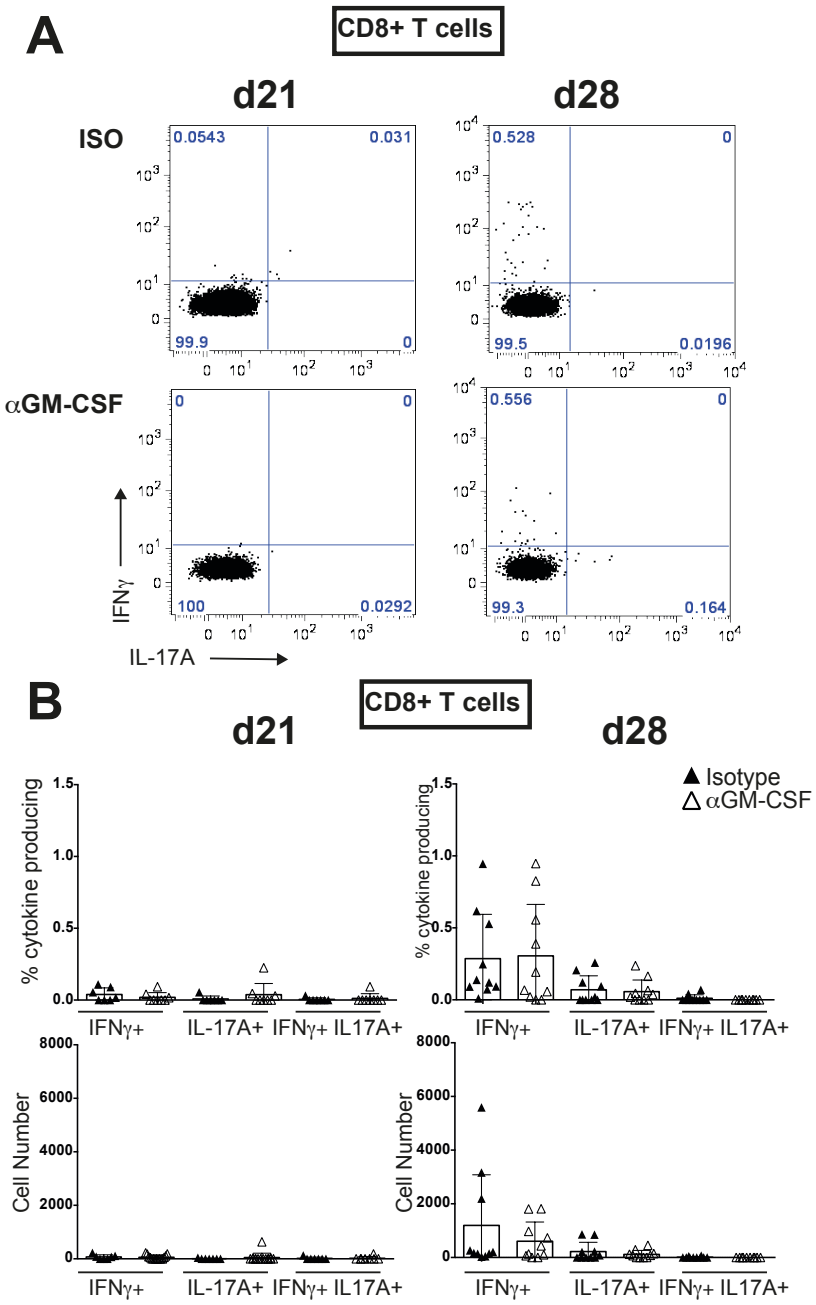

Figure 4.8 GM-CSF neutralisation during Mtb infection does not impact IFNγ or IL-17 production by CD8$^+$ T cells in susceptible CBA/J mice

CBA/J mice were infected and treated with αGM-CSF or ISO as shown in Figure 4.1. Mice were sacrificed at day 21 and 28 post infection. Lungs were homogenized by passage through a 70μm filter. 1x10^6 cells were restimulated with 20μg PPD and 2μg αCD28 mAb for 16h before the addition of BFA for a further 4h. Cells were then harvested and stained with the following to assess cytokine production: γδ TCR FITC, GM-CSF PE, CD8 PerCP e710, Thy1.2 PE Cy7, IFNγ e450, CD4 v500, IL-17A APC, CD3 APCe780. CD8$^+$ T cells were identified as CD3$^+$ Thy1.2$^+$ CD8$^+$. Representative flow cytometry plots from individual mice at day 21 or 28 post infection are shown **(A)**. Percentage and number of cytokine producing CD8$^+$ T cells at day 21 or 28 post infection **(B)**. Graphs show individual mice with mean ± SD. Data pooled from 2 independent experiments. 7-10 mice per group. Graphs show individual mice with mean ± SD

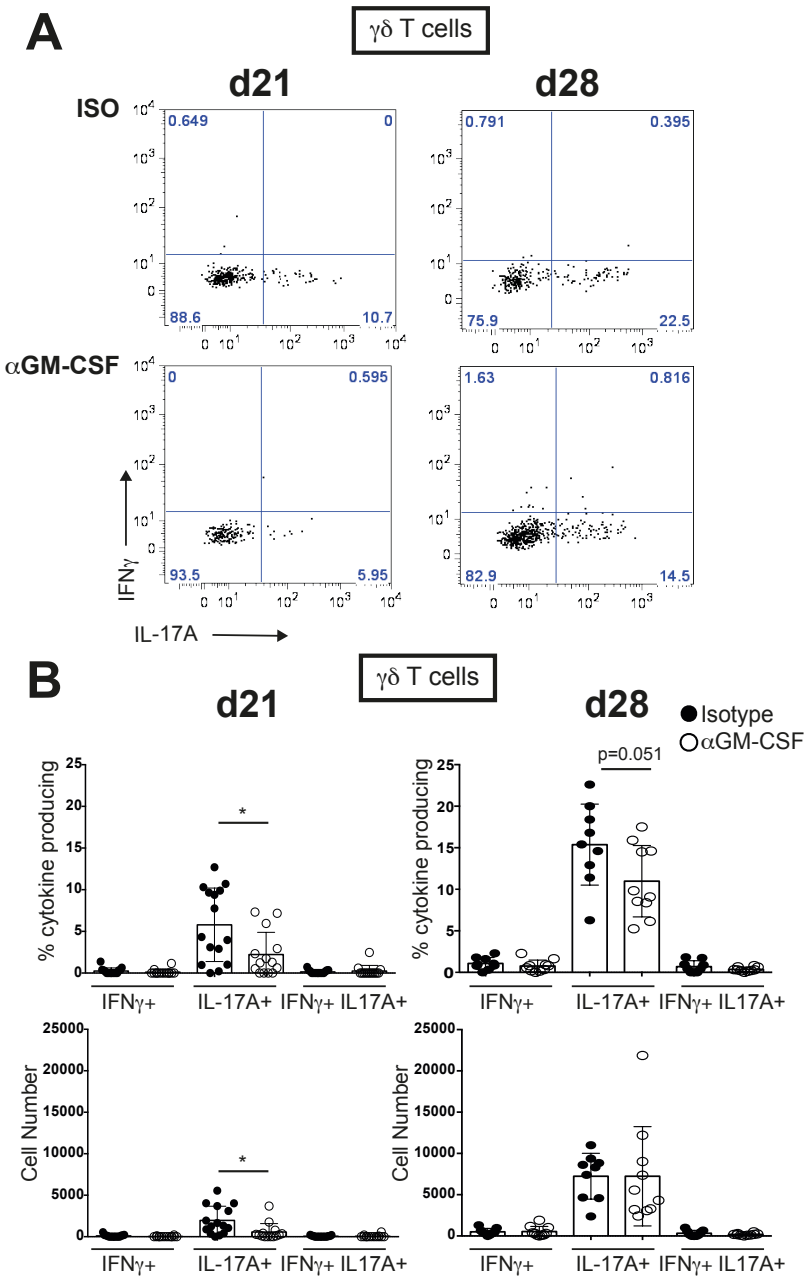

Figure 4.9 GM-CSF neutralisation during Mtb infection decreases early IL-17 production by γδ T cells in resistant C57BL/6 mice

C57BL/6 mice were infected and treated with αGM-CSF or ISO as shown in Figure 4.1. Mice were sacrificed at day 21 and 28 post infection. Lungs were homogenized by passage through a 70μm filter. $1x10^6$ cells were restimulated with 20μg PPD and 2μg αCD28 mAb for 16h before the addition of BFA for a further 4h. Cells were then harvested and stained with the following to assess cytokine production: γδ TCR FITC, GM-CSF PE, CD8 PerCP e710, Thy1.2 PE Cy7, IFNγ e450, CD4 v500, IL-17A APC, CD3 APCe780. γδ T cells were identified as $CD3^+$ $Thy1.2^+$ $CD4^-$ $CD8^-$ γδ TCR^+. Representative flow cytometry plots from individual mice at day 21 or 28 post infection are shown **(A)**. Percentage and number of cytokine producing γδ T cells at day 21 or 28 post infection **(B)**. Data pooled from 2 (d28) or 3 (d21) independent experiments. 9-15 mice per group. Graphs show individual mice with mean ± SD. ns – not significant p=0.051, *p<0.05 by unpaired student's t-test.

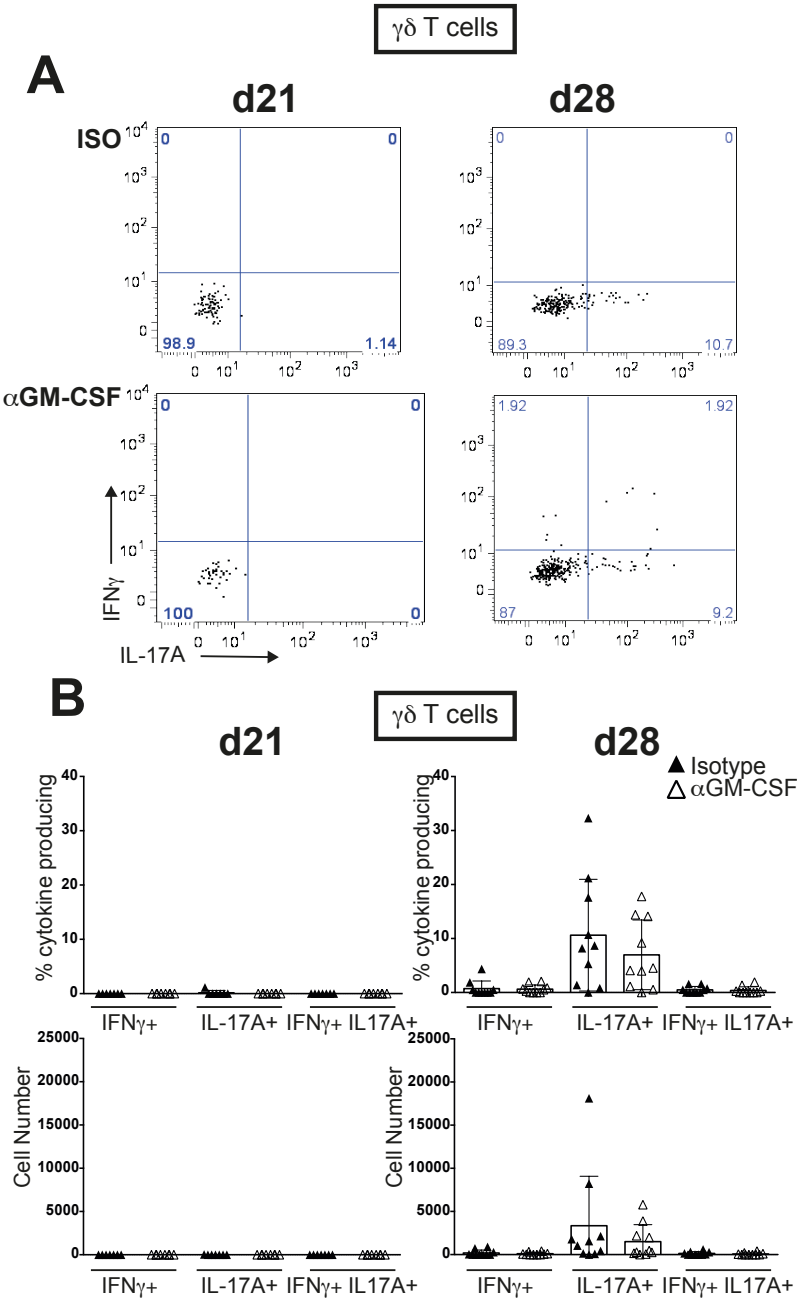

Figure 4.10 GM-CSF neutralisation during Mtb infection does not impact IFNγ or IL-17 production by γδ T cells in susceptible CBA/J mice

CBA/J mice were infected and treated with αGM-CSF or ISO as shown in Figure 4.1. Mice were sacrificed at day 21 and 28 post infection. Lungs were homogenized by passage through a 70μm filter. $1x10^6$ cells were restimulated with 20μg PPD and 2μg αCD28 mAb for 16h before the addition of BFA for a further 4h. Cells were then harvested and stained with the following to assess cytokine production: γδ TCR FITC, GM-CSF PE, CD8 PerCP e710, Thy1.2 PE Cy7, IFNγ e450, CD4 v500, IL-17A APC, CD3 APCe780. γδ T cells were identified as $CD3^+$ $Thy1.2^+$ $CD4^-$ $CD8^-$ γδ TCR^+. Representative flow cytometry plots from individual mice at day 21 or 28 post infection are shown **(A)**. Percentage and number of cytokine producing γδ T cells at day 21 or 28 post infection **(B)**. Graphs show individual mice with mean ± SD. Data pooled from 2 independent experiments. 7-10 mice per group. Graphs show individual mice with mean ± SD.

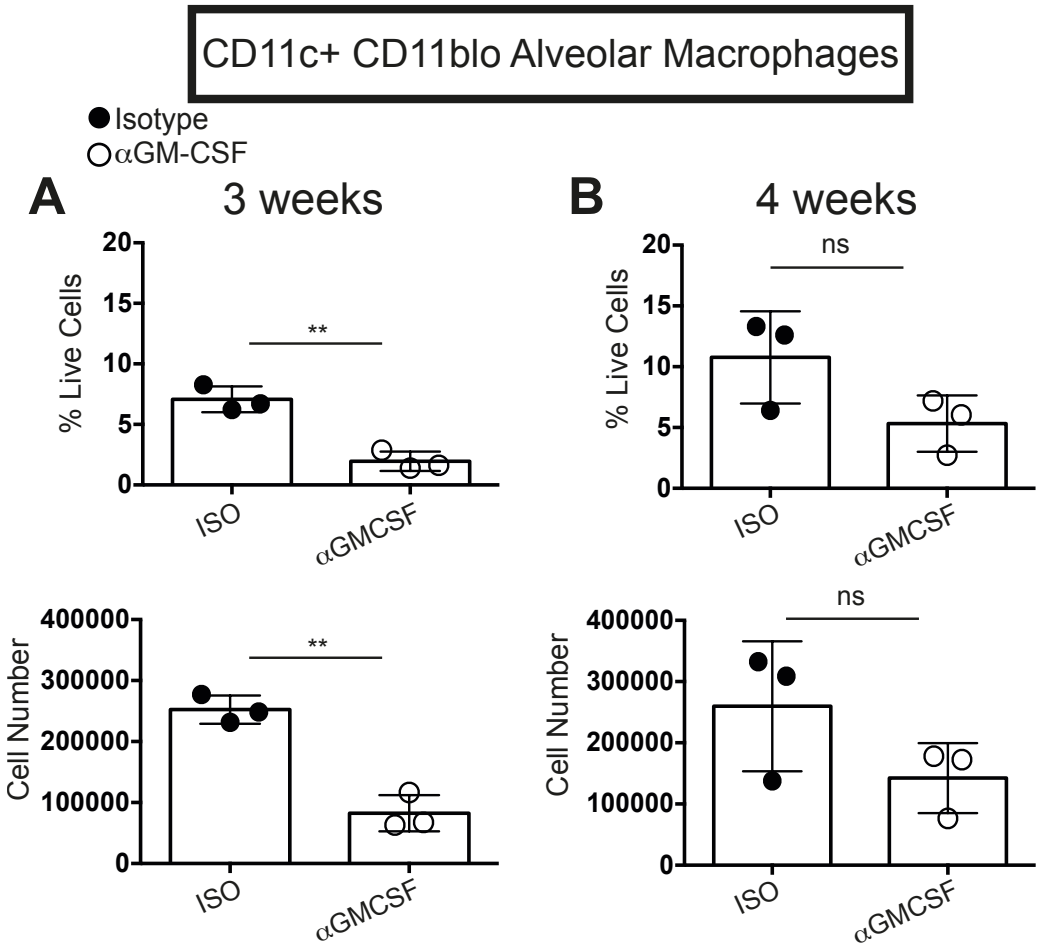

Figure 4.11 GM-CSF is required in the steady state to maintain CD11c$^+$ CD11b lo alveolar macrophage populations in resistant C57BL/6 mice

C57BL/6 mice were i.p. injected with 1mg anti-GM-CSF (αGM-CSF) or Isotype (ISO). Mice then received twice weekly i.p. injections of aGM-CSF or ISO for 3 weeks or 4 weeks. Mice were sacrificed after 3 or 4 weeks of antibody treatment. Lungs were harvested and digested with Collagenase D before being homogenized through passage through a 70μm filter. Cell suspensions were stained with the following to identify myeloid populations: Ly6G FITC, NK1.1 PE, Ly6C PerCP Cy5.5, CD11b PE Cy7, CD11c v450, F4/80 APC, MHC class II APCe780. Percentage and number of CD11c$^+$ CD11b lo alveolar macrophages following 3 weeks **(A)** or 4 weeks **(B)** of antibody treatment. Data shown from one experiment, with 3 mice per group. Graphs show individual mice with mean ± SD. ns – not significant, *p<0.05 **p<0.01 by unpaired student's t-test.

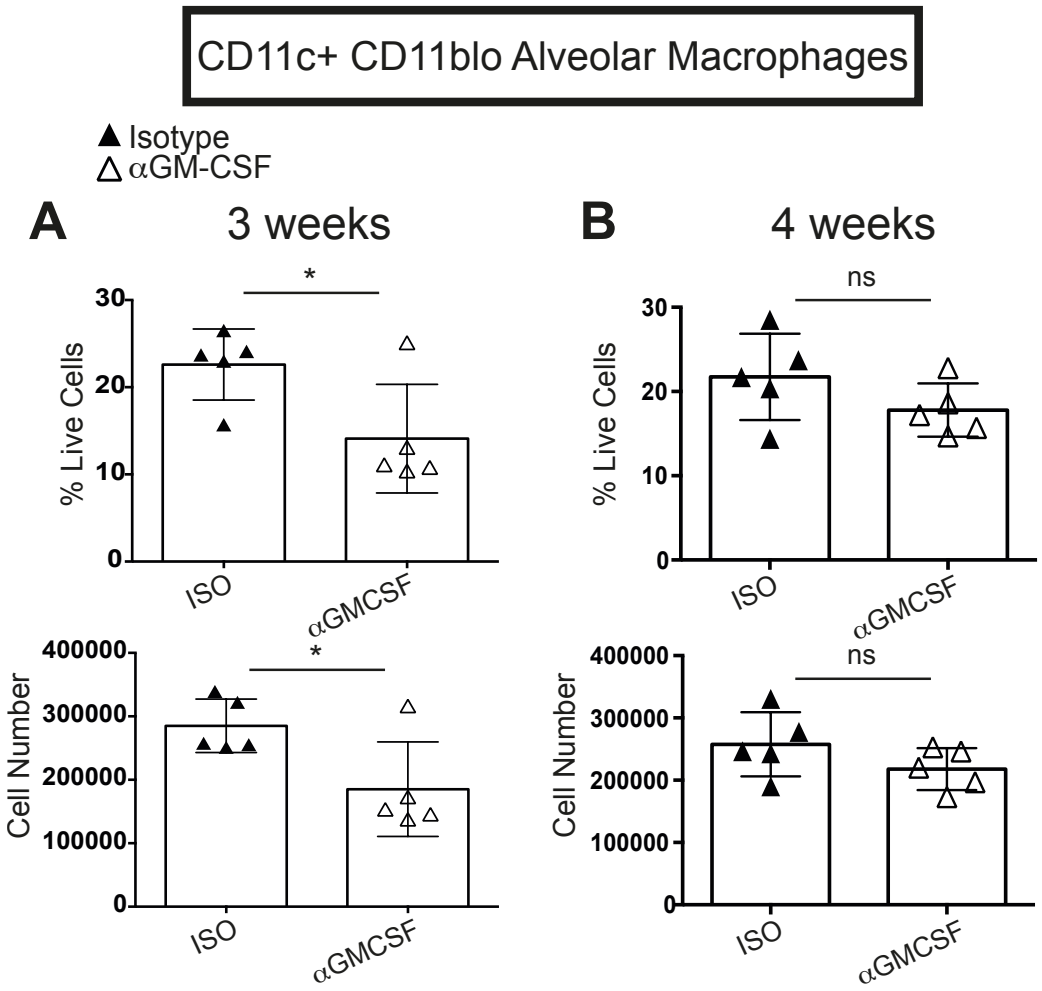

Figure 4.12 GM-CSF is required in the steady state to maintain CD11c$^+$ CD11b lo alveolar macrophage populations in susceptible CBA/J mice

CBA/J mice were i.p. injected with 1mg anti-GM-CSF (αGM-CSF) or Isotype (ISO). Mice then received twice weekly i.p. injections of aGM-CSF or ISO for 3 weeks or 4 weeks. Mice were sacrificed after 3 or 4 weeks of antibody treatment. Lungs were harvested and digested with Collagenase D before being homogenized through passage through a 70μm filter. Cell suspensions were stained with the following to identify myeloid populations: Ly6G FITC, CD11c PE, Ly6C PerCP Cy5.5, CD11b PE Cy7, CD86 Brilliant Violet 421, F4/80 APC, MHC class II APCe780. Percentage and number of CD11c$^+$ CD11b lo alveolar macrophages following 3 weeks **(A)** or 4 weeks **(B)** of antibody treatment. Data shown from one experiment, with 5 mice per group. Graphs show individual mice with mean ± SD. ns – not significant, *$p<0.05$ by unpaired student's t-test.

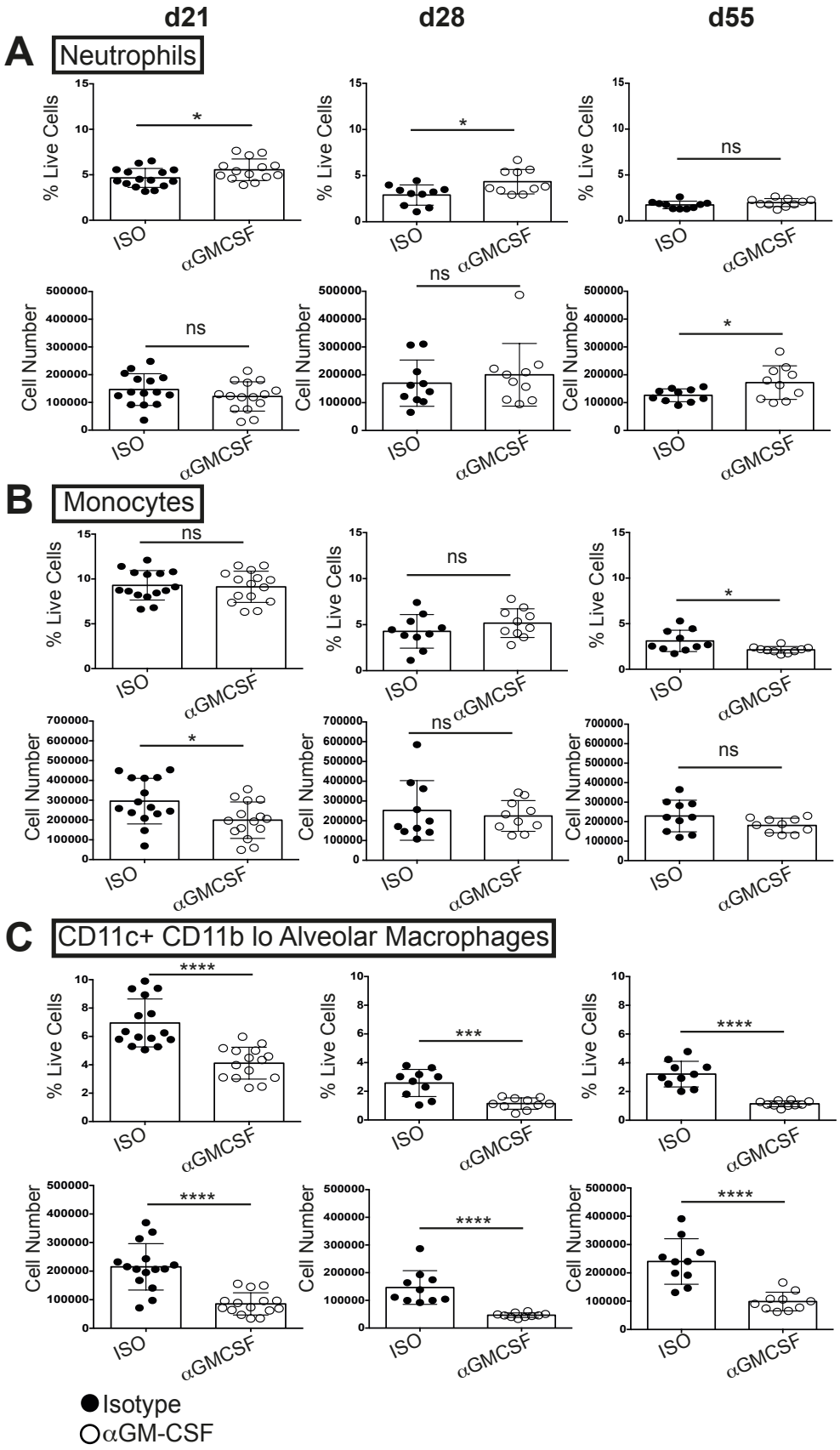

Figure 4.13 Significant early decrease in CD11c^{+} CD11b alveolar macrophage populations with GM-CSF neutralisation during Mtb infection in resistant C57BL/6 mice

C57BL/6 mice were infected and treated with αGM-CSF or ISO as shown in Figure 4.1. Mice were sacrificed at day 21, 28 and 55 post infection. Lungs were homogenized by passage through a 70μm filter. Single cell suspensions were stained with the following antibodies to assess percentages and calculate numbers of myeloid populations by flow cytometry: Ly6G FITC, CD11c PE, Ly6C PerCP Cy5.5, CD11b PE Cy7, CD86 Brilliant Violet 421, CD8 v500, F4/80 APC, MHC class II APCe780. Percentage and number of neutrophils (defined as $CD11b^+$ $Ly6G^+$) at day 21, 28 and 55 post infection **(A)**. Percentage and number of monocytes (defined as $CD11b^+$ $Ly6G^-$ Ly6C hi) at day 21, 28 and 55 post infection **(B)**. Percentage and number of $CD11c^+$ CD11b lo alveolar macrophages (defined as $CD11c^+$ CD11b lo $Ly6G^-$) at day 21, 28 and 55 post infection **(C)**. Data pooled from 2 (d28, d55) or 3 (d21) independent experiments. 10-15 mice per group. Graphs show individual mice with mean ± SD. ns – not significant *p<0.05, **p<0.01, ***p<0.001, ****p<0.0001 by unpaired student's t-test.

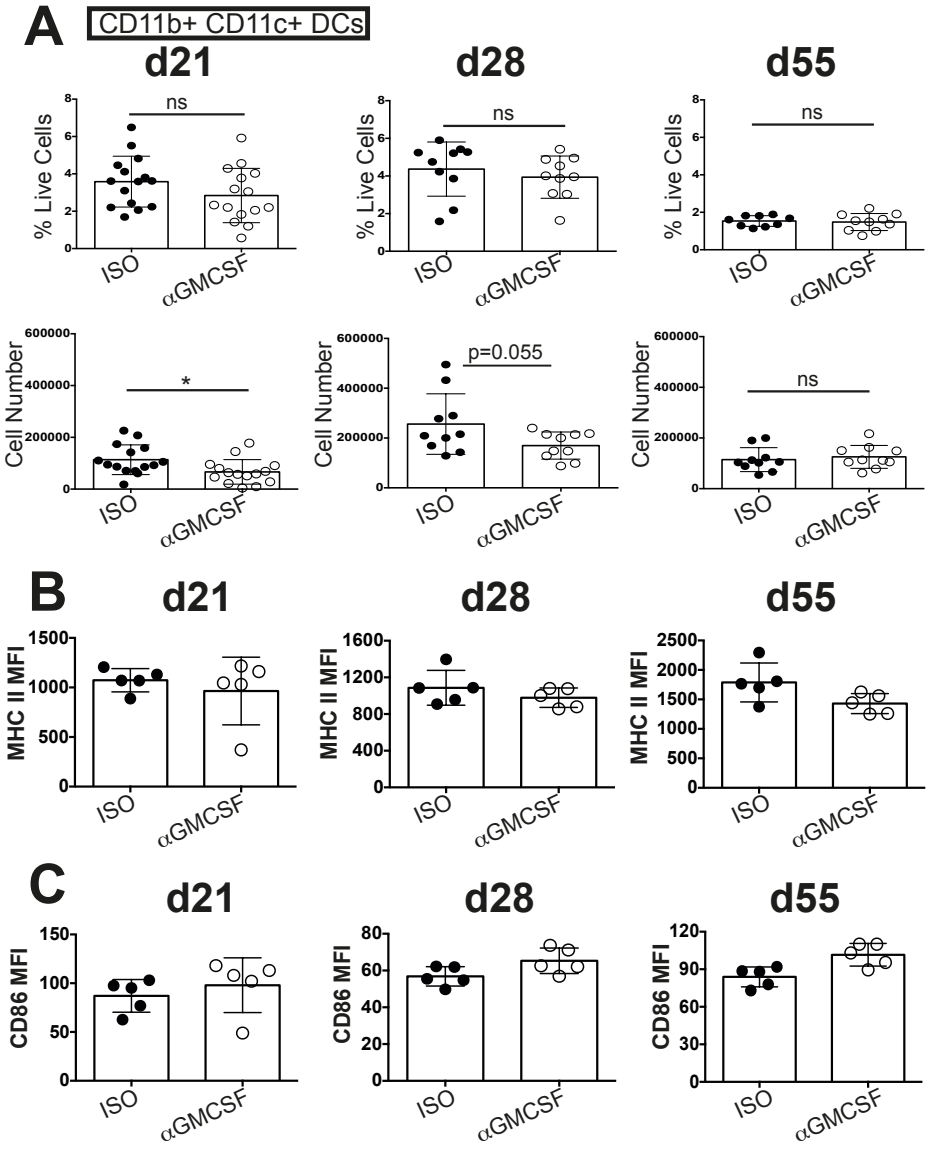

Figure 4.14 GM-CSF neutralisation leads to an early decrease numbers of CD11b$^+$ CD11c$^+$ DCs in the lung during Mtb infection in resistant C57BL/6 mice

C57BL/6 mice were infected and treated with αGM-CSF or ISO as shown in Figure 4.1. Mice were sacrificed at day 21, 28 and 55 post infection. Lungs were homogenized by passage through a 70μm filter. Single cell suspensions were stained with the following antibodies to assess percentages and calculate numbers of myeloid populations by flow cytometry: Ly6G FITC, CD11c PE, Ly6C PerCP Cy5.5, CD11b PE Cy7, CD86 Brilliant Violet 421, CD8 v500, F4/80 APC, MHC class II APCe780. Percentage and number of CD11b$^+$ CD11c$^+$ DCs (defined as Ly6G$^-$ CD11b$^+$ CD11c$^+$) at day 21, 28 and 55 post infection **(A)**. Mean Fluorescence Intensity (MFI) for MHC class II (MHC II) at day 21, 28 and 55 post infection **(B)** MFI for CD86 day 21, 28 and 55 post infection **(C)** Percentage and number graphs **(A)** shown data pooled from 2 (d28, d55) or 3 (d21) independent experiments with 10-15 mice per group. **(B)** and **(C)** graphs representative of 2 (d28, d55) or 3 (d21) independent experiments with 5-7 mice per group. Graphs show values for individual mice with mean ± SD. ns – not significant p=0.055, *p<0.05, by unpaired student's t-test.

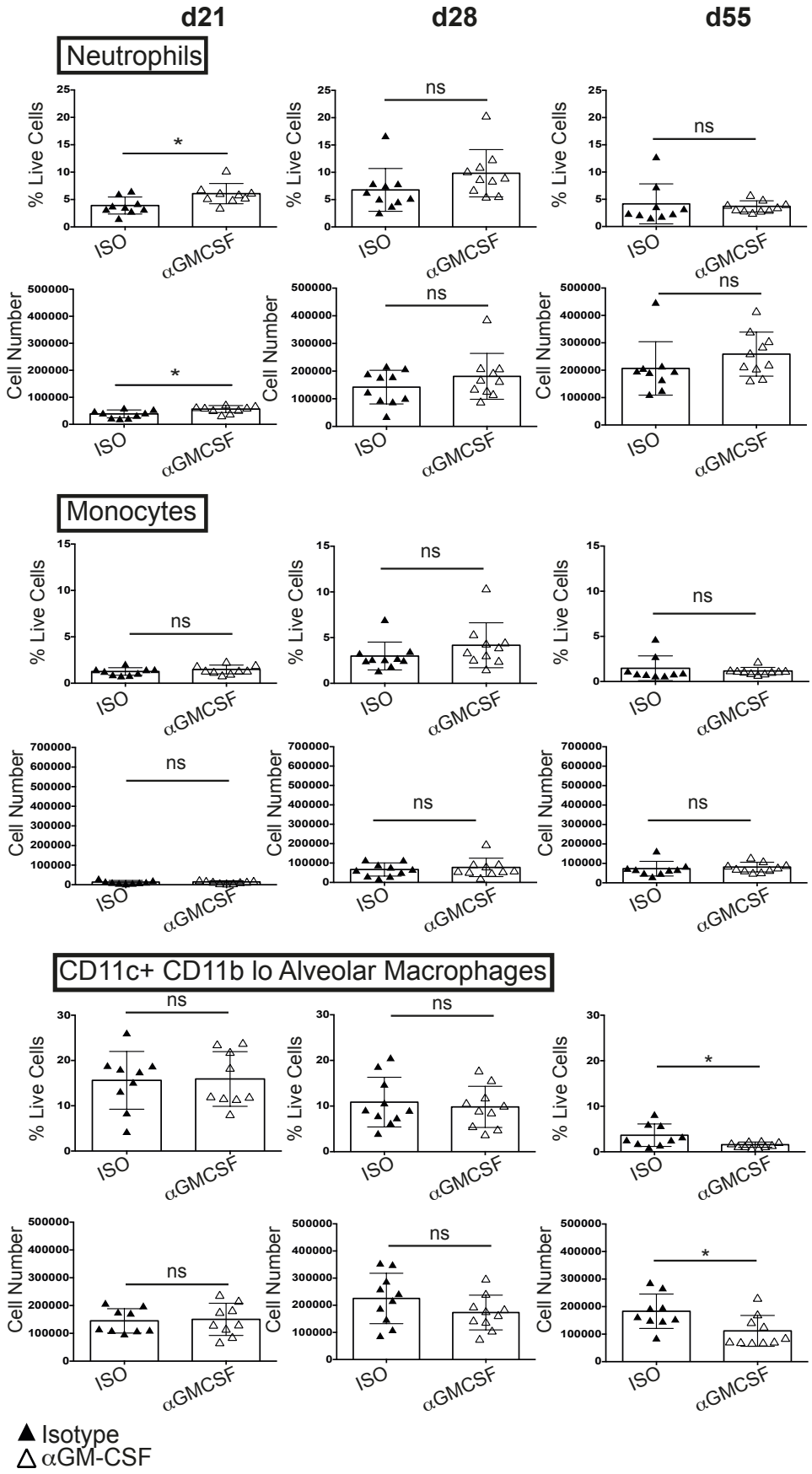

Figure 4.15 Significant late decrease in CD11c^{+} CD11b alveolar macrophage populations with GM-CSF neutralisation during Mtb infection in susceptible CBA/J mice

CBA/J mice were infected and treated with αGM-CSF or ISO as shown in **Figure 4.1**. Mice were sacrificed at day 21, 28 and 55 post infection. Lungs were homogenized by passage through a 70μm filter. Single cell suspensions were stained with the following antibodies to assess percentages and calculate numbers of myeloid populations by flow cytometry: Ly6G FITC, CD11c PE, Ly6C PerCP Cy5.5, CD11b PE Cy7, CD86 Brilliant Violet 421, CD8 v500, F4/80 APC, MHC class II APCe780. Percentage and number of neutrophils (defined as $CD11b^{+}$ $Ly6G^{+}$) at day 21, 28 and 55 post infection **(A)**. Percentage and number of monocytes (defined as $CD11b^{+}$ $Ly6G^{-}$ Ly6C hi) at day 21, 28 and 55 post infection **(B)**. Percentage and number of $CD11c^{+}$ $CD11b^{lo}$ alveolar macrophages (defined as $CD11c^{+}$ $CD11b^{lo}$ Ly6G-) at day 21, 28 and 55 post infection **(C)**. Data pooled from 2 independent experiments. 9-10 mice per group. Graphs show individual mice with mean ± SD. ns – not significant *$p<0.05$ by unpaired student's t-test.

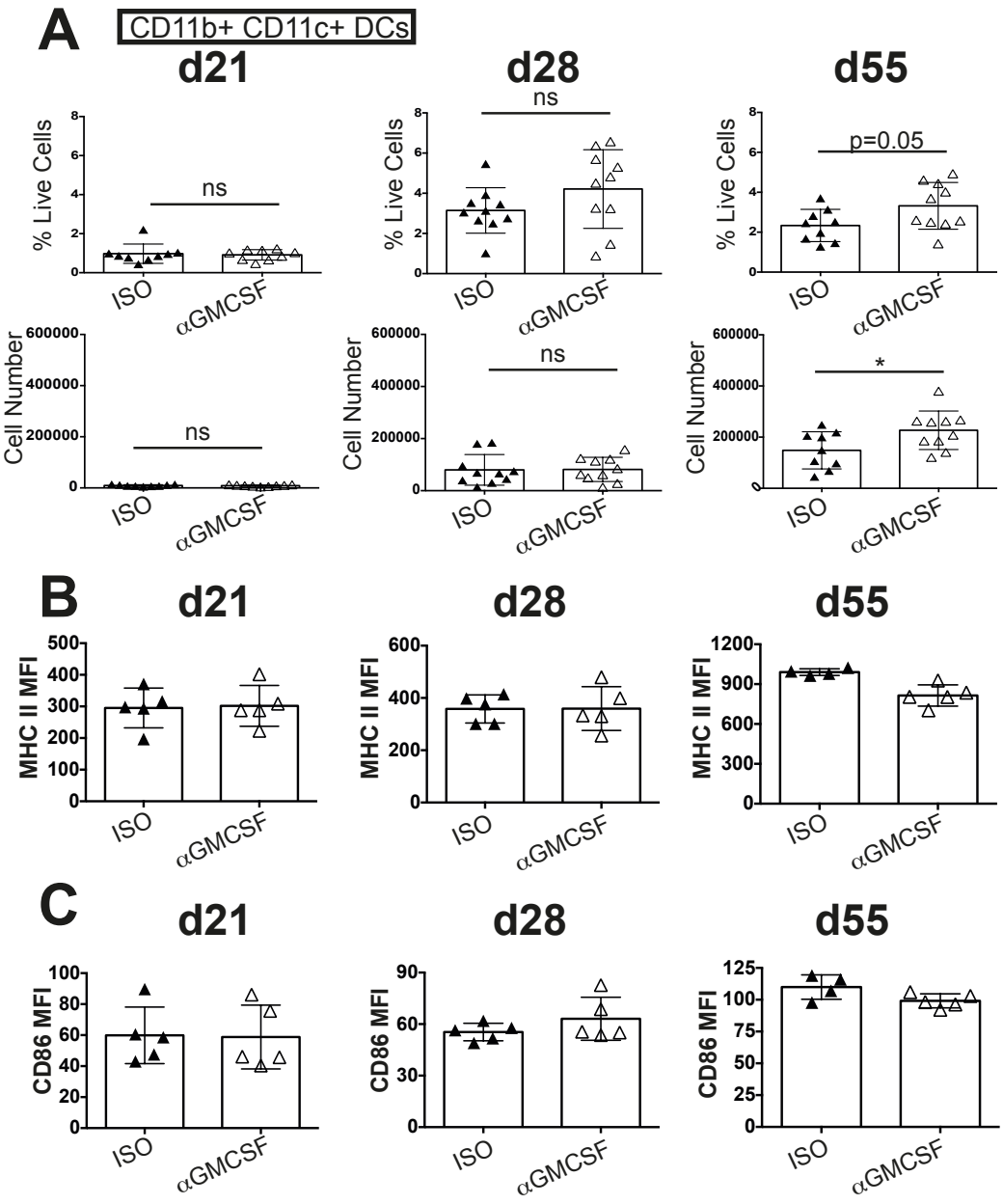

Figure 4.16 GM-CSF neutralisation leads to a late increase in CD11b$^+$ CD11c$^+$ DC populations in susceptible CBA/J mice

CBA/J mice were infected and treated with αGM-CSF or ISO as shown in **Figure 4.1**. Mice were sacrificed at day 21, 28 and 55 post infection. Lungs were homogenized by passage through a 70μm filter. Single cell suspensions were stained with the following antibodies to assess percentages and calculate numbers of myeloid populations by flow cytometry: Ly6G FITC, CD11c PE, Ly6C PerCP Cy5.5, CD11b PE Cy7, CD86 Brilliant Violet 421, CD8 v500, F4/80 APC, MHC class II APCe780. Percentage and number of CD11b$^+$ CD11c$^+$ DCs (defined as Ly6G$^-$ CD11b$^+$ CD11c$^+$) at day 21, 28 and 55 post infection **(A)**. Mean Fluorescence Intensity (MFI) for MHC class II (MHC II) at day 21, 28 and 55 post infection **(B)** MFI for CD86 day 21, 28 and 55 post infection **(C)** Percentage and number graphs **(A)** shown data pooled from 2 independent experiments with 9-10 mice per group. **(B)** and **(C)** graphs representative of 2 independent experiments with 4-5 mice per group. Graphs show values for individual mice with mean ± SD. ns – not significant p=0.05, *p<0.05, by unpaired student's t-test.

Chapter 5: The role of Innate Lymphoid Cells in the immune response to *Mtb* infection

5.1 Investigating the role of Innate Lymphoid Cells in the innate immune response to *Mtb* infection: aims of the investigation

In order to determine whether innate lymphoid cells (ILCs) have a role in the innate response to *Mtb* infection we aimed to:

1) Identify and phenotype ILCs upon infection with virulent H37Rv and hyper-virulent HN878 *Mtb* strains in *Rag* deficient mice and determine whether ILCs are a source of GM-CSF in *Mtb* infection

2) Establish whether deficiency in ILC populations impacts the control of bacterial load during infection with hyper-virulent HN878

3) Assess the impact of ILC deficiency upon myeloid populations during hyper-virulent HN878 infection

4) Determine if GM-CSF is important in the innate immune response to hyper-virulent HN878 infection

5.2 Background

ILCs are a recently described cell population that morphologically resemble lymphocytes and express cell surface molecule and cytokines classically associated T cell populations (reviewed in Serafini et al., 2015; Spits and Cupedo, 2012). However, in contrast to T cell populations, ILCs develop independently of RAG recombinase and lack rearranged antigen specific receptors (reviewed in Serafini et al., 2015). They are mainly localised at mucosal surfaces including the intestine and lung, where they are suitably placed to respond to invasion by

pathogens (reviewed in Artis and Spits, 2015). ILCs are activated, in an antigen independent fashion, by signals derived from myeloid populations and epithelial cells (reviewed in Artis and Spits, 2015). Several different sub-types of ILC have been defined based on the cytokines they produce in response to specific signals: ILC1s, including classical NK cells, which produce IFNγ, require the transcription factor T-bet, and respond to IL-12, IL-15 and IL-18, ILC2s which produce IL-5, IL-13, IL-9 and IL-4, require GATA3 for maintenance, and respond to IL-2, IL-33, IL-25, TSLP, TL1A, and ILC3s which require RORγt, can express IL-17, IL-22 and in some cases IFNγ and respond to IL-23, IL-1β, TL1A and Retinoic Acid (reviewed in Artis and Spits, 2015; Sonnenberg and Artis, 2015; Spits et al., 2013; Walker et al., 2013). In addition to the cytokines described above ILC2s and ILC3s have also been found to produce GM-CSF (Moro et al., 2010; Mortha et al., 2014; Neill et al., 2010). Furthermore, "tissue resident" NK cells that express T-bet but lack Eomes expression have been described to produce GM-CSF (Daussy et al., 2014; Sojka et al., 2014) and an ILC1 population in the small intestine was recently described to express mRNA for GM-CSF (Robinette et al., 2015).

All ILC subsets have been described to have roles during a variety of infections. In the lung ILC2s have been described to induce airway hypersensitivity following influenza infection (Chang et al., 2011). A beneficial role for ILC2s during influenza infection has also been described with ILC2-derived amphiregulin being required to restore epithelial integrity following infection (Monticelli et al., 2011). IL-13 production by ILC2s is required for immunity during *Nippostrongylus brasiliensis* infection (Moro et al., 2010; Neill et al., 2010; Price et al., 2010; Spits and Cupedo, 2012). Furthermore, ILC2s have been described to interact with T cells in the response to *N. brasiliensis* infection (Oliphant et al., 2014). This interaction was required for an optimal Th2 response and also the ability of ILCs to reduce worm burden when transferred into IL-13 deficient mice (Oliphant et al., 2014). ILC2s are also described to promote tissue repair in the lung stages of *N. brasiliensis* infection in an IL-9 dependent manner (Mohapatra et al., 2015; Turner et al., 2013). IL-22 producing ILC3s have been described in the

lung in response to *Streptococcus pneumonia* (Van Maele et al., 2014). In the gut, ILC3-derived IL-22 is also important in the response to *Citrobacter rodentium* (Qiu et al., 2012; Satoh-Takayama et al., 2008; Sonnenberg et al., 2011). ILC3-derived IL-22 has also been shown to synergise with IFNλ (a type III IFN, also known as IL-28) for control of rotavirus infection (Hernandez et al., 2015). An IFNγ producing ILC subset derived from ILC3s has been shown to be important for mucus production upon *Salmonella typhimurium* infection but also to contribute to entercolitis (Klose et al., 2013). ILC1s (that are not conventional NK cells) have been described as source of IFNγ in response to *Toxoplasma gondii* infection (Klose et al., 2014). NK cells have a long established role in the response to various viral infections and intracellular pathogens (Bancroft, 1993; Biron et al., 1999) and their potential role in *Mtb* infection will be discussed below.

ILC2s are the main subset of ILCs present in the lung, although a small population of lung resident RORγt^{+} ILCs have been described (Van Maele et al., 2014), as have ILCs that are negative for the ILC2 marker T1/ST2 (Yagi et al., 2014). As ILCs are present in the lung, they are ideally placed to respond to *Mtb* infection. Furthermore, they possess the capacity to produce cytokines important in the immune response to *Mtb* including IFNγ (Cooper et al., 1993; Flynn et al., 1993), IL-17 (Freches et al., 2013; Gopal et al., 2014; Umemura et al., 2007) and GM-CSF (Gonzalez-Juarrero et al., 2005; Szeliga et al., 2008).

Currently, reports of ILCs in the mouse model of *Mtb* infection concern NK cells or "innate like lymphocytes" that could include NK cells and other ILCs. The O'Garra lab has previously shown in a vaccination model that "innate like lymphocytes" (expressing Thy1.2 but lacking expression of CD3, CD4, CD8 and the γδ TCR) produced IFNγ and IL-17 following *Mtb* challenge but these were not characterised further (Pitt et al., 2012b). In *Rag* deficient mice (*Rag* KO), which lack the RAG recombinase required for rearrangement of the antigen specific T and B lymphocytes, NK cell-derived IFNγ was suggested to be important to prevent

accumulation of granulocytes upon *Mtb* infection (Feng et al., 2006). The importance of NK cells was inferred through comparison of the *Rag* KO strain with the *Rag* KO common γ chain double knock out (*Rag* KO *Il2rg* KO) strain. The common γ chain forms part of the receptor for several cytokines including IL-2, IL-7 and IL-15 and is required for the development and maintenance of NK cells and other ILCs (reviewed in Serafini et al., 2015; Spits et al., 2013). As a result, *Rag* KO *Il2rg* KO mice lack not only NK cells, but all ILC populations, leaving the possibility that other ILC populations may also contribute to the increased susceptibility of *Rag* KO *Il2rg* KO mice to *Mtb* infection when compared to *Rag* KO mice.

In wild-type mice (with a complete immune system) NK cells were identified to produce IFNγ and perforin upon *Mtb* infection (Junqueira-Kipnis et al., 2003). However, this study found NK cell depletion did not impact outcome of the infection, although, only early time points were assessed (Junqueira-Kipnis et al., 2003). Mice overexpressing IL-15 have been shown to display decreased bacterial loads during BCG infection, accompanied by expanded NK cell populations and increased IFNγ production by $CD8^+$ T cells (Umemura et al., 2001). This increased resistance to infection was not seen when NK cells or $CD8^+$ T cells were depleted, suggesting NK cells can contribute to immunity to BCG infection (Umemura et al., 2001). In addition, IL-15 deficient mice, which lack NK cells and have defects in $CD8^+$ T cell memory populations, show slightly higher bacterial loads in chronic infection and defects in cell recruitment to the lung (Lazarevic et al., 2005). Although not assessed, it is possible that a lack of NK cells contributed to the higher bacterial loads in chronic infection observed in these mice. Thus further investigation is needed to determine the role of ILCs during *Mtb* infection.

Different strains of *Mtb* have different virulence and are described to induce different immune responses. Indeed, HN878 is a clinical isolate which belongs to the W-Beijing family (Sreevatsan et al., 1997) and is described to be more virulent than the lab adapted *Mtb* strain H37Rv, with mice displaying shorter survival times upon infection with HN878 compared to

H37Rv (Manca et al., 2001). HN878 is described to contain glycolipids that lead to low production of inflammatory cytokines by both human and mouse macrophages when compared to the lab-adapted *Mtb* strain H37Rv (Portevin et al., 2011; Reed et al., 2004). In addition, in the rabbit model of TB, HN878 induced an early inflammatory response with increased recruitment of innate cells in the lung in comparison to another clinical isolate CDC1551 (Subbian et al., 2013). This was suggested to impact the outcome of infection (Subbian et al., 2013). Studies using multiple strains of *Mtb* have aided elucidation of factors involved in the response to *Mtb* infection. In the mouse model, HN878 infection failed to induce a lasting Th1 response and induced high levels of type I IFNs in comparison to other *Mtb* strains (Manca et al., 2001; Manca et al., 2005; Ordway et al., 2007). Subsequently, type I IFN induction was shown to contribute to the increased virulence of this *Mtb* strain (Manca et al., 2005), clarifying a detrimental role of type I IFNs in *Mtb* infection. These studies highlight the differences in the immune response between different strains of *Mtb*. Although use of H37Rv in immunological studies is beneficial to allow inter-lab comparison, certain factors in the immune response may be more evident upon infection with more virulent strains, as exemplified by type I IFNs in HN878 infection. Therefore assessment of the response of ILCs to both H37Rv and HN878 will aid our investigation and understanding of their role in *Mtb* infection.

5.3 Determining whether ILCs respond to *Mtb* infection

In order to identify whether ILCs respond to *Mtb* infection we used two models of infection: infection with the hyper-virulent *Mtb* strain HN878 and infection with the virulent lab-adapted strain H37Rv both in *Rag* KO mice. Use of H37Rv allows us to assess the response of ILCs to a well established and commonly used strain of *Mtb* but use of HN878, a recent clinical isolate, is arguably a more clinically relevant isolate and may reveal aspects of the immune response not apparent during H37Rv infection. *Rag* KO mice lack the RAG recombinase required for rearrangement of the antigen specific T and B lymphocytes, resulting in absence of adaptive lymphocytes include T, B, NKT and γδ T cells. However, as ILCs do not require recombination of antigen specific receptors these populations are maintained in *Rag* KO mice. Use of the *Rag* KO mouse allowed us to assess the role of ILCs in T cell independent immunity to *Mtb* infection, which could be relevant in patients with defective T cells response such as in HIV infection (Feng et al., 2006) or in individuals suggested to clear or control infection without mounting an adaptive immune response (Young et al., 2009). Furthermore, as many of the factors required for ILC development are also required for T cell development, use of *Rag* KO mice allowed us to take a genetic approach to assess their function, which would not be possible in a wild-type model.

5.3.1 Increase in T-bet positive ILCs upon H37Rv infection

Rag KO mice were infected via the aerosol route with approximately 100 CFU of the lab-adapted strain H37Rv. Lungs were then isolated at days 14, 21 and 25 post infection and digested with Collagenase D, as described in Materials and Methods. Flow cytometry was performed to identify ILC populations, with the gating strategy shown in **Figure 5.1**. The lineage cocktail (to exclude non ILCs) included CD49b (DX5), CD3, CD5, CD27, CD11b, CD11c, NK1.1, B220 and TCRβ and gates for CD127 (IL-7 receptor α), CD25 (IL-2 receptor α chain), T1/ST2 and T-bet were set using fluorescence minus one (FMO) or isotype controls

(Monticelli et al., 2011). ILCs (excluding NK cells) were defined as Lineage (Lin)$^-$ Thy1.2$^+$ CD127$^+$ CD25$^+$ based on previous publications (Monticelli et al., 2011).

We first determined how the percentage and number of the total ILC population, defined as Lin$^-$ Thy1.2$^+$ CD127$^+$ CD25$^+$ changed over the course of infection (**Figure 5.2**). We found that there was no change in the total ILC population at d14 post infection. By day 21 post infection there was a small decrease in the percentage of ILCs as a percentage of total live cells ($p<0.05$ compared to uninfected controls) but a small increase in their total number ($p<0.05$ compared to uninfected controls). This small increase in their number was also evident at day 25 post infection ($p<0.05$ compared to uninfected controls), although infection had no impact on the proportion of ILCs as a percentage of total live cells.

We next phenotyped the ILCs further upon H37Rv infection. In the lung ILC2s are described to be the predominant ILC population, although a small population of T1/ST2 negative ILCs have also been described in the lung (Yagi et al., 2014), as have a small population of RORγt$^+$ ILCs (Van Maele et al., 2014). We defined ILC2s as T1/ST2^{hi} (as shown in gating strategy **Figure 5.1**) based on previous publications (Monticelli et al., 2011; Spits et al., 2013).

In addition to T1/ST2^{hi} ILC2s, we identified a population of T1/ST2^{lo} ILCs in the lung and assessed expression of RORγt and T-bet within this population. We could not detect RORγt expression in ILCs upon H37Rv infection (data not shown). We identified a population of T-bet expressing T1/ST2^{lo} ILCs at day 21 post H37Rv infection (**Figure 5.3**, gates were set using a FMO control), with an increase in the percentage ($p<0.01$ compared to uninfected controls) and number ($p<0.05$ compared to uninfected controls) of T-bet$^+$ ILCs. This increase in percentage and number T-bet expressing ILCs was also evident at day 25 post infection (**Figure 5.3**) (percentage $p<0.05$, number $p<0.05$ compared to uninfected controls).

5.3.2 ILCs produce IFNγ but not GM-CSF in response to virulent H37Rv infection

Having established that there is a change in the population of ILCs present in the lung upon *Mtb* infection we next assessed the ability of ILCs to produce cytokines in response to H37Rv infection. Intracellular cytokine staining was performed upon lung cell cultures from infected or uninfected mice, stimulated for 2 hours with PMA and Ionomycin in the presence of brefeldin A.

ILCs were identified (defined as Lin^- $Thy1.2^+$ $CD127^+$ $CD25^+$) and the gates for cytokine production were again set using isotype controls (data not shown). Upon H37Rv infection cytokine production was undetectable at day 15 post infection (data not shown). We found that ILCs produced IFNγ at day 25 post infection but not at day 21 post infection (**Figure 5.4**). We observed increases in the percentage (d25 $p<0.001$ compared to uninfected controls) and number (d25 $p<0.05$ compared to uninfected controls) of IFNγ producing ILCs at day 25 post H37Rv infection. There was evidence of a trend towards GM-CSF production by ILCs at day 21 and day 25 post infection, but this did not reach significance. We also assessed IL-17 production by ILCs following H37Rv infection. IL-17 producing ILCs were undetectable at days 14, 21 and 25 post H37Rv infection (data not shown).

As conventional NK cells could also be a source of both of IFNγ and GM-CSF (Biron et al., 1999) and are present in the *Rag* KO mouse, we assessed whether these cells produced cytokine upon H37Rv infection. Lung cell cultures from infected or uninfected mice were stimulated for 2h with PMA and Ionomycin in the presence of brefeldin A, as above and then intracellular cytokine staining was performed. We found that NK cells (defined as $NK1.1^+$ $DX5^+$) produce IFNγ but not GM-CSF upon H37Rv infection at day 21 and day 25 post H37Rv infection (**Figure 5.5**). Both the percentage of IFNγ producing NK cells (d21 $p<0.01$, d25 $p<0.01$

compared to uninfected controls) and the number (d21 $p<0.05$, d25 $p<0.05$ compared to uninfected controls) increased upon H37Rv infection.

5.3.3 Increase in T-bet positive ILCs upon hyper-virulent HN878 infection

We observed activation of ILCs upon H37Rv infection. However, as HN878 is a clinical isolate, it may better reflect the response to *Mtb* in a clinical setting. We were therefore interested in how ILCs respond to this *Mtb* strain and investigated whether ILCs responded to HN878 infection in the same way as in H37Rv infection.

Rag KO mice were infected via the aerosol route with approximately 100 CFU of hyper-virulent HN878, via the aerosol route. Lungs were then isolated at days 15, 21 and 25 post infection and digested with Collagenase D, as described above and in the materials and methods. Flow cytometry was performed to identify ILC populations, with the gating strategy shown in **Figure 5.1**, and analysed as for H37Rv infection described above.

We first assessed the impact of infection on the total ILC population (**Figure 5.6**). Upon hyper-virulent HN878 infection the percentage of ILCs (as defined above), as a percentage of total live cells, in the lung remained the same at day 15 post infection but decreased from d21 post infection ($p<0.001$ compared to uninfected controls) and this decrease was maintained to day 25 post infection ($p<0.001$ compared to uninfected controls). However, the overall number of ILCs did not change over the time points assessed, which may reflect changes in other cell populations.

As for H37Rv infection, we next phenotyped the ILCs further upon HN878 infection. We defined ILC2s as T1/ST2^{hi} (as discussed above and shown in gating strategy **Figure 5.1**). We identified a population of T1/ST2^{lo} ILCs in the lung and assessed expression of T-bet and

RORγt in the T1/ST2^{lo} population upon HN878 infection. We could not detect RORγt expression in ILCs upon HN878 infection as for H37Rv (data not shown). We did observe an increase in T-bet^{+} ILCs beginning at d15 post HN878 infection both in percentage ($p< 0.01$ compared to uninfected controls) and number ($p< 0.0001$ compared to uninfected controls) (**Figure 5.7**, gates set using an FMO control,). The increase in T-bet^{+} ILCs was most evident at day 21 and day 25 post infection where there was a larger increase in the percentage (day 21 $p<0.0001$, day 25 $p<0.001$ compared to uninfected controls) and number (day 21 $p<0.0001$, day 25 $p<0.001$ compared to uninfected controls) of these ILCs in HN878 infected mice compared to uninfected controls.

5.3.4 ILCs produce IFNγ and GM-CSF in response to hyper-virulent HN878 infection

Having identified a change in ILC populations present in the lung upon HN878 infection, we next assessed the ability of ILCs to produce cytokines in response to HN878 infection, as described above for H37Rv infection. Intracellular cytokine staining was performed on lung cell cultures from infected or uninfected mice, stimulated for 2 hours with PMA and Ionomycin in the presence of brefeldin A.

Upon HN878 infection we found that ILCs (defined as Lin^{-} Thy1.2^{+} CD127^{+} CD25^{+}) produced IFNγ and GM-CSF at day 21 and day 25 post infection (**Figure 5.8**), whereas no cytokine production was detectable at day 15 post infection (data not shown). The gates for cytokine production were set using isotype controls (data not shown). We observed increases in the percentage (IFNγ d21 $p<0.01$, d25 $p<0.001$; GM-CSF d21 $p<0.01$, d25 $p<0.01$ compared to uninfected controls) and number (IFNγ d21 $p<0.001$, d25 $p<0.01$; GM-CSF d21 $p<0.01$, d25 $p<0.05$ compared to uninfected controls) of cytokine producing ILCs upon HN878 infection. We also assessed IL-17 and IL-22 production by ILCs at day 21 and day 25 post infection. We did not observe IL-22 production at either time point (data not shown). Low levels of IL-17

producing ILCs were inconsistently observed at both day 21 and day 25 post HN878 infection (data not shown).

Cytokine production by NK cells was also assessed upon HN878 infection as described for H37Rv infection. Following stimulation with PMA and Ionomycin for 2h in the presence of brefeldin A, intracellular cytokine staining was carried out. We found that NK cells (defined as $NK1.1^{+}$ $DX5^{+}$) produce IFNγ upon *Mtb* infection at day 21 (percentage $p<0.01$, number $p<0.001$) and also at day 25 post infection (percentage $p<0.05$, number $p<0.05$) (**Figure 5.9**). We did not observe production of GM-CSF at either time point by NK cells. However, GM-CSF producing "tissue resident" NK cells that are $NK1.1^{+}$ $DX5^{-}$ have been described in the liver (Daussy et al., 2014; Sojka et al., 2014). However, preliminary data suggests that $NK1.1^{+}$ $DX5^{-}$ cells are not a source of GM-CSF (or IFNγ) during HN878 infection (data not shown) although this requires confirmation.

5.4 Assessing the functional significance of ILCs in the outcome of *Mtb* infection

We found that ILCs respond to H37Rv and HN878 infection; however, the response of ILCs differed between the two *Mtb* strains. ILCs responded earlier and to a greater extent to HN878 infection than to H37Rv infection. Furthermore, HN878 is a more clinically relevant *Mtb* strain. We therefore decided to assess their functional significance in the outcome of infection with HN878.

In order to determine whether ILCs were important for the outcome of *Mtb* infection we took a genetic approach, utilising the dependence of ILCs on cytokines that signal via receptors containing the common γ chain (*Il2rg*). NK cells and some ILC1s are dependent upon IL-15 for development (Kennedy et al., 2000; Klose et al., 2014; Ranson et al., 2003; Vosshenrich et al., 2005). Deficiency in response to this cytokine will lead to deficiency in NK cells and some ILC1s, whilst other ILC subsets are preserved, as they depend upon IL-7 for their development and/or maintenance (Fuchs et al., 2013; Moro et al., 2010; Satoh-Takayama et al., 2010; Serafini et al., 2015; Spits et al., 2013). We utilised the differential requirement of NK cells and other ILCs for IL-7 and IL-15 in order to assess the importance of IL-15 dependent and/or IL-7 dependent ILCs in the response to HN878 infection.

The ILC populations present in *Rag* KO, *Rag* KO IL-15 Receptor knock out (*Rag* KO *Il-15r* KO), *Rag* KO IL-7 knock out (*Rag* KO *Il7* KO) and *Rag* KO *Il2rg* KO mice were assessed in the lungs of uninfected mice by flow cytometry and are shown in **Figure 5.10** and summarised in **Table 5.1**. As expected *Rag* KO *Il7* KO and *Rag* KO *Il2rg* KO retained a small population of Lin^- $Thy1.2^+$ cells but these were CD127 negative (**Figure 5.10A**). In contrast *Rag* KO *Il15r* KO mice retained an equivalent ILC population to that seen in the *Rag* KO mice (**Figure 5.10A**). *Rag* KO *Il-15r* KO mice, along with *Rag* KO *Il2rg* KO mice lacked $NK1.1^+$ cells,

which were retained in the *Rag* KO *Il7* KO mice (**Figure 5.10B**). Although there appeared to be a decrease in the percentage of NK1.1^{+} NK cells in *Rag* KO *Il7* KO mice (**Figure 5.10B**), this was inconsistent and their numbers were equivalent.

Table 5.1 Summary of cell populations present and absent in mice used to determine a functional role for ILCs in Mtb infection

	Cell types present		
Strain	**T/B cells**	**NK cells (NK1.1^{+})**	**ILCs**
Rag KO	No	Yes	Yes
Rag KO *Il7* KO	No	Yes	No
Rag KO *Il15r* KO	No	No	Yes
Rag KO *Il2rg* KO	No	No	Yes

In order to assess whether IL-15 dependent ILCs and other ILCs had a role in *Mtb* infection, *Rag* KO mice were infected with HN878 alongside *Rag* KO *Il15r* KO and *Rag* KO *Il2rg* KO. Weight loss was assessed over the course of infection and the bacterial load in the lung was assessed at day 21 post infection. Bacterial loads in the lung at day 21 post infection were determined by serial dilutions as described in Materials and Methods and are shown in **Figure 5.11A**. We found an increase in bacterial load at day 21 post infection in the *Rag* KO *Il15r* KO compared to the *Rag* KO ($p<0.0001$). The bacterial load was increased further in the *Rag* KO *Il2rg* KO compared to the *Rag* KO *Il15r* KO ($p<0.01$). This increase in bacterial load in the *Rag* KO *Il15r* KO and *Rag* KO *Il2rg* KO was accompanied by weight loss in both strains beginning after day 18 of infection (**Figure 5.11B**). However, such a pattern of weight loss was not observed in the *Rag* KO mouse (**Figure 5.11B**).

Rag KO *Il2rg* KO mice are deficient for NK cells and all other ILCs (**Figure 5.10**, **Table 5.1**). In order to determine whether IL-7 dependent ILCs have a role in *Mtb* infection in the presence

of NK cells and IL-15 dependent ILCs, we compared HN878 infection in the *Rag* KO and the *Rag* KO *Il7* KO. At day 21 post infection we found a small decrease in the bacterial load in the lung in *Rag* KO *Il7* KO compared to *Rag* KO mice ($p<0.01$) (**Figure 5.12A**). We reasoned that because disruption in early events in infection can potentially impact bacterial loads at later time points, the impact of ILC deficiency upon bacterial load may only be evident at a later time point. We therefore infected *Rag* KO and *Rag* KO *Il7* KO mice with HN878 and assessed bacterial load at day 25 post infection. We found that on average over 5 independent experiments there was an increase in bacterial loads in the *Rag* KO *Il7* KO compared to *Rag* KO mice at day 25 post-infection ($p<0.01$) (**Figure 5.12A**). However, this increased bacterial load data did show some variation between experiments as can be seen in the spread of bacterial load in the *Rag* KO *Il7* KO mice in **Figure 5.12A**. We observed minimal differences in the pattern of weight loss over the course of infection (**Figure 5.12B**).

5.5 Deficiency in ILCs leads to increased recruitment of neutrophils to the lung upon hyper-virulent HN878 infection

NK cells and ILCs produce IFNγ and/or GM-CSF in response to *Mtb* infection and we show that deficiency in IL-15 dependent and/or IL-7 dependent ILCs is detrimental to the outcome of infection. IFNγ and GM-CSF both activate macrophages to control bacterial growth (North and Jung, 2004; Pasula et al., 2015; Rothchild et al., 2014). Furthermore, IFNγ is also important for control of neutrophilia and the prevention of immunopathology (Desvignes et al., 2012; Feng et al., 2006; Nandi and Behar, 2011). Given that IFNγ and GM-CSF can influence myeloid populations, we next investigated the impact of IL-15 dependent and/or IL-7 dependent ILCs on the myeloid populations present upon HN878 infection.

Rag KO, *Rag* KO *Il15r* KO and *Rag* KO *Il2rg* KO mice were infected with HN878 and myeloid populations were assessed at day 21 post infection by flow cytometry. At day 21 post HN878 infection the percentage and number of neutrophils (defined as $Ly6G^{+}$ $CD11b^{+}$) present in the lung was increased in *Rag* KO *Il15r* KO compared to the *Rag* KO (percentage $p<0.05$, number $p<0.05$) and also in the *Rag* KO *Il2rg* KO compared to the *Rag* KO (percentage $p<0.01$, number $p<0.001$) as shown in **Figure 5.13A**. Also at day 21 post HN878 infection the percentage and number of $CD11c^{+}$ $CD11b^{lo}$ alveolar macrophages was lower in *Rag* KO *Il15r* KO compared to *Rag* KO (percentage $p<0.01$, number $p<0.05$) and also in the *Rag* KO *Il2rg* KO compared to *Rag* KO (percentage $p<0.0001$, number $p<0.01$) as shown in **Figure 5.13B**. In addition the percentage and number of $CD11c^{+}$ $CD11b^{lo}$ alveolar macrophages was lower in *Rag* KO *Il2rg* KO compared to *Rag* KO *Il15r* KO (percentage $p<0.01$, number $p<0.01$) as shown in **Figure 5.13B**.

Myeloid populations were also assessed by flow cytometry in the *Rag* KO and *Rag* KO *Il7* KO 25 days following HN878 infection. We found there was a very slight trend towards an increase

in the percentage of neutrophils (defined as above as $Ly6G^+$ $CD11b^+$) (**Figure 5.14A**) present in the lung in the *Rag* KO *Il7* KO compared to the *Rag* KO but this was not significant. However, the number of neutrophils present in the lung in *Rag* KO *Il7* KO was significantly increased compared to *Rag* KO (**Figure 5.14A**) ($p<0.05$). No significant differences in populations of $CD11c^+$ $CD11b^{lo}$ alveolar macrophages were observed (**Figure 5.14B**).

Neutrophils have been linked to susceptibility to *Mtb* infection (Eruslanov et al., 2005; Keller et al., 2006; Marzo et al., 2014) and accumulation of neutrophils can contribute to immunopathology (Feng et al., 2006; Nandi and Behar, 2011). Given that we observed an increase in neutrophils upon HN878 infection in the *Rag* KO *Il15r* KO and *Rag* KO *Il2rg* KO, we investigated whether this was detrimental to control of infection and contributing to susceptibility of these strains of mice to *Mtb* infection. To address this we infected *Rag* KO, *Rag* KO *Il15r* KO and *Rag* KO *Il2rg* KO mice with HN878 and depleted neutrophils from day 10 post infection using a monoclonal antibody against Ly6G (clone 1A8, isotype GL117). An outline of the experiment is shown in **Figure 5.15A**. Depletion of neutrophils increased the amount of weight loss following infection in all strains but most notably in *Rag* KO *Il15r* KO mice (**Figure 5.15B**). The weight loss was so pronounced in one *Rag* KO *Il2rg* KO treated with αLy6G, it was sacrificed before the end of the experiment.

The bacterial load in the lungs was determined as described in Materials and Methods. Neutrophil depletion did not impact the bacterial load in the *Rag* KO mice (**Figure 5.15C**). In the *Rag* KO *Il15r* KO mice neutrophil depletion led to a decrease in bacterial load by approximately $0.65\log_{10}$. In contrast, and somewhat surprisingly, in the *Rag* KO *Il2rg* KO mice neutrophil depletion did not impact the control of bacterial load.

5.6 GM-CSF is crucial to the immune response to HN878 infection

5.6.1 GM-CSF is important to the innate immune response to HN878

We identified ILCs as a source of GM-CSF upon HN878 infection. We therefore hypothesised that GM-CSF production by ILCs was important for their protective contribution to the immune response to HN878 infection. In order to test this we treated mice with a monoclonal antibody against GM-CSF (clone MP1-22E9) or an isotype control antibody (clone GL117) throughout infection in *Rag* KO and *Rag* KO *Il7* KO mice (outline of experiment shown in **Figure 5.16A**).

We found that GM-CSF had a protective role in the innate immune response to HN878 infection as there was a dramatic increase in bacterial load at day 25 post infection in *Rag* KO mice treated with anti-GM-CSF mAb compared to isotype controls (**Figure 5.16B**, $p<0.05$). This increase in bacterial load surpassed that seen in the *Rag* KO *Il7* KO. In *Rag* KO *Il7* KO mice treated with anti-GM-CSF mAb we also observed an increase in bacterial load compared to isotype controls (**Figure 5.16B** $p<0.05$), suggesting additional cellular sources of GM-CSF.

5.6.2 GM-CSF is crucial to the immune response to HN878 infection in a wild-type mouse

In Chapter 4 we assessed the impact of GM-CSF neutralisation upon the outcome of H37Rv infection, however we did not assess GM-CSF neutralisation during hyper-virulent HN878 infection. Given the dramatic increase in HN878 bacterial load in *Rag* KO mice treated with αGM-CSF mAb, we were interested to investigate the impact of GM-CSF neutralisation upon the outcome of HN878 infection in wild-type mice. In order to investigate this GM-CSF was neutralised throughout HN878 infection in intact *Mtb* resistant C57BL/6 mice. An outline of the experiment is shown in **Figure 5.17A**. The bacterial loads in the lung were increased dramatically when GM-CSF was neutralised from day 21 post infection onwards (**Figure**

5.17B). We assessed the populations of lymphocytes present in the lung upon infection using flow cytometry. At day 21 post infection there was a strong trend towards a decrease in the percentage and number of $CD4^+$ T cells (defined as $CD3^+$ $Thy1.2^+$ $CD4^+$) in those mice where GM-CSF had been neutralised (**Figure 5.17C**). At day 21 post infection the percentage and number of $CD8^+$ T cells (define as $CD3^+$ $Thy1.2^+$ $CD8^+$) was significantly lower in mice where GM-CSF had been neutralised (data not shown) but there was no effect on the presence of γδ T cells (defined as $CD3^+$ $Thy1.2^+$ $CD4^-$ $CD8^-$ γδ TCR^+) (data not shown).

Having found that GM-CSF was required for T cell recruitment to the lung upon HN878 infection, we assessed the ability of $CD4^+$ T cells to produce cytokines. At day 21 post infection, lung homogenates were stimulated with PPD for 16 hours before the addition of brefeldin A for a final 4 hours. Cells were then harvested and intracellular cytokine staining was performed to identify $CD4^+$ T cell populations producing IFNγ and IL-17 ($CD4^+$ T cells defined as above). Although there was a trend towards a lower $CD4^+$ T cell population in the absence of GM-CSF there did not appear to be a defect in the ability of $CD4^+$ T cells to produce IFNγ following restimulation as the percentage and number of IFNγ producing T cells were similar between those mice treated with anti-GM-CSF and the isotype controls (**Figure 5.17D**).

5.7 Discussion

It is well established that a protective immune response to *Mtb* is dependent upon $CD4^+$ T cells (Mogues et al., 2001; Saunders et al., 2002). However, the contribution of subsets of innate lymphocytes such as NK cells to the immune response is less well understood with conflicting reports of their importance in different immunological settings (Feng et al., 2006; Junqueira-Kipnis et al., 2003). This, coupled with the recent description of other ILCs underlines the requirement for further study of these subsets. As the predominant ILC population in the lung are ILC2s it is also possible these cells could be detrimental to control of *Mtb* infection through promotion of a type 2 response. Alternatively ILCs could provide early sources of cytokines important in control of *Mtb* and also provide T cell independent protection.

5.7.1 Differential response of ILCs to HN878 and H37Rv infection

We have shown that ILCs respond to both hyper-virulent HN878 and also virulent H37Rv infection in *Rag* KO mice with a population of T-bet positive ILCs present in the lung upon *Mtb* infection. A T-bet positive ILC subset has not been previously described in the lung. However, a small population of $ROR\gamma t^+$ ILCs have been described in the lung using RORγt reporter mice (Van Maele et al., 2014). In addition, a population of ILCs negative for T1/ST2 (an ILC2 marker) were identified in the lung (Yagi et al., 2014). The $T\text{-}bet^+$ ILCs we identified upon *Mtb* infection could derive from these previously described non-ILC2 (potentially $ROR\gamma t^+$) populations in the lung. Indeed, a transition from an ILC3 phenotype ($ROR\gamma t^+$) to an ILC1-like phenotype has been described in both mice and humans, where there is downregulation of RORγt and upregulation of T-bet (Bernink et al., 2015; Klose et al., 2013; Serafini et al., 2015; Vonarbourg et al., 2010). However, we were unable to detect RORγt expression in any ILC population in the lung in naïve or infected mice. Use of a RORγt reporter mouse would facilitate identification of ILCs expressing RORγt in the lung. It is possible that we were unable to detect

RORγt expression is that these cells are "ex ILC3s" and have downregulated RORγt such that they are RORγt lo/negative, and have upregulated T-bet allowing IFNγ expression, as has been described for NKp46^{+} CCR6^{-} ILC3s in the gut (Klose et al., 2013; Vonarbourg et al., 2010). Assessment of the expression of NKp46 and CCR6 on the T-bet expressing cells as well as use of a RORγt fate reporter mouse would enable us to determine if the T-bet expressing ILCs observed originate from RORγt dependent ILC3s as has been previously described. Alternatively the T-bet expressing ILCs could represent ILC1s that have not derived from ILC3s (Klose et al., 2014). However, these cells are described to be CD27^{+} and NK1.1^{+}, markers not expressed by the T-bet^{+} ILCs we identified (Klose et al., 2014; Serafini et al., 2015).

We found IFNγ and GM-CSF production by ILCs in response to HN878 infection from day 21 post infection but only IFNγ in response to H37Rv at day 25 post infection. Both IFNγ and GM-CSF are important for control of *Mtb* infection (Cooper et al., 1993; Flynn et al., 1993; Gonzalez-Juarrero et al., 2005; Szeliga et al., 2008), thus production of these cytokines by ILCs could contribute to protection against *Mtb* infection.

The response of ILCs to *Mtb* infection differed depending on the infecting strain. The expression of T-bet was more pronounced in response to hyper-virulent HN878 infection than during virulent H37Rv infection and ILCs producing GM-CSF were only evident during HN878 infection. Differences in the immune response to *Mtb* strains have been established (Subbian et al., 2013; Portevin et al., 2011; Reed et al., 2004; Manca et al., 2001; Manca et al., 2005; Ordway et al., 2007). In rabbits HN878 has been seen to induce an early granulocyte response when compared to another clinical isolate CDC1551, which was suggested to impact the subsequent outcome of infection (Subbian et al., 2013). Furthermore, HN878 induces higher levels of type I IFNs than other clinical isolates (Manca et al., 2001). It is possible that the differences in the immune responses induced between the two strains could explain the

differences in the level of T-bet expression, kinetics of IFNγ expression and also GM-CSF expression in ILCs that we report here. As ILCs can be activated by factors produced by myeloid populations (reviewed in Artis and Spits, 2015), the early increased granulocyte response in HN878 infection could contribute to the kinetics of cytokine production and the level of T-bet expression. Furthermore, the bacterial loads at the time points assessed are higher in HN878 infection compared to H37Rv infection (data not shown). Thus it is possible that the differences we observe in cytokine production between H37Rv and HN878 at the time points assessed, result from differences in bacterial loads at that time point. Assessment of the ILC response at a later time point in H37Rv infection may be more similar to that observed following HN878 infection but this remains to be assessed.

5.7.2 NK cells and other ILCs are important for the innate response to Mtb infection

Having identified that ILCs respond to *Mtb* infection in *Rag* KO mice we used a genetic approach to assess whether ILCs have a functional role in *Mtb* infection. Such an approach would not have been possible in the context of an adaptive response. We utilised the requirement of ILCs for cytokines that signal via the common γ chain. NK cells and $NK1.1^{+}$ ILC1s are dependent upon IL-15 (Klose et al., 2014; Ranson et al., 2003) whereas other ILC subsets are dependent upon IL-7 (Moro et al., 2010; Satoh-Takayama et al., 2010; Serafini et al., 2015; Vonarbourg and Diefenbach, 2012).

We show that *Rag* KO *Il15r* KO mice (lacking T, B and IL-15 dependent ILCs) are more susceptible to HN878 infection than *Rag* KO mice at day 21 post infection. Furthermore, we show that *Rag* KO *Il2rg* KO mice (lacking T, B, NK cells and all other ILCs) are more susceptible than *Rag* KO *Il15r* KO mice at day 21 post infection. Therefore we show that IL-15 dependent ILCs are important for the innate control of *Mtb* infection, and can infer that other ILC populations also contribute to control which leads to the difference in susceptibility

between the *Rag* KO *Il15r* KO and *Rag* KO *Il2rg* KO. This result demonstrates a role for IL-15 dependent ILCs in *Mtb* infection in *Rag* KO mice, along with IFNγ production by NK cells, and is in keeping with previous literature (Feng et al., 2006). However, our data also suggests an additional role for other ILC populations. However, in the context of an adaptive response, it has been shown that depletion of NK cells during *Mtb* infection does not impact the control of infection at day 21 post infection (Junqueira-Kipnis et al., 2003). A consideration is that the immune setting may influence the importance of NK cells in response to *Mtb* infection. For example, dramatic immunomodulation can occur in humans during HIV infection at least partly through depletion of $CD4^+$ T cells, increasing susceptibility to *Mtb* infection and reactivation (Geldmacher et al., 2012). In this situation, in the absence of an effective $CD4^+$ T cell response, it is possible NK cells have a more pronounced role in the immune response to *Mtb* infection.

Rag KO *Il7* KO mice were not more susceptible to HN878 infection than *Rag* KO mice at day 21 post infection. However, at day 25 post infection *Rag* KO *Il7* KO displayed higher bacterial loads. This finding, taken together with findings in the *Rag* KO *Il15r* KO, suggests that IL-15 dependent ILCs are more important than IL-7 dependent ILCs to the innate immune response to *Mtb* infection, as the effect of deficiency in IL-15 dependent ILCs is evident earlier and is more severe. However, collectively our data shows both are involved.

The predominant population of ILCs in the naïve lung are ILC2s, which promote type 2 immune response producing cytokines such as IL-5 and IL-13 (Artis and Spits, 2015; Monticelli et al., 2011; Yagi et al., 2014). Type 2 responses are suggested to be detrimental to control of *Mtb* infection potentially through suppression of protective Th1 responses (reviewed in O'Garra et al., 2013). As mentioned earlier, it was possible that ILC2s could have been detrimental to control of *Mtb* infection potentially through promotion of type 2 responses. However, *Rag* KO *Il7* KO mice, which lack ILC2 populations, do not show increased control of bacterial infection suggesting this scenario does not occur. It is possible that cytokines that expand and activate

ILC2s such as IL-33 and IL-25 (reviewed in Artis and Spits, 2015) are not induced upon *Mtb* infection, meaning ILC2s are not activated to promote a type 2 response. However, further work will be required to confirm expression of such cytokines and the activation of ILC2s for example through assessment of their production of IL-5 and IL-13. Additionally, it has recently been suggested that IFNγ limits the expansion of ILC2s, their induction of eosinophilia and IL-5 expression upon *N. brasiliensis* infection (Molofsky et al., 2015). In line with this, production of IFNγ upon *Mtb* infection may act to suppress the response of ILC2s.

In order to assess the function of IL-7 dependent ILCs during *Mtb* infection we utilised the *Rag* KO *Il7* KO mouse. However, although ILCs are dependent on IL-7 for their development and/or maintenance (reviewed in Serafini et al., 2015; Vonarbourg and Diefenbach, 2012), it has been suggested that deficiency in IL-7 only reduces ILC numbers and does not lead to complete deficiency due to the ability of TSLP, another cytokine that signals via the α subunit of the IL-7 receptor (IL-7Rα), to compensate for loss of IL-7 (Hoyler et al., 2012; Vonarbourg et al., 2010). Although we found that there was loss of a Lin^- $Thy1.2^+$ $CD127^+$ population in the *Rag* KO *Il7* KO, use of an *Il7rα* deficient mouse strain may provide a more complete deficiency in ILCs and confirm our results.

Taken together, we show a protective role for ILCs, including NK cells, in the immune response to *Mtb* infection in the absence of an adaptive immune system in *Rag* KO mice. Further work assessing the response of ILCs in a wild type mouse would be beneficial to our understanding of the their response upon *Mtb* infection. Indeed, it has been reported that NK cells and other ILCs from *Rag* deficient mice are hyper-responsive (Karo et al., 2014), which could influence their response to *Mtb* infection. It is also important to consider potential additional roles of ILCs in the initiation and regulation of the adaptive immune response. Indeed ILCs have been described to interact with T cells to influence outcome of infection, initiate allergic responses and regulate T cell response to commensal bacteria (Gold et al., 2014; Halim et al., 2014; Hepworth et al.,

2015; Hepworth et al., 2013; Mortha et al., 2014; Oliphant et al., 2014) and thus ILCs could have additional roles in *Mtb* infection, which requires further investigation. However, use of the *Rag* deficient mouse has allowed us to take a genetic approach to determine the relative importance of different ILCs during *Mtb* infection, which would not have been possible in the presence of an adaptive immune system.

5.7.3 Deficiency in NK cells and/or other ILCs leads to neutrophilia upon Mtb infection

We observed that the increased bacterial loads observed in the absence of NK cells and/or other ILCs correlated with accumulation of neutrophils upon *Mtb* infection. IFNγ has been described to regulate neutrophils in *Mtb* infection through suppressing their recruitment and survival (Desvignes et al., 2012; Nandi and Behar, 2011). We would hypothesise that in the absence of NK cells and/or other ILCs there is impairment in IFNγ production in infection. Therefore the absence of IFNγ leads to higher numbers of neutrophils in the lung, which could contribute to immunopathology or provide a permissive environment for bacterial growth (Eruslanov et al., 2005; Nandi and Behar, 2011).

In order to determine whether neutrophil accumulation was detrimental to control of infection and contributing to susceptibility to *Mtb* infection in ILC deficient animals, we depleted neutrophils using an αLy6G mAb. In all strains depletion of neutrophils led to more weight loss over the course of infection, although this was most pronounced in *Rag* KO *Il15r* KO mice. This could suggest that neutrophils are contributing to control of the immune response and thus, in their absence, the increased level of weight loss reflects a more exaggerated immune response. Alternatively, this could suggest neutrophils are contributing to control of infection and in their absence disease is exacerbated.

In contrast to the weight loss observed, depletion of neutrophils had different effects on the control of bacterial load in the different mouse strains. Neutrophil depletion led to lower bacterial loads in *Rag* KO *Il15r* KO mice, suggesting that neutrophils in *Rag* KO *Il15r* KO mice are detrimental to control of infection. The lower bacterial load in the context of increased weight loss when neutrophils are depleted suggests that neutrophils may be functioning to suppress the immune response to *Mtb*. Indeed neutrophils have been described to be a source of the immunosuppressive cytokine IL-10 during *Mtb* infection (Dorhoi et al., 2010; Dorhoi et al., 2013; Zhang et al., 2009), although further investigation will be required to confirm this hypothesis. The lower bacterial load in the absence of neutrophils could also suggest that neutrophils provide a permissive environment for *Mtb* growth as has been previously suggested (Eruslanov et al., 2005).

However, in contrast to *Rag* KO *Il15r* KO, in *Rag* KO and *Rag* KO *Il2rg* KO neutrophil depletion did not impact control of bacterial load. A possible explanation for the different impact of neutrophil depletion in *Rag* KO *Il15r* KO and *Rag* KO *Il2rg* KO is that lower proportions and numbers of $CD11c^{+}$ $CD11b^{lo}$ macrophages were present in the lung in *Rag* KO *Il2rg* KO compared to *Rag* KO *Il15r* KO. If neutrophils are suppressing the anti-mycobacterial response in alveolar macrophages to facilitate bacterial growth in *Rag* KO *Il15r* KO, this may not be evident in *Rag* KO *Il2rg* KO as the population is lacking. Furthermore, *Rag* KO *Il2rg* KO mice will have deficiencies in populations producing macrophage activating cytokines such as IFNγ and GM-CSF (Flynn and Chan, 2001; Pasula et al., 2015; Rothchild et al., 2014). Therefore, even in the absence of neutrophils, macrophages may still not be sufficiently activated to control bacterial growth. Further work will be required to determine if the state of macrophage activation differs between *Rag* KO *Il15r* KO and *Rag* KO *Il2rg* KO and how neutrophil depletion affects this.

5.7.4 GM-CSF is crucial to the innate and adaptive response to Mtb infection

We found that ILCs, but not conventional NK cells, were a source of GM-CSF upon *Mtb* infection. We therefore hypothesised that GM-CSF production by ILCs may be an important factor for their protective role in *Mtb* infection. Neutralisation of GM-CSF in the *Rag* KO and *Rag* KO *Il7* KO mice revealed that GM-CSF was an important factor for the innate control of *Mtb* infection, with an increase in bacterial load in *Rag* KO mice treated with αGM-CSF compared to isotype controls. This increase in bacterial load upon αGM-CSF treatment was also evident in the *Rag* KO *Il7* KO mice. This suggests that, although ILCs are a source of GM-CSF, there are other sources of GM-CSF that contribute to protection upon *Mtb* infection. GM-CSF producing "tissue resident" NK cells that are $DX5^-$ have been described in the liver (Daussy et al., 2014; Sojka et al., 2014). It is possible that there is a population of NK cells, distinct from conventional NK cells, present in *Mtb* infection that produce GM-CSF. Although, very few tissue resident NK cells, expressing the same markers as the GM-CSF producing liver tissue resident NK cells, were found in the lung (Sojka et al., 2014). In keeping with this, our preliminary results suggest that $NK1.1^+$ $DX5^-$ cells are not a source of GM-CSF during *Mtb* infection, although confirmation of these results is required. Production of GM-CSF by various other cell types present in the lung including fibroblasts, type II pneumocytes and macrophages has also been reported (Gasson, 1991; Trapnell and Whitsett, 2002). These populations could also contribute to GM-CSF production during *Mtb* infection and this will require further investigation.

We were surprised to see such a dramatic phenotype in the *Rag* KO mice when GM-CSF was neutralised during HN878 infection, as previous work in mice lacking GM-CSF suggested a defect in antigen presenting function, lymphocyte recruitment and IFNγ production by $CD4^+$ T cells in the lung was responsible for their enhanced susceptibility to less virulent *Mtb* infection (Gonzalez-Juarrero et al., 2005). However, GM-CSF has been described to restrict

mycobacterial growth in macrophages *in vitro* (Denis and Ghadirian, 1990; Pasula et al., 2015; Rothchild et al., 2014). In the *Rag* KO GM-CSF neutralisation could impair macrophage activation and control of mycobacterial growth, leading to increased bacterial loads.

In Chapter 4 we investigated the role of GM-CSF during H37Rv infection in *Mtb* resistant and *Mtb* susceptible mouse strains. Given the dramatic phenotype in *Rag* KO mice when GM-CSF was neutralised during HN878 infection, we investigated the role of GM-CSF in wild type mice infected with the hyper-virulent HN878 *Mtb* strain. There was an increase in bacterial load in mice treated with αGM-CSF from day 21 post infection. We observed a strong trend towards a decrease in proportion and number of $CD4^+$ T cells in the lung at day 21 post infection. However, there did not appear to be a defect in their ability to produce IFNγ. This suggests that, in keeping with the literature, GM-CSF is important for the recruitment of $CD4^+$ T cells to the lung (Gonzalez-Juarrero et al., 2005). However, as we did not observe a defect in their IFNγ production this suggests those present are functional. $CD4^+$ T cells could be impaired for production of another factor (e.g. TNFα) that we are not measuring, resulting in impaired control of *Mtb* infection. Another likely possibility is that GM-CSF is affecting the function of myeloid populations due to the ability of GM-CSF to activate macrophages to restrict mycobacterial growth (Denis and Ghadirian, 1990; Flynn and Chan, 2001; Pasula et al., 2015; Rothchild et al., 2014). Therefore, the absence of GM-CSF may affect macrophage ability to control bacterial load. It is likely that both the impact of GM-CSF upon the recruitment of T cells and its effect upon macrophage activation will contribute to the increased susceptibility of wild-type mice to HN878 infection when GM-CSF is neutralised.

Overall we show that a population of T-bet^+ ILCs are present upon infection with either the lab-adapted *Mtb* strain H37Rv or the hyper-virulent strain HN878. Furthermore, ILCs are a source of cytokines following infection with either strain of *Mtb*. Deficiency in NK cells and/or other ILCs increases susceptibility to HN878 infection and leads to accumulation of neutrophils in the

lung, which in the absence of NK cells, are detrimental to control of bacterial load. Furthermore, we show that GM-CSF is crucial to control bacterial loads in HN878 infection in both *Rag* KO and wild-type mice. Further work is required to determine the mechanisms by which ILCs are protective and also response of ILCs to *Mtb* infection in the context of an adaptive immune system.

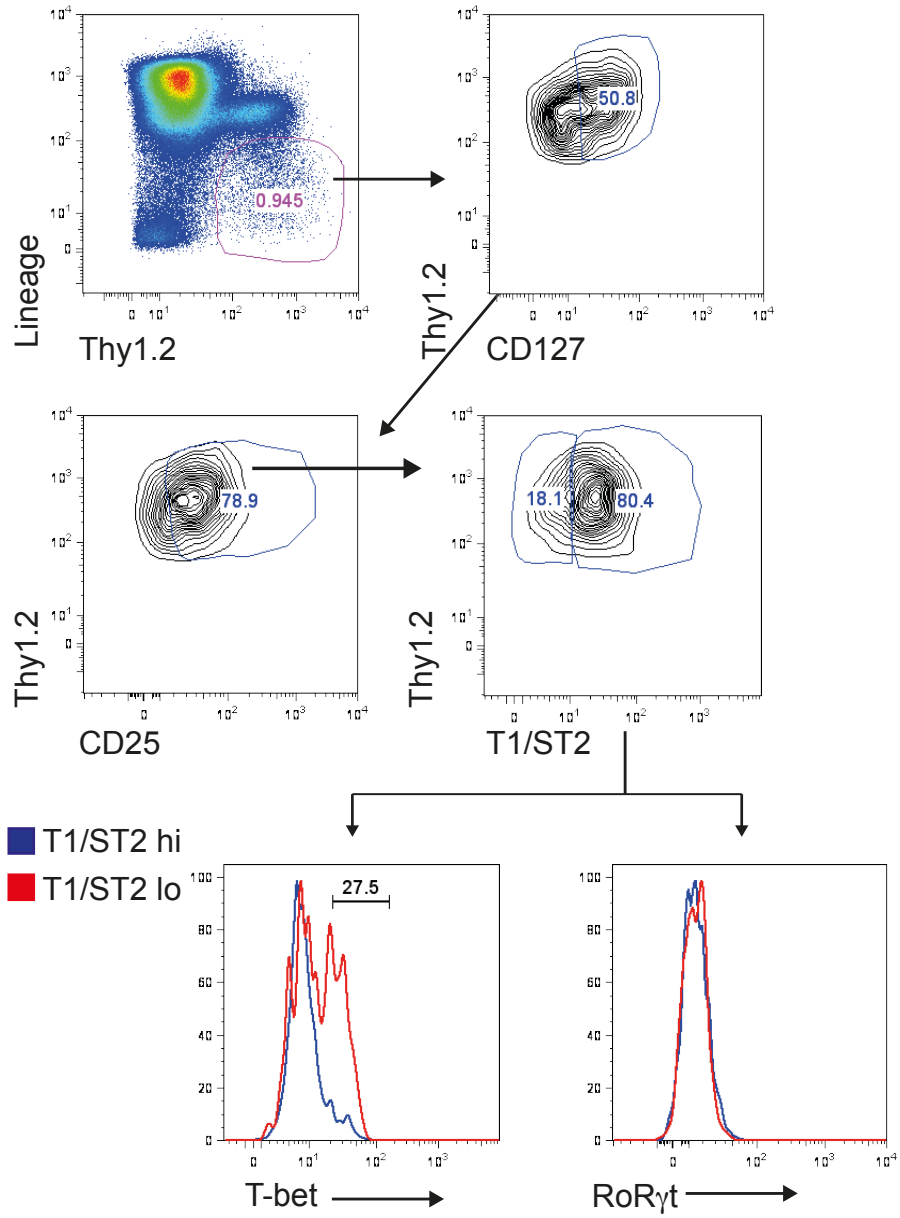

Figure 5.1 Identification of Innate Lymphoid cells - gating strategy and definition of ILCs

Rag KO mice were infected with approximately 100 CFU of the hyper-virulent *Mtb* strain HN878 via the aerosol route. At day 21 post infection lungs were harvested and digested by incubation with collagenase D, as described in the materials and methods. Single cell suspensions from the lung were obtained by passage through a 70µm filter. Single cell suspensions were stained with the following antibodies: T1/ST2 FITC, CD127 PE, RORγt PerCP e710, Thy1.2 PE Cy7, T-bet Pacific Blue, Sca-1 v500, CD25 APC e780 and Lineage markers: CD49b (DX5) APC, CD3 APC, CD5 APC, CD27 APC, CD11b APC, CD11c APC, NK1.1 APC, B220 APC, TCRβ APC. ILCs were identified as Lin^{-} $Thy1.2^{+}$ $CD127^{+}$ $CD25^{+}$ and further phenotyped based on expression of T1/ST2, T-bet and RORγt. Flow cytometery plots shown are from one mouse representative of infected mice at day 21 post infection. The same gating strategy was used to identify ILCs in uninfected mice and also in H37Rv infected mice.

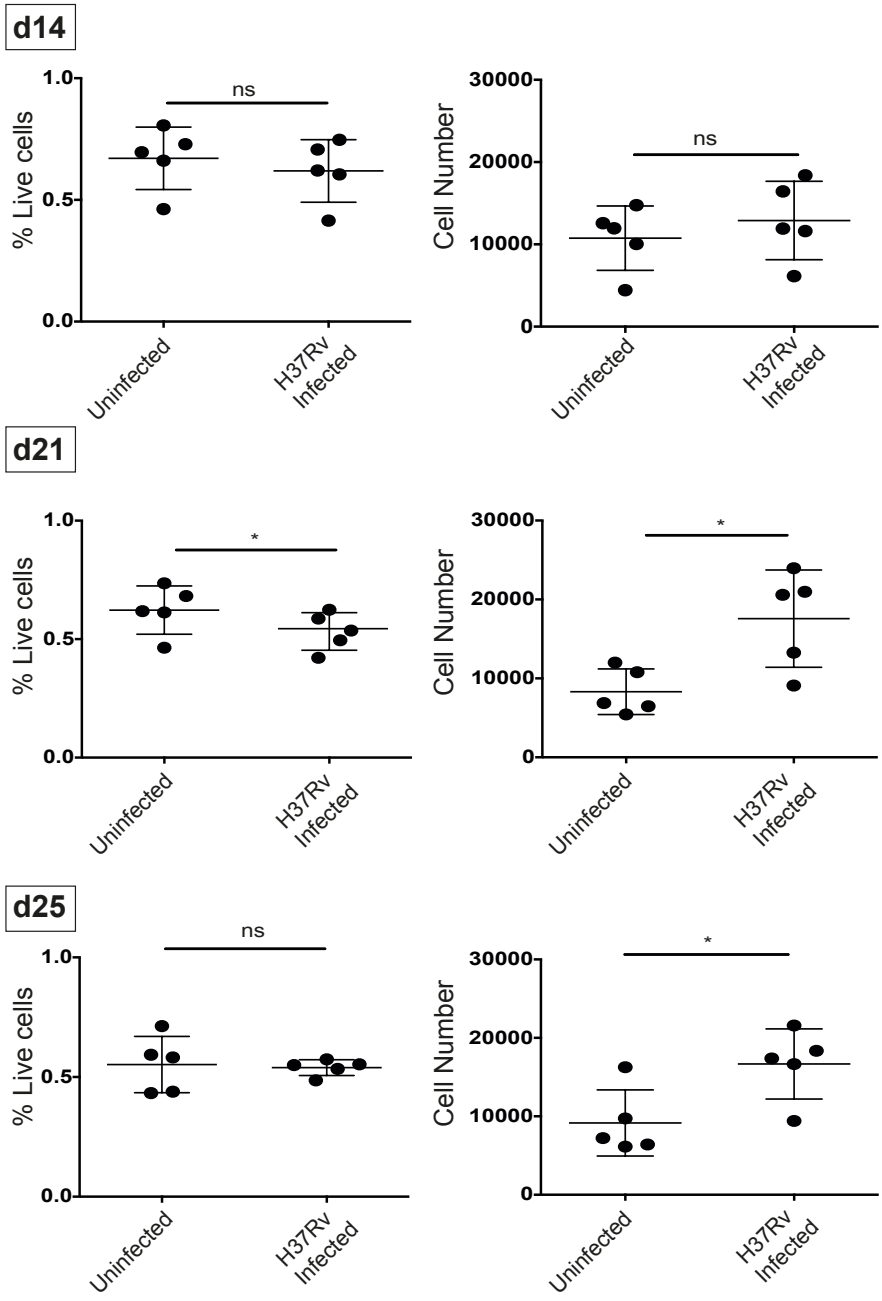

Figure 5.2 H37Rv infection induces a small increase in total numbers of Lin- Thy1.2$^+$ CD127$^+$ CD25$^+$ ILCs in the lung

Rag KO mice were left uninfected or infected with approximately 100 CFU of the lab-adapted *Mtb* strain H37Rv via the aerosol route. At days 14, 21 and 25 post infection mice were sacrificed. Lungs were harvested and digested with collagenase D as described in the materials and methods. Single cell suspensions from the lung were obtained by passage through a 70μm filter. Single cell suspensions were stained with the following antibodies: T1/ST2 FITC, CD127 PE, RORγt PerCP e710, Thy1.2 PE Cy7, T-bet Pacific Blue, Sca-1 v500, CD25 APC e780 and Lineage markers (Lin): CD49b (DX5) APC, CD3 APC, CD5 APC, CD27 APC, CD11b APC, CD11c APC, NK1.1 APC, B220 APC, TCRβ APC. Percentage and number of ILCs defined as Lin$^-$ Thy1.2$^+$ CD127$^+$ CD25$^+$ at day 14, 21 and 25 post infection are shown. Graphs show individual mice with mean ± SD. Individual time points are from independent experiments. Data representative of 1(d14), 2 (d25) or 3 (d21) independent experiments. 5 mice per group. ns – not significant, * $p<0.05$ by unpaired student's t-test.

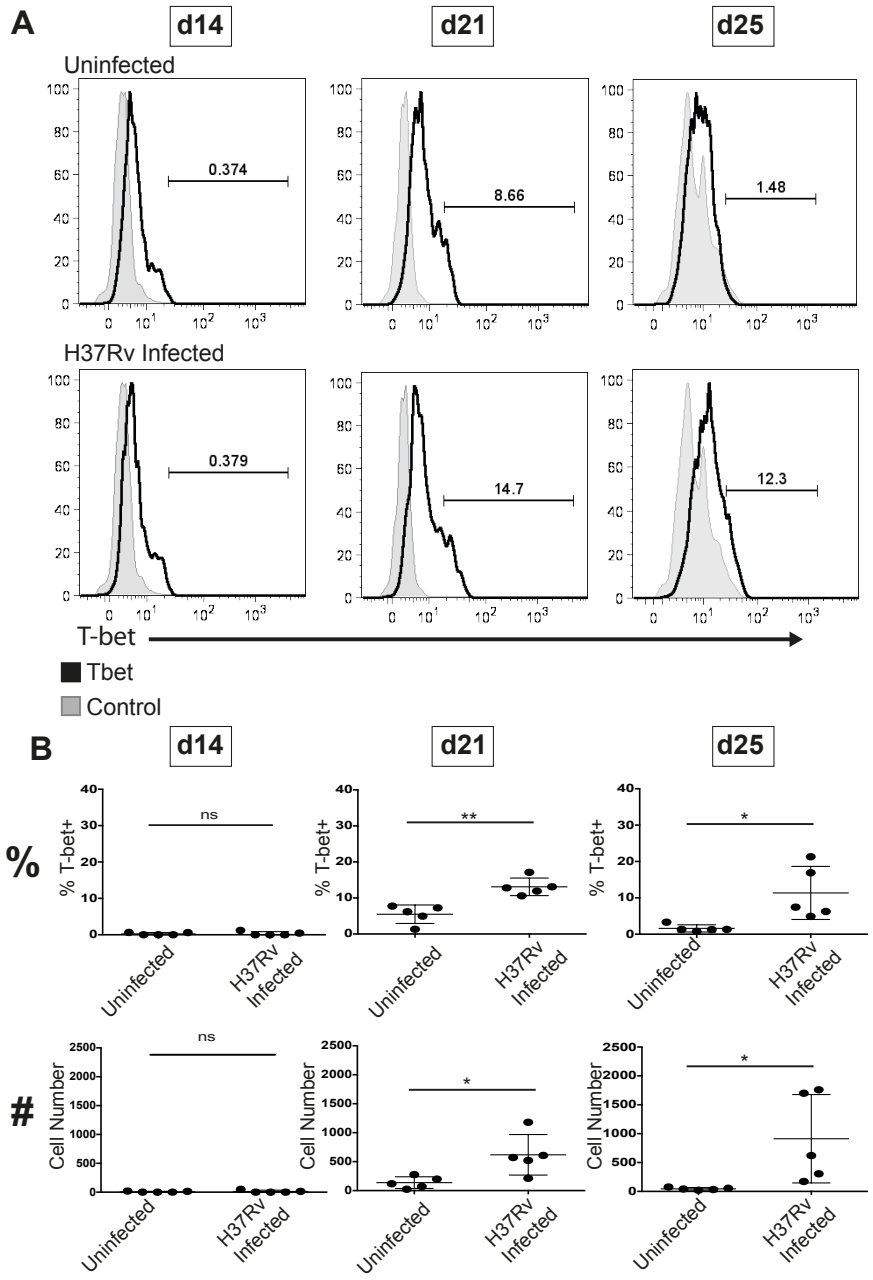

Figure 5.3 H37Rv infection in Rag KO mice leads to an increase in T-bet$^+$ ILCs in the lung

Rag KO mice were left uninfected or infected with approximately 100 CFU of the lab-adapted *Mtb* strain H37Rv via the aerosol route. At days 14, 21 and 25 post infection mice were sacrificed. Lungs were harvested and digested with collagenase D as described in the materials and methods. Single cell suspensions from the lung were obtained by passage through a 70μm filter. Single cell suspensions were stained with the following antibodies: T1/ST2 FITC, CD127 PE, RORγt PerCP e710, Thy1.2 PE Cy7, T-bet Pacific Blue, Sca-1 v500, CD25 APC e780 and Lineage markers (Lin): CD49b (DX5) APC, CD3 APC, CD5 APC, CD27 APC, CD11b APC, CD11c APC, NK1.1 APC, B220 APC, TCRβ APC. Histograms showing T-bet expression in Lin$^-$ Thy1.2$^+$ CD127$^+$ CD25$^+$ T1/ST2^{lo}ILCs at day 14, 21 and 25 post infection are shown **(A)**. Histograms are concatenated from all individuals in the group. Percentage and number of T-bet$^+$ Lin$^-$ Thy1.2$^+$ CD127$^+$ CD25$^+$ T1/ST2^{lo} ILCs **(B)** Graphs show individual mice with mean ± SD. Individual time points are from independent experiments. Data representative of 1(d14) or 2 (d21 and d25) independent experiments. 5 mice per group. ns – not significant, * $p<0.05$ by unpaired student's t-test.

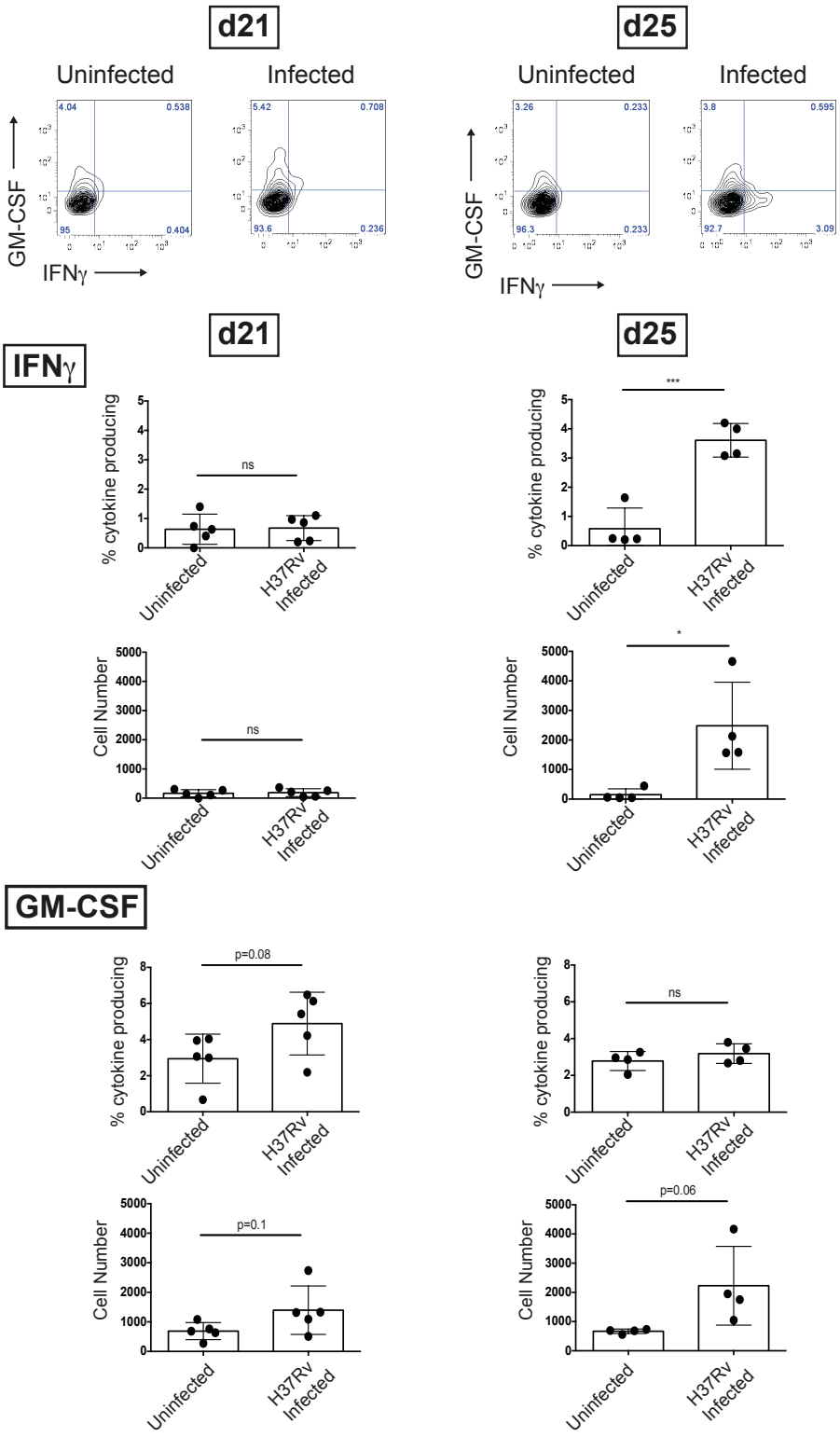

Figure 5.4 Innate Lymphoid cells are a source of IFNγ following H37Rv infection of Rag KO mice

Rag KO mice were left uninfected or infected with approximately 100 CFU of the lab-adapted *Mtb* strain H37Rv via the aerosol route. At days 21 and 25 post infection mice were sacrificed. Lungs were harvested and digested with collagenase D as described in the materials and methods. Single cell suspensions from the lung were obtained by passage through a 70μm filter. $5x10^5$ cells were restimulated with 50ng/ml PMA and 500ng/ml ionomycin in the presence of Brefeldin A for 2 hours. Cells were then harvested and stained with the following to identify

IFNγ and GM-CSF production by ILCs: GM-CSF FITC, CD127 PE, Lineage markers (Lin): CD49b (DX5) PerCP e710, CD3 PerCP Cy5.5, CD5 PerCP Cy5.5, CD27 PerCP Cy5.5, CD11b PerCP Cy5.5, CD11c PerCP Cy5.5, NK1.1 PerCP Cy5.5, B220 PerCP Cy5.5, TCRβ PerCP Cy5.5, Thy1.2 PE Cy7, IFNγ e450 and CD25 APC e780. ILCs were identified as Lin^- $Thy1.2^+$ $CD127^+$ $CD25^+$. Representative flow cytometry plots from individual mice at day 21 or 25 post infection are shown. Graphs of percentage and number of IFNγ or GM-CSF producing ILCs are shown at day 21 and 25 post infection. Graphs show individual mice with mean ± SD. Individual time points are from independent experiments. Data representative of 1 (GM-CSF d21 and 25) or 2 (IFNγ d21 and 25) independent experiments. 4-5 mice per group. ns – not significant, p=0.06, p=0.08, p=0.01, * $p<0.05$, *** $p<0.001$ by unpaired student's t-test.

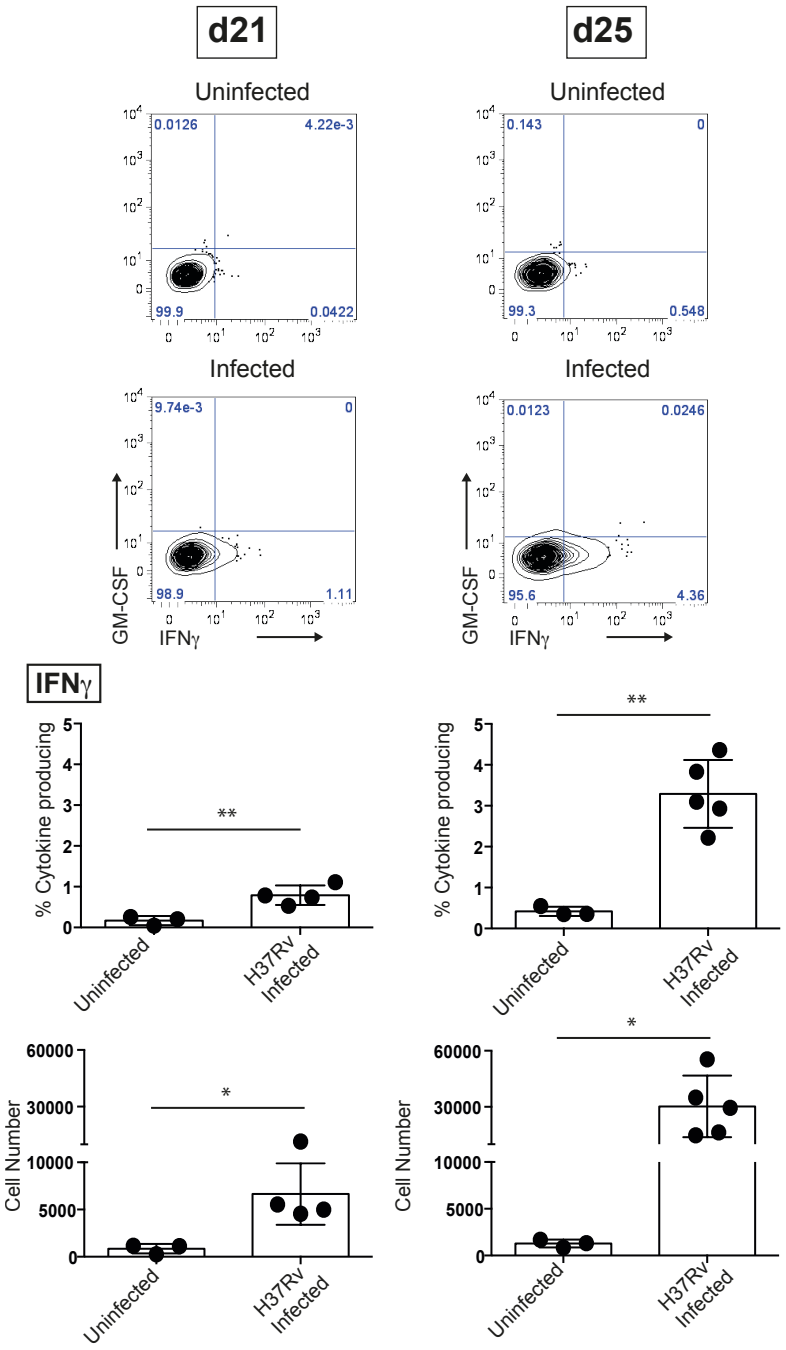

Figure 5.5 Conventional NK cells produce IFNγ not GM-CSF upon H37Rv Infection

Rag KO mice were left uninfected or infected with approximately 100 CFU of the lab-adapted *Mtb* strain H37Rv via the aerosol route. At days 21 and 25 post infection mice were sacrificed. Lungs were harvested and digested with collagenase D as described in the materials and methods. Single cell suspensions from the lung were obtained by passage through a 70µm filter. $5x10^5$ cells were restimulated with 50ng/ml PMA and 500ng/ml ionomycin in the presence of Brefeldin A for 2 hours. Cells were then harvested and stained with the following to identify IFNγ and GM-CSF production by conventional NK cells: GM-CSF FITC, NK1.1 PE, CD27 PerCP Cy5.5, CD11b PE Cy7, IFNγ e450 and CD49b (DX5) APC. NK cells were identified as $NK1.1^+$ $DX5^+$ ($CD11b^{lo-hi}$). Representative flow cytometry plots from individual mice at day 21 or 25 post infection are shown. Graphs of percentage and number of IFNγ NK cells are shown at day 21 and 25 post infection. Graphs show individual mice with mean ± SD. Data representative of 1 independent experiment. 3-5 mice per group. * $p<0.05$, *** $p<0.001$ by unpaired student's t-test.

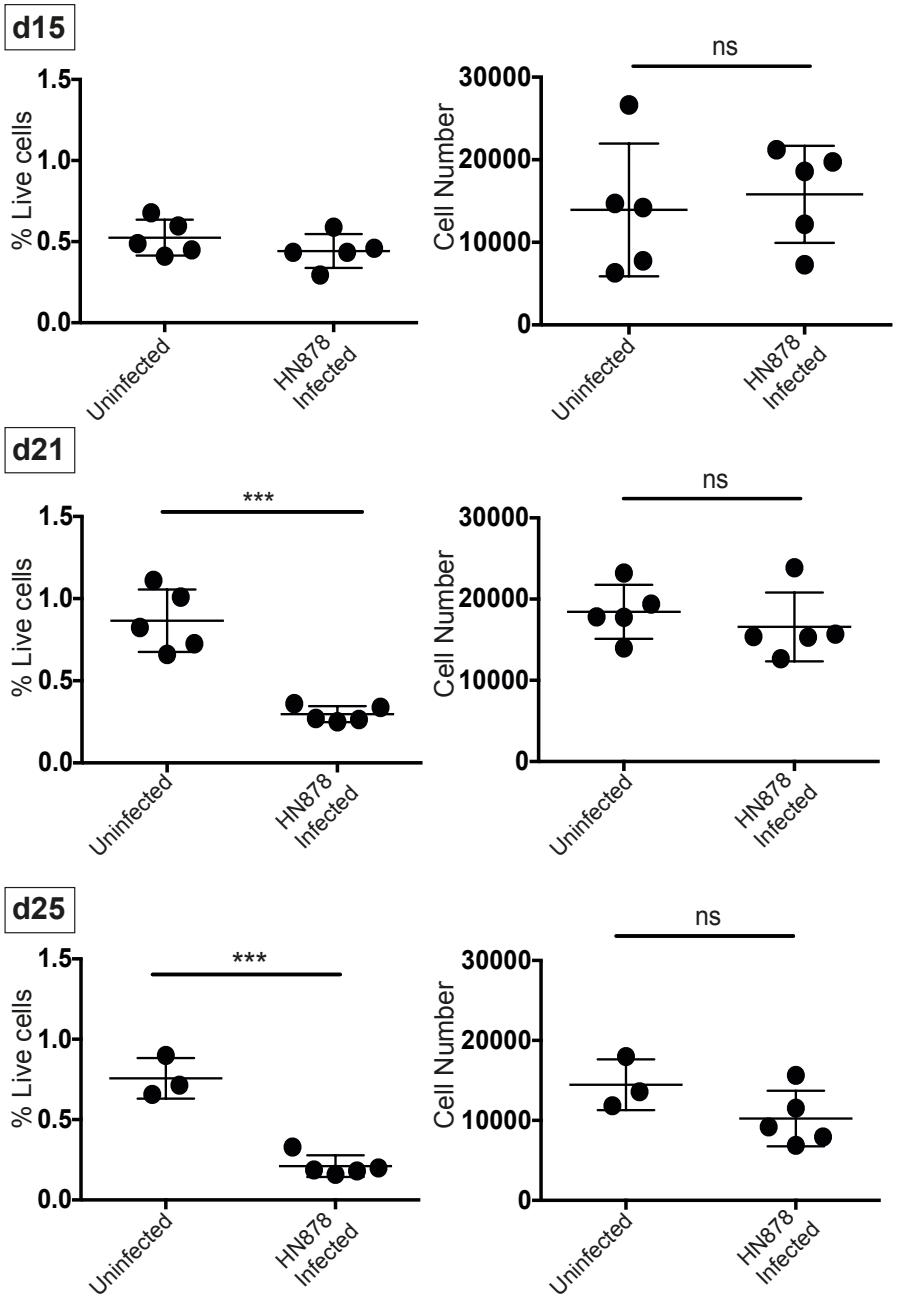

Figure 5.6 HN878 infection does not impact total numbers of Lin- Thy1.2$^+$ CD127$^+$ CD25$^+$ ILCs in the lung

Rag KO mice were left uninfected or infected with approximately 100 CFU of the hyper-virulent *Mtb* strain HN878 via the aerosol route. At days 15, 21 and 25 post infection mice were sacrificed. Lungs were harvested and digested with collagenase D as described in the materials and methods. Single cell suspensions from the lung were obtained by passage through a 70μm filter. Single cell suspensions were stained with the following antibodies: T1/ST2 FITC, CD127 PE, RORγt PerCP e710, Thy1.2 PE Cy7, T-bet Pacific Blue, Sca-1 v500, CD25 APC e780 and Lineage markers (Lin): CD49b (DX5) APC, CD3 APC, CD5 APC, CD27 APC, CD11b APC, CD11c APC, NK1.1 APC, B220 APC, TCRβ AP. Percentage and number of ILCs defined as Lin$^-$ Thy1.2$^+$ CD127$^+$ CD25$^+$ at day 15, 21 and 25 post infection are shown. Graphs show individual mice with mean ± SD. Individual time points are from independent experiments. Data representative of 3 (d14), 5 (d21) or 4 (d25) independent experiments. 3-5 mice per group. ns – not significant, *** $p<0.001$ by unpaired student's t-test.

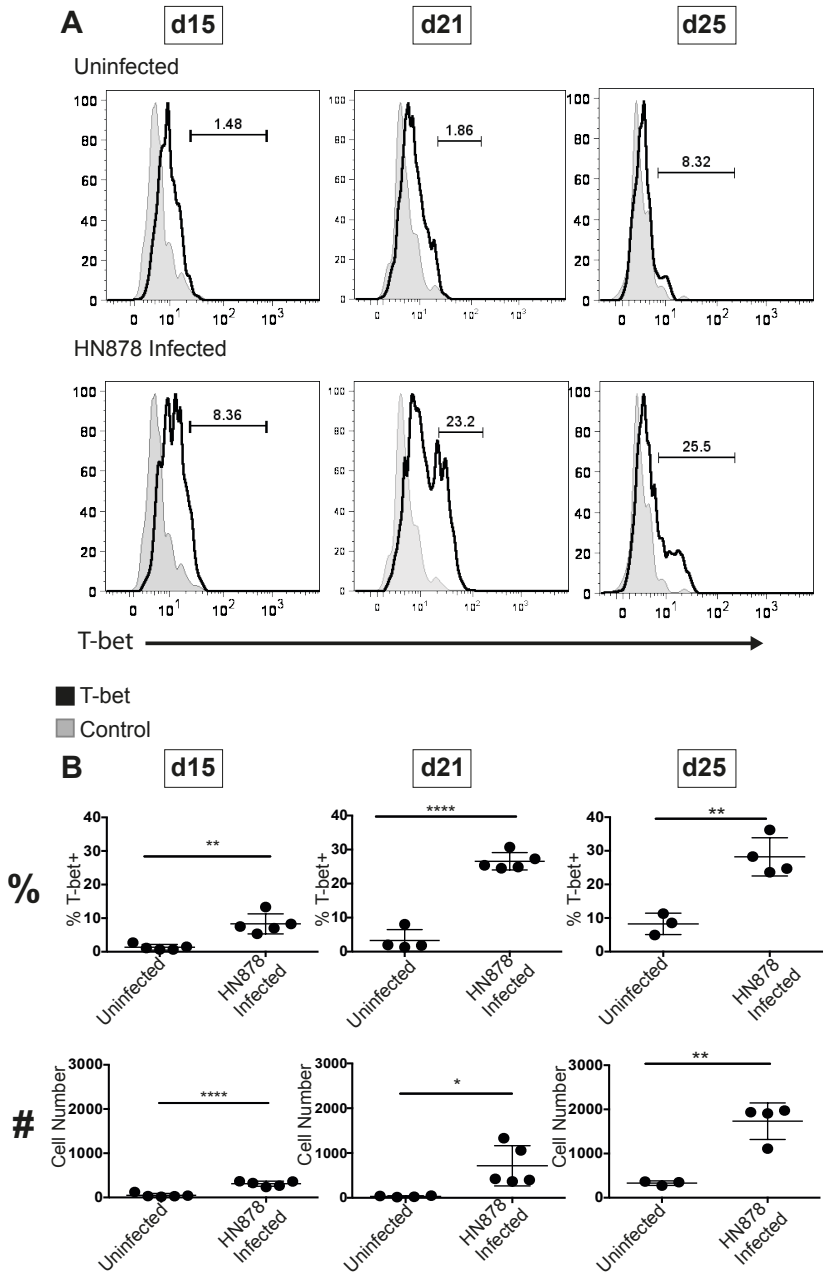

Figure 5.7 HN878 infection in Rag deficient mice leads to an increase in T-bet$^+$ ILCs in the lung

Rag KO mice were left uninfected or infected with approximately 100 CFU of the hyper-virulent *Mtb* strain HN878 via the aerosol route. At days 14, 21 and 25 post infection mice were sacrificed. Lungs were harvested and digested with collagenase D as described in the materials and methods. Single cell suspensions from the lung were obtained by passage through a 70μm filter. Single cell suspensions were stained with the following antibodies: T1/ST2 FITC, CD127 PE, RORγt PerCP e710, Thy1.2 PE Cy7, T-bet Pacific Blue, Sca-1 v500, CD25 APC e780 and Lineage markers (Lin): CD49b (DX5) APC, CD3 APC, CD5 APC, CD27 APC, CD11b APC, CD11c APC, NK1.1 APC, B220 APC, TCRβ APC. Histograms showing T-bet expression in Lin$^-$ Thy1.2$^+$ CD127$^+$ CD25$^+$ T1/ST2^{lo} ILCs at day 14, 21 and 25 post infection are shown **(A)**. Histograms are concatenated from all individuals in the group. Percentage and number of T-bet$^+$ Lin$^-$ Thy1.2$^+$ CD127$^+$ CD25$^+$ T1/ST2^{lo} ILCs **(B)** Graphs show individual mice with mean ± SD. Individual time points are from independent experiments. Data representative of 2 (d14) or 5 (d21) or 4 (d25) independent experiments. 3-5 mice per group. ns – not significant, * $p<0.05$ by unpaired student's t-test.

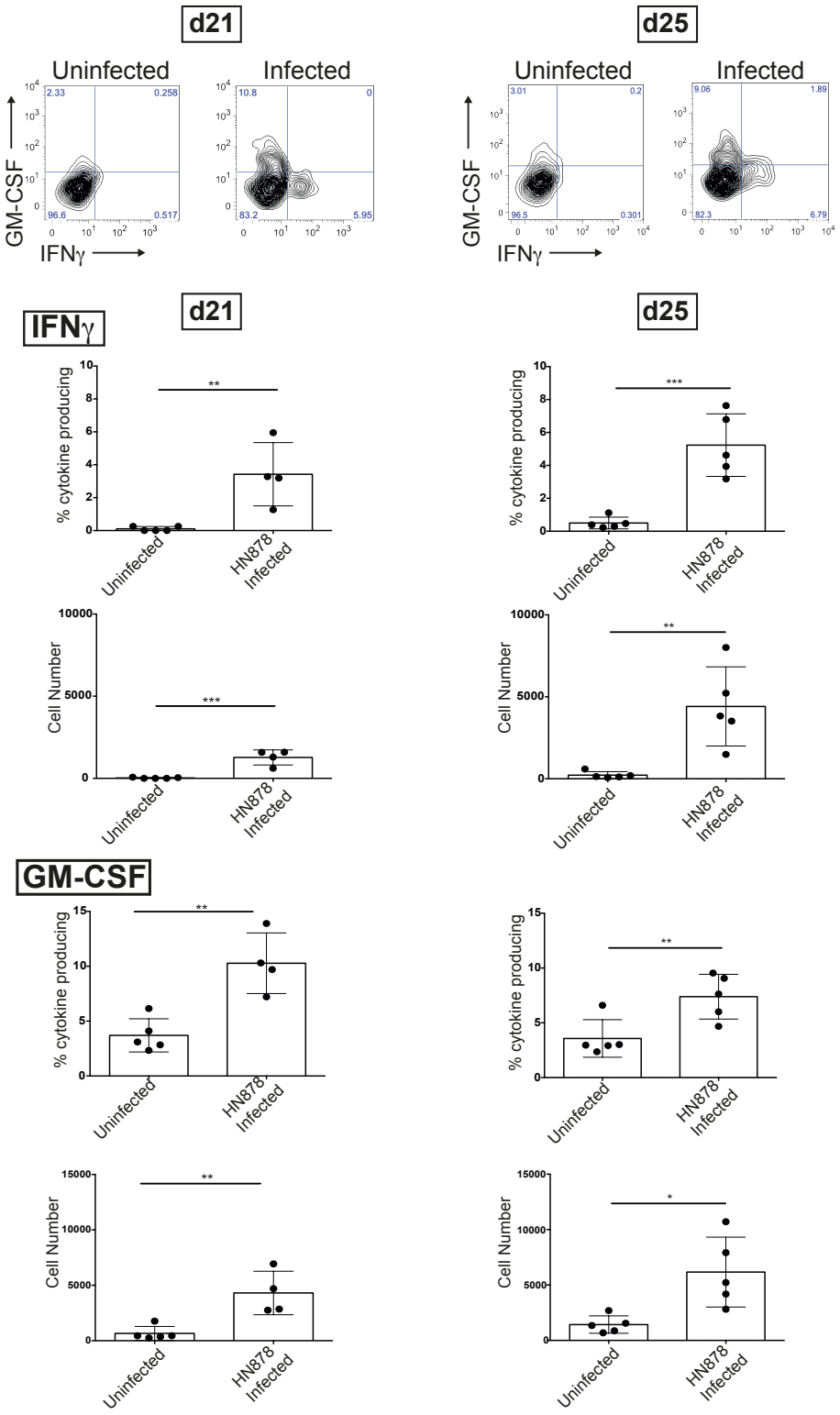

Figure 5.8 Innate Lymphoid cells are a source of IFNγ and GM-CSF upon HN878 infection in Rag KO mice

Rag KO mice were left uninfected or infected with approximately 100 CFU of the hyper-virulent *Mtb* strain HN878 via the aerosol route. At days 21 and 25 post infection mice were sacrificed. Lungs were harvested and digested with collagenase D as described in the materials and methods. Single cell suspensions from the lung were obtained by passage through a 70μm filter. $5x10^5$ cells were restimulated with 50ng/ml PMA and 500ng/ml ionomycin in the presence of Brefeldin A for 2 hours. Cells were then harvested and stained with the following to

identify IFNγ and GM-CSF production by ILCs: GM-CSF FITC, CD127 PE, Lineage markers (Lin): CD49b (DX5) PerCP e710, CD3 PerCP Cy5.5, CD5 PerCP Cy5.5, CD27 PerCP Cy5.5, CD11b PerCP Cy5.5, CD11c PerCP Cy5.5, NK1.1 PerCP Cy5.5, B220 PerCP Cy5.5, TCRβ PerCP Cy5.5, Thy1.2 PE Cy7, IFNγ e450 and CD25 APC e780. ILCs were identified as Lin^- $Thy1.2^+$ $CD127^+$ $CD25^+$. Representative flow cytometry plots from individual mice at day 21 or 25 post infection are shown. Graphs of percentage and number of IFNγ or GM-CSF producing ILCs are shown at day 21 and 25 post infection. Graphs show individual mice with mean ± SD. Individual time points are from independent experiments. Data representative of 3 (GM-CSF d21 and 25, IFNγ d25) or 4 (IFNγ d21) independent experiments. 4-5 mice per group. ns – not significant, * $p<0.05$, ** $p<0.01$, *** $p<0.001$ by unpaired student's t-test.

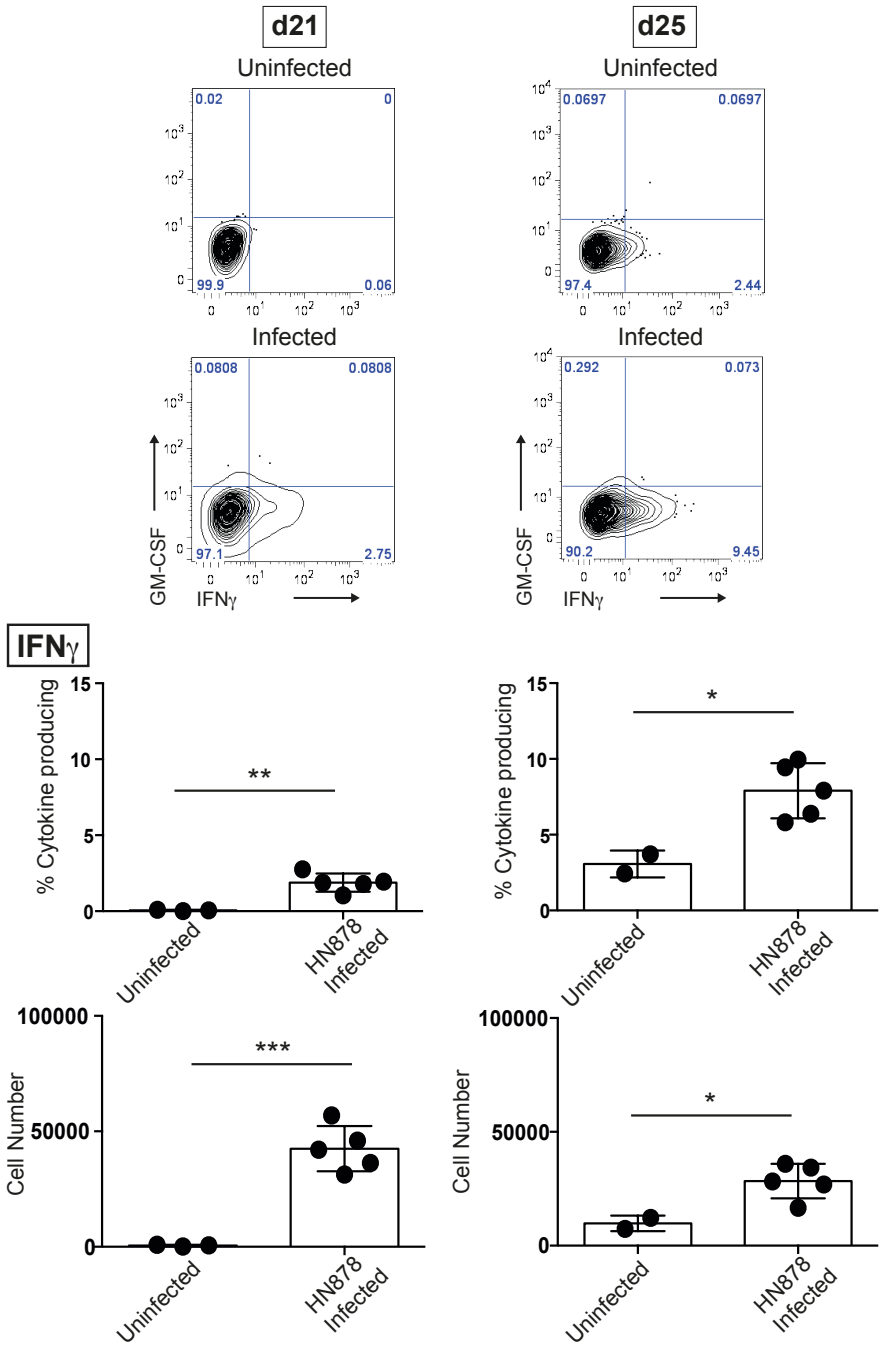

Figure 5.9 Conventional NK cells produce IFNγ not GM-CSF upon HN878 infection

Rag KO mice were left uninfected or infected with approximately 100 CFU of the hyper-virulent *Mtb* strain HN878 via the aerosol route. At days 21 and 25 post infection mice were sacrificed. Lungs were harvested and digested with collagenase D as described in the materials and methods. Single cell suspensions from the lung were obtained by passage through a 70μm filter. $5x10^5$ cells were restimulated with 50ng/ml PMA and 500ng/ml ionomycin in the presence of Brefeldin A for 2 hours. Cells were then harvested and stained with the following to identify IFNγ and GM-CSF production by conventional NK cells: GM-CSF FITC, NK1.1 PE, CD27 PerCP Cy5.5, CD11b PE Cy7, IFNγ e450 and CD49b (DX5) APC. NK cells were identified as $NK1.1^+$ $DX5^+$ ($CD11b^{lo-hi}$). Representative flow cytometry plots from individual mice at day 21 or 25 post infection are shown. Graphs of percentage and number of IFNγ NK cells are shown at day 21 and 25 post infection. Graphs show individual mice with mean ± SD. Data representative of 2 (d21) or 3 (d25) independent experiments. 2-5 mice per group. * $p<0.05$, ** $p<0.01$, *** $p<0.001$ by unpaired student's t-test.

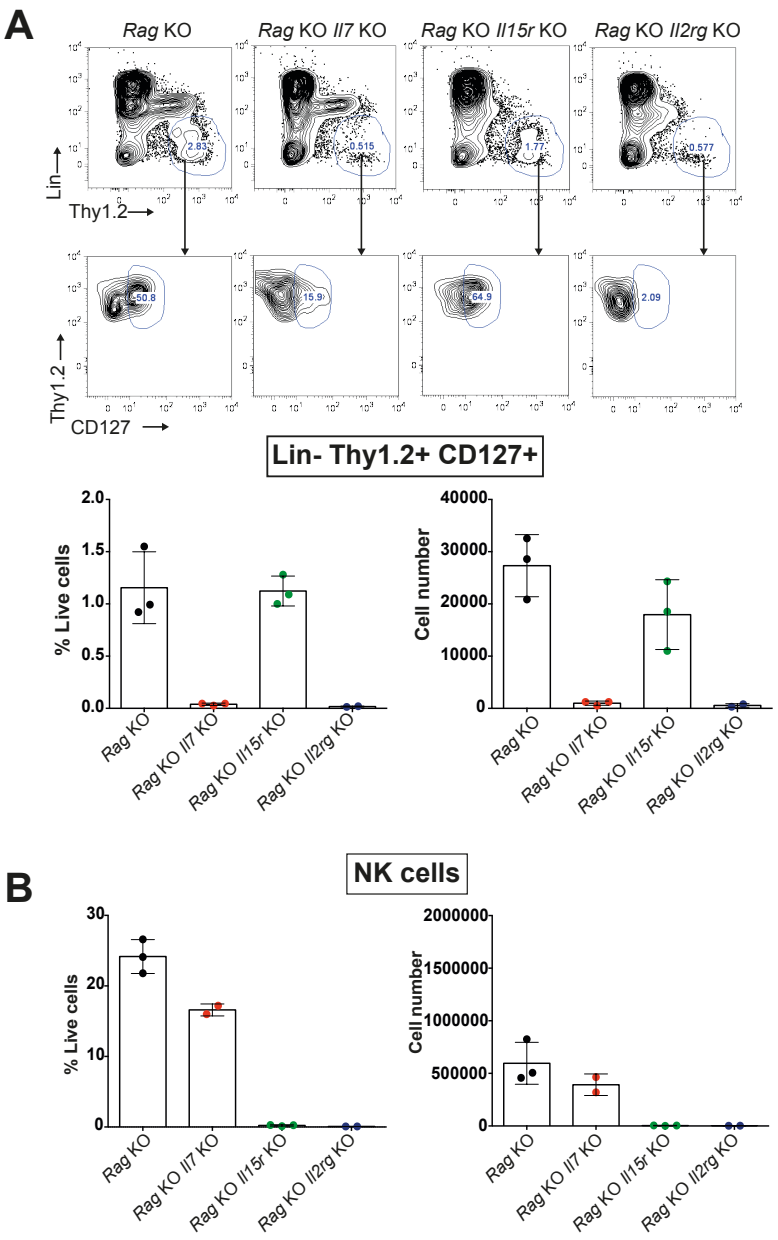

Figure 5.10 Phenotyping deficiencies of ILC populations in Rag KO Il7 KO, Rag KO Il15r KO and Rag KO Il2rg KO mice

Lungs were harvested from naïve *Rag* KO, *Rag* KO *Il7* KO, *Rag* KO *Il15r* KO and *Rag* KO *Il2rg* KO mice. Single cell suspensions were obtained following digestion with collagenase D and passage through a 70μm filter. Flow cytometry plots and graphs of percentage and number of ILCs in the 4 different mouse strains **(A)**. ILCs were defined as Lin^- $Thy1.2^+$ $CD127^+$ following staining with the following antibody cocktail: T1/ST2 FITC, CD127 PE, RORγt PerCP e710, Thy1.2 PE Cy7, T-bet Pacific Blue, Sca-1 v500, CD25 APC e780 and Lineage markers (Lin): CD49b (DX5) APC, CD3 APC, CD5 APC, CD27 APC, CD11b APC, CD11c APC, NK1.1 APC, B220 APC, TCRβ APC. Graphs of percentage and number of NK cells in the 4 different mouse strains **(B)**. NK cells were defined as $NK1.1^+$ following staining with the following antibodies: Ly6G FITC, PE NK1.1, PerCP Cy5.5 Ly6C, F4/80 PE Cy7, CD11c v450, CD11b v500, CD115 APC, MHC II APC e780. Representative flow cytometry plots from individual mice are shown. Graphs show individual mice with mean ± SD. 2-3 mice per group. Comparisons of ILCs and NK cells in all four strains was performed twice. Comparison of only *Rag* KO, *Rag* KO *Il15r* KO, *Rag* KO *Il2rg* KO was performed twice and comparison of *Rag* KO and *Rag* KO *Il7* KO four times.

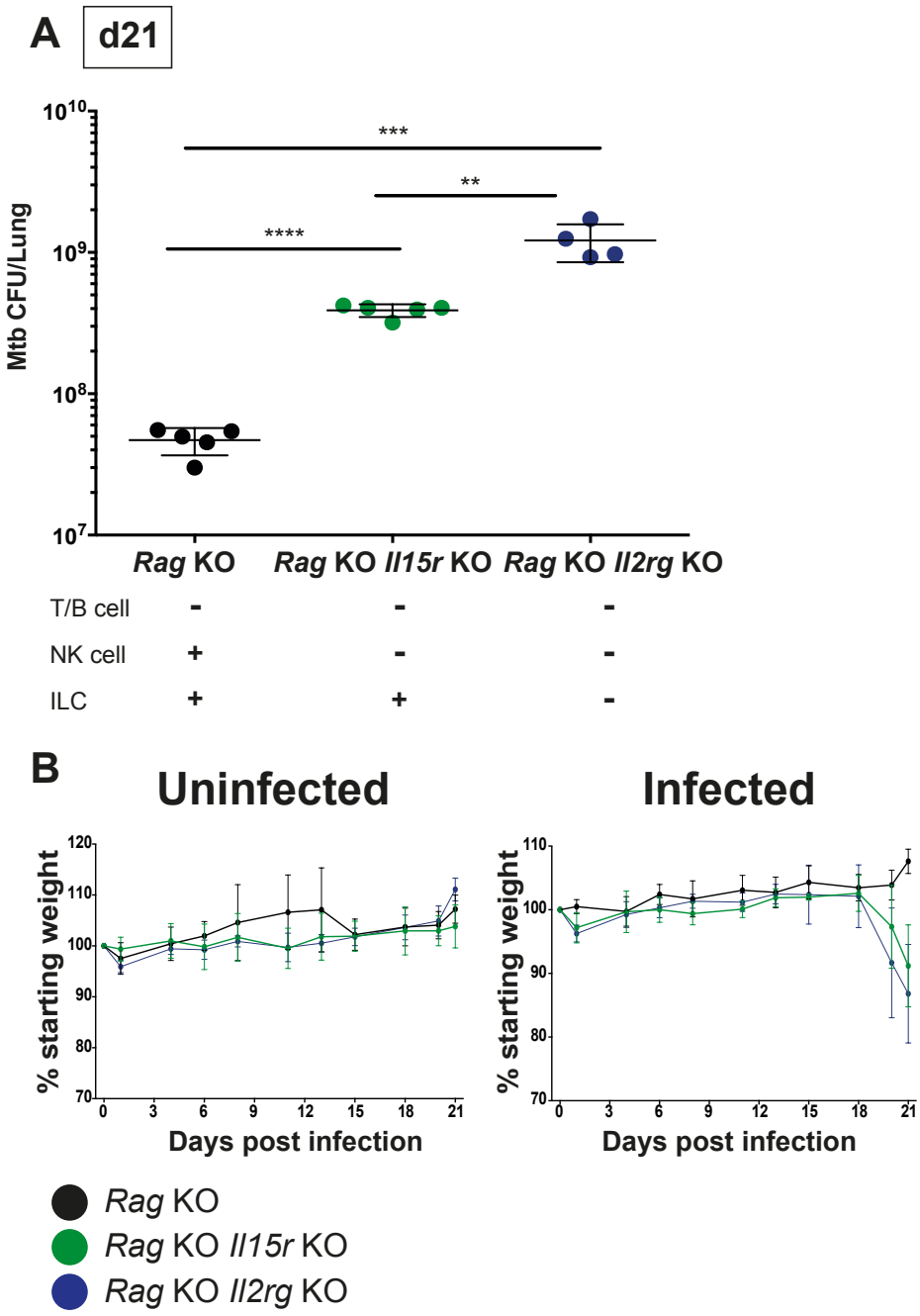

Figure 5.11 IL-15 dependent ILCs have a protective role in the innate immune response to HN878 infection

Rag KO, *Rag* KO *Il15r* KO and *Rag* KO *Il2rg* KO mice were infected with approximately 100 CFU of the hyper-virulent *Mtb* strain HN878 via the aerosol route. At day 21 post infection lungs were harvested and digested in collagenase D. Single cell suspensions were obtained and serially diluted and plated to determine bacterial loads in the lung. Graph show individual mice with mean ± SD **(A)**. Weight loss was monitored over the course of infection. Graph shows mean ± SD **(B)**. 4-5 mice per group. Data representative of 3 independent experiments. ** $p<0.01$, *** $p<0.001$, **** $p<0.0001$ by unpaired student's t-test.

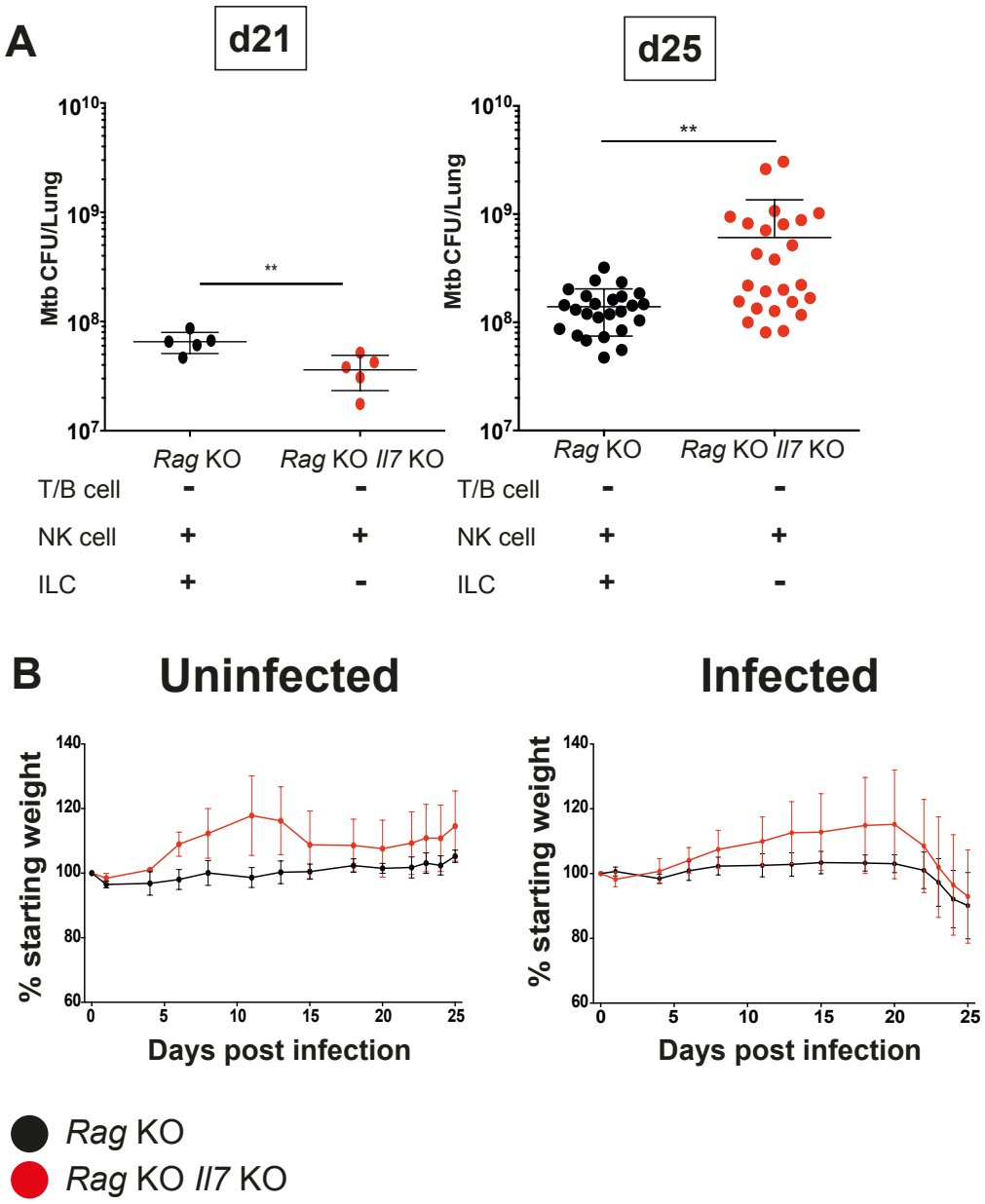

Figure 5.12 IL-7 dependent ILCs are required in the innate immune response to HN878 infection.

Rag KO and *Rag* KO *Il7* KO mice were infected with approximately 100 CFU of the hyper-virulent *Mtb* strain HN878 via the aerosol route. At day 21 or 25 post infection lungs were harvested and digested in collagenase D. Single cell suspensions were obtained and serially diluted and plated to determine bacterial loads in the lung. Graph show individual mice with mean ± SD **(A)**. Bacterial loads at day 21 representative of 1 independent experiment. Bacterial loads at day 25 show data pooled from 5 independent experiments. Weight loss was monitored over the course of infection. Graph shows mean ± SD **(B)**. Weight loss representative of 4 independent experiments. 5-25 mice per group. ** $p<0.01$ by unpaired student's t-test.

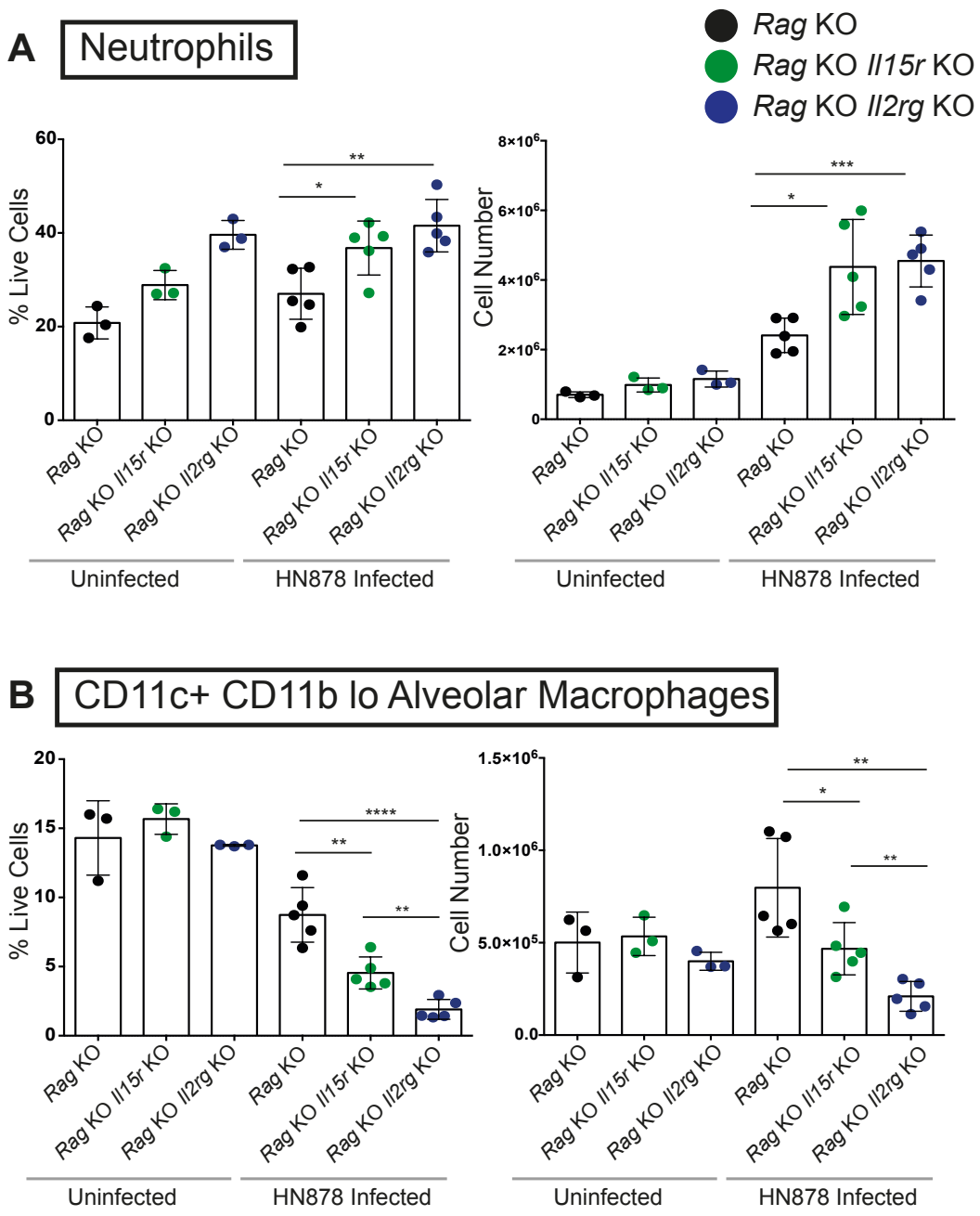

Figure 5.13 The absence of IL-15 and/or IL-7 dependent ILCs during HN878 infection leads to neutrophil accumulation and a decrease in alveolar macrophages

Rag KO, *Rag* KO *Il15r* KO and *Rag* KO *Il2rg* KO mice were infected with approximately 100 CFU of the hyper-virulent *Mtb* strain HN878 via the aerosol route. At day 21 post infection lungs were harvested and digested in collagenase D. Single cell suspensions were obtained and stained with the following to identify myeloid populations: Ly6G FITC, PE NK1.1, PerCP Cy5.5 Ly6C, F4/80 PE Cy7, CD11c v450, CD11b v500, CD115 APC, MHC II APC e780. Percentage and number of neutrophils (defined as $Ly6G^{+}$ $CD11b^{+}$) at day 21 post infection **(A)**. Percentage and number of $CD11c^{+}$ $CD11b^{lo}$ alveolar macrophages (defined as $Ly6G^{-}$ $CD11c^{+}$ $CD11b^{lo}$) at day 21 post infection **(B)**. Graphs show individual mice with mean ± SD. 3-5 mice per group. Data representative of 3 independent experiments. * $p<0.05$, ** $p<0.01$, *** $p<0.001$ **** $p<0.0001$ by unpaired student's t-test.

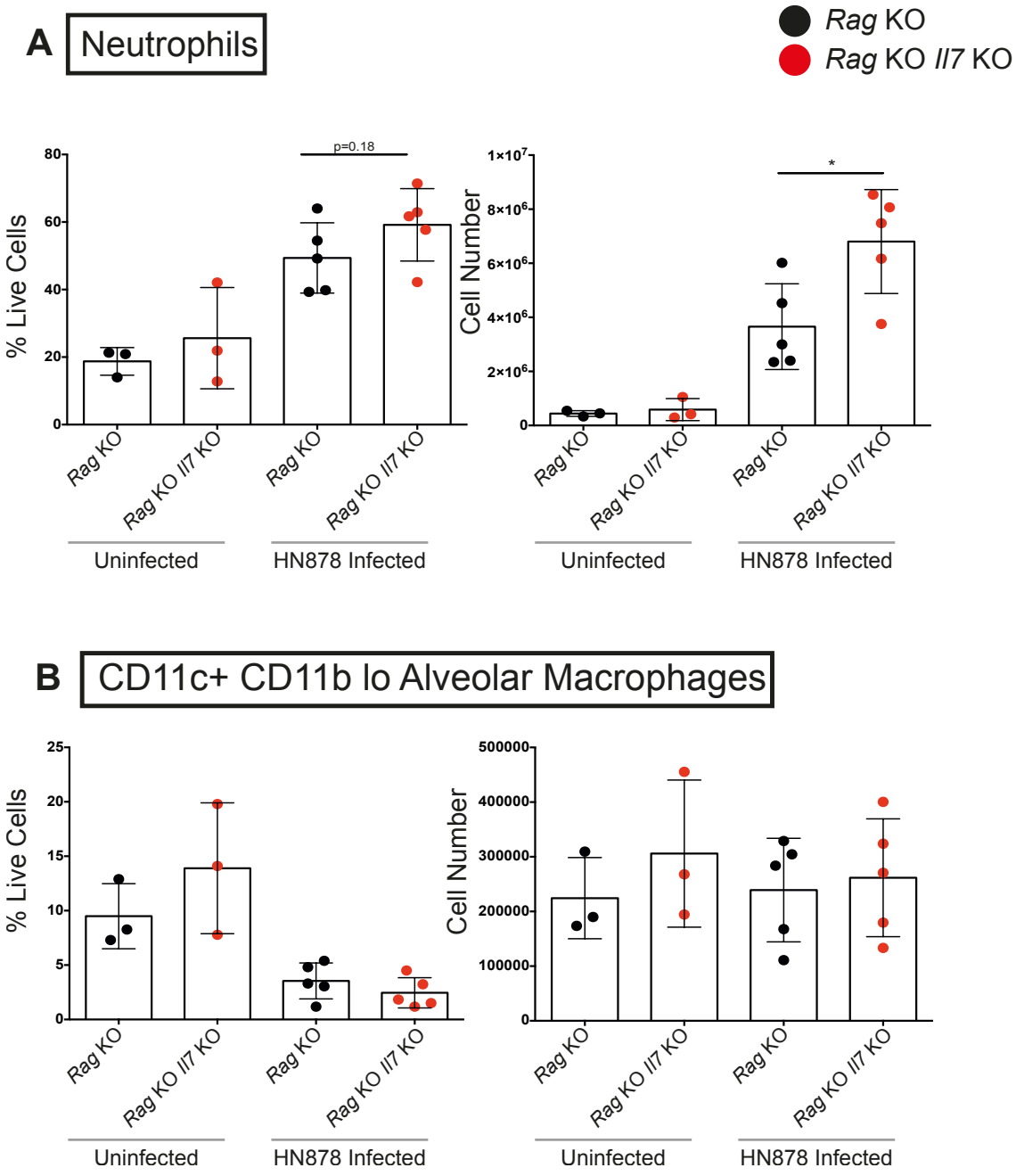

Figure 5.14 Neutrophils accumulate in response to HN878 infection in the absence of IL-7 dependent ILCs

Rag KO and *Rag* KO *Il7* KO mice were infected with approximately 100 CFU the hyper-virulent *Mtb* strain HN878 via the aerosol route. At day 25 post infection lungs were harvested and digested in collagenase D. Single cell suspensions were obtained and stained with the following to identify myeloid populations: Ly6G FITC, PE NK1.1, PerCP Cy5.5 Ly6C, F4/80 PE Cy7, CD11c v450, CD11b v500, CD115 APC, MHC II APC e780. Percentage and number of neutrophils (defined as $Ly6G^{+}$ $CD11b^{+}$) at day 25 post infection **(A)**. Percentage and number of $CD11c^{+}$ $CD11b^{lo}$ alveolar macrophages (defined as $Ly6G^{-}$ $CD11c^{+}$ $CD11b^{lo}$) at day 25 post infection **(B)**. Graphs show individual mice with mean ± SD. 3-5 mice per group. Data representative of 4 independent experiments. p=0.18, * $p<0.05$ by unpaired student's t-test.

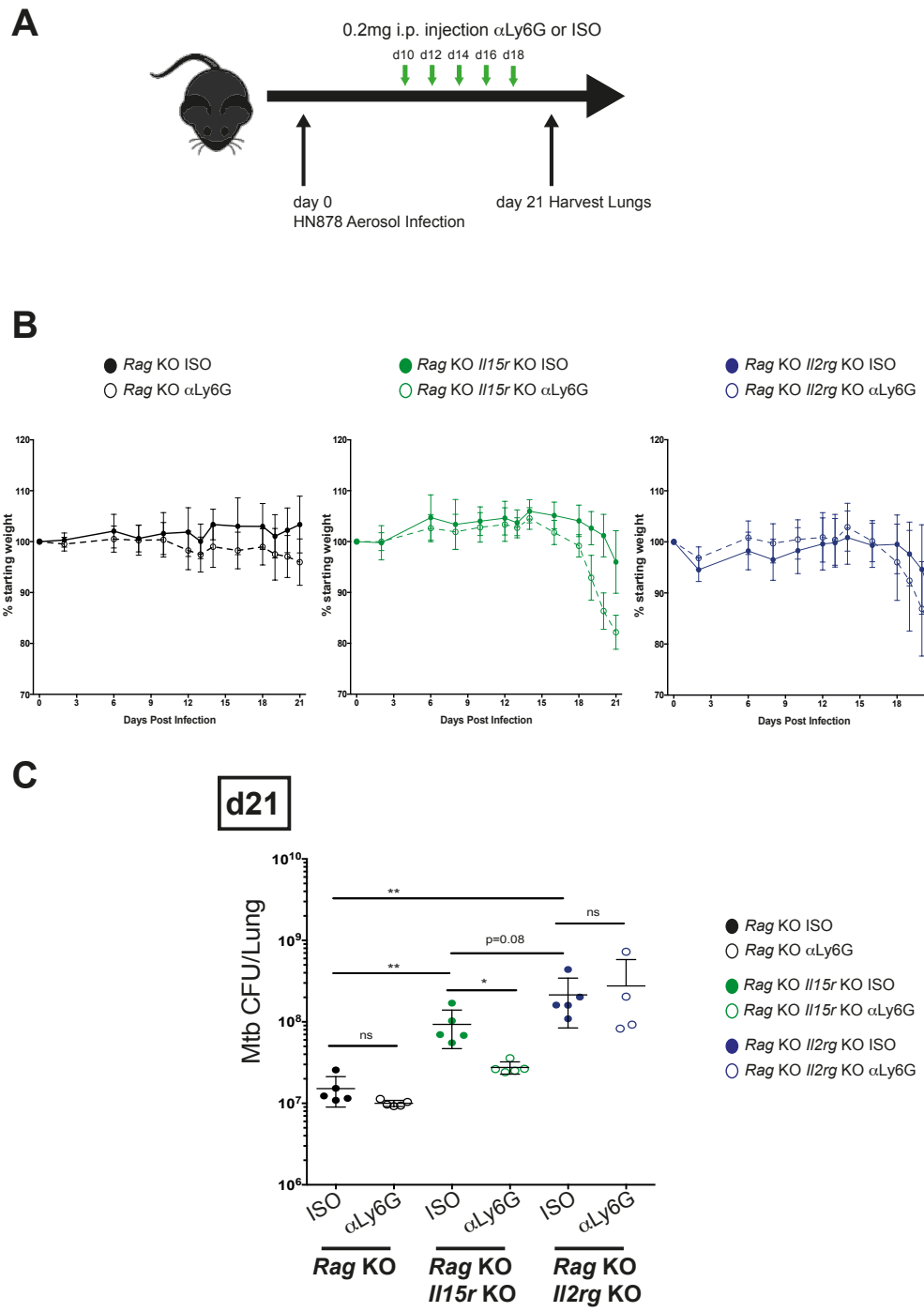

Figure 5.15 Depletion of neutrophils during HN878 infection increased weight loss of the course of infection and lowers Mtb bacterial load in Rag KO Il15r KO mice

Rag KO, *Rag* KO *Il15r* KO and *Rag* KO *Il2rg* KO mice were infected with approximately 100 CFU the hyper-virulent *Mtb* strain HN878 via the aerosol route. Mice received i.p. injections on days 10, 12, 14, 16 and 18 containing 0.2mg αLy6G (clone 1A8) or isotype (GL117). At day 21 post infection mice were sacrificed and lungs were harvested **(A)**. Weight loss was monitored over the course of infection. Graph shows mean ± SD. 7-8 mice per group **(B)**. Single cell suspensions from the lungs were obtained following digestion with collagenase D, as described in materials and methods. These were serially diluted and plated to determine bacterial loads in the lung at day 21 post infection. Graph shows individual mice with mean ± SD. 4-5 mice per group **(C)**. Data representative of 1 experiment. ns- not significant, p=0.08. *p<0.05, **p<0.01 by unpaired student's t-test.

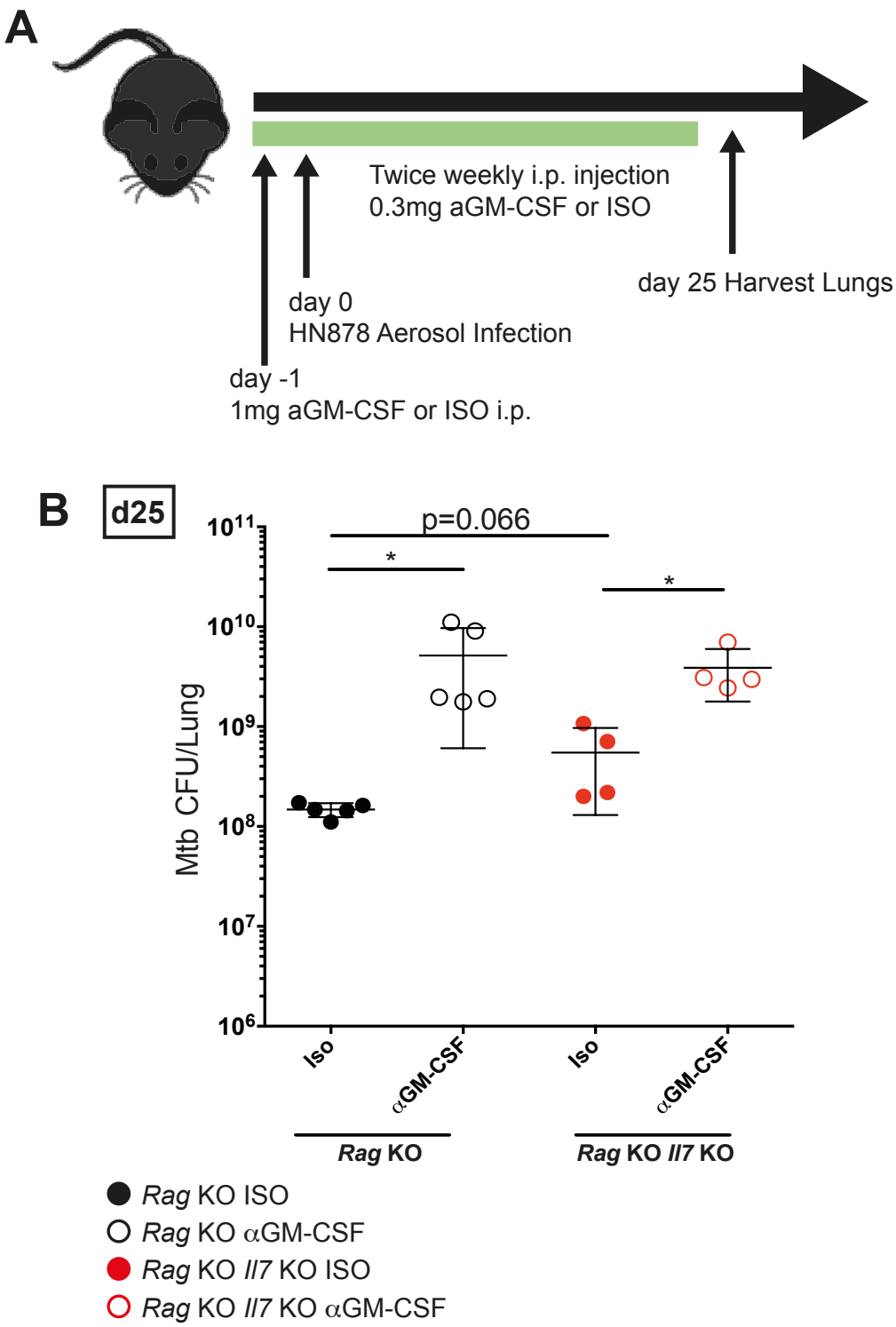

Figure 5.16 GM-CSF is crucial to the innate immune response to HN878 infection

Outline of experiment **(A)**. *Rag* KO and *Rag* KO *Il7* KO mice were i.p. injected with 1mg anti-GM-CSF (αGM-CSF, clone MP1-22E9) or Isotype (ISO, clone GL117) control the day prior to infection with approx. 100-200 CFU the hyper-virulent *Mtb* strain HN878, via aerosol route. Mice then received twice weekly i.p. injections of aGM-CSF or ISO. Mice were sacrificed at day 25 post infection. Single cell suspensions from the lungs were obtained following digestion with collagenase D, as described in materials and methods. These were serially diluted and plated to determine bacterial loads in the lung at day 25 post infection **(B)**. Graph shows individual mice with mean ± SD. 4-5 mice per group. Data representative of 1 experiment. p=0.066. *p<0.05 unpaired student's t-test.

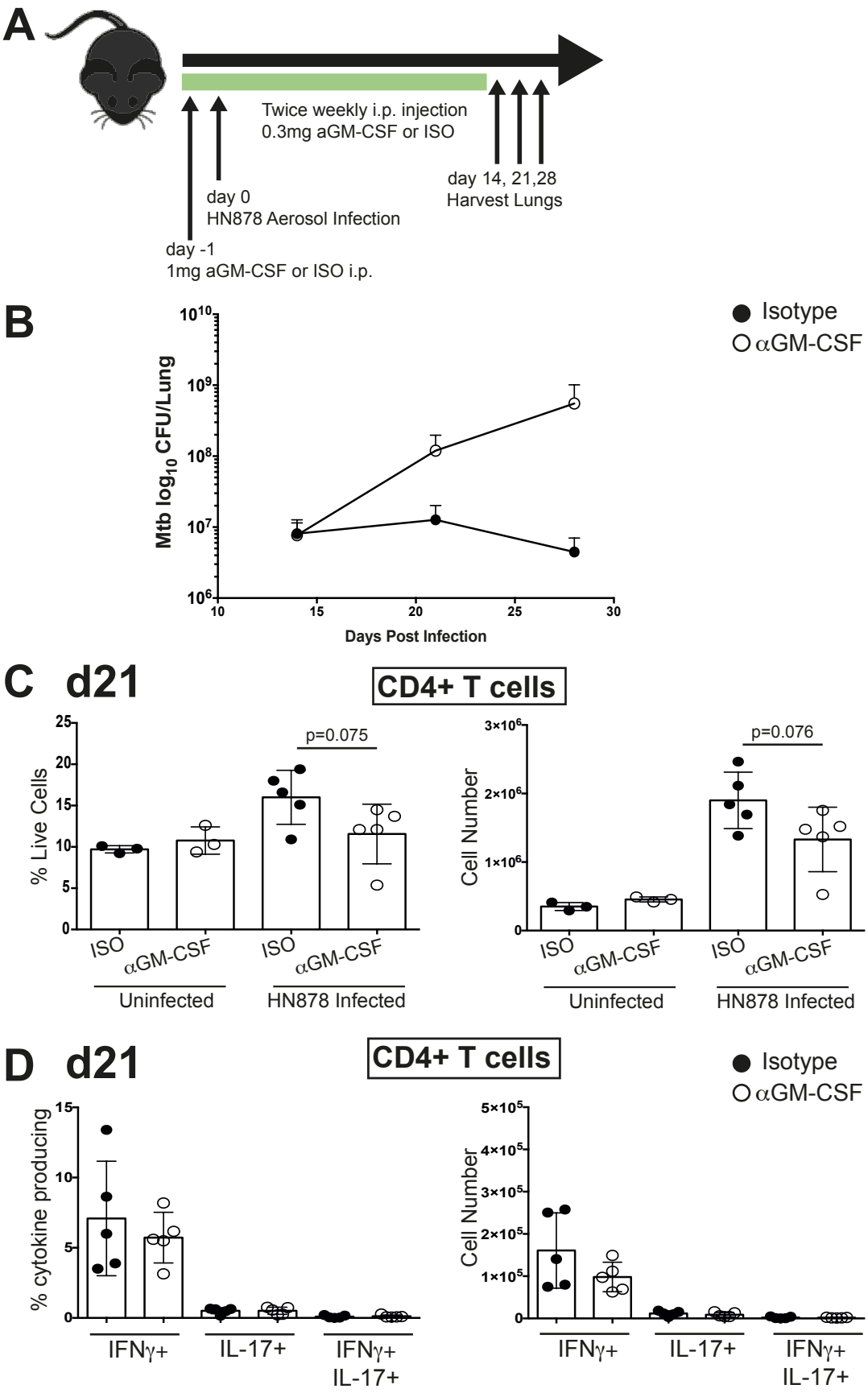

Figure 5.17 GM-CSF is crucial to the immune response to HN878 infection in wild type mice

Outline of experiment **(A)**. C57BL/6 mice were i.p. injected with 1mg anti-GM-CSF (αGM-CSF, clone MP1-22E9) or Isotype (ISO, GL117) control the day prior to infection with approx. 100-200 CFU the hyper-virulent *Mtb* strain HN878, via aerosol route. Mice then received twice weekly i.p. injections of αGM-CSF or ISO. Mice were sacrificed at day 14, 21 or 25 post infection. Single cell suspensions from the lungs were obtained following digestion with collagenase D, as described in materials and methods. These were serially diluted and plated to determine bacterial loads in the lung at days 14, 21 and 28 post infection. Graph shows mean ± SD. 5 mice per group **(B)**. Single cell suspensions were stained with the following antibodies to identify $CD4^+$ T cells: γδ TCR FITC, Thy1.2 PECy7, CD4 e450, CD8 v500 and CD3 APC. Percentage and number of $CD4^+$ T cells (defined as $Thy1.2^+$ $CD3^+$ $CD4^+$) at day 21 post infection **(C)**. Graphs show individual mice with mean ± SD. 3-5 mice per group**.** $1x10^6$ cells were restimulated with 20μg PPD and 2μg αCD28 mAb for 16h before the addition of BFA for a further 4h. Cells were then harvested and stained with the following to assess cytokine production: γδ TCR FITC, GM-CSF PE, CD8 PerCP e710, Thy1.2 PE Cy7, IFNγ e450, CD4 v500, IL-17A APC, CD3 APCe780. Percentage and number of cytokine producing $CD4^+$ T cells (defined as $CD3^+$ $Thy1.2^+$ $CD4^+$) at day 21 post infection **(D)**. Graphs show individual mice with mean ± SD. 5 mice per group. Data representative of 1 experiment. p=0.075, p=0.076 by unpaired student's t-test.

Chapter 6 General Discussion and Future Perspectives

TB is the second leading cause of death from infectious disease, with an estimated 1.5 million deaths in 2013 (WHO, 2014b). Currently the only licensed vaccine, BCG, affords variable protection against TB disease (Fine, 1995). Novel vaccine regimes are under development but an incomplete understanding of a protective response to *Mtb* hinders the rational design of vaccines. There is a significant delay in the onset of an immune response capable of controlling *Mtb* bacterial growth (reviewed in Cooper, 2009). It is argued that the delay in the control of bacterial growth allows *Mtb* to manipulate its environment, such that when a potentially protective response is expressed, it can be ineffective (reviewed in Cooper, 2009; Orme et al., 2015). Therefore, a possible avenue to improve vaccination is to manipulate the speed at which the T cell response is expressed (reviewed in Cooper, 2009). Furthermore a more detailed understanding of how innate lymphocytes such as NK cells, NKT cells, MAIT cells and ILCs respond to *Mtb* infection and influence the early response to infection will further our understanding of a protective response to *Mtb*. If possible, augmenting the response of such rapidly responding innate lymphocyte populations may provide another way in which vaccination can be improved (Zufferey et al., 2013).

6.1 IL-10R blockade improves the protective effect of BCG vaccination, influencing early immune events following *Mtb* challenge

6.1.1 Influence of IL-10R blockade during BCG vaccination on the adaptive response following Mtb challenge in Mtb susceptible mice

IL-10 is detrimental to control of *Mtb* infection, and increased IL-10 levels during *Mtb* infection have been linked with increased susceptibility (Beamer et al., 2008; Redford et al., 2010; Turner et al., 2002). Previous work from the O'Garra lab has shown that IL-10 also suppresses the response to BCG vaccination and the protection it affords against *Mtb* challenge in both *Mtb*

resistant and *Mtb* susceptible mouse models (Pitt et al., 2012b). In resistant mice, increased control of *Mtb* bacterial load when BCG vaccination was administered in the context of αIL-10R mAb correlated with an accelerated arrival of and enhanced IFNγ producing $CD4^+$ T cells (Pitt et al., 2012b). However, the early immune response in *Mtb* susceptible mice was not assessed. Acceleration in the onset of an adaptive immune response is one way in which vaccination can be improved, given the expression of an adaptive immune response is considerably delayed in response to *Mtb* infection (reviewed in Cooper, 2009). Chapter 3 of this thesis investigated whether BCG vaccination in the context of αIL-10R mAb, accelerated the arrival of the adaptive response in susceptible CBA/J mice. In contrast to resistant C57BL/6 mice, the increased protection in chronic infection afforded by this vaccine regime was not accompanied by significantly accelerated recruitment of IFNγ producing $CD4^+$ T cells in susceptible CBA/J mice, although increased levels of IFNγ were observed at later time points (Pitt et al., 2012b). The differences identified between resistant and susceptible mouse strains highlight the importance of selecting appropriate models to investigate vaccine candidates.

Although BCG vaccination in the context of αIL-10R did not lead to accelerated recruitment of IFNγ producing $CD4^+$ T cells, increased protection in chronic infection did correlate with accelerated and increased production of IL-17 by γδ T cells and $CD8^+$ T cells and GM-CSF by $CD4^+$ T cells. This result supports the idea that modulation of the early events following *Mtb* infection can positively impact the subsequent course of infection and that IFNγ may not be the sole determinant of protection, as has been previously reported (Abebe, 2012; Kagina et al., 2010; Mittrucker et al., 2007).

In addition to the speed of the onset of a T cell response, its appropriate localisation within the lung could be an important factor in increasing protection against *Mtb* infection. Indeed, T cells localised in the lung parenchyma were able to confer superior levels of protection against *Mtb* upon transfer than those localised in the vasculature (Sakai et al., 2014). IL-17 is described to be

important to induce chemokines to recruit (CXCL9, CXCL10, CXCL11) and localise (CXCL13) T cells in the recall response following vaccination (Gopal et al., 2013; Khader et al., 2007). The functional significance of the increased levels of IL-17 and GM-CSF upon *Mtb* challenge identified in the lungs of mice vaccinated with BCG in the context of αIL-10R is unclear. However, as IL-17 has been described to be involved in the localisation of T cells within the lung, further investigation into chemokine induction and histological analysis will allow assessment of localisation of T cells in granulomas, providing insight into how increased protection is achieved.

In contrast to the role of IL-17 in the recall response following vaccination, the role of GM-CSF has not been investigated and is not regularly measured in animal studies assessing vaccine efficacy. However, increased GM-CSF production was observed in the lung following *Mtb* challenge in mice vaccinated with the recombinant BCG VPM1002 compared to parental BCG (Desel et al., 2011) and increased GM-CSF expression in PBMCs of previously BCG vaccinated individuals upon BCG challenge has been observed (Matsumiya et al., 2015). Taken together with our results correlating increased production of GM-CSF with protection, could suggest that vaccine regimes that increase GM-CSF production could be beneficial.

6.1.2 Potential to improve vaccination against Mtb infection by modulating the innate immune response

In addition to accelerating the onset of adaptive immunity, BCG vaccination could also increase protection against *Mtb* challenge through modulation of the innate immune response. Indeed, "trained immunity" has been described, where innate cells display increased response to secondary and/or heterologous infection, and this is suggested to contribute to the epidemiological observation that BCG vaccination provides protection against heterologous infection (Freyne et al., 2015; Quintin et al., 2014). BCG induced trained immunity has been

demonstrated in humans where BCG vaccination led to NOD2 dependent epigenetic reprogramming of monocytes resulting in increased production of pro-inflammatory cytokines by PBMCs when stimulated ex vivo with *Mtb*, or the heterologous infections *Candida albicans* or *Staphylococcus aureus* (Kleinnijenhuis et al., 2012). Furthermore, BCG vaccination of SCID mice afforded protection against lethal *Candia albicans* infection, demonstrating a T and B cell independent mechanism (Kleinnijenhuis et al., 2012). The protection afforded by BCG against *Candida albincans* infection was subsequently shown to be at least partially dependent upon NK cells (Kleinnijenhuis et al., 2014).

An avenue through which vaccination against *Mtb* could potentially be improved is in harnessing and augmenting the response of innate lymphocytes such as NK cells. In humans NK cells have also been demonstrated to produce IFNγ following BCG vaccination (Zufferey et al., 2013). Furthermore, MHC class II expressing NK cells have been demonstrated to expand following BCG stimulation and have increased cytotoxic capacity in comparison to MHC class II negative cells (Evans et al., 2011). Such cells were found to expand in response to IL-2 (Evans et al., 2011). Therefore one way in which NK cell responses could be augmented is to increase IL-2 production upon *Mtb* challenge. Indeed a positive correlation between IL-2 production by T cells and NK cell activation was found in Tanzanian children vaccinated with the malaria vaccine candidate RTS,S/AS01 (Horowitz et al., 2012). Furthermore therapeutic vaccination of chronically infected HIV patients led to IL-2 production by $CD4^+$ T cells, which was suggested to lead to an increased IFNγ production by NK cells (Jost et al., 2014). Both these studies suggest that innate lymphocyte responses can be augmented through increasing IL-2 production by T cells.

As well as augmenting the NK cell response through increased cytokine production by T cells, it has been suggested that NK cells can themselves develop immune memory, where antigen specific NK cells persist and can mount enhanced responses upon challenge (Paust and von

Andrian, 2011). For example, hapten induced contact hypersensitivity can be elicited in T and B cell deficient mice (O'Leary et al., 2006). Hapten specific NK cells were found to persist for at least 4 weeks, reside in the liver and have the capacity to transfer sensitivity to naïve mice (O'Leary et al., 2006). Subsequently it was shown that NK memory could also be induced following viral infection (Paust et al., 2010; Sun et al., 2009). In addition to these findings in mice, recently it has been reported that antigen specific NK cell memory is also induced in NHP following Simian Immunodeficiency Virus infection or following vaccination (Reeves et al., 2015). These results suggest that as NK cells can display features of immune memory there is potential for vaccine strategies to harness this to improve protection.

In Chapter 3 of this thesis we identified increased IFNγ levels at day 21 post *Mtb* challenge in PPD restimulated lung cultures from mice vaccinated with BCG in the context of αIL-10R mAb. It is possible that NK cells and/or other ILCs provide this early IFNγ and therefore assessment of the cytokine response of innate lymphocytes to *Mtb* infection following BCG vaccination in the context of αIL-10R treatment is required.

6.1.3 Could IL-10 suppress the immune response to other vaccines?

Although it is unlikely that IL-10R blockade using mAb will be clinically viable, given the expense and practicalities of receiving multiple injections, our results do highlight the potential of IL-10 to suppress protective responses to BCG vaccination. This raises the question whether IL-10 is also suppressive in other candidate vaccine regimes. IL-10 can be induced by type I IFNs in various settings, including *Mtb* infection (Mayer-Barber et al., 2011; McNab et al., 2014; Teles et al., 2013). Several of the vaccine candidates currently in clinical trials will induce type I IFNs for example, MVA (the vector used for MVA85A) is described to induce type I IFNs (Waibler et al., 2007) and the adjuvant IC31 (which is used for the vaccine candidates H1, H4 and H56) contains TLR9 agonists which will induce type I IFN (Akira and Takeda, 2004).

Thus this induction of type I IFNs could be accompanied by IL-10 expression and decreased induction of key cytokines such as IL-12 and IL-1, leading to suboptimal induction of a protective response. Investigation of whether novel vaccine candidates induce IL-10 and whether this suppresses the induction of an optimal response to novel vaccine candidates could aid our understanding of how to improve them.

Understanding other mechanisms of immunosuppression, in addition to IL-10, will also increase our ability to improve vaccination. Indeed increased Treg frequency following vaccination with MVA85A in volunteers correlated with a low response to the vaccine as defined by IFNγ release in response to antigen 85A peptides (Matsumiya et al., 2013). Furthermore, increased basal levels of Indoleamine 2,3-dioxygenase activity (which suppresses T cell function), prior to vaccination, in South African adults compared to UK adults correlated with a lower response to MVA85A vaccination, as defined by IFNγ release in response to antigen 85A peptides (Tanner et al., 2014). By understanding factors that negatively impact the immunogenicity of a vaccine, there is potential to improve vaccination and identify individuals in which vaccination may be less effective.

6.1.4 Could IL-10R blockade during BCG vaccination also increase protection upon challenge with clinical isolates of Mtb?

Assessment of the ability of a vaccine to protect against clinically relevant isolates could further our understanding of protective responses and enable better prediction of those vaccine regimes with the potential to be protective in a clinical setting (McShane and Williams, 2014). Although αIL-10R blockade during BCG enhances the protection against challenge with the lab strain of *Mtb* H37Rv, assessment of its ability to protect against clinical isolates of *Mtb* would also be important. It is known that different strains of *Mtb* induce different responses in several animal models (Manca et al., 2001; Ordway et al., 2007; Reed et al., 2004; Subbian et al., 2013) and

also in human monocytes (Newton et al., 2006; Portevin et al., 2011). Furthermore, BCG vaccinated mice challenged with clinical isolates of *Mtb* display lower bacterial load in the lung compared to controls for a shorter time than those challenged with the lab-adapted strain H37Rv (Grode et al., 2005; Ordway et al., 2011). Assessment of whether increased IL-17 and GM-CSF correlates with increased control of bacterial load in mice vaccinated with BCG in the context of αIL-10R blockade challenged with a clinical isolate of *Mtb,* will provide further support that vaccine regimes that aim to achieve this could be beneficial.

6.2 GM-CSF is required for the protective response following primary *Mtb* infection

GM-CSF is known to be required for the immune response to *Mtb* infection following studies of GM-CSF deficient mice (Gonzalez-Juarrero et al., 2005). However, GM-CSF deficient mice develop a lung disease that resembles pulmonary alveolar proteinosis (Dranoff et al., 1994; Stanley et al., 1994; Trapnell and Whitsett, 2002), which leads to basal defects that can confound interpretation of these results. Using antibody neutralisation of GM-CSF, we were able to assess the role of GM-CSF during *Mtb* infection in both resistant and susceptible mice, without basal defects that could impact the immune response to *Mtb* infection. Results in this thesis show that in both resistant and susceptible mice, GM-CSF is protective in the immune response to infection with the lab *Mtb* strain H37Rv. Furthermore, GM-CSF neutralisation dramatically increases susceptibility of *Mtb* resistant mice and *Rag* deficient mice to infection with the hyper-virulent *Mtb* strain HN878. Our results showing that GM-CSF neutralisation during *Mtb* infection can increase susceptibility to *Mtb* could be clinically relevant. Several clinical trials are underway to assess the use of antibodies targeting the GM-CSFRα or GM-CSF in treatment of rheumatoid arthritis and/or multiple sclerosis (Hamilton, 2015). Patients receiving treatment targeting GM-CSF may be at increased risk of tuberculosis infection or reactivation as has been described in patients treated with anti-TNF mAbs (Keane et al., 2001)

and thus patients should be closely monitored. Assessment of the impact of GM-CSF neutralisation in latently infected NHP would provide valuable information regarding how treatments targeting GM-CSF could impact the outcome of *Mtb* infection in human patients.

6.3 Innate lymphoid cells in the immune response to *Mtb*

Previous work from the O'Garra lab demonstrated that an "innate-like lymphocyte" population, lacking CD3, CD4, CD8 and γδ TCR but expressing Thy1.2, was a source of IFNγ and IL-17 upon *Mtb* challenge in mice vaccinated with BCG in the context of αIL-10R blockade but these were not characterised further (Pitt et al., 2012b). NK cells and the recently described ILCs could be contained within this population. Although NK cells respond to *Mtb* infection (Feng et al., 2006; Junqueira-Kipnis et al., 2003), the role of other ILCs has not been addressed. The rapidity with which these cells respond during infection could mean they influence the early immune response to *Mtb* infection, but this is still an outstanding question (Orme et al., 2015). Chapter 5 of this thesis investigated the response and role of NK cells and ILCs in the innate immune response to *Mtb* infection. Using *Rag* KO mice our results demonstrated that ILCs respond to infection with both the lab-adapted strain H37Rv and hyper virulent HN878, with a subset of ILCs expressing T-bet upon infection. ILCs were a source of cytokines during *Mtb* infection, producing IFNγ upon H37Rv infection, and IFNγ and GM-CSF upon HN878 infection. Furthermore work in this thesis demonstrated that IL-15 and IL-7 dependent ILCs are important in the control of HN878 bacterial loads, although our data shows that IL-15 dependent ILCs are more important in the protective response against HN878 infection. Furthermore, subsequent experiments employing histology to assess lung pathology have demonstrated increased lung pathology in the absence of IL-15 dependent ILCs alone and further increased pathology in the absence of IL-15 and IL-7 dependent ILCs. It is possible that ILCs, along with NK cells and other innate lymphocytes will contribute to immunity in individuals suggested to be capable of clearing *Mtb* infection without mounting an adaptive

response (Barry et al., 2009; Young et al., 2009). More investigation is required to determine the mechanisms for this innate clearance, which is hindered by the difficulties in identifying such individuals.

In addition to an increase in bacterial loads, we observed an accumulation of neutrophils in the lung during *Mtb* infection in the absence of IL-15 dependent ILCs and/or IL-7 dependent ILCs. Given that IFNγ has been described to regulate neutrophil accumulation and survival during *Mtb* infection (Desvignes et al., 2012; Feng et al., 2006; Nandi and Behar, 2011), we hypothesise that the accumulation of neutrophils we observe is a result of decreased levels of IFNγ in the lung. We aim to assess the protein levels of IFNγ, as well as other cytokines (such as GM-CSF, IL-17, G-CSF), in the lungs of *Mtb* infected mice lacking IL-15 dependent and/or IL-7 dependent ILCs, to identify potential candidates that could contribute to the observed neutrophilia. Indeed mRNA has been collected from the lungs of the three different mouse strains as well as supernatants from restimulation of lung cell suspensions, analysis of which will provide such information.

The role of neutrophils during *Mtb* infection is debated, with some reports suggesting they provide a niche for bacterial growth and others suggesting they are capable of restricting bacterial growth (Eruslanov et al., 2005; Lowe et al., 2012; Yang et al., 2012). In Chapter 5 of this thesis we show that the accumulation of neutrophils in the absence of IL-15 dependent ILCs was detrimental to control of bacterial load but not in the absence of both IL-15 and IL-7 dependent ILCs (*Rag* KO *Il2rg* KO). This result reinforces the complex role for neutrophils during *Mtb* infection and suggests that it is context dependent. Further work will attempt to address why neutrophils appear to have different roles in *Rag* KO *Il15r* KO and *Rag* KO *Il2rg* KO. Insight will be provided by assessing differences in neutrophil function between *Rag* KO *Il15r* KO and *Rag* KO *Il2rg* KO mice through assessment of their bacterial loads and expression of cytokines. Furthermore, assessment of how (or if) macrophage activation differs between the

two mouse strains, and how neutrophils impacts this, could provide an explanation for the apparent differences in the contribution of neutrophils to control of bacterial load.

6.4 Future Perspectives

6.4.1 The affect of IL-10 receptor blockade during BCG vaccination upon the response of ILCs to Mtb challenge

A future experiment to assess how the early response of ILCs upon *Mtb* challenge is impacted by IL-10R blockade during BCG vaccination will further understanding of both ILC responses upon *Mtb* infection and potential avenues by which IL-10R blockade enhances the protective affect of BCG vaccination. This could be achieved through analysing the cytokine responses of ILCs (as described in Chapter 5) at day 14, 21 and 28 post *Mtb* challenge. Furthermore, given the studies discussed above that suggest IL-2 production by $CD4^+$ T cells can increase NK cell responses, assessment of how IL-10R blockade during BCG vaccination impacts IL-2 production by $CD4^+$ T cells could provide insight into the mechanism by which ILC responses could be modulated by this vaccine regime.

6.4.2 What are the sources of GM-CSF during Mtb infection?

Many cell types have the capacity to produce GM-CSF including ILCs, NK cells, NKT cells, T cells, myeloid cells such as macrophages as well as fibroblasts and endothelial cells (Daussy et al., 2014; Gasson, 1991; Moro et al., 2010; Mortha et al., 2014; Robinette et al., 2015; Sojka et al., 2014). Although we identify ILCs as a source of GM-CSF, results neutralising GM-CSF in *Rag* KO mice suggest there are other sources. Experiments to assess the other cellular sources of GM-CSF, in addition to ILCs, are required. This could be achieved partly through performing intracellular cytokine staining on myeloid populations. Use of a GM-CSF reporter

mouse, where GM-CSF expression is accompanied by expression of a fluorescent protein such as GFP, would be beneficial to identifying cellular sources of GM-CSF both in the naïve and infected state, especially given the technical difficulties of performing intracellular cytokine staining on myeloid populations. However, to our knowledge, such a mouse is currently unavailable.

6.4.3 The mechanism for the protective role of GM-CSF during Mtb infection

The mechanism for the protective role of GM-CSF during *Mtb* infection remains unclear. In order to try to determine this, experiments utilising histology would be important. Lung histology could be used to assess the impact of GM-CSF neutralisation upon granuloma structure. In addition, immunohistochemistry could be utilised to assess the location of T cells within the lung and individual granulomas, which could be important given the recent data suggesting the location of T cells influence their protective capacity (Sakai et al., 2014; Srivastava and Ernst, 2013). Furthermore immunohistochemistry staining for iNOS within the infected lung could be used to assess the influence of GM-CSF upon macrophage activation, which could contribute to the protective role of GM-CSF in both wild-type and *Rag* deficient mice. Additionally, staining infected lung sections to identify mycobacteria (e.g. using a Ziehl Neelsen stain) may provide information regarding how GM-CSF influences bacterial loads within myeloid cells as well as within the granuloma. The work to assess the influence of GM-CSF upon activation of myeloid subsets could be supported by *in vitro* work assessing the influence of GM-CSF upon restriction of bacterial growth and expression of pro-inflammatory molecules.

6.4.4 The role of ILCs and their importance as a source of GM-CSF during Mtb infection

The results presented in this thesis provide evidence that ILCs are capable of responding to *Mtb* infection, however an outstanding question remains: what is their role in the context of an adaptive immune response? Use of flowcytometry to identify ILCs and their cytokine production in a wild-type mouse is required. In order to assess the functional importance of ILCs in the context of an adaptive immune response anti-Thy1 antibody mediated depletion of ILCs could be utilised with concomitant transfer of congenically marked T cells. Such an experimental design will lead to a T cell response (as these would be congenically marked and therefore not recognised by the depleting antibody) in the absence of ILCs. As well as the potential to identify the importance of ILCs as an early source of cytokines, this experiment would enable assessment of the influence of ILCs upon the T cell response. This could be important, especially given recent data highlighting the ability of ILCs to influence the adaptive response (Gold et al., 2014; Halim et al., 2014; Hepworth et al., 2015; Hepworth et al., 2013; Mortha et al., 2014; Oliphant et al., 2014).

In order to further investigate the importance of ILCs as a source of GM-CSF during *Mtb* infection a similar experiment utilising depletion of ILCs using anti-Thy1 antibody mediated depletion with concomitant transfer of congenically marked T cells and GM-CSF sufficient or deficient ILCs could be conducted. This would allow assessment of the outcome of infection in the context of absence of ILC derived GM-CSF. Such an experimental design would show whether GM-CSF deficiency specifically in ILCs is important for the outcome of *Mtb* infection in the context of an adaptive immune response.

6.5 Concluding remarks

An incomplete understanding of the protective immune response to *Mtb* hinders development of successful vaccines against *Mtb*. Improved vaccine strategies are required if the aim of a TB free world by 2050 is to be achieved (WHO, 2006). Work in this thesis has aimed to further our

understanding of factors that contribute to a protective response. It demonstrates early and increased levels of GM-CSF and IL-17 correlate with increased control of bacterial load in chronic infection. Furthermore, GM-CSF is important for optimal protection in the recall response. These results taken together suggest augmenting production of GM-CSF could be beneficial to improve vaccination. GM-CSF is also important in primary *Mtb* infection, which is of clinical relevance given on-going clinical trials assessing use of monoclonal antibodies against GM-CSF or its receptor in treatment of rheumatoid arthritis or multiple sclerosis (Hamilton, 2015).

This thesis also aimed to further our understanding of the role of NK cells and ILCs in the early, innate response to *Mtb* infection. ILCs are a source of GM-CSF upon *Mtb* infection and contribute to protection in the innate immune response to *Mtb* infection. Innate lymphocytes (including ILCs, NK cells and MAIT cells) could provide an early source of cytokines, influencing the outcome of infection. Further investigation into these cell populations in humans will advance our understanding of these cell populations and their contribution to the immune response to *Mtb*. Furthermore, investigation into whether their responses can be augmented by vaccines could provide strategies to improve vaccination. Improving our understanding of a protective immune response to *Mtb* will facilitate development of improved vaccines and novel biological therapies, and potentially contribute to control of the global TB epidemic.

Chapter 7 References

Aagaard, C., T. Hoang, J. Dietrich, P.J. Cardona, A. Izzo, G. Dolganov, G.K. Schoolnik, J.P. Cassidy, R. Billeskov, and P. Andersen. 2011. A multistage tuberculosis vaccine that confers efficient protection before and after exposure. *Nat Med* 17:189-194.

Abadie, V., E. Badell, P. Douillard, D. Ensergueix, P.J. Leenen, M. Tanguy, L. Fiette, S. Saeland, B. Gicquel, and N. Winter. 2005. Neutrophils rapidly migrate via lymphatics after Mycobacterium bovis BCG intradermal vaccination and shuttle live bacilli to the draining lymph nodes. *Blood* 106:1843-1850.

Abdalla, H., L. Srinivasan, S. Shah, K.D. Mayer-Barber, A. Sher, F.S. Sutterwala, and V. Briken. 2012. Mycobacterium tuberculosis infection of dendritic cells leads to partially caspase-1/11-independent IL-1beta and IL-18 secretion but not to pyroptosis. *Plos One* 7:e40722.

Abebe, F. 2012. Is interferon-gamma the right marker for bacille Calmette-Guerin-induced immune protection? The missing link in our understanding of tuberculosis immunology. *Clin Exp Immunol* 169:213-219.

Abel, B., M. Tameris, N. Mansoor, S. Gelderbloem, J. Hughes, D. Abrahams, L. Makhethe, M. Erasmus, M. de Kock, L. van der Merwe, A. Hawkridge, A. Veldsman, M. Hatherill, G. Schirru, M.G. Pau, J. Hendriks, G.J. Weverling, J. Goudsmit, D. Sizemore, J.B. McClain, M. Goetz, J. Gearhart, H. Mahomed, G.D. Hussey, J.C. Sadoff, and W.A. Hanekom. 2010. The novel tuberculosis vaccine, AERAS-402, induces robust and polyfunctional CD4+ and CD8+ T cells in adults. *Am J Respir Crit Care Med* 181:1407-1417.

Abel, B., N. Thieblemon, V.J.F. Quesniaux, N. Brown, J. Mpagi, K. Miyake, F. Bihl, and B. Ryffel. 2002. Toll-like receptor 4 expression is required to control chronic Mycobacterium tuberculosis infection in mice. *J. Immunol.* 169:3155-3162.

Abubakar, I., M. Zignol, D. Falzon, M. Raviglione, L. Ditiu, S. Masham, I. Adetifa, N. Ford, H. Cox, S.D. Lawn, B.J. Marais, T.D. McHugh, P. Mwaba, M. Bates, M. Lipman, L. Zijenah, S. Logan, R. McNerney, A. Zumla, K. Sarda, P. Nahid, M. Hoelscher, M. Pletschette, Z.A. Memish, P. Kim, R. Hafner, S. Cole, G.B. Migliori, M. Maeurer, M. Schito, and A. Zumla. 2013. Drug-resistant tuberculosis: time for visionary political leadership. *Lancet Infect Dis* 13:529-539.

Akira, S., and K. Takeda. 2004. Toll-like receptor signalling. *Nature reviews* 4:499-511.

Alcais, A., C. Fieschi, L. Abel, and J.L. Casanova. 2005. Tuberculosis in children and adults: two distinct genetic diseases. *J Exp Med* 202:1617-1621.

Almeida, A.S., P.M. Lago, N. Boechat, R.C. Huard, L.C.O. Lazzarini, A.R. Santos, M. Nociari, H. Zhu, B.M. Perez-Sweeney, H. Bang, Q. Ni, J. Huang, A.L. Gibson, V.C. Flores, L.R. Pecanha, A.L. Kritski, J.R. Lapa e Silva, and J.L. Ho. 2009. Tuberculosis Is Associated with a Down-Modulatory Lung Immune Response That Impairs Th1-Type Immunity. *J. Immunol.* 183:718-731.

Altare, F., A. Ensser, A. Breiman, J. Reichenbach, J.E. Baghdadi, A. Fischer, J.F. Emile, J.L. Gaillard, E. Meinl, and J.L. Casanova. 2001. Interleukin-12 receptor beta1 deficiency in a patient with abdominal tuberculosis. *J Infect Dis* 184:231-236.

Andersen, P., and S.H. Kaufmann. 2014. Novel Vaccination Strategies against Tuberculosis. *Cold Spring Harbor perspectives in medicine* 4:

Anderson, C.F., M. Oukka, V.J. Kuchroo, and D. Sacks. 2007. CD4(+)CD25(-)Foxp3(-) Th1 cells are the source of IL-10-mediated immune suppression in chronic cutaneous leishmaniasis. *Journal of Experimental Medicine* 204:285-297.

Antonelli, L.R.V., A.G. Rothfuchs, R. Goncalves, E. Roffe, A.W. Cheever, A. Bafica, A.M. Salazar, C.G. Feng, and A. Sher. 2010. Intranasal Poly-IC treatment exacerbates tuberculosis in mice through the pulmonary recruitment of a pathogen-permissive monocyte/macrophage population. *Journal of Clinical Investigation* 120:1674-1682.

Apt, A., and I. Kramnik. 2009. Man and mouse TB: contradictions and solutions. *Tuberculosis (Edinb)* 89:195-198.

Arbues, A., J.I. Aguilo, J. Gonzalo-Asensio, D. Marinova, S. Uranga, E. Puentes, C. Fernandez, A. Parra, P.J. Cardona, C. Vilaplana, V. Ausina, A. Williams, S. Clark, W. Malaga, C. Guilhot, B. Gicquel, and C. Martin. 2013. Construction, characterization and preclinical evaluation of

MTBVAC, the first live-attenuated M. tuberculosis-based vaccine to enter clinical trials. *Vaccine* 31:4867-4873.

Artis, D., and H. Spits. 2015. The biology of innate lymphoid cells. *Nature* 517:293-301.

Bafica, A., C.A. Scanga, C.G. Feng, C. Leifer, A. Cheever, and A. Sher. 2005a. TLR9 regulates Th1 responses and cooperates with TLR2 in mediating optimal resistance to Mycobacterium tuberculosis. *J Exp Med* 202:1715-1724.

Bafica, A., C.A. Scanga, C. Serhan, F. Machado, S. White, A. Sher, and J. Aliberti. 2005b. Host control of Mycobacterium tuberculosis is regulated by 5-lipoxygenase-dependent lipoxin production. *J Clin Invest* 115:1601-1606.

Ballinger, M.N., R. Paine, 3rd, C.H. Serezani, D.M. Aronoff, E.S. Choi, T.J. Standiford, G.B. Toews, and B.B. Moore. 2006. Role of granulocyte macrophage colony-stimulating factor during gram-negative lung infection with Pseudomonas aeruginosa. *American journal of respiratory cell and molecular biology* 34:766-774.

Bancroft, G.J. 1993. The role of natural killer cells in innate resistance to infection. *Curr Opin Immunol* 5:503-510.

Barber, D.L., K.D. Mayer-Barber, C.G. Feng, A.H. Sharpe, and A. Sher. 2011. CD4 T cells promote rather than control tuberculosis in the absence of PD-1-mediated inhibition. *J Immunol* 186:1598-1607.

Barnes, P.F., S.Z. Lu, J.S. Abrams, E. Wang, M. Yamamura, and R.L. Modlin. 1993. CYTOKINE PRODUCTION AT THE SITE OF DISEASE IN HUMAN TUBERCULOSIS. *Infect. Immun.* 61:3482-3489.

Barry, C.E., III, H.I. Boshoff, V. Dartois, T. Dick, S. Ehrt, J. Flynn, D. Schnappinger, R.J. Wilkinson, and D. Young. 2009. The spectrum of latent tuberculosis: rethinking the biology and intervention strategies. *Nature Reviews Microbiology* 7:845-855.

Beamer, G.L., J. Cyktor, B. Carruthers, and J. Turner. 2011. H-2 alleles contribute to antigen 85-specific interferon-gamma responses during Mycobacterium tuberculosis infection. *Cell Immunol* 271:53-61.

Beamer, G.L., D.K. Flaherty, B.D. Assogba, P. Stromberg, M. Gonzalez-Juarrero, R.d.W. Malefyt, B. Vesosky, and J. Turner. 2008. Interleukin-10 promotes Mycobacterium tuberculosis disease progression in CBA/J mice. *J. Immunol.* 181:5545-5550.

Bean, A.G., D.R. Roach, H. Briscoe, M.P. France, H. Korner, J.D. Sedgwick, and W.J. Britton. 1999. Structural deficiencies in granuloma formation in TNF gene-targeted mice underlie the heightened susceptibility to aerosol Mycobacterium tuberculosis infection, which is not compensated for by lymphotoxin. *J Immunol* 162:3504-3511.

Becher, B., A. Schlitzer, J. Chen, F. Mair, H.R. Sumatoh, K.W. Teng, D. Low, C. Ruedl, P. Riccardi-Castagnoli, M. Poidinger, M. Greter, F. Ginhoux, and E.W. Newell. 2014. High-dimensional analysis of the murine myeloid cell system. *Nat Immunol* 15:1181-1189.

Behar, S.M. 2013. Antigen-specific CD8(+) T cells and protective immunity to tuberculosis. *Advances in experimental medicine and biology* 783:141-163.

Behar, S.M., C.C. Dascher, M.J. Grusby, C.R. Wang, and M.B. Brenner. 1999. Susceptibility of mice deficient in CD1D or TAP1 to infection with Mycobacterium tuberculosis. *J Exp Med* 189:1973-1980.

Behar, S.M., C.J. Martin, M.G. Booty, T. Nishimura, X. Zhao, H.X. Gan, M. Divangahi, and H.G. Remold. 2011. Apoptosis is an innate defense function of macrophages against Mycobacterium tuberculosis. *Mucosal Immunol* 4:279-287.

Behler, F., R. Maus, J. Bohling, S. Knippenberg, G. Kirchhof, M. Nagata, D. Jonigk, N. Izykowski, L. Magel, T. Welte, S. Yamasaki, and U.A. Maus. 2015. Macrophage-inducible C-type lectin Mincle-expressing dendritic cells contribute to control of splenic Mycobacterium bovis BCG infection in mice. *Infect Immun* 83:184-196.

Behler, F., K. Steinwede, L. Balboa, B. Ueberberg, R. Maus, G. Kirchhof, S. Yamasaki, T. Welte, and U.A. Maus. 2012. Role of Mincle in alveolar macrophage-dependent innate immunity against mycobacterial infections in mice. *J Immunol* 189:3121-3129.

Belkaid, Y., K.F. Hoffmann, S. Mendez, S. Kamhawi, M.C. Udey, T.A. Wynn, and D.L. Sacks. 2001. The role of interleukin (IL)-10 in the persistence of Leishmania major in the skin after healing and the therapeutic potential of anti-IL-10 receptor antibody for sterile cure. *Journal of Experimental Medicine* 194:1497-1506.

Belkaid, Y., C.A. Piccirillo, S. Mendez, E.M. Shevach, and D.L. Sacks. 2002. CD4(+)CD25(+) regulatory T cells control Leishmania major persistence and immunity. *Nature* 420:502-507.

Belyakov, I.M., and J.D. Ahlers. 2009. What Role Does the Route of Immunization Play in the Generation of Protective Immunity against Mucosal Pathogens? *J. Immunol.* 183:6883-6892.

Bermudez, L.E., and L.S. Young. 1990. Recombinant granulocyte-macrophage colony-stimulating factor activates human macrophages to inhibit growth or kill Mycobacterium avium complex. *J Leukoc Biol* 48:67-73.

Bernink, J.H., L. Krabbendam, K. Germar, E. de Jong, K. Gronke, M. Kofoed-Nielsen, J.M. Munneke, M.D. Hazenberg, J. Villaudy, C.J. Buskens, W.A. Bemelman, A. Diefenbach, B. Blom, and H. Spits. 2015. Interleukin-12 and -23 Control Plasticity of CD127 Group 1 and Group 3 Innate Lymphoid Cells in the Intestinal Lamina Propria. *Immunity*

Bernink, J.H., C.P. Peters, M. Munneke, A.A. Te Velde, S.L. Meijer, K. Weijer, H.S. Hreggvidsdottir, S.E. Heinsbroek, N. Legrand, C.J. Buskens, W.A. Bemelman, J.M. Mjosberg, and H. Spits. 2013. Human type 1 innate lymphoid cells accumulate in inflamed mucosal tissues. *Nat Immunol* 14:221-229.

Berry, M.P.R., C.M. Graham, F.W. McNab, Z. Xu, S.A.A. Bloch, T. Oni, K.A. Wilkinson, R. Banchereau, J. Skinner, R.J. Wilkinson, C. Quinn, D. Blankenship, R. Dhawan, J.J. Cush, A. Mejias, O. Ramilo, O.M. Kon, V. Pascual, J. Banchereau, D. Chaussabel, and A. O'Garra. 2010. An interferon-inducible neutrophil-driven blood transcriptional signature in human tuberculosis. *Nature* 466:973-U998.

Bertholet, S., G.C. Ireton, D.J. Ordway, H.P. Windish, S.O. Pine, M. Kahn, T. Phan, I.M. Orme, T.S. Vedvick, S.L. Baldwin, R.N. Coler, and S.G. Reed. 2010. A defined tuberculosis vaccine candidate boosts BCG and protects against multidrug-resistant Mycobacterium tuberculosis. *Sci Transl Med* 2:53ra74.

Bezbradica, J.S., L.E. Gordy, A.K. Stanic, S. Dragovic, T. Hill, J. Hawiger, D. Unutmaz, L. Van Kaer, and S. Joyce. 2006. Granulocyte-macrophage colony-stimulating factor regulates effector differentiation of invariant natural killer T cells during thymic ontogeny. *Immunity* 25:487-497.

Biron, C.A., K.B. Nguyen, G.C. Pien, L.P. Cousens, and T.P. Salazar-Mather. 1999. Natural killer cells in antiviral defense: function and regulation by innate cytokines. *Annu Rev Immunol* 17:189-220.

Blomgran, R., L. Desvignes, V. Briken, and J.D. Ernst. 2012. Mycobacterium tuberculosis inhibits neutrophil apoptosis, leading to delayed activation of naive CD4 T cells. *Cell host & microbe* 11:81-90.

Blomgran, R., and J.D. Ernst. 2011. Lung neutrophils facilitate activation of naive antigen-specific CD4+ T cells during Mycobacterium tuberculosis infection. *J Immunol* 186:7110-7119.

Boehme, C.C., P. Nabeta, D. Hillemann, M.P. Nicol, S. Shenai, F. Krapp, J. Allen, R. Tahirli, R. Blakemore, R. Rustomjee, A. Milovic, M. Jones, S.M. O'Brien, D.H. Persing, S. Ruesch-Gerdes, E. Gotuzzo, C. Rodrigues, D. Alland, and M.D. Perkins. 2010. Rapid molecular detection of tuberculosis and rifampin resistance. *N Engl J Med* 363:1005-1015.

Boer, M.C., S.A. Joosten, and T.H. Ottenhoff. 2015. Regulatory T-Cells at the Interface between Human Host and Pathogens in Infectious Diseases and Vaccination. *Frontiers in immunology* 6:217.

Bogunovic, D., M. Byun, L.A. Durfee, A. Abhyankar, O. Sanal, D. Mansouri, S. Salem, I. Radovanovic, A.V. Grant, P. Adimi, N. Mansouri, S. Okada, V.L. Bryant, X.F. Kong, A. Kreins, M.M. Velez, B. Boisson, S. Khalilzadeh, U. Ozcelik, I.A. Darazam, J.W. Schoggins, C.M. Rice, S. Al-Muhsen, M. Behr, G. Vogt, A. Puel, J. Bustamante, P. Gros, J.M. Huibregtse, L. Abel, S.

Boisson-Dupuis, and J.L. Casanova. 2012. Mycobacterial disease and impaired IFN-gamma immunity in humans with inherited ISG15 deficiency. *Science* 337:1684-1688.

Bogunovic, M., F. Ginhoux, J. Helft, L. Shang, D. Hashimoto, M. Greter, K. Liu, C. Jakubzick, M.A. Ingersoll, M. Leboeuf, E.R. Stanley, M. Nussenzweig, S.A. Lira, G.J. Randolph, and M. Merad. 2009. Origin of the lamina propria dendritic cell network. *Immunity* 31:513-525.

Bold, T.D., and J.D. Ernst. 2012. CD4+ T cell-dependent IFN-gamma production by CD8+ effector T cells in Mycobacterium tuberculosis infection. *J Immunol* 189:2530-2536.

Borie, R., C. Danel, M.P. Debray, C. Taille, M.C. Dombret, M. Aubier, R. Epaud, and B. Crestani. 2011. Pulmonary alveolar proteinosis. *European respiratory review : an official journal of the European Respiratory Society* 20:98-107.

Bosio, C.M., D. Gardner, and K.L. Elkins. 2000. Infection of B cell-deficient mice with CDC 1551, a clinical isolate of Mycobacterium tuberculosis: Delay in dissemination and development of lung pathology. *J. Immunol.* 164:6417-6425.

Brandt, L., J. Feino Cunha, A. Weinreich Olsen, B. Chilima, P. Hirsch, R. Appelberg, and P. Andersen. 2002. Failure of the Mycobacterium bovis BCG vaccine: some species of environmental mycobacteria block multiplication of BCG and induction of protective immunity to tuberculosis. *Infect Immun* 70:672-678.

Brestoff, J.R., B.S. Kim, S.A. Saenz, R.R. Stine, L.A. Monticelli, G.F. Sonnenberg, J.J. Thome, D.L. Farber, K. Lutfy, P. Seale, and D. Artis. 2015. Group 2 innate lymphoid cells promote beiging of white adipose tissue and limit obesity. *Nature* 519:242-246.

Brooks, D.G., A.M. Lee, H. Elsaesser, D.B. McGavern, and M.B.A. Oldstone. 2008. IL-10 blockade facilitates DNA vaccine-induced T cell responses and enhances clearance of persistent virus infection. *Journal of Experimental Medicine* 205:533-541.

Brooks, D.G., M.J. Trifilo, K.H. Edelmann, L. Teyton, D.B. McGavern, and M.B.A. Oldstone. 2006. Interleukin-10 determines viral clearance or persistence in vivo. *Nature Medicine* 12:1301-1309.

Buonocore, S., P.P. Ahern, H.H. Uhlig, Ivanov, II, D.R. Littman, K.J. Maloy, and F. Powrie. 2010. Innate lymphoid cells drive interleukin-23-dependent innate intestinal pathology. *Nature* 464:1371-1375.

Burgess, A.W., and D. Metcalf. 1980. The nature and action of granulocyte-macrophage colony stimulating factors. *Blood* 56:947-958.

Campbell, I.K., M.J. Rich, R.J. Bischof, A.R. Dunn, D. Grail, and J.A. Hamilton. 1998. Protection from collagen-induced arthritis in granulocyte-macrophage colony-stimulating factor-deficient mice. *J Immunol* 161:3639-3644.

Capuano, S.V., D.A. Croix, S. Pawar, A. Zinovik, A. Myers, P.L. Lin, S. Bissel, C. Fuhrman, E. Klein, and J.L. Flynn. 2003. Experimental Mycobacterium tuberculosis infection of cynomolgus Macaques closely resembles the various manifestations of human M-tuberculosis infection. *Infect. Immun.* 71:5831-5844.

Carmona, J., A. Cruz, L. Moreira-Teixeira, C. Sousa, J. Sousa, N.S. Osorio, A.L. Saraiva, S. Svenson, G. Kallenius, J. Pedrosa, F. Rodrigues, A.G. Castro, and M. Saraiva. 2013. Strains Are Differentially Recognized by TLRs with an Impact on the Immune Response. *PLoS One* 8:e67277.

Carotta, S., S.H. Pang, S.L. Nutt, and G.T. Belz. 2011. Identification of the earliest NK-cell precursor in the mouse BM. *Blood* 117:5449-5452.

Casanova, J.L. 2001. Mendelian susceptibility to mycobacterial infection in man. *Swiss Med. Wkly.* 131:445-454.

Casanova, J.L., and L. Abel. 2002. Genetic dissection of immunity to mycobacteria: The human model. *Annu. Rev. Immunol.* 20:581-620.

Chackerian, A., J. Alt, V. Perera, and S.M. Behar. 2002a. Activation of NKT cells protects mice from tuberculosis. *Infect Immun* 70:6302-6309.

Chackerian, A.A., J.M. Alt, T.V. Perera, C.C. Dascher, and S.M. Behar. 2002b. Dissemination of Mycobacterium tuberculosis is influenced by host factors and precedes the initiation of T-cell immunity. *Infect. Immun.* 70:4501-4509.

Chackerian, A.A., T.V. Perera, and S.M. Behar. 2001. Gamma interferon-producing CD4+ T lymphocytes in the lung correlate with resistance to infection with Mycobacterium tuberculosis. *Infect Immun* 69:2666-2674.

Chakravarty, S.D., G.F. Zhu, M.C. Tsai, V.P. Mohan, S. Marino, D.E. Kirschner, L.Q. Huang, J. Flynn, and J. Chan. 2008. Tumor necrosis factor blockade in chronic murine tuberculosis enhances granulomatous inflammation and disorganizes granulomas in the lungs. *Infect. Immun.* 76:916-926.

Chan, J., Y. Xing, R.S. Magliozzo, and B.R. Bloom. 1992. KILLING OF VIRULENT MYCOBACTERIUM-TUBERCULOSIS BY REACTIVE NITROGEN INTERMEDIATES PRODUCED BY ACTIVATED MURINE MACROPHAGES. *Journal of Experimental Medicine* 175:1111-1122.

Chang, Y.J., H.Y. Kim, L.A. Albacker, N. Baumgarth, A.N. McKenzie, D.E. Smith, R.H. Dekruyff, and D.T. Umetsu. 2011. Innate lymphoid cells mediate influenza-induced airway hyper-reactivity independently of adaptive immunity. *Nat Immunol* 12:631-638.

Chaudhry, A., R.M. Samstein, P. Treuting, Y. Liang, M.C. Pils, J.M. Heinrich, R.S. Jack, F.T. Wunderlich, J.C. Bruning, W. Muller, and A.Y. Rudensky. 2011. Interleukin-10 signaling in regulatory T cells is required for suppression of Th17 cell-mediated inflammation. *Immunity* 34:566-578.

Chegou, N.N., K.G. Hoek, M. Kriel, R.M. Warren, T.C. Victor, and G. Walzl. 2011. Tuberculosis assays: past, present and future. *Expert review of anti-infective therapy* 9:457-469.

Chen, L., J. Wang, A. Zganiacz, and Z. Xing. 2004. Single intranasal mucosal Mycobacterium bovis BCG vaccination confers improved protection compared to subcutaneous vaccination against pulmonary tuberculosis. *Infect Immun* 72:238-246.

Chen, M., M. Divangahi, H. Gan, D.S. Shin, S. Hong, D.M. Lee, C.N. Serhan, S.M. Behar, and H.G. Remold. 2008. Lipid mediators in innate immunity against tuberculosis: opposing roles of PGE2 and LXA4 in the induction of macrophage death. *J Exp Med* 205:2791-2801.

Cherrier, M., S. Sawa, and G. Eberl. 2012. Notch, Id2, and RORgammat sequentially orchestrate the fetal development of lymphoid tissue inducer cells. *J Exp Med* 209:729-740.

Cilfone, N.A., C.B. Ford, S. Marino, J.T. Mattila, H.P. Gideon, J.L. Flynn, D.E. Kirschner, and J.J. Linderman. 2015. Computational modeling predicts IL-10 control of lesion sterilization by balancing early host immunity-mediated antimicrobial responses with caseation during mycobacterium tuberculosis infection. *J Immunol* 194:664-677.

Clay, H., H.E. Volkman, and L. Ramakrishnan. 2008. Tumor necrosis factor signaling mediates resistance to mycobacteria by inhibiting bacterial growth and macrophage death. *Immunity* 29:283-294.

Codarri, L., G. Gyulveszi, V. Tosevski, L. Hesske, A. Fontana, L. Magnenat, T. Suter, and B. Becher. 2011. RORgammat drives production of the cytokine GM-CSF in helper T cells, which is essential for the effector phase of autoimmune neuroinflammation. *Nat Immunol* 12:560-567.

Constantinides, M.G., B.D. McDonald, P.A. Verhoef, and A. Bendelac. 2014. A committed precursor to innate lymphoid cells. *Nature* 508:397-401.

Cooper, A.M. 2009. Cell-Mediated Immune Responses in Tuberculosis. In Annu. Rev. Immunol. 393-422.

Cooper, A.M., D.K. Dalton, T.A. Stewart, J.P. Griffin, D.G. Russell, and I.M. Orme. 1993. DISSEMINATED TUBERCULOSIS IN INTERFERON-GAMMA GENE-DISRUPTED MICE. *Journal of Experimental Medicine* 178:2243-2247.

Cooper, A.M., A. Kipnis, J. Turner, J. Magram, J. Ferrante, and I.M. Orme. 2002. Mice lacking bioactive IL-12 can generate protective, antigen-specific cellular responses to mycobacterial infection only if the IL-12 p40 subunit is present. *J. Immunol.* 168:1322-1327.

Cooper, A.M., J. Magram, J. Ferrante, and I.M. Orme. 1997. Interleukin 12 (IL-12) is crucial to the development of protective immunity in mice intravenously infected with Mycobacterium tuberculosis. *Journal of Experimental Medicine* 186:39-45.

Cooper, A.M., J.E. Pearl, J.V. Brooks, S. Ehlers, and I.M. Orme. 2000a. Expression of the nitric oxide synthase 2 gene is not essential for early control of Mycobacterium tuberculosis in the murine lung. *Infect. Immun.* 68:6879-6882.

Cooper, A.M., A.D. Roberts, E.R. Rhoades, J.E. Callahan, D.M. Getzy, and I.M. Orme. 1995. THE ROLE OF INTERLEUKIN-12 IN ACQUIRED-IMMUNITY TO MYCOBACTERIUM-TUBERCULOSIS INFECTION. *Immunology* 84:423-432.

Cooper, A.M., B.H. Segal, A.A. Frank, S.M. Holland, and I.M. Orme. 2000b. Transient loss of resistance to pulmonary tuberculosis in p47(phox-/-) mice. *Infect Immun* 68:1231-1234.

Corbett, E.L., C.J. Watt, N. Walker, D. Maher, B.G. Williams, M.C. Raviglione, and C. Dye. 2003. The growing burden of tuberculosis: global trends and interactions with the HIV epidemic. *Archives of internal medicine* 163:1009-1021.

Cowley, S.C., and K.L. Elkins. 2003. CD4+ T cells mediate IFN-gamma-independent control of Mycobacterium tuberculosis infection both in vitro and in vivo. *J Immunol* 171:4689-4699.

Cruz, A., A.G. Fraga, J.J. Fountain, J. Rangel-Moreno, E. Torrado, M. Saraiva, D.R. Pereira, T.D. Randall, J. Pedrosa, A.M. Cooper, and A.G. Castro. 2010. Pathological role of interleukin 17 in mice subjected to repeated BCG vaccination after infection with Mycobacterium tuberculosis. *Journal of Experimental Medicine* 207:1609-1616.

Cruz, A., S.A. Khader, E. Torrado, A. Fraga, J.E. Pearl, J. Pedrosa, A.M. Cooper, and A.G. Castro. 2006. Cutting edge: IFN-gamma regulates the induction and expansion of IL-17-producing CD4 T cells during mycobacterial infection. *J. Immunol.* 177:1416-1420.

Cruz, A., E. Torrado, J. Carmona, A.G. Fraga, P. Costa, F. Rodrigues, R. Appelberg, M. Correia-Neves, A.M. Cooper, M. Saraiva, J. Pedrosa, and A.G. Castro. 2015. BCG vaccination-induced long-lasting control of Mycobacterium tuberculosis correlates with the accumulation of a novel population of CD4(+)IL-17(+)TNF(+)IL-2(+) T cells. *Vaccine* 33:85-91.

Cyktor, J.C., B. Carruthers, G.L. Beamer, and J. Turner. 2013a. Clonal Expansions of CD8(+) T Cells with IL-10 Secreting Capacity Occur during Chronic Mycobacterium tuberculosis Infection. *Plos One* 8:e58612.

Cyktor, J.C., B. Carruthers, R.A. Kominsky, G.L. Beamer, P. Stromberg, and J. Turner. 2013b. IL-10 Inhibits Mature Fibrotic Granuloma Formation during Mycobacterium tuberculosis Infection. *J Immunol* 190:2778-2790.

D'Souza, C.D., A.M. Cooper, A.A. Frank, R.J. Mazzaccaro, B.R. Bloom, and I.M. Orme. 1997. An anti-inflammatory role for gamma delta T lymphocytes in acquired immunity to Mycobacterium tuberculosis. *J Immunol* 158:1217-1221.

Dai, W.J., G. Kohler, and F. Brombacher. 1997. Both innate and acquired immunity to Listeria monocytogenes infection are increased in IL-10-deficient mice. *J. Immunol.* 158:2259-2267.

Dallenga, T., B. Corleis, and U.E. Schaible. 2015. Infection of Human Neutrophils to Study Virulence Properties of Mycobacterium tuberculosis. *Methods in molecular biology (Clifton, N.J.)* 1285:343-355.

Darrah, P.A., D.L. Bolton, A.A. Lackner, D. Kaushal, P.P. Aye, S. Mehra, J.L. Blanchard, P.J. Didier, C.J. Roy, S.S. Rao, D.A. Hokey, C.A. Scanga, D.R. Sizemore, J.C. Sadoff, M. Roederer, and R.A. Seder. 2014. Aerosol vaccination with AERAS-402 elicits robust cellular immune responses in the lungs of rhesus macaques but fails to protect against high-dose Mycobacterium tuberculosis challenge. *J Immunol* 193:1799-1811.

Darrah, P.A., S.T. Hegde, D.T. Patel, R.W.B. Lindsay, L. Chen, M. Roederer, and R.A. Seder. 2010. IL-10 production differentially influences the magnitude, quality, and protective capacity of Th1 responses depending on the vaccine platform. *Journal of Experimental Medicine* 207:1421-1433.

Daussy, C., F. Faure, K. Mayol, S. Viel, G. Gasteiger, E. Charrier, J. Bienvenu, T. Henry, E. Debien, U.A. Hasan, J. Marvel, K. Yoh, S. Takahashi, I. Prinz, S. de Bernard, L. Buffat, and T. Walzer.

2014. T-bet and Eomes instruct the development of two distinct natural killer cell lineages in the liver and in the bone marrow. *J Exp Med* 211:563-577.

Davis, J.M., and L. Ramakrishnan. 2009. The Role of the Granuloma in Expansion and Dissemination of Early Tuberculous Infection. *Cell* 136:37-49.

Day, C.L., M. Tameris, N. Mansoor, M. van Rooyen, M. de Kock, H. Geldenhuys, M. Erasmus, L. Makhethe, E.J. Hughes, S. Gelderbloem, A. Bollaerts, P. Bourguignon, J. Cohen, M.A. Demoitie, P. Mettens, P. Moris, J.C. Sadoff, A. Hawkridge, G.D. Hussey, H. Mahomed, O. Ofori-Anyinam, and W.A. Hanekom. 2013. Induction and regulation of T-cell immunity by the novel tuberculosis vaccine M72/AS01 in South African adults. *Am J Respir Crit Care Med* 188:492-502.

Demangel, C., P. Bertolino, and W.J. Britton. 2002. Autocrine IL-10 impairs dendritic cell (DC)-derived immune responses to mycobacterial infection by suppressing DC trafficking to draining lymph nodes and local IL-12 production. *European Journal of Immunology* 32:994-1002.

Denis, M. 1991. Tumor necrosis factor and granulocyte macrophage-colony stimulating factor stimulate human macrophages to restrict growth of virulent Mycobacterium avium and to kill avirulent M. avium: killing effector mechanism depends on the generation of reactive nitrogen intermediates. *J Leukoc Biol* 49:380-387.

Denis, M., and E. Ghadirian. 1990. Granulocyte-macrophage colony-stimulating factor restricts growth of tubercle bacilli in human macrophages. *Immunology letters* 24:203-206.

Desel, C., A. Dorhoi, S. Bandermann, L. Grode, B. Eisele, and S.H. Kaufmann. 2011. Recombinant BCG DeltaureC hly+ induces superior protection over parental BCG by stimulating a balanced combination of type 1 and type 17 cytokine responses. *J Infect Dis* 204:1573-1584.

Desvignes, L., A.J. Wolf, and J.D. Ernst. 2012. Dynamic roles of type I and type II IFNs in early infection with Mycobacterium tuberculosis. *J Immunol* 188:6205-6215.

Dhiman, R., S. Periasamy, P.F. Barnes, A.G. Jaiswal, P. Paidipally, A.B. Barnes, A. Tvinnereim, and R. Vankayalapati. 2012. NK1.1+ cells and IL-22 regulate vaccine-induced protective immunity against challenge with Mycobacterium tuberculosis. *J Immunol* 189:897-905.

Diefenbach, A., M. Colonna, and S. Koyasu. 2014. Development, differentiation, and diversity of innate lymphoid cells. *Immunity* 41:354-365.

Divangahi, M., M. Chen, H. Gan, D. Desjardins, T.T. Hickman, D.M. Lee, S. Fortune, S.M. Behar, and H.G. Remold. 2009. Mycobacterium tuberculosis evades macrophage defenses by inhibiting plasma membrane repair. *Nat Immunol* 10:899-906.

Divangahi, M., D. Desjardins, C. Nunes-Alves, H.G. Remold, and S.M. Behar. 2010. Eicosanoid pathways regulate adaptive immunity to Mycobacterium tuberculosis. *Nat Immunol* 11:751-758.

Divangahi, M., S. Mostowy, F. Coulombe, R. Kozak, L. Guillot, F. Veyrier, K.S. Kobayashi, R.A. Flavell, P. Gros, and M.A. Behr. 2008. NOD2-deficient mice have impaired resistance to Mycobacterium tuberculosis infection through defective innate and adaptive immunity. *J Immunol* 181:7157-7165.

do Rosario, A.P.F., T. Lamb, P. Spence, R. Stephens, A. Lang, A. Roers, W. Muller, A. O'Garra, and J. Langhorne. 2012. IL-27 Promotes IL-10 Production by Effector Th1 CD4(+) T Cells: A Critical Mechanism for Protection from Severe Immunopathology during Malaria Infection. *J. Immunol.* 188:1178-1190.

Dorhoi, A., C. Desel, V. Yeremeev, L. Pradl, V. Brinkmann, H.J. Mollenkopf, K. Hanke, O. Gross, J. Ruland, and S.H. Kaufmann. 2010. The adaptor molecule CARD9 is essential for tuberculosis control. *J Exp Med* 207:777-792.

Dorhoi, A., M. Iannaccone, M. Farinacci, K.C. Fae, J. Schreiber, P. Moura-Alves, G. Nouailles, H.J. Mollenkopf, D. Oberbeck-Muller, S. Jorg, E. Heinemann, K. Hahnke, D. Lowe, F. Del Nonno, D. Goletti, R. Capparelli, and S.H. Kaufmann. 2013. MicroRNA-223 controls susceptibility to tuberculosis by regulating lung neutrophil recruitment. *J Clin Invest* 123:4836-4848.

Dorhoi, A., G. Nouailles, S. Jorg, K. Hagens, E. Heinemann, L. Pradl, D. Oberbeck-Muller, M.A. Duque-Correa, S.T. Reece, J. Ruland, R. Brosch, J. Tschopp, O. Gross, and S.H. Kaufmann. 2012.

Activation of the NLRP3 inflammasome by Mycobacterium tuberculosis is uncoupled from susceptibility to active tuberculosis. *Eur J Immunol* 42:374-384.

Dorman, S.E., and R.E. Chaisson. 2007. From magic bullets back to the magic mountain: the rise of extensively drug-resistant tuberculosis. *Nat Med* 13:295-298.

Dou, J., Q. Tang, F. Yu, H. Yang, F. Zhao, W. Xu, J. Wang, W. Hu, K. Hu, C. Liou, X. Feng He, and Y. Wang. 2010. Investigation of immunogenic effect of the BCG priming and Ag85A- GM-CSF boosting in Balb/c mice model. *Immunobiology* 215:133-142.

Dranoff, G., A.D. Crawford, M. Sadelain, B. Ream, A. Rashid, R.T. Bronson, G.R. Dickersin, C.J. Bachurski, E.L. Mark, J.A. Whitsett, and et al. 1994. Involvement of granulocyte-macrophage colony-stimulating factor in pulmonary homeostasis. *Science* 264:713-716.

Dranoff, G., and R.C. Mulligan. 1994. Activities of granulocyte-macrophage colony-stimulating factor revealed by gene transfer and gene knockout studies. *Stem cells (Dayton, Ohio)* 12 Suppl 1:173-182; discussion 182-174.

Drennan, M.B., D. Nicolle, V.J.F. Quesniaux, M. Jacobs, N. Allie, J. Mpagi, C. Fremond, H. Wagner, C. Kirschning, and B. Ryffel. 2004. Toll-like receptor 2-deficient mice succumb to Mycobacterium tuberculosis infection. *Am. J. Pathol.* 164:49-57.

Dye, C., S. Scheele, P. Dolin, V. Pathania, and M.C. Raviglione. 1999. Consensus statement. Global burden of tuberculosis: estimated incidence, prevalence, and mortality by country. WHO Global Surveillance and Monitoring Project. *JAMA* 282:677-686.

Eberl, G., S. Marmon, M.J. Sunshine, P.D. Rennert, Y. Choi, and D.R. Littman. 2004. An essential function for the nuclear receptor RORgamma(t) in the generation of fetal lymphoid tissue inducer cells. *Nat Immunol* 5:64-73.

Ejrnaes, M., C.M. Filippi, M.M. Martinic, E.M. Ling, L.M. Togher, S. Crotty, and M.G. von Herrath. 2006. Resolution of a chronic viral infection after interleukin-10 receptor blockade. *Journal of Experimental Medicine* 203:2461-2472.

El Daker, S., A. Sacchi, M. Tempestilli, C. Carducci, D. Goletti, V. Vanini, V. Colizzi, F.N. Lauria, F. Martini, and A. Martino. 2015. Granulocytic Myeloid Derived Suppressor Cells Expansion during Active Pulmonary Tuberculosis Is Associated with High Nitric Oxide Plasma Level. *PLoS One* 10:e0123772.

El-Behi, M., B. Ciric, H. Dai, Y. Yan, M. Cullimore, F. Safavi, G.X. Zhang, B.N. Dittel, and A. Rostami. 2011. The encephalitogenicity of T(H)17 cells is dependent on IL-1- and IL-23-induced production of the cytokine GM-CSF. *Nat Immunol* 12:568-575.

Eruslanov, E.B., I.V. Lyadova, T.K. Kondratieva, K.B. Majorov, I.V. Scheglov, M.O. Orlova, and A.S. Apt. 2005. Neutrophil responses to Mycobacterium tuberculosis infection in genetically susceptible and resistant mice. *Infect Immun* 73:1744-1753.

Eruslanov, E.B., K.B. Majorov, M.O. Orlova, V.V. Mischenko, T.K. Kondratieva, A.S. Apt, and I.V. Lyadova. 2004. Lung cell responses to M. tuberculosis in genetically susceptible and resistant mice following intratracheal challenge. *Clin Exp Immunol* 135:19-28.

Esin, S., and G. Batoni. 2015. Natural killer cells: a coherent model for their functional role in Mycobacterium tuberculosis infection. *J Innate Immun* 7:11-24.

Eum, S.Y., J.H. Kong, M.S. Hong, Y.J. Lee, J.H. Kim, S.H. Hwang, S.N. Cho, L.E. Via, and C.E. Barry, 3rd. 2010. Neutrophils are the predominant infected phagocytic cells in the airways of patients with active pulmonary TB. *Chest* 137:122-128.

Evans, J.H., A. Horowitz, M. Mehrabi, E.L. Wise, J.E. Pease, E.M. Riley, and D.M. Davis. 2011. A distinct subset of human NK cells expressing HLA-DR expand in response to IL-2 and can aid immune responses to BCG. *Eur J Immunol* 41:1924-1933.

Feng, C.G., D. Jankovic, M. Kullberg, A. Cheever, C.A. Scanga, S. Hieny, P. Caspar, G.S. Yap, and A. Sher. 2005. Maintenance of pulmonary Th1 effector function in chronic tuberculosis requires persistent IL-12 production. *J. Immunol.* 174:4185-4192.

Feng, C.G., M. Kaviratne, A.G. Rothfuchs, A. Cheever, S. Hieny, H.A. Young, T.A. Wynn, and A. Sher. 2006. NK cell-derived IFN-gamma differentially regulates innate resistance and neutrophil

response in T cell-deficient hosts infected with Mycobacterium tuberculosis. *J Immunol* 177:7086-7093.

Fine, P.E. 1995. Variation in protection by BCG: implications of and for heterologous immunity. *Lancet* 346:1339-1345.

Fiorentino, D.F., M.W. Bond, and T.R. Mosmann. 1989. Two types of mouse T helper cell. IV. Th2 clones secrete a factor that inhibits cytokine production by Th1 clones. *J Exp Med* 170:2081-2095.

Fleetwood, A.J., T. Lawrence, J.A. Hamilton, and A.D. Cook. 2007. Granulocyte-macrophage colony-stimulating factor (CSF) and macrophage CSF-dependent macrophage phenotypes display differences in cytokine profiles and transcription factor activities: implications for CSF blockade in inflammation. *J Immunol* 178:5245-5252.

Fletcher, H.A., R. Tanner, R.S. Wallis, J. Meyer, Z.R. Manjaly, S. Harris, I. Satti, R.F. Silver, D. Hoft, B. Kampmann, K.B. Walker, H.M. Dockrell, U. Fruth, L. Barker, M.J. Brennan, and H. McShane. 2013. Inhibition of mycobacterial growth in vitro following primary but not secondary vaccination with Mycobacterium bovis BCG. *Clin Vaccine Immunol* 20:1683-1689.

Flynn, J.L. 2006. Lessons from experimental Mycobacterium tuberculosis infections. *Microbes Infect.* 8:1179-1188.

Flynn, J.L., and J. Chan. 2001. Immunology of tuberculosis. *Annu. Rev. Immunol.* 19:93-129.

Flynn, J.L., J. Chan, and P.L. Lin. 2011. Macrophages and control of granulomatous inflammation in tuberculosis. *Mucosal Immunol* 4:271-278.

Flynn, J.L., J. Chan, K.J. Triebold, D.K. Dalton, T.A. Stewart, and B.R. Bloom. 1993. AN ESSENTIAL ROLE FOR INTERFERON-GAMMA IN RESISTANCE TO MYCOBACTERIUM-TUBERCULOSIS INFECTION. *Journal of Experimental Medicine* 178:2249-2254.

Flynn, J.L., H.P. Gideon, J.T. Mattila, and P.L. Lin. 2015. Immunology studies in non-human primate models of tuberculosis. *Immunol Rev* 264:60-73.

Flynn, J.L., M.M. Goldstein, J. Chan, K.J. Triebold, K. Pfeffer, C.J. Lowenstein, R. Schreiber, T.W. Mak, and B.R. Bloom. 1995a. TUMOR-NECROSIS-FACTOR-ALPHA IS REQUIRED IN THE PROTECTIVE IMMUNE-RESPONSE AGAINST MYCOBACTERIUM-TUBERCULOSIS IN MICE. *Immunity* 2:561-572.

Flynn, J.L., M.M. Goldstein, K.J. Triebold, B. Koller, and B.R. Bloom. 1992. MAJOR HISTOCOMPATIBILITY COMPLEX CLASS-I-RESTRICTED T-CELLS ARE REQUIRED FOR RESISTANCE TO MYCOBACTERIUM-TUBERCULOSIS INFECTION. *Proceedings of the National Academy of Sciences of the United States of America* 89:12013-12017.

Flynn, J.L., M.M. Goldstein, K.J. Triebold, J. Sypek, S. Wolf, and B.R. Bloom. 1995b. IL-12 increases resistance of BALB/c mice to Mycobacterium tuberculosis infection. *J Immunol* 155:2515-2524.

Forbes, E.K., C. Sander, E.O. Ronan, H. McShane, A.V.S. Hill, P.C.L. Beverley, and E.Z. Tchilian. 2008. Multifunctional, high-level cytokine-producing Th1 cells in the lung, but not spleen, correlate with protection against Mycobacterium tuberculosis aerosol challenge in mice. *J. Immunol.* 181:4955-4964.

Fort, M.M., J. Cheung, D. Yen, J. Li, S.M. Zurawski, S. Lo, S. Menon, T. Clifford, B. Hunte, R. Lesley, T. Muchamuel, S.D. Hurst, G. Zurawski, M.W. Leach, D.M. Gorman, and D.M. Rennick. 2001. IL-25 induces IL-4, IL-5, and IL-13 and Th2-associated pathologies in vivo. *Immunity* 15:985-995.

Fortin, A., L. Abel, J.L. Casanova, and P. Gros. 2007. Host genetics of mycobacterial diseases in mice and men: forward genetic studies of BCG-osis and tuberculosis. *Annu Rev Genomics Hum Genet* 8:163-192.

Freches, D., H. Korf, O. Denis, X. Havaux, K. Huygen, and M. Romano. 2013. Mice genetically inactivated in interleukin-17A receptor are defective in long-term control of Mycobacterium tuberculosis infection. *Immunology* 140:220-231.

Fremond, C.M., D. Togbe, E. Doz, S. Rose, V. Vasseur, I. Maillet, M. Jacobs, B. Ryffel, and V.F.J. Quesniaux. 2007. IL-1 receptor-mediated signal is an essential component of MyD88-dependent innate response to Mycobacterium tuberculosis infection. *J. Immunol.* 179:1178-1189.

Fremond, C.M., V. Yeremeev, D.M. Nicolle, M. Jacobs, V.F. Quesniaux, and B. Ryffel. 2004. Fatal Mycobacterium tuberculosis infection despite adaptive immune response in the absence of MyD88. *J Clin Invest* 114:1790-1799.

Freyne, B., A. Marchant, and N. Curtis. 2015. BCG-associated heterologous immunity, a historical perspective: intervention studies in animal models of infectious diseases. *Transactions of the Royal Society of Tropical Medicine and Hygiene* 109:287.

Fuchs, A., W. Vermi, J.S. Lee, S. Lonardi, S. Gilfillan, R.D. Newberry, M. Cella, and M. Colonna. 2013. Intraepithelial Type 1 Innate Lymphoid Cells Are a Unique Subset of IL-12- and IL-15-Responsive IFN-gamma-Producing Cells. *Immunity*

Gabrilovich, D.I., and S. Nagaraj. 2009. Myeloid-derived suppressor cells as regulators of the immune system. *Nature reviews* 9:162-174.

Gaffen, S.L., R. Jain, A.V. Garg, and D.J. Cua. 2014. The IL-23-IL-17 immune axis: from mechanisms to therapeutic testing. *Nature reviews* 14:585-600.

Gallegos, A.M., J.W. van Heijst, M. Samstein, X. Su, E.G. Pamer, and M.S. Glickman. 2011. A gamma interferon independent mechanism of CD4 T cell mediated control of M. tuberculosis infection in vivo. *PLoS Pathog* 7:e1002052.

Gandotra, S., S. Jang, P.J. Murray, P. Salgame, and S. Ehrt. 2007. Nucleotide-binding oligomerization domain protein 2-deficient mice control infection with Mycobacterium tuberculosis. *Infect Immun* 75:5127-5134.

Gao, X., J. Chen, Z. Tong, G. Yang, Y. Yao, F. Xu, and J. Zhou. 2015. Interleukin-10 promoter gene polymorphisms and susceptibility to tuberculosis: a meta-analysis. *PLoS One* 10:e0127496.

Garcia-Contreras, L., Y.L. Wong, P. Muttil, D. Padilla, J. Sadoff, J. Derousse, W.A. Germishuizen, S. Goonesekera, K. Elbert, B.R. Bloom, R. Miller, P.B. Fourie, A. Hickey, and D. Edwards. 2008. Immunization by a bacterial aerosol. *Proc Natl Acad Sci U S A* 105:4656-4660.

Gascoyne, D.M., E. Long, H. Veiga-Fernandes, J. de Boer, O. Williams, B. Seddon, M. Coles, D. Kioussis, and H.J. Brady. 2009. The basic leucine zipper transcription factor E4BP4 is essential for natural killer cell development. *Nat Immunol* 10:1118-1124.

Gasson, J.C. 1991. Molecular physiology of granulocyte-macrophage colony-stimulating factor. *Blood* 77:1131-1145.

Gazzinelli, R.T., M. Wysocka, S. Hieny, T. SchartonKersten, A. Cheever, R. Kuhn, W. Muller, G. Trinchieri, and A. Sher. 1996. In the absence of endogenous IL-1O, mice acutely infected with Toxoplasma gondii succumb to a lethal immune response dependent on CD4(+) T cells and accompanied by overproduction of IL-12, IFN-gamma, and TNF-alpha. *J. Immunol.* 157:798-805.

Geiger, T.L., M.C. Abt, G. Gasteiger, M.A. Firth, M.H. O'Connor, C.D. Geary, T.E. O'Sullivan, M.R. van den Brink, E.G. Pamer, A.M. Hanash, and J.C. Sun. 2014. Nfil3 is crucial for development of innate lymphoid cells and host protection against intestinal pathogens. *J Exp Med* 211:1723-1731.

Geijtenbeek, T.B., and Y. van Kooyk. 2003. Pathogens target DC-SIGN to influence their fate DC-SIGN functions as a pathogen receptor with broad specificity. *APMIS : acta pathologica, microbiologica, et immunologica Scandinavica* 111:698-714.

Geldmacher, C., A. Zumla, and M. Hoelscher. 2012. Interaction between HIV and Mycobacterium tuberculosis: HIV-1-induced CD4 T-cell depletion and the development of active tuberculosis. *Current opinion in HIV and AIDS* 7:268-275.

Gerosa, F., C. Nisii, S. Righetti, R. Micciolo, M. Marchesini, A. Cazzadori, and G. Trinchieri. 1999. CD4(+) T cell clones producing both interferon-gamma and interleukin-10 predominate in bronchoalveolar lavages of active pulmonary tuberculosis patients. *Clinical Immunology* 92:224-234.

Gideon, H.P., and J.L. Flynn. 2011. Latent tuberculosis: what the host "sees"? *Immunologic Research* 50:202-212.

Gideon, H.P., J. Phuah, A.J. Myers, B.D. Bryson, M.A. Rodgers, M.T. Coleman, P. Maiello, T. Rutledge, S. Marino, S.M. Fortune, D.E. Kirschner, P.L. Lin, and J.L. Flynn. 2015. Variability in tuberculosis granuloma T cell responses exists, but a balance of pro- and anti-inflammatory cytokines is associated with sterilization. *PLoS Pathog* 11:e1004603.

Gladiator, A., N. Wangler, K. Trautwein-Weidner, and S. LeibundGut-Landmann. 2013. Cutting edge: IL-17-secreting innate lymphoid cells are essential for host defense against fungal infection. *J Immunol* 190:521-525.

Gold, M.C., S. Cerri, S. Smyk-Pearson, M.E. Cansler, T.M. Vogt, J. Delepine, E. Winata, G.M. Swarbrick, W.J. Chua, Y.Y. Yu, O. Lantz, M.S. Cook, M.D. Null, D.B. Jacoby, M.J. Harriff, D.A. Lewinsohn, T.H. Hansen, and D.M. Lewinsohn. 2010. Human mucosal associated invariant T cells detect bacterially infected cells. *PLoS biology* 8:e1000407.

Gold, M.C., R.J. Napier, and D.M. Lewinsohn. 2015. MR1-restricted mucosal associated invariant T (MAIT) cells in the immune response to Mycobacterium tuberculosis. *Immunol Rev* 264:154-166.

Gold, M.J., F. Antignano, T.Y. Halim, J.A. Hirota, M.R. Blanchet, C. Zaph, F. Takei, and K.M. McNagny. 2014. Group 2 innate lymphoid cells facilitate sensitization to local, but not systemic, TH2-inducing allergen exposures. *J Allergy Clin Immunol* 133:1142-1148.

Gong, J.H., M. Zhang, R.L. Modlin, P.S. Linsley, D. Iyer, Y. Lin, and P.F. Barnes. 1996. Interleukin-10 downregulates Mycobacterium tuberculosis-induced Th1 responses and CTLA-4 expression. *Infect Immun* 64:913-918.

Gonzalez-Juarrero, M., J.M. Hattle, A. Izzo, A.P. Junqueira-Kipnis, T.S. Shim, B.C. Trapnell, A.M. Cooper, and I.M. Orme. 2005. Disruption of granulocyte macrophage-colony stimulating factor production in the lungs severely affects the ability of mice to control Mycobacterium tuberculosis infection. *Journal of Leukocyte Biology* 77:914-922.

Gonzalez-Juarrero, M., O.C. Turner, J. Turner, P. Marietta, J.V. Brooks, and I.M. Orme. 2001. Temporal and spatial arrangement of lymphocytes within lung granulomas induced by aerosol infection with Mycobacterium tuberculosis. *Infect Immun* 69:1722-1728.

Goonetilleke, N.P., H. McShane, C.M. Hannan, R.J. Anderson, R.H. Brookes, and A.V. Hill. 2003. Enhanced immunogenicity and protective efficacy against Mycobacterium tuberculosis of bacille Calmette-Guerin vaccine using mucosal administration and boosting with a recombinant modified vaccinia virus Ankara. *J Immunol* 171:1602-1609.

Gopal, R., Y. Lin, N. Obermajer, S. Slight, N. Nuthalapati, M. Ahmed, P. Kalinski, and S.A. Khader. 2012. IL-23-dependent IL-17 drives Th1-cell responses following Mycobacterium bovis BCG vaccination. *European Journal of Immunology* 42:364-373.

Gopal, R., L. Monin, S. Slight, U. Uche, E. Blanchard, B.A. Fallert Junecko, R. Ramos-Payan, C.L. Stallings, T.A. Reinhart, J.K. Kolls, D. Kaushal, U. Nagarajan, J. Rangel-Moreno, and S.A. Khader. 2014. Unexpected role for IL-17 in protective immunity against hypervirulent Mycobacterium tuberculosis HN878 infection. *PLoS Pathog* 10:e1004099.

Gopal, R., J. Rangel-Moreno, S. Slight, Y. Lin, H.F. Nawar, B.A. Fallert Junecko, T.A. Reinhart, J. Kolls, T.D. Randall, T.D. Connell, and S.A. Khader. 2013. Interleukin-17-dependent CXCL13 mediates mucosal vaccine-induced immunity against tuberculosis. *Mucosal Immunol*

Gringhuis, S.I., J. den Dunnen, M. Litjens, M. van der Vlist, and T.B. Geijtenbeek. 2009. Carbohydrate-specific signaling through the DC-SIGN signalosome tailors immunity to Mycobacterium tuberculosis, HIV-1 and Helicobacter pylori. *Nat Immunol* 10:1081-1088.

Grode, L., P. Seiler, S. Baumann, J. Hess, V. Brinkmann, A. Nasser Eddine, P. Mann, C. Goosmann, S. Bandermann, D. Smith, G.J. Bancroft, J.M. Reyrat, D. van Soolingen, B. Raupach, and S.H. Kaufmann. 2005. Increased vaccine efficacy against tuberculosis of recombinant Mycobacterium bovis bacille Calmette-Guerin mutants that secrete listeriolysin. *J Clin Invest* 115:2472-2479.

Gruppo, V., O.C. Turner, I.M. Orme, and J. Turner. 2002. Reduced up-regulation of memory and adhesion/integrin molecules in susceptible mice and poor expression of immunity to pulmonary tuberculosis. *Microbiology (Reading, England)* 148:2959-2966.

Guilliams, M., I. De Kleer, S. Henri, S. Post, L. Vanhoutte, S. De Prijck, K. Deswarte, B. Malissen, H. Hammad, and B.N. Lambrecht. 2013. Alveolar macrophages develop from fetal monocytes that differentiate into long-lived cells in the first week of life via GM-CSF. *J Exp Med* 210:1977-1992.

Gupta, U.D., and V.M. Katoch. 2005. Animal models of tuberculosis. *Tuberculosis (Edinb)* 85:277-293.

Halim, T.Y., A. MacLaren, M.T. Romanish, M.J. Gold, K.M. McNagny, and F. Takei. 2012. Retinoic-acid-receptor-related orphan nuclear receptor alpha is required for natural helper cell development and allergic inflammation. *Immunity* 37:463-474.

Halim, T.Y., C.A. Steer, L. Matha, M.J. Gold, I. Martinez-Gonzalez, K.M. McNagny, A.N. McKenzie, and F. Takei. 2014. Group 2 innate lymphoid cells are critical for the initiation of adaptive T helper 2 cell-mediated allergic lung inflammation. *Immunity* 40:425-435.

Hamilton, J.A. 2002. GM-CSF in inflammation and autoimmunity. *Trends Immunol* 23:403-408.

Hamilton, J.A. 2008. Colony-stimulating factors in inflammation and autoimmunity. *Nature reviews* 8:533-544.

Hamilton, J.A. 2015. GM-CSF as a target in inflammatory/autoimmune disease: current evidence and future therapeutic potential. *Expert review of clinical immunology* 11:457-465.

Hams, E., R.M. Locksley, A.N. McKenzie, and P.G. Fallon. 2013. Cutting edge: IL-25 elicits innate lymphoid type 2 and type II NKT cells that regulate obesity in mice. *J Immunol* 191:5349-5353.

Hanke, T. 2008. STEP trial and HIV-1 vaccines inducing T-cell responses. *Expert Rev Vaccines* 7:303-309.

Harper, J., C. Skerry, S.L. Davis, R. Tasneen, M. Weir, I. Kramnik, W.R. Bishai, M.G. Pomper, E.L. Nuermberger, and S.K. Jain. 2012. Mouse model of necrotic tuberculosis granulomas develops hypoxic lesions. *J Infect Dis* 205:595-602.

Hashimoto, D., A. Chow, C. Noizat, P. Teo, M.B. Beasley, M. Leboeuf, C.D. Becker, P. See, J. Price, D. Lucas, M. Greter, A. Mortha, S.W. Boyer, E.C. Forsberg, M. Tanaka, N. van Rooijen, A. Garcia-Sastre, E.R. Stanley, F. Ginhoux, P.S. Frenette, and M. Merad. 2013. Tissue-resident macrophages self-maintain locally throughout adult life with minimal contribution from circulating monocytes. *Immunity* 38:792-804.

Heidenreich, S., J.H. Gong, A. Schmidt, M. Nain, and D. Gemsa. 1989. Macrophage activation by granulocyte/macrophage colony-stimulating factor. Priming for enhanced release of tumor necrosis factor-alpha and prostaglandin E2. *J Immunol* 143:1198-1205.

Heitmann, L., H. Schoenen, S. Ehlers, R. Lang, and C. Holscher. 2013. Mincle is not essential for controlling Mycobacterium tuberculosis infection. *Immunobiology* 218:506-516.

Hepworth, M.R., T.C. Fung, S.H. Masur, J.R. Kelsen, F.M. McConnell, J. Dubrot, D.R. Withers, S. Hugues, M.A. Farrar, W. Reith, G. Eberl, R.N. Baldassano, T.M. Laufer, C.O. Elson, and G.F. Sonnenberg. 2015. Group 3 innate lymphoid cells mediate intestinal selection of commensal bacteria-specific CD4+ T cells. *Science*

Hepworth, M.R., L.A. Monticelli, T.C. Fung, C.G. Ziegler, S. Grunberg, R. Sinha, A.R. Mantegazza, H.L. Ma, A. Crawford, J.M. Angelosanto, E.J. Wherry, P.A. Koni, F.D. Bushman, C.O. Elson, G. Eberl, D. Artis, and G.F. Sonnenberg. 2013. Innate lymphoid cells regulate CD4+ T-cell responses to intestinal commensal bacteria. *Nature* 498:113-117.

Hernandez, P.P., T. Mahlakoiv, I. Yang, V. Schwierzeck, N. Nguyen, F. Guendel, K. Gronke, B. Ryffel, C. Holscher, L. Dumoutier, J.C. Renauld, S. Suerbaum, P. Staeheli, and A. Diefenbach. 2015. Interferon-lambda and interleukin 22 act synergistically for the induction of interferon-stimulated genes and control of rotavirus infection. *Nat Immunol*

Hesseling, A.C., H. Rabie, B.J. Marais, M. Manders, M. Lips, H.S. Schaaf, R.P. Gie, M.F. Cotton, P.D. van Helden, R.M. Warren, and N. Beyers. 2006. Bacille Calmette-Guerin vaccine-induced

disease in HIV-infected and HIV-uninfected children. *Clinical infectious diseases : an official publication of the Infectious Diseases Society of America* 42:548-558.

Holscher, C., N. Reiling, U.E. Schaible, A. Holscher, C. Bathmann, D. Korbel, I. Lenz, T. Sonntag, S. Kroger, S. Akira, H. Mossmann, C.J. Kirschning, H. Wagner, M. Freudenberg, and S. Ehlers. 2008. Containment of aerogenic Mycobacterium tuberculosis infection in mice does not require MyD88 adaptor function for TLR2, -4 and -9. *Eur J Immunol* 38:680-694.

Horowitz, A., J.C. Hafalla, E. King, J. Lusingu, D. Dekker, A. Leach, P. Moris, J. Cohen, J. Vekemans, T. Villafana, P.H. Corran, P. Bejon, C.J. Drakeley, L. von Seidlein, and E.M. Riley. 2012. Antigen-specific IL-2 secretion correlates with NK cell responses after immunization of Tanzanian children with the RTS,S/AS01 malaria vaccine. *J Immunol* 188:5054-5062.

Hoyler, T., C.S. Klose, A. Souabni, A. Turqueti-Neves, D. Pfeifer, E.L. Rawlins, D. Voehringer, M. Busslinger, and A. Diefenbach. 2012. The transcription factor GATA-3 controls cell fate and maintenance of type 2 innate lymphoid cells. *Immunity* 37:634-648.

Hsieh, C.S., S.E. Macatonia, C.S. Tripp, S.F. Wolf, A. Ogarra, and K.M. Murphy. 1993. DEVELOPMENT OF TH1 CD4+ T-CELLS THROUGH IL-12 PRODUCED BY LISTERIA-INDUCED MACROPHAGES. *Science* 260:547-549.

Hsu, D.H., R. de Waal Malefyt, D.F. Fiorentino, M.N. Dang, P. Vieira, J. de Vries, H. Spits, T.R. Mosmann, and K.W. Moore. 1990. Expression of interleukin-10 activity by Epstein-Barr virus protein BCRF1. *Science* 250:830-832.

Huard, R.C., S. Chitale, M. Leung, L.C. Lazzarini, H. Zhu, E. Shashkina, S. Laal, M.B. Conde, A.L. Kritski, J.T. Belisle, B.N. Kreiswirth, J.R. Lapa e Silva, and J.L. Ho. 2003. The Mycobacterium tuberculosis complex-restricted gene cfp32 encodes an expressed protein that is detectable in tuberculosis patients and is positively correlated with pulmonary interleukin-10. *Infect Immun* 71:6871-6883.

Huber, S., N. Gagliani, E. Esplugues, W. O'Connor, Jr., F.J. Huber, A. Chaudhry, M. Kamanaka, Y. Kobayashi, C.J. Booth, A.Y. Rudensky, M.G. Roncarolo, M. Battaglia, and R.A. Flavell. 2011. Th17 cells express interleukin-10 receptor and are controlled by Foxp3(-) and Foxp3+ regulatory CD4+ T cells in an interleukin-10-dependent manner. *Immunity* 34:554-565.

Hunter, C.A., L.A. EllisNeyes, T. Slifer, S. Kanaly, G. Grunig, M. Fort, D. Rennick, and F.G. Araujo. 1997. IL-10 is required to prevent immune hyperactivity during infection with Trypanosoma cruzi. *J. Immunol.* 158:3311-3316.

Idoko, O.T., O.A. Owolabi, P.K. Owiafe, P. Moris, A. Odutola, A. Bollaerts, E. Ogundare, E. Jongert, M.A. Demoitie, O. Ofori-Anyinam, and M.O. Ota. 2014. Safety and immunogenicity of the M72/AS01 candidate tuberculosis vaccine when given as a booster to BCG in Gambian infants: an open-label randomized controlled trial. *Tuberculosis (Edinb)* 94:564-578.

Inaba, K., M. Inaba, N. Romani, H. Aya, M. Deguchi, S. Ikehara, S. Muramatsu, and R.M. Steinman. 1992. Generation of large numbers of dendritic cells from mouse bone marrow cultures supplemented with granulocyte/macrophage colony-stimulating factor. *J Exp Med* 176:1693-1702.

Jankovic, D., M.C. Kullberg, C.G. Feng, R.S. Goldszmid, C.M. Collazo, M. Wilson, T.A. Wynn, M. Kamanaka, R.A. Flavell, and A. Sheri. 2007. Conventional T-bet(+)Foxp3(-) Th1 cells are the major source of host-protective regulatory IL-10 during intracellular protozoan infection. *Journal of Experimental Medicine* 204:273-283.

Josefowicz, S.Z., L.F. Lu, and A.Y. Rudensky. 2012. Regulatory T cells: mechanisms of differentiation and function. *Annu Rev Immunol* 30:531-564.

Joshi, R., A.L. Reingold, D. Menzies, and M. Pai. 2006. Tuberculosis among health-care workers in low- and middle-income countries: a systematic review. *PLoS medicine* 3:e494.

Jost, S., P.J. Tomezsko, K. Rands, I. Toth, M. Lichterfeld, R.T. Gandhi, and M. Altfeld. 2014. CD4+ T-cell help enhances NK cell function following therapeutic HIV-1 vaccination. *J Virol* 88:8349-8354.

Jung, Y.J., L. Ryan, R. LaCourse, and R.J. North. 2003. Increased interleukin-10 expression is not responsible for failure of T helper 1 immunity to resolve airborne Mycobacterium tuberculosis infection in mice. *Immunology* 109:295-299.

Jung, Y.J., L. Ryan, R. LaCourse, and R.J. North. 2005. Properties and protective value of the secondary versus primary T helper type 1 response to airborne Mycobacterium tuberculosis infection in mice. *J Exp Med* 201:1915-1924.

Junqueira-Kipnis, A.P., A. Kipnis, A. Jamieson, M.G. Juarrero, A. Diefenbach, D.H. Raulet, J. Turner, and I.M. Orme. 2003. NK cells respond to pulmonary infection with Mycobacterium tuberculosis, but play a minimal role in protection. *J Immunol* 171:6039-6045.

Kagina, B.M., B. Abel, T.J. Scriba, E.J. Hughes, A. Keyser, A. Soares, H. Gamieldien, M. Sidibana, M. Hatherill, S. Gelderbloem, H. Mahomed, A. Hawkridge, G. Hussey, G. Kaplan, and W.A. Hanekom. 2010. Specific T cell frequency and cytokine expression profile do not correlate with protection against tuberculosis after bacillus Calmette-Guerin vaccination of newborns. *Am J Respir Crit Care Med* 182:1073-1079.

Kagina, B.M., M.D. Tameris, H. Geldenhuys, M. Hatherill, B. Abel, G.D. Hussey, T.J. Scriba, H. Mahomed, J.C. Sadoff, W.A. Hanekom, N. Mansoor, J. Hughes, M. de Kock, W. Whatney, H. Africa, C. Krohn, A. Veldsman, A.L. Kany, M. Douoguih, M.G. Pau, J. Hendriks, B. McClainc, J. Benko, M.A. Snowden, and D.A. Hokey. 2014. The novel tuberculosis vaccine, AERAS-402, is safe in healthy infants previously vaccinated with BCG, and induces dose-dependent CD4 and CD8T cell responses. *Vaccine* 32:5908-5917.

Kamath, A.B., and S.M. Behar. 2005. Anamnestic responses of mice following Mycobacterium tuberculosis infection. *Infect Immun* 73:6110-6118.

Kamath, A.B., J. Woodworth, X. Xiong, C. Taylor, Y. Weng, and S.M. Behar. 2004. Cytolytic CD8+ T cells recognizing CFP10 are recruited to the lung after Mycobacterium tuberculosis infection. *J Exp Med* 200:1479-1489.

Kamath, A.T., T. Hanke, H. Briscoe, and W.J. Britton. 1999. Co-immunization with DNA vaccines expressing granulocyte-macrophage colony-stimulating factor and mycobacterial secreted proteins enhances T-cell immunity, but not protective efficacy against Mycobacterium tuberculosis. *Immunology* 96:511-516.

Karo, J.M., D.G. Schatz, and J.C. Sun. 2014. The RAG recombinase dictates functional heterogeneity and cellular fitness in natural killer cells. *Cell* 159:94-107.

Kaufmann, S.H., M.F. Cotton, B. Eisele, M. Gengenbacher, L. Grode, A.C. Hesseling, and G. Walzl. 2014. The BCG replacement vaccine VPM1002: from drawing board to clinical trial. *Expert Rev Vaccines* 13:619-630.

Keane, J., S. Gershon, R.P. Wise, E. Mirabile-Levens, J. Kasznica, W.D. Schwieterman, J.N. Siegel, and M.M. Braun. 2001. Tuberculosis associated with infliximab, a tumor necrosis factor (alpha)-neutralizing agent. *New England Journal of Medicine* 345:1098-1104.

Keller, C., R. Hoffmann, R. Lang, S. Brandau, C. Hermann, and S. Ehlers. 2006. Genetically determined susceptibility to tuberculosis in mice causally involves accelerated and enhanced recruitment of granulocytes. *Infect Immun* 74:4295-4309.

Kennedy, M.K., M. Glaccum, S.N. Brown, E.A. Butz, J.L. Viney, M. Embers, N. Matsuki, K. Charrier, L. Sedger, C.R. Willis, K. Brasel, P.J. Morrissey, K. Stocking, J.C. Schuh, S. Joyce, and J.J. Peschon. 2000. Reversible defects in natural killer and memory CD8 T cell lineages in interleukin 15-deficient mice. *J Exp Med* 191:771-780.

Kerkhoff, A.D., R. Wood, D.M. Lowe, M. Vogt, and S.D. Lawn. 2013. Blood neutrophil counts in HIV-infected patients with pulmonary tuberculosis: association with sputum mycobacterial load. *PLoS One* 8:e67956.

Khader, S.A., G.K. Bell, J.E. Pearl, J.J. Fountain, J. Rangel-Moreno, G.E. Cilley, F. Shen, S.M. Eaton, S.L. Gaffen, S.L. Swain, R.M. Locksley, L. Haynes, T.D. Randall, and A.M. Cooper. 2007. IL-23 and IL-17 in the establishment of protective pulmonary CD4(+) T cell responses after vaccination and during Mycobacterium tuberculosis challenge. *Nature Immunology* 8:369-377.

Khader, S.A., and A.M. Cooper. 2008. IL-23 and IL-17 in tuberculosis. *Cytokine* 41:79-83.

Khader, S.A., S. Partida-Sanchez, G. Bell, D.M. Jelley-Gibbs, S. Swain, J.E. Pearl, N. Ghilardi, F.J. deSauvage, F.E. Lund, and A.M. Cooper. 2006. Interleukin 12p40 is required for dendritic cell migration and T cell priming after Mycobacterium tuberculosis infection. *Journal of Experimental Medicine* 203:1805-1815.

Khader, S.A., J.E. Pearl, K. Sakamoto, L. Gilmartin, G.K. Bell, D.M. Jelley-Gibbs, N. Ghilardi, F. deSauvage, and A.M. Cooper. 2005. IL-23 compensates for the absence of IL-12p70 and is essential for the IL-17 response during tuberculosis but is dispensable for protection and antigen-specific IFN-gamma responses if IL-12p70 is available. *J. Immunol.* 175:788-795.

King, I.L., M.A. Kroenke, and B.M. Segal. 2010. GM-CSF-dependent, CD103+ dermal dendritic cells play a critical role in Th effector cell differentiation after subcutaneous immunization. *J Exp Med* 207:953-961.

Klein Wolterink, R.G., N. Serafini, M. van Nimwegen, C.A. Vosshenrich, M.J. de Bruijn, D. Fonseca Pereira, H. Veiga Fernandes, R.W. Hendriks, and J.P. Di Santo. 2013. Essential, dose-dependent role for the transcription factor Gata3 in the development of IL-5+ and IL-13+ type 2 innate lymphoid cells. *Proc Natl Acad Sci U S A* 110:10240-10245.

Kleinnijenhuis, J., J. Quintin, F. Preijers, L.A. Joosten, D.C. Ifrim, S. Saeed, C. Jacobs, J. van Loenhout, D. de Jong, H.G. Stunnenberg, R.J. Xavier, J.W. van der Meer, R. van Crevel, and M.G. Netea. 2012. Bacille Calmette-Guerin induces NOD2-dependent nonspecific protection from reinfection via epigenetic reprogramming of monocytes. *Proc Natl Acad Sci U S A* 109:17537-17542.

Kleinnijenhuis, J., J. Quintin, F. Preijers, L.A. Joosten, C. Jacobs, R.J. Xavier, J.W. van der Meer, R. van Crevel, and M.G. Netea. 2014. BCG-induced trained immunity in NK cells: Role for non-specific protection to infection. *Clinical immunology (Orlando, Fla.)* 155:213-219.

Klose, C.S., M. Flach, L. Mohle, L. Rogell, T. Hoyler, K. Ebert, C. Fabiunke, D. Pfeifer, V. Sexl, D. Fonseca-Pereira, R.G. Domingues, H. Veiga-Fernandes, S.J. Arnold, M. Busslinger, I.R. Dunay, Y. Tanriver, and A. Diefenbach. 2014. Differentiation of type 1 ILCs from a common progenitor to all helper-like innate lymphoid cell lineages. *Cell* 157:340-356.

Klose, C.S., E.A. Kiss, V. Schwierzeck, K. Ebert, T. Hoyler, Y. d'Hargues, N. Goppert, A.L. Croxford, A. Waisman, Y. Tanriver, and A. Diefenbach. 2013. A T-bet gradient controls the fate and function of CCR6-RORgammat+ innate lymphoid cells. *Nature* 494:261-265.

Knaul, J.K., S. Jorg, D. Oberbeck-Mueller, E. Heinemann, L. Scheuermann, V. Brinkmann, H.J. Mollenkopf, V. Yeremeev, S.H. Kaufmann, and A. Dorhoi. 2014. Lung-residing myeloid-derived suppressors display dual functionality in murine pulmonary tuberculosis. *Am J Respir Crit Care Med* 190:1053-1066.

Koch, R. 1882. The Etiology of tuberculosis. *Berliner Klinischen Wochenscrift* 15:221-230.

Kozakiewicz, L., J. Phuah, J. Flynn, and J. Chan. 2013. The role of B cells and humoral immunity in Mycobacterium tuberculosis infection. *Advances in experimental medicine and biology* 783:225-250.

Kramnik, I., W.F. Dietrich, P. Demant, and B.R. Bloom. 2000. Genetic control of resistance to experimental infection with virulent Mycobacterium tuberculosis. *Proc Natl Acad Sci U S A* 97:8560-8565.

Kursar, M., M. Koch, H.W. Mittrucker, G. Nouailles, K. Bonhagen, T. Kamradt, and S.H. Kaufmann. 2007. Cutting Edge: Regulatory T cells prevent efficient clearance of Mycobacterium tuberculosis. *J Immunol* 178:2661-2665.

Ladel, C.H., C. Blum, A. Dreher, K. Reifenberg, and S.H. Kaufmann. 1995. Protective role of gamma/delta T cells and alpha/beta T cells in tuberculosis. *Eur J Immunol* 25:2877-2881.

Lamkanfi, M. 2011. Emerging inflammasome effector mechanisms. *Nature reviews* 11:213-220.

Lawn, S.D., G. Meintjes, H. McIlleron, A.D. Harries, and R. Wood. 2013. Management of HIV-associated tuberculosis in resource-limited settings: a state-of-the-art review. *BMC medicine* 11:253.

Lawn, S.D., and A.I. Zumla. 2011. Tuberculosis. *Lancet* 378:57-72.

Lazarevic, V., D.J. Yankura, S.J. DiVito, and J.L. Flynn. 2005. Induction of Mycobacterium tuberculosis-specific primary and secondary T-cell responses in interleukin-15-deficient mice. *Infect Immun* 73:2910-2922.

Le Bourhis, L., E. Martin, I. Peguillet, A. Guihot, N. Froux, M. Core, E. Levy, M. Dusseaux, V. Meyssonnier, V. Premel, C. Ngo, B. Riteau, L. Duban, D. Robert, S. Huang, M. Rottman, C. Soudais, and O. Lantz. 2010. Antimicrobial activity of mucosal-associated invariant T cells. *Nat Immunol* 11:701-708.

Lee, J.S., M. Cella, K.G. McDonald, C. Garlanda, G.D. Kennedy, M. Nukaya, A. Mantovani, R. Kopan, C.A. Bradfield, R.D. Newberry, and M. Colonna. 2012. AHR drives the development of gut ILC22 cells and postnatal lymphoid tissues via pathways dependent on and independent of Notch. *Nat Immunol* 13:144-151.

Leemans, J.C., N.P. Juffermans, S. Florquin, N. van Rooijen, M.J. Vervoordeldonk, A. Verbon, S.J. van Deventer, and T. van der Poll. 2001. Depletion of alveolar macrophages exerts protective effects in pulmonary tuberculosis in mice. *J Immunol* 166:4604-4611.

LeVine, A.M., J.A. Reed, K.E. Kurak, E. Cianciolo, and J.A. Whitsett. 1999. GM-CSF-deficient mice are susceptible to pulmonary group B streptococcal infection. *J Clin Invest* 103:563-569.

Li, C., I. Corraliza, and J. Langhorne. 1999. A defect in interleukin-10 leads to enhanced malarial disease in Plasmodium chabaudi chabaudi infection in mice. *Infect. Immun.* 67:4435-4442.

Lin, P.L., J. Dietrich, E. Tan, R.M. Abalos, J. Burgos, C. Bigbee, M. Bigbee, L. Milk, H.P. Gideon, M. Rodgers, C. Cochran, K.M. Guinn, D.R. Sherman, E. Klein, C. Janssen, J.L. Flynn, and P. Andersen. 2012. The multistage vaccine H56 boosts the effects of BCG to protect cynomolgus macaques against active tuberculosis and reactivation of latent Mycobacterium tuberculosis infection. *J Clin Invest* 122:303-314.

Lin, P.L., C.B. Ford, M.T. Coleman, A.J. Myers, R. Gawande, T. Ioerger, J. Sacchettini, S.M. Fortune, and J.L. Flynn. 2014. Sterilization of granulomas is common in active and latent tuberculosis despite within-host variability in bacterial killing. *Nat Med* 20:75-79.

Lin, P.L., A. Myers, L.K. Smith, C. Bigbee, M. Bigbee, C. Fuhrman, H. Grieser, I. Chiosea, N.N. Voitenek, S.V. Capuano, E. Klein, and J.L. Flynn. 2010. Tumor Necrosis Factor Neutralization Results in Disseminated Disease in Acute and Latent Mycobacterium tuberculosis Infection With Normal Granuloma Structure in a Cynomolgus Macaque Model. *Arthritis and Rheumatism* 62:340-350.

Lin, P.L., M. Rodgers, L. Smith, M. Bigbee, A. Myers, C. Bigbee, I. Chiosea, S.V. Capuano, C. Fuhrman, E. Klein, and J.L. Flynn. 2009. Quantitative comparison of active and latent tuberculosis in the cynomolgus macaque model. *Infect Immun* 77:4631-4642.

Lindenstrom, T., N.P. Knudsen, E.M. Agger, and P. Andersen. 2013. Control of chronic mycobacterium tuberculosis infection by CD4 KLRG1- IL-2-secreting central memory cells. *J Immunol* 190:6311-6319.

Liu, Q., W. Li, D. Li, Y. Feng, and C. Tao. 2015. The association of interleukin-10 -1082, -819, -592 polymorphisms and tuberculosis risk. *Saudi medical journal* 36:407-417.

Lockhart, E., A.M. Green, and J.L. Flynn. 2006. IL-17 production is dominated by gamma delta T cells rather than CD4 T cells during Mycobacterium tuberculosis infection. *J. Immunol.* 177:4662-4669.

Loebbermann, J., C. Schnoeller, H. Thornton, L. Durant, N.P. Sweeney, M. Schuijs, A. O'Garra, C. Johansson, and P.J. Openshaw. 2012. IL-10 regulates viral lung immunopathology during acute respiratory syncytial virus infection in mice. *PLoS One* 7:e32371.

Lowe, D.M., A.K. Bandara, G.E. Packe, R.D. Barker, R.J. Wilkinson, C.J. Griffiths, and A.R. Martineau. 2013. Neutrophilia independently predicts death in tuberculosis. *The European respiratory journal* 42:1752-1757.

Lowe, D.M., P.S. Redford, R.J. Wilkinson, A. O'Garra, and A.R. Martineau. 2012. Neutrophils in tuberculosis: friend or foe? *Trends Immunol* 33:14-25.

Luabeya, A.K., B.M. Kagina, M.D. Tameris, H. Geldenhuys, S.T. Hoff, Z. Shi, I. Kromann, M. Hatherill, H. Mahomed, W.A. Hanekom, P. Andersen, T.J. Scriba, E. Schoeman, C. Krohn, C.L. Day, H.

Africa, L. Makhethe, E. Smit, Y. Brown, S. Suliman, E.J. Hughes, P. Bang, M.A. Snowden, B. McClain, and G.D. Hussey. 2015. First-in-human trial of the post-exposure tuberculosis vaccine H56:IC31 in Mycobacterium tuberculosis infected and non-infected healthy adults. *Vaccine*

Macatonia, S.E., N.A. Hosken, M. Litton, P. Vieira, C.S. Hsieh, J.A. Culpepper, M. Wysocka, G. Trinchieri, K.M. Murphy, and A. O'Garra. 1995. Dendritic cells produce IL-12 and direct the development of Th1 cells from naive CD4+ T cells. *J Immunol* 154:5071-5079.

MacMicking, J.D., R.J. North, R. LaCourse, J.S. Mudgett, S.K. Shah, and C.F. Nathan. 1997. Identification of nitric oxide synthase as a protective locus against tuberculosis. *Proceedings of the National Academy of Sciences of the United States of America* 94:5243-5248.

Maglione, P.J., and J. Chan. 2009. How B cells shape the immune response against Mycobacterium tuberculosis. *European Journal of Immunology* 39:676-686.

Maglione, P.J., J. Xu, A. Casadevall, and J. Chan. 2008. Fc gamma receptors regulate immune activation and susceptibility during Mycobacterium tuberculosis infection. *J Immunol* 180:3329-3338.

Maglione, P.J., J. Xu, and J. Chan. 2007. B cells moderate inflammatory progression and enhance bacterial containment upon pulmonary challenge with Mycobacterium tuberculosis. *J. Immunol.* 178:7222-7234.

Mahairas, G.G., P.J. Sabo, M.J. Hickey, D.C. Singh, and C.K. Stover. 1996. Molecular analysis of genetic differences between Mycobacterium bovis BCG and virulent M. bovis. *Journal of bacteriology* 178:1274-1282.

Manca, C., L. Tsenova, A. Bergtold, S. Freeman, M. Tovey, J.M. Musser, C.E. Barry, V.H. Freedman, and G. Kaplan. 2001. Virulence of a Mycobacterium tuberculosis clinical isolate in mice is determined by failure to induce Th1 type immunity and is associated with induction of IFN-alpha/beta. *Proceedings of the National Academy of Sciences of the United States of America* 98:5752-5757.

Manca, C., L. Tsenova, S. Freeman, A.K. Barczak, M. Tovey, P.J. Murray, C. Barry, and G. Kaplan. 2005. Hypervirulent M-tuberculosis W/Beijing strains upregulate type IIFNs and increase expression of negative regulators of the Jak-Stat pathway. *Journal of Interferon and Cytokine Research* 25:694-701.

Manjaly Thomas, Z.R., and H. McShane. 2015. Aerosol immunisation for TB: matching route of vaccination to route of infection. *Transactions of the Royal Society of Tropical Medicine and Hygiene* 109:175-181.

Marakalala, M.J., R. Guler, L. Matika, G. Murray, M. Jacobs, F. Brombacher, A.G. Rothfuchs, A. Sher, and G.D. Brown. 2011. The Syk/CARD9-coupled receptor Dectin-1 is not required for host resistance to Mycobacterium tuberculosis in mice. *Microbes and infection / Institut Pasteur* 13:198-201.

Martineau, A.R., P.M. Timms, G.H. Bothamley, Y. Hanifa, K. Islam, A.P. Claxton, G.E. Packe, J.C. Moore-Gillon, M. Darmalingam, R.N. Davidson, H.J. Milburn, L.V. Baker, R.D. Barker, N.J. Woodward, T.R. Venton, K.E. Barnes, C.J. Mullett, A.K. Coussens, C.M. Rutterford, C.A. Mein, G.R. Davies, R.J. Wilkinson, V. Nikolayevskyy, F.A. Drobniewski, S.M. Eldridge, and C.J. Griffiths. 2011. High-dose vitamin D(3) during intensive-phase antimicrobial treatment of pulmonary tuberculosis: a double-blind randomised controlled trial. *Lancet* 377:242-250.

Marzo, E., C. Vilaplana, G. Tapia, J. Diaz, V. Garcia, and P.J. Cardona. 2014. Damaging role of neutrophilic infiltration in a mouse model of progressive tuberculosis. *Tuberculosis (Edinb)* 94:55-64.

Matsumiya, M., I. Satti, A. Chomka, S.A. Harris, L. Stockdale, J. Meyer, H.A. Fletcher, and H. McShane. 2015. Gene Expression and Cytokine Profile Correlate With Mycobacterial Growth in a Human BCG Challenge Model. *J Infect Dis* 211:1499-1509.

Matsumiya, M., E. Stylianou, K. Griffiths, Z. Lang, J. Meyer, S.A. Harris, R. Rowland, A.M. Minassian, A.A. Pathan, H. Fletcher, and H. McShane. 2013. Roles for Treg expansion and HMGB1 signaling through the TLR1-2-6 axis in determining the magnitude of the antigen-specific immune response to MVA85A. *PLoS One* 8:e67922.

Mattila, J.T., P. Maiello, T. Sun, L.E. Via, and J.L. Flynn. 2015. Granzyme B-expressing neutrophils correlate with bacterial load in granulomas from Mycobacterium tuberculosis-infected cynomolgus macaques. *Cell Microbiol*

Mayer-Barber, K.D., B.B. Andrade, D.L. Barber, S. Hieny, C.G. Feng, P. Caspar, S. Oland, S. Gordon, and A. Sher. 2011. Innate and Adaptive Interferons Suppress IL-1 alpha and IL-1 beta Production by Distinct Pulmonary Myeloid Subsets during Mycobacterium tuberculosis Infection. *Immunity* 35:1023-1034.

Mayer-Barber, K.D., B.B. Andrade, S.D. Oland, E.P. Amaral, D.L. Barber, J. Gonzales, S.C. Derrick, R. Shi, N.P. Kumar, W. Wei, X. Yuan, G. Zhang, Y. Cai, S. Babu, M. Catalfamo, A.M. Salazar, L.E. Via, C.E. Barry, 3rd, and A. Sher. 2014. Host-directed therapy of tuberculosis based on interleukin-1 and type I interferon crosstalk. *Nature* 511:99-103.

Mayer-Barber, K.D., D.L. Barber, K. Shenderov, S.D. White, M.S. Wilson, A. Cheever, D. Kugler, S. Hieny, P. Caspar, G. Nunez, D. Schlueter, R.A. Flavell, F.S. Sutterwala, and A. Sher. 2010. Cutting Edge: Caspase-1 Independent IL-1 beta Production Is Critical for Host Resistance to Mycobacterium tuberculosis and Does Not Require TLR Signaling In Vivo. *J. Immunol.* 184:3326-3330.

Mayer-Barber, K.D., and A. Sher. 2015. Cytokine and lipid mediator networks in tuberculosis. *Immunol Rev* 264:264-275.

McNab, F., K. Mayer-Barber, A. Sher, A. Wack, and A. O'Garra. 2015. Type I interferons in infectious disease. *Nature reviews* 15:87-103.

McNab, F.W., J. Ewbank, A. Howes, L. Moreira-Teixeira, A. Martirosyan, N. Ghilardi, M. Saraiva, and A. O'Garra. 2014. Type I IFN induces IL-10 production in an IL-27-independent manner and blocks responsiveness to IFN-gamma for production of IL-12 and bacterial killing in Mycobacterium tuberculosis-infected macrophages. *J Immunol* 193:3600-3612.

McNab, F.W., J. Ewbank, R. Rajsbaum, E. Stavropoulos, A. Martirosyan, P.S. Redford, X. Wu, C.M. Graham, M. Saraiva, P. Tsichlis, D. Chaussabel, S.C. Ley, and A. O'Garra. 2013. TPL-2-ERK1/2 signaling promotes host resistance against intracellular bacterial infection by negative regulation of type I IFN production. *J Immunol* 191:1732-1743.

McShane, H., and A. Williams. 2014. A review of preclinical animal models utilised for TB vaccine evaluation in the context of recent human efficacy data. *Tuberculosis (Edinb)* 94:105-110.

Medina, E., and R.J. North. 1998. Resistance ranking of some common inbred mouse strains to Mycobacterium tuberculosis and relationship to major histocompatibility complex haplotype and Nramp1 genotype. *Immunology* 93:270-274.

Medzhitov, R., and C. Janeway, Jr. 2000. Innate immune recognition: mechanisms and pathways. *Immunol Rev* 173:89-97.

Mielke, L.A., J.R. Groom, L.C. Rankin, C. Seillet, F. Masson, T. Putoczki, and G.T. Belz. 2013. TCF-1 controls ILC2 and NKp46+RORgammat+ innate lymphocyte differentiation and protection in intestinal inflammation. *J Immunol* 191:4383-4391.

Min, L., S.A. Mohammad Isa, W. Shuai, C.B. Piang, F.W. Nih, M. Kotaka, and C. Ruedl. 2010. Cutting edge: granulocyte-macrophage colony-stimulating factor is the major CD8+ T cell-derived licensing factor for dendritic cell activation. *J Immunol* 184:4625-4629.

Minassian, A.M., I. Satti, I.D. Poulton, J. Meyer, A.V. Hill, and H. McShane. 2012. A human challenge model for Mycobacterium tuberculosis using Mycobacterium bovis bacille Calmette-Guerin. *J Infect Dis* 205:1035-1042.

Mishra, B.B., P. Moura-Alves, A. Sonawane, N. Hacohen, G. Griffiths, L.F. Moita, and E. Anes. 2010. Mycobacterium tuberculosis protein ESAT-6 is a potent activator of the NLRP3/ASC inflammasome. *Cell Microbiol* 12:1046-1063.

Mishra, B.B., V.A. Rathinam, G.W. Martens, A.J. Martinot, H. Kornfeld, K.A. Fitzgerald, and C.M. Sassetti. 2013. Nitric oxide controls the immunopathology of tuberculosis by inhibiting NLRP3 inflammasome-dependent processing of IL-1beta. *Nat Immunol* 14:52-60.

Mittrucker, H.W., U. Steinhoff, A. Kohler, M. Krause, D. Lazar, P. Mex, D. Miekley, and S.H. Kaufmann. 2007. Poor correlation between BCG vaccination-induced T cell responses and protection against tuberculosis. *Proc Natl Acad Sci U S A* 104:12434-12439.

Mjosberg, J., J. Bernink, K. Golebski, J.J. Karrich, C.P. Peters, B. Blom, A.A. te Velde, W.J. Fokkens, C.M. van Drunen, and H. Spits. 2012. The transcription factor GATA3 is essential for the function of human type 2 innate lymphoid cells. *Immunity* 37:649-659.

Mogues, T., M.E. Goodrich, L. Ryan, R. LaCourse, and R.J. North. 2001. The relative importance of T cell subsets in immunity and immunopathology of Airborne Mycobacterium tuberculosis infection in mice. *Journal of Experimental Medicine* 193:271-280.

Mohan, V.P., C.A. Scanga, K.M. Yu, H.M. Scott, K.E. Tanaka, E. Tsang, M.C. Tsai, J.L. Flynn, and J. Chan. 2001. Effects of tumor necrosis factor alpha on host immune response in chronic persistent tuberculosis: Possible role for limiting pathology. *Infect. Immun.* 69:1847-1855.

Mohapatra, A., S.J. Van Dyken, C. Schneider, J.C. Nussbaum, H.E. Liang, and R.M. Locksley. 2015. Group 2 innate lymphoid cells utilize the IRF4-IL-9 module to coordinate epithelial cell maintenance of lung homeostasis. *Mucosal Immunol*

Molofsky, A.B., J.C. Nussbaum, H.E. Liang, S.J. Van Dyken, L.E. Cheng, A. Mohapatra, A. Chawla, and R.M. Locksley. 2013. Innate lymphoid type 2 cells sustain visceral adipose tissue eosinophils and alternatively activated macrophages. *J Exp Med* 210:535-549.

Molofsky, A.B., F. Van Gool, H.E. Liang, S.J. Van Dyken, J.C. Nussbaum, J. Lee, J.A. Bluestone, and R.M. Locksley. 2015. Interleukin-33 and Interferon-gamma Counter-Regulate Group 2 Innate Lymphoid Cell Activation during Immune Perturbation. *Immunity*

Monin, L., K.L. Griffiths, S. Slight, Y. Lin, J. Rangel-Moreno, and S.A. Khader. 2015. Immune requirements for protective Th17 recall responses to Mycobacterium tuberculosis challenge. *Mucosal Immunol*

Monticelli, L.A., G.F. Sonnenberg, M.C. Abt, T. Alenghat, C.G. Ziegler, T.A. Doering, J.M. Angelosanto, B.J. Laidlaw, C.Y. Yang, T. Sathaliyawala, M. Kubota, D. Turner, J.M. Diamond, A.W. Goldrath, D.L. Farber, R.G. Collman, E.J. Wherry, and D. Artis. 2011. Innate lymphoid cells promote lung-tissue homeostasis after infection with influenza virus. *Nat Immunol* 12:1045-1054.

Moore, K.W., R.D. Malefyt, R.L. Coffman, and A. O'Garra. 2001. Interleukin-10 and the interleukin-10 receptor. *Annu. Rev. Immunol.* 19:683-765.

Moro, K., T. Yamada, M. Tanabe, T. Takeuchi, T. Ikawa, H. Kawamoto, J. Furusawa, M. Ohtani, H. Fujii, and S. Koyasu. 2010. Innate production of T(H)2 cytokines by adipose tissue-associated c-Kit(+)Sca-1(+) lymphoid cells. *Nature* 463:540-544.

Morrison, J., M. Pai, and P.C. Hopewell. 2008. Tuberculosis and latent tuberculosis infection in close contacts of people with pulmonary tuberculosis in low-income and middle-income countries: a systematic review and meta-analysis. *Lancet Infect Dis* 8:359-368.

Mortha, A., A. Chudnovskiy, D. Hashimoto, M. Bogunovic, S.P. Spencer, Y. Belkaid, and M. Merad. 2014. Microbiota-Dependent Crosstalk Between Macrophages and ILC3 Promotes Intestinal Homeostasis. *Science*

Murai, M., O. Turovskaya, G. Kim, R. Madan, C.L. Karp, H. Cheroutre, and M. Kronenberg. 2009. Interleukin 10 acts on regulatory T cells to maintain expression of the transcription factor Foxp3 and suppressive function in mice with colitis. *Nat Immunol* 10:1178-1184.

Murray, P.J. 2006. Understanding and exploiting the endogenous interleukin-10/STAT3-mediated anti-inflammatory response. *Curr Opin Pharmacol* 6:379-386.

Murray, P.J., and R.A. Young. 1999. Increased antimycobacterial immunity in interleukin-10-deficient mice. *Infect Immun* 67:3087-3095.

Nambiar, J.K., A.A. Ryan, C.U. Kong, W.J. Britton, and J.A. Triccas. 2010. Modulation of pulmonary DC function by vaccine-encoded GM-CSF enhances protective immunity against Mycobacterium tuberculosis infection. *Eur J Immunol* 40:153-161.

Nandi, B., and S.M. Behar. 2011. Regulation of neutrophils by interferon-gamma limits lung inflammation during tuberculosis infection. *J Exp Med* 208:2251-2262.

Nathan, C., and M.U. Shiloh. 2000. Reactive oxygen and nitrogen intermediates in the relationship between mammalian hosts and microbial pathogens. *Proc Natl Acad Sci U S A* 97:8841-8848.

Ndiaye, B.P., F. Thienemann, M. Ota, B.S. Landry, M. Camara, S. Dieye, T.N. Dieye, H. Esmail, R. Goliath, K. Huygen, V. January, I. Ndiaye, T. Oni, M. Raine, M. Romano, I. Satti, S. Sutton, A. Thiam, K.A. Wilkinson, S. Mboup, R.J. Wilkinson, and H. McShane. 2015. Safety, immunogenicity, and efficacy of the candidate tuberculosis vaccine MVA85A in healthy adults infected with HIV-1: a randomised, placebo-controlled, phase 2 trial. *The Lancet. Respiratory medicine* 3:190-200.

Neill, D.R., S.H. Wong, A. Bellosi, R.J. Flynn, M. Daly, T.K. Langford, C. Bucks, C.M. Kane, P.G. Fallon, R. Pannell, H.E. Jolin, and A.N. McKenzie. 2010. Nuocytes represent a new innate effector leukocyte that mediates type-2 immunity. *Nature* 464:1367-1370.

Newton, S.M., R.J. Smith, K.A. Wilkinson, M.P. Nicol, N.J. Garton, K.J. Staples, G.R. Stewart, J.R. Wain, A.R. Martineau, S. Fandrich, T. Smallie, B. Foxwell, A. Al-Obaidi, J. Shafi, K. Rajakumar, B. Kampmann, P.W. Andrew, L. Ziegler-Heitbrock, M.R. Barer, and R.J. Wilkinson. 2006. A deletion defining a common Asian lineage of Mycobacterium tuberculosis associates with immune subversion. *Proc Natl Acad Sci U S A* 103:15594-15598.

Nishinakamura, R., R. Wiler, U. Dirksen, Y. Morikawa, K. Arai, A. Miyajima, S. Burdach, and R. Murray. 1996. The pulmonary alveolar proteinosis in granulocyte macrophage colony-stimulating factor/interleukins 3/5 beta c receptor-deficient mice is reversed by bone marrow transplantation. *J Exp Med* 183:2657-2662.

North, R.J. 1998. Mice incapable of making IL-4 or IL-10 display normal resistance to infection with Mycobacterium tuberculosis. *Clinical and Experimental Immunology* 113:55-58.

North, R.J., and Y.J. Jung. 2004. Immunity to tuberculosis. *Annu. Rev. Immunol.* 22:599-623.

Novikov, A., M. Cardone, R. Thompson, K. Shenderov, K.D. Kirschman, K.D. Mayer-Barber, T.G. Myers, R.L. Rabin, G. Trinchieri, A. Sher, and C.G. Feng. 2011. Mycobacterium tuberculosis Triggers Host Type I IFN Signaling To Regulate IL-1 beta Production in Human Macrophages. *J. Immunol.* 187:2540-2547.

O'Garra, A., F.J. Barrat, A.G. Castro, A. Vicari, and C. Hawrylowicz. 2008. Strategies for use of IL-10 or its antagonists in human disease. *Immunol Rev* 223:114-131.

O'Garra, A., P.S. Redford, F.W. McNab, C.I. Bloom, R.J. Wilkinson, and M.P. Berry. 2013. The immune response in tuberculosis. *Annu Rev Immunol* 31:475-527.

O'Leary, J.G., M. Goodarzi, D.L. Drayton, and U.H. von Andrian. 2006. T cell- and B cell-independent adaptive immunity mediated by natural killer cells. *Nat Immunol* 7:507-516.

Okamoto Yoshida, Y., M. Umemura, A. Yahagi, R.L. O'Brien, K. Ikuta, K. Kishihara, H. Hara, S. Nakae, Y. Iwakura, and G. Matsuzaki. 2010. Essential role of IL-17A in the formation of a mycobacterial infection-induced granuloma in the lung. *Journal of immunology (Baltimore, Md. : 1950)* 184:4414-4422.

Oliphant, C.J., Y.Y. Hwang, J.A. Walker, M. Salimi, S.H. Wong, J.M. Brewer, A. Englezakis, J.L. Barlow, E. Hams, S.T. Scanlon, G.S. Ogg, P.G. Fallon, and A.N. McKenzie. 2014. MHCII-mediated dialog between group 2 innate lymphoid cells and CD4(+) T cells potentiates type 2 immunity and promotes parasitic helminth expulsion. *Immunity* 41:283-295.

Ordway, D., M. Henao-Tamayo, M. Harton, G. Palanisamy, J. Troudt, C. Shanley, R.J. Basaraba, and I.M. Orme. 2007. The hypervirulent Mycobacterium tuberculosis strain HN878 induces a potent TH1 response followed by rapid down-regulation. *J Immunol* 179:522-531.

Ordway, D.J., S. Shang, M. Henao-Tamayo, A. Obregon-Henao, L. Nold, M. Caraway, C.A. Shanley, R.J. Basaraba, C.G. Duncan, and I.M. Orme. 2011. Mycobacterium bovis BCG-mediated protection against W-Beijing strains of Mycobacterium tuberculosis is diminished concomitant with the emergence of regulatory T cells. *Clin Vaccine Immunol* 18:1527-1535.

Orme, I.M., and F.M. Collins. 1983. Protection against Mycobacterium tuberculosis infection by adoptive immunotherapy. Requirement for T cell-deficient recipients. *J Exp Med* 158:74-83.

Orme, I.M., R.T. Robinson, and A.M. Cooper. 2015. The balance between protective and pathogenic immune responses in the TB-infected lung. *Nat Immunol* 16:57-63.

Pacheco, A.G., C.C. Cardoso, and M.O. Moraes. 2008. IFNG +874T/A, IL10 -1082G/A and TNF -308G/A polymorphisms in association with tuberculosis susceptibility: a meta-analysis study. *Hum Genet* 123:477-484.

Paine, R., 3rd, A.M. Preston, S. Wilcoxen, H. Jin, B.B. Siu, S.B. Morris, J.A. Reed, G. Ross, J.A. Whitsett, and J.M. Beck. 2000. Granulocyte-macrophage colony-stimulating factor in the innate immune response to Pneumocystis carinii pneumonia in mice. *J Immunol* 164:2602-2609.

Pan, H., B.S. Yan, M. Rojas, Y.V. Shebzukhov, H. Zhou, L. Kobzik, D.E. Higgins, M.J. Daly, B.R. Bloom, and I. Kramnik. 2005. Ipr1 gene mediates innate immunity to tuberculosis. *Nature* 434:767-772.

Pasula, R., A.K. Azad, J.C. Gardner, L.S. Schlesinger, and F.X. McCormack. 2015. Keratinocyte growth factor administration attenuates murine pulmonary Mycobacterium tuberculosis infection through GM-CSF-dependent macrophage activation and phagolysosome fusion. *J Biol Chem*

Paust, S., H.S. Gill, B.Z. Wang, M.P. Flynn, E.A. Moseman, B. Senman, M. Szczepanik, A. Telenti, P.W. Askenase, R.W. Compans, and U.H. von Andrian. 2010. Critical role for the chemokine receptor CXCR6 in NK cell-mediated antigen-specific memory of haptens and viruses. *Nat Immunol* 11:1127-1135.

Paust, S., and U.H. von Andrian. 2011. Natural killer cell memory. *Nat Immunol* 12:500-508.

Philips, J.A., and J.D. Ernst. 2012. Tuberculosis Pathogenesis and Immunity. In Annual Review of Pathology: Mechanisms of Disease, Vol 7. A.K. Abbas, S.J. Galli, and P.M. Howley, editors. Annual Reviews, Palo Alto. 353-384.

Phuah, J.Y., J.T. Mattila, P.L. Lin, and J.L. Flynn. 2012. Activated B cells in the granulomas of nonhuman primates infected with Mycobacterium tuberculosis. *Am J Pathol* 181:508-514.

Pichugin, A.V., B.S. Yan, A. Sloutsky, L. Kobzik, and I. Kramnik. 2009. Dominant role of the sst1 locus in pathogenesis of necrotizing lung granulomas during chronic tuberculosis infection and reactivation in genetically resistant hosts. *Am J Pathol* 174:2190-2201.

Pitt, J.M., S. Blankley, H. McShane, and A. O'Garra. 2012a. Vaccination against tuberculosis: How can we better BCG? *Microb Pathog*

Pitt, J.M., E. Stavropoulos, P.S. Redford, A.M. Beebe, G.J. Bancroft, D.B. Young, and A. O'Garra. 2012b. Blockade of IL-10 Signaling during Bacillus Calmette-Guerin Vaccination Enhances and Sustains Th1, Th17, and Innate Lymphoid IFN-gamma and IL-17 Responses and Increases Protection to Mycobacterium tuberculosis Infection. *J Immunol* 189:4079-4087.

Portevin, D., S. Gagneux, I. Comas, and D. Young. 2011. Human macrophage responses to clinical isolates from the Mycobacterium tuberculosis complex discriminate between ancient and modern lineages. *PLoS Pathog* 7:e1001307.

Price, A.E., H.E. Liang, B.M. Sullivan, R.L. Reinhardt, C.J. Eisley, D.J. Erle, and R.M. Locksley. 2010. Systemically dispersed innate IL-13-expressing cells in type 2 immunity. *Proc Natl Acad Sci U S A* 107:11489-11494.

Qiu, J., J.J. Heller, X. Guo, Z.M. Chen, K. Fish, Y.X. Fu, and L. Zhou. 2012. The aryl hydrocarbon receptor regulates gut immunity through modulation of innate lymphoid cells. *Immunity* 36:92-104.

Quintin, J., S.C. Cheng, J.W. van der Meer, and M.G. Netea. 2014. Innate immune memory: towards a better understanding of host defense mechanisms. *Curr Opin Immunol* 29:1-7.

Ramakrishnan, L. 2012. Revisiting the role of the granuloma in tuberculosis. *Nature reviews* 12:352-366.

Ramakrishnan, L. 2013. Looking within the zebrafish to understand the tuberculous granuloma. *Advances in experimental medicine and biology* 783:251-266.

Rankin, L.C., J.R. Groom, M. Chopin, M.J. Herold, J.A. Walker, L.A. Mielke, A.N. McKenzie, S. Carotta, S.L. Nutt, and G.T. Belz. 2013. The transcription factor T-bet is essential for the development of NKp46(+) innate lymphocytes via the Notch pathway. *Nat Immunol* 14:389-395.

Ranson, T., C.A. Vosshenrich, E. Corcuff, O. Richard, W. Muller, and J.P. Di Santo. 2003. IL-15 is an essential mediator of peripheral NK-cell homeostasis. *Blood* 101:4887-4893.

Redford, P.S., A. Boonstra, S. Read, J. Pitt, C. Graham, E. Stavropoulos, G.J. Bancroft, and A. O'Garra. 2010. Enhanced protection to Mycobacterium tuberculosis infection in IL-10-deficient mice is accompanied by early and enhanced Th1 responses in the lung. *European Journal of Immunology* 40:2200-2210.

Redford, P.S., K.D. Mayer-Barber, F.W. McNab, E. Stavropoulos, A. Wack, A. Sher, and A. O'Garra. 2014. Influenza A virus impairs control of Mycobacterium tuberculosis coinfection through a type I interferon receptor-dependent pathway. *J Infect Dis* 209:270-274.

Redford, P.S., P.J. Murray, and A. O'Garra. 2011. The role of IL-10 in immune regulation during M. tuberculosis infection. *Mucosal Immunology* 4:261-270.

Reed, M.B., P. Domenech, C. Manca, H. Su, A.K. Barczak, B.N. Kreiswirth, G. Kaplan, and C.E. Barry, 3rd. 2004. A glycolipid of hypervirulent tuberculosis strains that inhibits the innate immune response. *Nature* 431:84-87.

Reeves, R.K., H. Li, S. Jost, E. Blass, H. Li, J.L. Schafer, V. Varner, C. Manickam, L. Eslamizar, M. Altfeld, U.H. von Andrian, and D.H. Barouch. 2015. Antigen-specific NK cell memory in rhesus macaques. *Nat Immunol* 16:927-932.

Reichman, L.B. 1979. Tuberculin skin testing. The state of the art. *Chest* 76:764-770.

Reiley, W.W., M.D. Calayag, S.T. Wittmer, J.L. Huntington, J.E. Pearl, J.J. Fountain, C.A. Martino, A.D. Roberts, A.M. Cooper, G.M. Winslow, and D.L. Woodland. 2008. ESAT-6-specific CD4 T cell responses to aerosol Mycobacterium tuberculosis infection are initiated in the mediastinal lymph nodes. *Proceedings of the National Academy of Sciences of the United States of America* 105:10961-10966.

Reiley, W.W., S. Shafiani, S.T. Wittmer, G. Tucker-Heard, J.J. Moon, M.K. Jenkins, K.B. Urdahl, G.M. Winslow, and D.L. Woodland. 2010. Distinct functions of antigen-specific CD4 T cells during murine Mycobacterium tuberculosis infection. *Proc Natl Acad Sci U S A* 107:19408-19413.

Reiling, N., C. Holscher, A. Fehrenbach, S. Kroger, C.J. Kirschning, S. Goyert, and S. Ehlers. 2002. Cutting edge: Toll-like receptor (TLR)2- and TLR4-mediated pathogen recognition in resistance to airborne infection with Mycobacterium tuberculosis. *J. Immunol.* 169:3480-3484.

Rhoades, E.R., A.A. Frank, and I.M. Orme. 1997. Progression of chronic pulmonary tuberculosis in mice aerogenically infected with virulent Mycobacterium tuberculosis. *Tubercle and lung disease : the official journal of the International Union against Tuberculosis and Lung Disease* 78:57-66.

Richeldi, L. 2006. An update on the diagnosis of tuberculosis infection. *Am J Respir Crit Care Med* 174:736-742.

Ritz, N., B. Dutta, S. Donath, D. Casalaz, T.G. Connell, M. Tebruegge, R. Robins-Browne, W.A. Hanekom, W.J. Britton, and N. Curtis. 2012. The influence of bacille Calmette-Guerin vaccine strain on the immune response against tuberculosis: a randomized trial. *Am J Respir Crit Care Med* 185:213-222.

Ritz, N., W.A. Hanekom, R. Robins-Browne, W.J. Britton, and N. Curtis. 2008. Influence of BCG vaccine strain on the immune response and protection against tuberculosis. *FEMS microbiology reviews* 32:821-841.

Roach, D.R., E. Martin, A.G.D. Bean, D.M. Rennick, H. Briscoe, and W.J. Britton. 2001. Endogenous inhibition of antimycobacterial immunity by IL-10 varies between mycobacterial species. *Scand. J. Immunol.* 54:163-170.

Robinette, M.L., A. Fuchs, V.S. Cortez, J.S. Lee, Y. Wang, S.K. Durum, S. Gilfillan, and M. Colonna. 2015. Transcriptional programs define molecular characteristics of innate lymphoid cell classes and subsets. *Nat Immunol* 16:306-317.

Robinson, R.T., I.M. Orme, and A.M. Cooper. 2015. The onset of adaptive immunity in the mouse model of tuberculosis and the factors that compromise its expression. *Immunol Rev* 264:46-59.

Roca, F.J., and L. Ramakrishnan. 2013. TNF dually mediates resistance and susceptibility to mycobacteria via mitochondrial reactive oxygen species. *Cell* 153:521-534.

Rothchild, A.C., P. Jayaraman, C. Nunes-Alves, and S.M. Behar. 2014. iNKT Cell Production of GM-CSF Controls Mycobacterium tuberculosis. *PLoS Pathog* 10:e1003805.

Rothfuchs, A.G., A. Bafica, C.G. Feng, J.G. Egen, D.L. Williams, G.D. Brown, and A. Sher. 2007. Dectin-1 interaction with Mycobacterium tuberculosis leads to enhanced IL-12p40 production by splenic dendritic cells. *J Immunol* 179:3463-3471.

Rowland, R., and H. McShane. 2011. Tuberculosis vaccines in clinical trials. *Expert Rev. Vaccines* 10:645-658.

Russell, D.G., P.J. Cardona, M.J. Kim, S. Allain, and F. Altare. 2009. Foamy macrophages and the progression of the human tuberculosis granuloma. *Nat Immunol* 10:943-948.

Russell, D.G., B.C. VanderVen, W. Lee, R.B. Abramovitch, M.J. Kim, S. Homolka, S. Niemann, and K.H. Rohde. 2010. Mycobacterium tuberculosis wears what it eats. *Cell host & microbe* 8:68-76.

Ryan, A.A., T.M. Wozniak, E. Shklovskaya, M.A. O'Donnell, B. Fazekas de St Groth, W.J. Britton, and J.A. Triccas. 2007. Improved protection against disseminated tuberculosis by Mycobacterium bovis bacillus Calmette-Guerin secreting murine GM-CSF is associated with expansion and activation of APCs. *J Immunol* 179:8418-8424.

Sada-Ovalle, I., A. Chiba, A. Gonzales, M.B. Brenner, and S.M. Behar. 2008. Innate invariant NKT cells recognize Mycobacterium tuberculosis-infected macrophages, produce interferon-gamma, and kill intracellular bacteria. *PLoS Pathog* 4:e1000239.

Sakai, S., K.D. Kauffman, J.M. Schenkel, C.C. McBerry, K.D. Mayer-Barber, D. Masopust, and D.L. Barber. 2014. Cutting Edge: Control of Mycobacterium tuberculosis Infection by a Subset of Lung Parenchyma-Homing CD4 T Cells. *J Immunol* 192:2965-2969.

Samstein, M., H.A. Schreiber, I.M. Leiner, B. Susac, M.S. Glickman, and E.G. Pamer. 2013. Essential yet limited role for CCR2(+) inflammatory monocytes during Mycobacterium tuberculosis-specific T cell priming. *eLife* 2:e01086.

Satoh-Takayama, N., S. Lesjean-Pottier, P. Vieira, S. Sawa, G. Eberl, C.A. Vosshenrich, and J.P. Di Santo. 2010. IL-7 and IL-15 independently program the differentiation of intestinal CD3-NKp46+ cell subsets from Id2-dependent precursors. *J Exp Med* 207:273-280.

Satoh-Takayama, N., N. Serafini, T. Verrier, A. Rekiki, J.C. Renauld, G. Frankel, and J.P. Di Santo. 2014. The chemokine receptor CXCR6 controls the functional topography of interleukin-22 producing intestinal innate lymphoid cells. *Immunity* 41:776-788.

Satoh-Takayama, N., C.A. Vosshenrich, S. Lesjean-Pottier, S. Sawa, M. Lochner, F. Rattis, J.J. Mention, K. Thiam, N. Cerf-Bensussan, O. Mandelboim, G. Eberl, and J.P. Di Santo. 2008. Microbial flora drives interleukin 22 production in intestinal NKp46+ cells that provide innate mucosal immune defense. *Immunity* 29:958-970.

Satti, I., J. Meyer, S.A. Harris, Z.R. Manjaly Thomas, K. Griffiths, R.D. Antrobus, R. Rowland, R.L. Ramon, M. Smith, S. Sheehan, H. Bettinson, and H. McShane. 2014. Safety and immunogenicity of a candidate tuberculosis vaccine MVA85A delivered by aerosol in BCG-vaccinated healthy adults: a phase 1, double-blind, randomised controlled trial. *Lancet Infect Dis* 14:939-946.

Saunders, B.M., A.A. Frank, I.M. Orme, and A.M. Cooper. 2002. CD4 is required for the development of a protective granulomatous response to pulmonary tuberculosis. *Cellular Immunology* 216:65-72.

Scanga, C.A., A. Bafica, C.G. Feng, A.W. Cheever, S. Hieny, and A. Sher. 2004. MyD88-deficient mice display a profound loss in resistance to Mycobacterium tuberculosis associated with partially impaired Th1 cytokine and nitric oxide synthase 2 expression. *Infect. Immun.* 72:2400-2404.

Scanga, C.A., V.P. Mohan, H. Joseph, K.M. Yu, J. Chan, and J.L. Flynn. 1999. Reactivation of latent tuberculosis: Variations on the Cornell murine model. *Infect. Immun.* 67:4531-4538.

Scanga, C.A., V.P. Mohan, K. Tanaka, D. Alland, J.L. Flynn, and J. Chan. 2001. The inducible nitric oxide synthase locus confers protection against aerogenic challenge of both clinical and laboratory strains of Mycobacterium tuberculosis in mice. *Infect. Immun.* 69:7711-7717.

Scanga, C.A., V.P. Mohan, K. Yu, H. Joseph, K. Tanaka, J. Chan, and J.L. Flynn. 2000. Depletion of CD4(+) T cells causes reactivation of murine persistent tuberculosis despite continued expression of interferon gamma and nitric oxide synthase 2. *J Exp Med* 192:347-358.

Schaible, U.E., H.L. Collins, F. Priem, and S.H. Kaufmann. 2002. Correction of the iron overload defect in beta-2-microglobulin knockout mice by lactoferrin abolishes their increased susceptibility to tuberculosis. *J Exp Med* 196:1507-1513.

Schneider, C., S.P. Nobs, M. Kurrer, H. Rehrauer, C. Thiele, and M. Kopf. 2014. Induction of the nuclear receptor PPAR-gamma by the cytokine GM-CSF is critical for the differentiation of fetal monocytes into alveolar macrophages. *Nat Immunol* 15:1026-1037.

Schutz, C., G. Meintjes, F. Almajid, R.J. Wilkinson, and A. Pozniak. 2010. Clinical management of tuberculosis and HIV-1 co-infection. *The European respiratory journal* 36:1460-1481.

Scott-Browne, J.P., S. Shafiani, G. Tucker-Heard, K. Ishida-Tsubota, J.D. Fontenot, A.Y. Rudensky, M.J. Bevan, and K.B. Urdahl. 2007. Expansion and function of Foxp3-expressing T regulatory cells during tuberculosis. *J Exp Med* 204:2159-2169.

Seehus, C.R., P. Aliahmad, B. de la Torre, I.D. Iliev, L. Spurka, V.A. Funari, and J. Kaye. 2015. The development of innate lymphoid cells requires TOX-dependent generation of a common innate lymphoid cell progenitor. *Nat Immunol* 16:599-608.

Seillet, C., L.C. Rankin, J.R. Groom, L.A. Mielke, J. Tellier, M. Chopin, N.D. Huntington, G.T. Belz, and S. Carotta. 2014. Nfil3 is required for the development of all innate lymphoid cell subsets. *J Exp Med*

Serafini, N., R.G. Klein Wolterink, N. Satoh-Takayama, W. Xu, C.A. Vosshenrich, R.W. Hendriks, and J.P. Di Santo. 2014. Gata3 drives development of RORgammat+ group 3 innate lymphoid cells. *J Exp Med* 211:199-208.

Serafini, N., C.A. Vosshenrich, and J.P. Di Santo. 2015. Transcriptional regulation of innate lymphoid cell fate. *Nature reviews*

Seymour, J.F., and J.J. Presneill. 2002. Pulmonary alveolar proteinosis: progress in the first 44 years. *Am J Respir Crit Care Med* 166:215-235.

Shafiani, S., C. Dinh, J.M. Ertelt, A.O. Moguche, I. Siddiqui, K.S. Smigiel, P. Sharma, D.J. Campbell, S.S. Way, and K.B. Urdahl. 2013. Pathogen-specific Treg cells expand early during mycobacterium tuberculosis infection but are later eliminated in response to Interleukin-12. *Immunity* 38:1261-1270.

Shafiani, S., G. Tucker-Heard, A. Kariyone, K. Takatsu, and K.B. Urdahl. 2010. Pathogen-specific regulatory T cells delay the arrival of effector T cells in the lung during early tuberculosis. *J Exp Med* 207:1409-1420.

Shibata, Y., P.Y. Berclaz, Z.C. Chroneos, M. Yoshida, J.A. Whitsett, and B.C. Trapnell. 2001. GM-CSF regulates alveolar macrophage differentiation and innate immunity in the lung through PU.1. *Immunity* 15:557-567.

Silva, B.D., M.M. Trentini, A.C. da Costa, A. Kipnis, and A.P. Junqueira-Kipnis. 2014. Different phenotypes of CD8+ T cells associated with bacterial load in active tuberculosis. *Immunology letters* 160:23-32.

Silva, R.A., and R. Appelberg. 2001. Blocking the receptor for interleukin 10 protects mice from lethal listeriosis. *Antimicrobial Agents and Chemotherapy* 45:1312-1314.

Silva, R.A., T.F. Pais, and R. Appelberg. 2001. Blocking the receptor for IL-10 improves antimycobacterial chemotherapy and vaccination. *J. Immunol.* 167:1535-1541.

Slight, S.R., J. Rangel-Moreno, R. Gopal, Y. Lin, B.A. Fallert Junecko, S. Mehra, M. Selman, E. Becerril-Villanueva, J. Baquera-Heredia, L. Pavon, D. Kaushal, T.A. Reinhart, T.D. Randall, and S.A. Khader. 2013. CXCR5(+) T helper cells mediate protective immunity against tuberculosis. *J Clin Invest* 123:712-726.

Slobedman, B., P.A. Barry, J.V. Spencer, S. Avdic, and A. Abendroth. 2009. Virus-Encoded Homologs of Cellular Interleukin-10 and Their Control of Host Immune Function. *Journal of Virology* 83:9618-9629.

Smaill, F., M. Jeyanathan, M. Smieja, M.F. Medina, N. Thanthrige-Don, A. Zganiacz, C. Yin, A. Heriazon, D. Damjanovic, L. Puri, J. Hamid, F. Xie, R. Foley, J. Bramson, J. Gauldie, and Z. Xing. 2013. A human type 5 adenovirus-based tuberculosis vaccine induces robust T cell responses in humans despite preexisting anti-adenovirus immunity. *Sci Transl Med* 5:205ra134.

Sojka, D.K., B. Plougastel-Douglas, L. Yang, M.A. Pak-Wittel, M.N. Artyomov, Y. Ivanova, C. Zhong, J.M. Chase, P.B. Rothman, J. Yu, J.K. Riley, J. Zhu, Z. Tian, and W.M. Yokoyama. 2014. Tissue-resident natural killer (NK) cells are cell lineages distinct from thymic and conventional splenic NK cells. *eLife* 3:e01659.

Sonnenberg, G.F., and D. Artis. 2015. Innate lymphoid cells in the initiation, regulation and resolution of inflammation. *Nat Med*

Sonnenberg, G.F., L.A. Monticelli, T. Alenghat, T.C. Fung, N.A. Hutnick, J. Kunisawa, N. Shibata, S. Grunberg, R. Sinha, A.M. Zahm, M.R. Tardif, T. Sathaliyawala, M. Kubota, D.L. Farber, R.G. Collman, A. Shaked, L.A. Fouser, D.B. Weiner, P.A. Tessier, J.R. Friedman, H. Kiyono, F.D. Bushman, K.M. Chang, and D. Artis. 2012. Innate lymphoid cells promote anatomical containment of lymphoid-resident commensal bacteria. *Science* 336:1321-1325.

Sonnenberg, G.F., L.A. Monticelli, M.M. Elloso, L.A. Fouser, and D. Artis. 2011. CD4(+) lymphoid tissue-inducer cells promote innate immunity in the gut. *Immunity* 34:122-134.

Sorgi, C.A., S. Rose, N. Court, D. Carlos, F.W. Paula-Silva, P.A. Assis, F.G. Frantz, B. Ryffel, V. Quesniaux, and L.H. Faccioli. 2012. GM-CSF priming drives bone marrow-derived macrophages to a pro-inflammatory pattern and downmodulates PGE2 in response to TLR2 ligands. *PLoS One* 7:e40523.

Spits, H., D. Artis, M. Colonna, A. Diefenbach, J.P. Di Santo, G. Eberl, S. Koyasu, R.M. Locksley, A.N. McKenzie, R.E. Mebius, F. Powrie, and E. Vivier. 2013. Innate lymphoid cells--a proposal for uniform nomenclature. *Nature reviews* 13:145-149.

Spits, H., and T. Cupedo. 2012. Innate lymphoid cells: emerging insights in development, lineage relationships, and function. *Annu Rev Immunol* 30:647-675.

Spooner, C.J., J. Lesch, D. Yan, A.A. Khan, A. Abbas, V. Ramirez-Carrozzi, M. Zhou, R. Soriano, J. Eastham-Anderson, L. Diehl, W.P. Lee, Z. Modrusan, R. Pappu, M. Xu, J. DeVoss, and H. Singh. 2013. Specification of type 2 innate lymphocytes by the transcriptional determinant Gfi1. *Nat Immunol* 14:1229-1236.

Sreevatsan, S., X. Pan, K.E. Stockbauer, N.D. Connell, B.N. Kreiswirth, T.S. Whittam, and J.M. Musser. 1997. Restricted structural gene polymorphism in the Mycobacterium tuberculosis complex indicates evolutionarily recent global dissemination. *Proc Natl Acad Sci U S A* 94:9869-9874.

Srivastava, S., and J.D. Ernst. 2013. Cutting edge: Direct recognition of infected cells by CD4 T cells is required for control of intracellular Mycobacterium tuberculosis in vivo. *J Immunol* 191:1016-1020.

Srivastava, S., and J.D. Ernst. 2014. Cell-to-cell transfer of M. tuberculosis antigens optimizes CD4 T cell priming. *Cell host & microbe* 15:741-752.

Srivastava, S., J.D. Ernst, and L. Desvignes. 2014. Beyond macrophages: the diversity of mononuclear cells in tuberculosis. *Immunol Rev* 262:179-192.

Stanley, E., G.J. Lieschke, D. Grail, D. Metcalf, G. Hodgson, J.A. Gall, D.W. Maher, J. Cebon, V. Sinickas, and A.R. Dunn. 1994. Granulocyte/macrophage colony-stimulating factor-deficient mice show no major perturbation of hematopoiesis but develop a characteristic pulmonary pathology. *Proc Natl Acad Sci U S A* 91:5592-5596.

Subbian, S., N. Bandyopadhyay, L. Tsenova, P. O'Brien, V. Khetani, N.L. Kushner, B. Peixoto, P. Soteropoulos, J.S. Bader, P.C. Karakousis, D. Fallows, and G. Kaplan. 2013. Early innate immunity determines outcome of Mycobacterium tuberculosis pulmonary infection in rabbits. *Cell communication and signaling : CCS* 11:60.

Subbian, S., L. Tsenova, P. O'Brien, G. Yang, N.L. Kushner, S. Parsons, B. Peixoto, D. Fallows, and G. Kaplan. 2012. Spontaneous latency in a rabbit model of pulmonary tuberculosis. *Am J Pathol* 181:1711-1724.

Subramanian Vignesh, K., J.A. Landero Figueroa, A. Porollo, J.A. Caruso, and G.S. Deepe, Jr. 2013. Granulocyte macrophage-colony stimulating factor induced Zn sequestration enhances macrophage superoxide and limits intracellular pathogen survival. *Immunity* 39:697-710.

Sugawara, I., T. Udagawa, and H. Yamada. 2004. Rat neutrophils prevent the development of tuberculosis. *Infect Immun* 72:1804-1806.

Sugawara, I., H. Yamada, S.C. Hua, and S. Mizuno. 2001. Role of interleukin (IL)-1 type 1 receptor in mycobacterial infection. *Microbiol. Immunol.* 45:743-750.

Sun, J.C., J.N. Beilke, and L.L. Lanier. 2009. Adaptive immune features of natural killer cells. *Nature* 457:557-561.

Szeliga, J., D.S. Daniel, C.H. Yang, Z. Sever-Chroneos, C. Jagannath, and Z.C. Chroneos. 2008. Granulocyte-macrophage colony stimulating factor-mediated innate responses in tuberculosis. *Tuberculosis (Edinb)* 88:7-20.

Tabarsi, P., M. Marjani, N. Mansouri, P. Farnia, S. Boisson-Dupuis, J. Bustamante, L. Abel, P. Adimi, J.L. Casanova, and D. Mansouri. 2011. Lethal Tuberculosis in a Previously Healthy Adult with IL-12 Receptor Deficiency. *J. Clin. Immunol.* 31:537-539.

Takeuchi, O., and S. Akira. 2010. Pattern recognition receptors and inflammation. *Cell* 140:805-820.

Tameris, M., H. Geldenhuys, A.K. Luabeya, E. Smit, J.E. Hughes, S. Vermaak, W.A. Hanekom, M. Hatherill, H. Mahomed, H. McShane, and T.J. Scriba. 2014. The candidate TB vaccine, MVA85A, induces highly durable Th1 responses. *PLoS One* 9:e87340.

Tameris, M.D., M. Hatherill, B.S. Landry, T.J. Scriba, M.A. Snowden, S. Lockhart, J.E. Shea, J.B. McClain, G.D. Hussey, W.A. Hanekom, H. Mahomed, and H. McShane. 2013. Safety and efficacy of MVA85A, a new tuberculosis vaccine, in infants previously vaccinated with BCG: a randomised, placebo-controlled phase 2b trial. *Lancet*

Tanner, R., K. Kakalacheva, E. Miller, A.A. Pathan, R. Chalk, C.R. Sander, T. Scriba, M. Tameris, T. Hawkridge, H. Mahomed, G. Hussey, W. Hanekom, A. Checkley, H. McShane, and H.A. Fletcher. 2014. Serum indoleamine 2,3-dioxygenase activity is associated with reduced immunogenicity following vaccination with MVA85A. *BMC infectious diseases* 14:660.

Teles, R.M., T.G. Graeber, S.R. Krutzik, D. Montoya, M. Schenk, D.J. Lee, E. Komisopoulou, K. Kelly-Scumpia, R. Chun, S.S. Iyer, E.N. Sarno, T.H. Rea, M. Hewison, J.S. Adams, S.J. Popper, D.A. Relman, S. Stenger, B.R. Bloom, G. Cheng, and R.L. Modlin. 2013. Type I interferon suppresses type II interferon-triggered human anti-mycobacterial responses. *Science* 339:1448-1453.

Tobin, D.M., F.J. Roca, S.F. Oh, R. McFarland, T.W. Vickery, J.P. Ray, D.C. Ko, Y. Zou, N.D. Bang, T.T. Chau, J.C. Vary, T.R. Hawn, S.J. Dunstan, J.J. Farrar, G.E. Thwaites, M.C. King, C.N. Serhan, and L. Ramakrishnan. 2012. Host genotype-specific therapies can optimize the inflammatory response to mycobacterial infections. *Cell* 148:434-446.

Tobin, D.M., J.C. Vary, Jr., J.P. Ray, G.S. Walsh, S.J. Dunstan, N.D. Bang, D.A. Hagge, S. Khadge, M.C. King, T.R. Hawn, C.B. Moens, and L. Ramakrishnan. 2010. The lta4h locus modulates susceptibility to mycobacterial infection in zebrafish and humans. *Cell* 140:717-730.

Trapnell, B.C., and J.A. Whitsett. 2002. Gm-CSF regulates pulmonary surfactant homeostasis and alveolar macrophage-mediated innate host defense. *Annual review of physiology* 64:775-802.

Trinchieri, G. 2003. Interleukin-12 and the regulation of innate resistance and adaptive immunity. *Nature reviews* 3:133-146.

Trunz, B.B., P. Fine, and C. Dye. 2006. Effect of BCG vaccination on childhood tuberculous meningitis and miliary tuberculosis worldwide: a meta-analysis and assessment of cost-effectiveness. *Lancet* 367:1173-1180.

Tsai, M.C., S. Chakravarty, G. Zhu, J. Xu, K. Tanaka, C. Koch, J. Tufariello, J. Flynn, and J. Chan. 2006. Characterization of the tuberculous granuloma in murine and human lungs: cellular composition and relative tissue oxygen tension. *Cell Microbiol* 8:218-232.

Tsiganov, E.N., E.M. Verbina, T.V. Radaeva, V.V. Sosunov, G.A. Kosmiadi, I.Y. Nikitina, and I.V. Lyadova. 2014. Gr-1dimCD11b+ immature myeloid-derived suppressor cells but not neutrophils are markers of lethal tuberculosis infection in mice. *J Immunol* 192:4718-4727.

Turner, J., M. Gonzalez-Juarrero, D.L. Ellis, R.J. Basaraba, A. Kipnis, I.M. Orme, and A.M. Cooper. 2002. In vivo IL-10 production reactivates chronic pulmonary tuberculosis in C57BL/6 mice. *J. Immunol.* 169:6343-6351.

Turner, J., M. Gonzalez-Juarrero, B.M. Saunders, J.V. Brooks, P. Marietta, D.L. Ellis, A.A. Frank, and A.M. Cooper. 2001. Immunological basis for reactivation of tuberculosis in mice. *Infect. Immun.* 69:3264-3270.

Turner, J.E., P.J. Morrison, C. Wilhelm, M. Wilson, H. Ahlfors, J.C. Renauld, U. Panzer, H. Helmby, and B. Stockinger. 2013. IL-9-mediated survival of type 2 innate lymphoid cells promotes damage control in helminth-induced lung inflammation. *J Exp Med* 210:2951-2965.

Uchida, K., D.C. Beck, T. Yamamoto, P.Y. Berclaz, S. Abe, M.K. Staudt, B.C. Carey, M.D. Filippi, S.E. Wert, L.A. Denson, J.T. Puchalski, D.M. Hauck, and B.C. Trapnell. 2007. GM-CSF autoantibodies and neutrophil dysfunction in pulmonary alveolar proteinosis. *N Engl J Med* 356:567-579.

Ulrichs, T., G.A. Kosmiadi, V. Trusov, S. Jorg, L. Pradl, M. Titukhina, V. Mishenko, N. Gushina, and S.H. Kaufmann. 2004. Human tuberculous granulomas induce peripheral lymphoid follicle-like structures to orchestrate local host defence in the lung. *The Journal of pathology* 204:217-228.

Umemura, M., H. Nishimura, K. Hirose, T. Matsuguchi, and Y. Yoshikai. 2001. Overexpression of IL-15 in vivo enhances protection against Mycobacterium bovis bacillus Calmette-Guerin infection via augmentation of NK and T cytotoxic 1 responses. *J Immunol* 167:946-956.

Umemura, M., A. Yahagi, S. Hamada, M.D. Begum, H. Watanabe, K. Kawakami, T. Suda, K. Sudo, S. Nakae, Y. Iwakura, and G. Matsuzaki. 2007. IL-17-mediated regulation of innate and acquired immune response against pulmonary Mycobacterium bovis bacille Calmette-Guerin infection. *J. Immunol.* 178:3786-3796.

Urdahl, K.B. 2014. Understanding and overcoming the barriers to T cell-mediated immunity against tuberculosis. *Seminars in immunology* 26:578-587.

Urdahl, K.B., S. Shafiani, and J.D. Ernst. 2011. Initiation and regulation of T-cell responses in tuberculosis. *Mucosal Immunology* 4:288-293.

van de Veerdonk, F.L., A.C. Teirlinck, J. Kleinnijenhuis, B.J. Kullberg, R. van Crevel, J.W. van der Meer, L.A. Joosten, and M.G. Netea. 2010. Mycobacterium tuberculosis induces IL-17A responses through TLR4 and dectin-1 and is critically dependent on endogenous IL-1. *J Leukoc Biol* 88:227-232.

Van Maele, L., C. Carnoy, D. Cayet, S. Ivanov, R. Porte, E. Deruy, J.A. Chabalgoity, J.C. Renauld, G. Eberl, A.G. Benecke, F. Trottein, C. Faveeuw, and J.C. Sirard. 2014. Activation of type 3 innate lymphoid cells and IL-22 secretion in lung during Streptococcus pneumoniae infection. *J Infect Dis*

Verbon, A., N. Juffermans, S.J. Van Deventer, P. Speelman, H. Van Deutekom, and T. Van Der Poll. 1999. Serum concentrations of cytokines in patients with active tuberculosis (TB) and after treatment. *Clin Exp Immunol* 115:110-113.

Verrall, A.J., M.G. Netea, B. Alisjahbana, P.C. Hill, and R. van Crevel. 2014. Early clearance of Mycobacterium tuberculosis: a new frontier in prevention. *Immunology* 141:506-513.

Verver, S., R.M. Warren, N. Beyers, M. Richardson, G.D. van der Spuy, M.W. Borgdorff, D.A. Enarson, M.A. Behr, and P.D. van Helden. 2005. Rate of reinfection tuberculosis after successful treatment is higher than rate of new tuberculosis. *Am J Respir Crit Care Med* 171:1430-1435.

Via, L.E., P.L. Lin, S.M. Ray, J. Carrillo, S.S. Allen, S.Y. Eum, K. Taylor, E. Klein, U. Manjunatha, J. Gonzales, E.G. Lee, S.K. Park, J.A. Raleigh, S.N. Cho, D.N. McMurray, J.L. Flynn, and C.E. Barry, 3rd. 2008. Tuberculous granulomas are hypoxic in guinea pigs, rabbits, and nonhuman primates. *Infect Immun* 76:2333-2340.

Vonarbourg, C., and A. Diefenbach. 2012. Multifaceted roles of interleukin-7 signaling for the development and function of innate lymphoid cells. *Seminars in immunology* 24:165-174.

Vonarbourg, C., A. Mortha, V.L. Bui, P.P. Hernandez, E.A. Kiss, T. Hoyler, M. Flach, B. Bengsch, R. Thimme, C. Holscher, M. Honig, U. Pannicke, K. Schwarz, C.F. Ware, D. Finke, and A. Diefenbach. 2010. Regulated expression of nuclear receptor RORgammat confers distinct

functional fates to NK cell receptor-expressing RORgammat(+) innate lymphocytes. *Immunity* 33:736-751.

Vosshenrich, C.A., T. Ranson, S.I. Samson, E. Corcuff, F. Colucci, E.E. Rosmaraki, and J.P. Di Santo. 2005. Roles for common cytokine receptor gamma-chain-dependent cytokines in the generation, differentiation, and maturation of NK cell precursors and peripheral NK cells in vivo. *J Immunol* 174:1213-1221.

Waibler, Z., M. Anzaghe, H. Ludwig, S. Akira, S. Weiss, G. Sutter, and U. Kalinke. 2007. Modified vaccinia virus Ankara induces toll-like receptor-independent type I interferon responses. *Journal of Virology* 81:12102-12110.

Walker, J.A., J.L. Barlow, and A.N. McKenzie. 2013. Innate lymphoid cells--how did we miss them? *Nature reviews* 13:75-87.

Walker, J.A., C.J. Oliphant, A. Englezakis, Y. Yu, S. Clare, H.R. Rodewald, G. Belz, P. Liu, P.G. Fallon, and A.N. McKenzie. 2015a. Bcl11b is essential for group 2 innate lymphoid cell development. *J Exp Med* 212:875-882.

Walker, N.F., J. Scriven, G. Meintjes, and R.J. Wilkinson. 2015b. Immune reconstitution inflammatory syndrome in HIV-infected patients. *HIV/AIDS (Auckland, N.Z.)* 7:49-64.

Wallgren, A. 1948. The time-table of tuberculosis. *Tubercle* 29:245-251.

Wang, J., A. Zganiacz, and Z. Xing. 2002. Enhanced immunogenicity of BCG vaccine by using a viral-based GM-CSF transgene adjuvant formulation. *Vaccine* 20:2887-2898.

Whitsett, J.A., S.E. Wert, and T.E. Weaver. 2015. Diseases of pulmonary surfactant homeostasis. *Annual review of pathology* 10:371-393.

WHO. 2006. The global plan to stop TB, 2006-2015 / Stop TB Partnership.

WHO. 2014a. Drug Resistant TB Surveillance and Response. Supplement Global Tuberculosis Report 2014.

WHO. 2014b. Global Tuberculosis report 2014.

Wolf, A.J., L. Desvignes, B. Linas, N. Banaiee, T. Tamura, K. Takatsu, and J.D. Ernst. 2008. Initiation of the adaptive immune response to Mycobacterium tuberculosis depends on antigen production in the local lymph node, not the lungs. *Journal of Experimental Medicine* 205:105-115.

Wolf, A.J., B. Linas, G.J. Trevejo-Nunez, E. Kincaid, T. Tamura, K. Takatsu, and J.D. Ernst. 2007. Mycobacterium tuberculosis infects dendritic cells with high frequency and impairs their function in vivo. *J. Immunol.* 179:2509-2519.

Wong, S.H., J.A. Walker, H.E. Jolin, L.F. Drynan, E. Hams, A. Camelo, J.L. Barlow, D.R. Neill, V. Panova, U. Koch, F. Radtke, C.S. Hardman, Y.Y. Hwang, P.G. Fallon, and A.N. McKenzie. 2012. Transcription factor RORalpha is critical for nuocyte development. *Nat Immunol* 13:229-236.

Woodworth, J.S., C.S. Aagaard, P.R. Hansen, J.P. Cassidy, E.M. Agger, and P. Andersen. 2014. Protective CD4 T cells targeting cryptic epitopes of Mycobacterium tuberculosis resist infection-driven terminal differentiation. *J Immunol* 192:3247-3258.

Woodworth, J.S., Y. Wu, and S.M. Behar. 2008. Mycobacterium tuberculosis-specific CD8+ T cells require perforin to kill target cells and provide protection in vivo. *J Immunol* 181:8595-8603.

Wozniak, T.M., A.A. Ryan, and W.J. Britton. 2006. Interleukin-23 restores immunity to Mycobacterium tuberculosis infection in IL-12p40-deficient mice and is not required for the development of IL-17-secreting T cell responses. *J. Immunol.* 177:8684-8692.

Wozniak, T.M., B.M. Saunders, A.A. Ryan, and W.J. Britton. 2010. Mycobacterium bovis BCG-specific Th17 cells confer partial protection against Mycobacterium tuberculosis infection in the absence of gamma interferon. *Infect Immun* 78:4187-4194.

Xu, W., R.G. Domingues, D. Fonseca-Pereira, M. Ferreira, H. Ribeiro, S. Lopez-Lastra, Y. Motomura, L. Moreira-Santos, F. Bihl, V. Braud, B. Kee, H. Brady, M.C. Coles, C. Vosshenrich, M. Kubo, J.P. Di Santo, and H. Veiga-Fernandes. 2015. NFIL3 Orchestrates the Emergence of Common Helper Innate Lymphoid Cell Precursors. *Cell reports* 10:2043-2054.

Yagi, R., C. Zhong, D.L. Northrup, F. Yu, N. Bouladoux, S. Spencer, G. Hu, L. Barron, S. Sharma, T. Nakayama, Y. Belkaid, K. Zhao, and J. Zhu. 2014. The Transcription Factor GATA3 Is Critical for the Development of All IL-7Ralpha-Expressing Innate Lymphoid Cells. *Immunity* 40:378-388.

Yang, C.T., C.J. Cambier, J.M. Davis, C.J. Hall, P.S. Crosier, and L. Ramakrishnan. 2012. Neutrophils exert protection in the early tuberculous granuloma by oxidative killing of mycobacteria phagocytosed from infected macrophages. *Cell host & microbe* 12:301-312.

Yang, Q., L.A. Monticelli, S.A. Saenz, A.W. Chi, G.F. Sonnenberg, J. Tang, M.E. De Obaldia, W. Bailis, J.L. Bryson, K. Toscano, J. Huang, A. Haczku, W.S. Pear, D. Artis, and A. Bhandoola. 2013. T cell factor 1 is required for group 2 innate lymphoid cell generation. *Immunity* 38:694-704.

Yokota, Y., A. Mansouri, S. Mori, S. Sugawara, S. Adachi, S. Nishikawa, and P. Gruss. 1999. Development of peripheral lymphoid organs and natural killer cells depends on the helix-loop-helix inhibitor Id2. *Nature* 397:702-706.

Yonekawa, A., S. Saijo, Y. Hoshino, Y. Miyake, E. Ishikawa, M. Suzukawa, H. Inoue, M. Tanaka, M. Yoneyama, M. Oh-Hora, K. Akashi, and S. Yamasaki. 2014. Dectin-2 is a direct receptor for mannose-capped lipoarabinomannan of mycobacteria. *Immunity* 41:402-413.

Young, D.B., H.P. Gideon, and R.J. Wilkinson. 2009. Eliminating latent tuberculosis. *Trends in Microbiology* 17:183-188.

Yu, X., Y. Wang, M. Deng, Y. Li, K.A. Ruhn, C.C. Zhang, and L.V. Hooper. 2014. The basic leucine zipper transcription factor NFIL3 directs the development of a common innate lymphoid cell precursor. *eLife* 3:

Yu, Y., C. Wang, S. Clare, J. Wang, S.C. Lee, C. Brandt, S. Burke, L. Lu, D. He, N.A. Jenkins, N.G. Copeland, G. Dougan, and P. Liu. 2015. The transcription factor Bcl11b is specifically expressed in group 2 innate lymphoid cells and is essential for their development. *J Exp Med* 212:865-874.

Zenaro, E., M. Donini, and S. Dusi. 2009. Induction of Th1/Th17 immune response by Mycobacterium tuberculosis: role of dectin-1, Mannose Receptor, and DC-SIGN. *J Leukoc Biol* 86:1393-1401.

Zhan, Y., Y. Xu, and A.M. Lew. 2012. The regulation of the development and function of dendritic cell subsets by GM-CSF: more than a hematopoietic growth factor. *Molecular immunology* 52:30-37.

Zhang, X., D. Bogunovic, B. Payelle-Brogard, V. Francois-Newton, S.D. Speer, C. Yuan, S. Volpi, Z. Li, O. Sanal, D. Mansouri, I. Tezcan, G.I. Rice, C. Chen, N. Mansouri, S.A. Mahdaviani, Y. Itan, B. Boisson, S. Okada, L. Zeng, X. Wang, H. Jiang, W. Liu, T. Han, D. Liu, T. Ma, B. Wang, M. Liu, J.Y. Liu, Q.K. Wang, D. Yalnizoglu, L. Radoshevich, G. Uze, P. Gros, F. Rozenberg, S.Y. Zhang, E. Jouanguy, J. Bustamante, A. Garcia-Sastre, L. Abel, P. Lebon, L.D. Notarangelo, Y.J. Crow, S. Boisson-Dupuis, J.L. Casanova, and S. Pellegrini. 2015. Human intracellular ISG15 prevents interferon-alpha/beta over-amplification and auto-inflammation. *Nature* 517:89-93.

Zhang, X., M. Divangahi, P. Ngai, M. Santosuosso, J. Millar, A. Zganiacz, J. Wang, J. Bramson, and Z. Xing. 2007. Intramuscular immunization with a monogenic plasmid DNA tuberculosis vaccine: Enhanced immunogenicity by electroporation and co-expression of GM-CSF transgene. *Vaccine* 25:1342-1352.

Zhang, X., L. Majlessi, E. Deriaud, C. Leclerc, and R. Lo-Man. 2009. Coactivation of Syk kinase and MyD88 adaptor protein pathways by bacteria promotes regulatory properties of neutrophils. *Immunity* 31:761-771.

Zhu, J., and W.E. Paul. 2008. CD4 T cells: fates, functions, and faults. *Blood* 112:1557-1569.

Zhu, J., H. Yamane, and W.E. Paul. 2010. Differentiation of effector CD4 T cell populations (*). *Annu Rev Immunol* 28:445-489.

Zufferey, C., S. Germano, B. Dutta, N. Ritz, and N. Curtis. 2013. The contribution of non-conventional T cells and NK cells in the mycobacterial-specific IFNgamma response in Bacille Calmette-Guerin (BCG)-immunized infants. *PLoS One* 8:e77334.

Appendices

Appendix 1

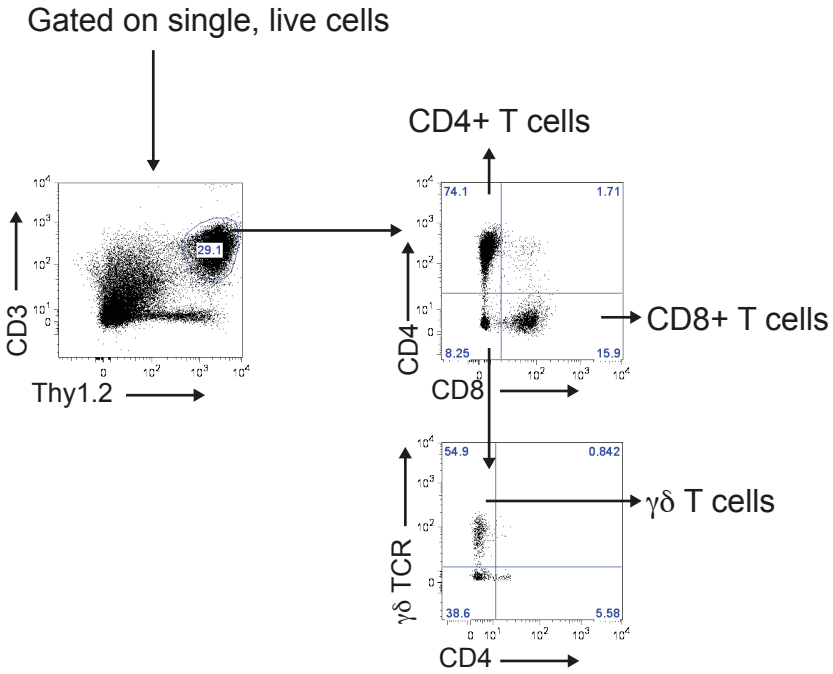

Appendix 1 Gating strategy to identify T cell populations

CBA/J mice were BCG vaccinated and challenged with *Mtb* as shown in **Figure 3.1**. Lungs were homogenized by passage through a 70μm filter. Samples were stained with the following antibodies to assess percentages and calculate numbers of lymphoid populations by flow cytometry: γδ TCR FITC, Thy1.2 PECy7, CD4 e450, CD8 v500 and CD3 APC. $CD4^+$ T cells were identified as $CD3^+$ $Thy1.2^+$ $CD4^+$, $CD8^+$ T cells as $CD3^+$ $Thy1.2^+$ and γδ T cells as $CD3^+$ $Thy1.2^+$ γδ TCR^+. Representative flow cytometry plots from the lung of a mouse BCG vaccinated in the context of αIL-10R mAb harvested at day 28 post infection is shown. The same gating strategy was used to identify T cell populations following *Mtb* infection and αGM-CSF treatment as shown in **Figure 4.1A.**

Appendix 2

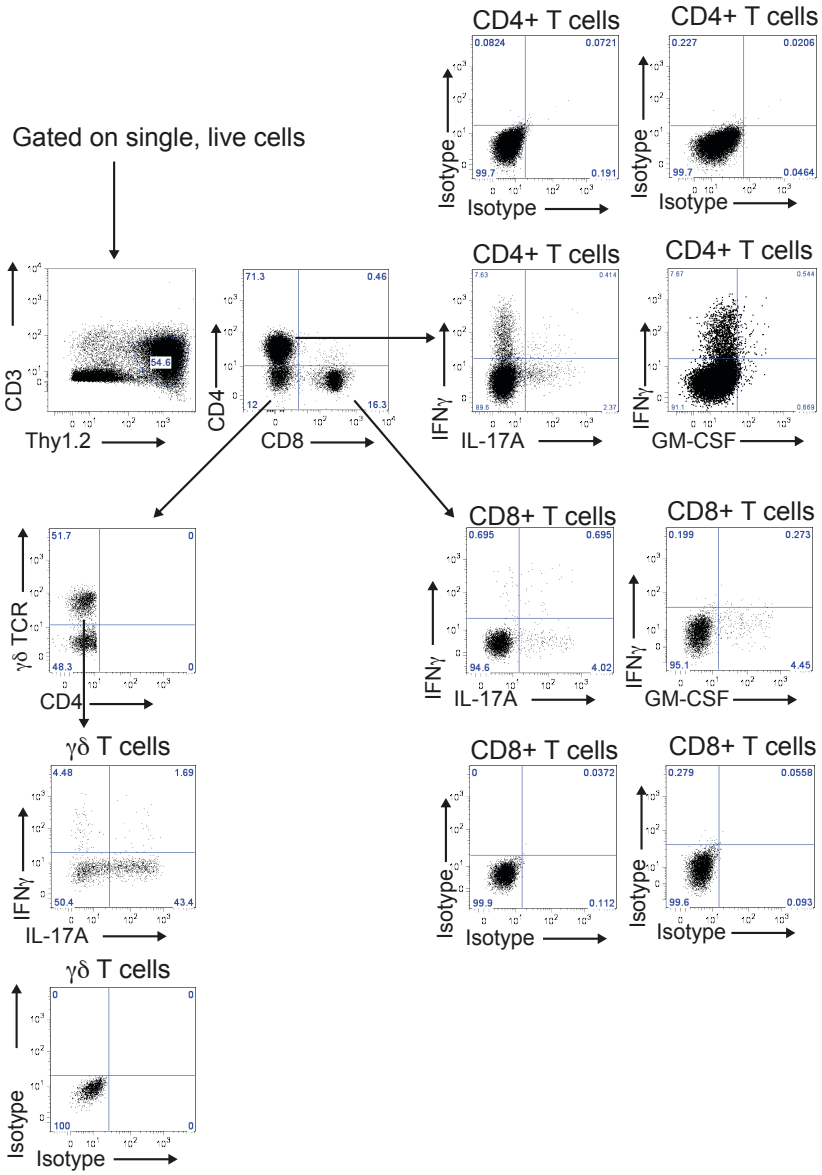

Appendix 2 Gating strategy to identify cytokine production by T cell populations.

CBA/J mice were BCG vaccinated and challenged with *Mtb* as shown in **Figure 3.1**. Lungs were homogenized by passage through a 70μm filter. $1x10^6$ cells were restimulated with 20μg PPD and 2μg αCD28 mAb for 16h before the addition of BFA for a further 4h. Cells were then harvested and stained with the following to assess cytokine production: γδ TCR FITC, GM-CSF PE, CD8 PerCP e710, Thy1.2 PE Cy7, IFNγ e450, CD4 v500, IL-17A APC, CD3 APCe780. $CD4^+$ T cells were identified as $CD3^+$ $Thy1.2^+$ $CD4^+$, $CD8^+$ T cells as $CD3^+$ $Thy1.2^+$ and γδ T cells as $CD3^+$ $Thy1.2^+$ γδ TCR^+. Cytokine gates set from isotype controls. Representative flow cytometry plots from the lung of a mouse BCG vaccinated in the context of αIL-10R mAb harvested at day 28 post infection is shown. The same gating strategy was used to identify cytokine producing T cells following *Mtb* infection and αGM-CSF treatment as shown in **Figure 4.1A.**

Appendix 3

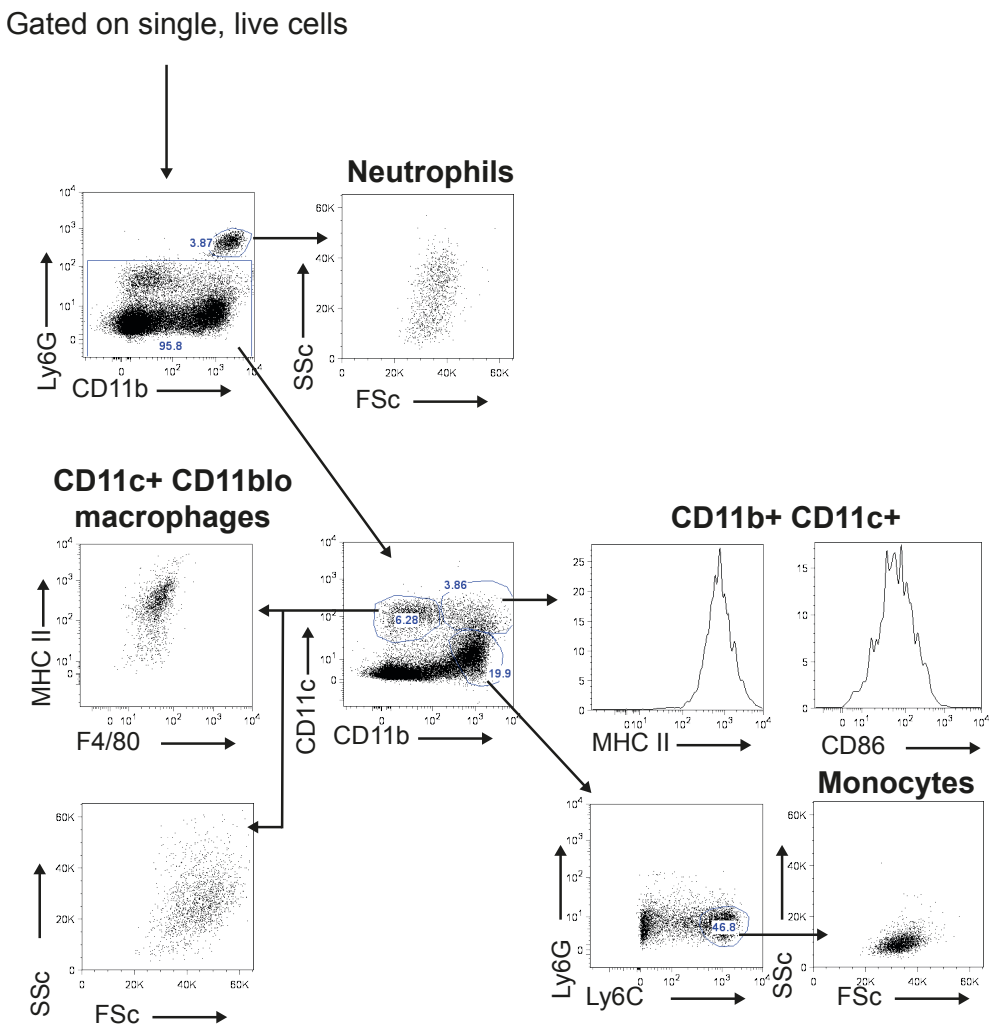

Appendix 3 Gating strategy to myeloid populations in the lung

C57BL/6 or CBA/J mice were treated with αGM-CSF or isotype control mAb as shown in **Figure 4.1A**. Lungs were homogenized by passage through a 70μm filter. Samples were stained with the following antibodies to assess percentages and calculate numbers of myeloid populations by flow cytometry: Ly6G FITC, CD11c PE, Ly6C PerCP Cy5.5, CD11b PECy7, CD86 Brilliant Violet 421, CD8 v500, F4/80 APC and MHC class II (MHC II) APCe780. Neutrophils were identified as Ly6G^{+} CD11b^{+}, CD11c^{+} CD11b^{lo} macrophages as Ly6G- CD11b^{lo} CD11c^{+}, monocytes as Ly6G- CD11b^{+} Ly6C^{+}, CD11b^{+} CD11c^{+} DCs as Ly6G- CD11b^{+} CD11c^{+}. Representative flow cytometry plots from the lung of an *Mtb* infected C57BL/6 mouse treated with isotype control at day 21 post infection.

Appendix 4

Poster Presentations:

- **Stimpson P**, "IL-10 signalling abrogation during BCG vaccination accelerates recruitment of GM-CSF producing not IFNγ producing $CD4^+$ T cells to the lung upon challenge with *Mycobacterium tuberculosis*." British Society for Immunology Congress 2014, December 2014, Brighton, UK.

Book Chapter:

- Howes A, **Stimpson P**, Redford P, Gabryšová L, O'Garra A. (2013). Interleukin 10: Cytokines in Anti-inflammation and Tolerance. In: Yoshimoto, T and Yoshimoto, T (ed.) *Cytokine Frontiers: Regulation of Immune Responses in Health and Disease*. Japan: Springer.